

THESIS FOR THE DEGREE OF DOCTOR OF PHILOSOPHY

# Environmental actions on concrete exposed in marine and road environments and its response

Consequences for the initiation of chloride induced  
reinforcement corrosion

ANDERS LINDVALL

Department of Building Technology  
Building Materials  
CHALMERS UNIVERSITY OF TECHNOLOGY  
Göteborg, Sweden 2003

ENVIRONMENTAL ACTIONS ON CONCRETE EXPOSED IN MARINE AND  
ROAD ENVIRONMENTS AND ITS RESPON

Consequences for the initiation of chloride induced reinforcement corrosion

ANDERS LINDVALL

ISBN 91-7291-371-1

© ANDERS LINDVALL, 2003

Doktorsavhandlingar vid Chalmers Tekniska Högskola

Ny serie nr 2053

ISSN 0346-718X

Department of Building Technology

Building Materials

Chalmers University of Technology

ISSN 1104-893X

Publication no P-03:2

Arbnr: 612

Department of Building Technology

Building Materials

Chalmers University of Technology

SE-412 96 Göteborg

Sweden

Telephone: +46 (0)31-772 1000

<http://www.chalmers.se>

Cover: The picture on the cover shows the author at the field station (for exposure in the marine tidal zone) in La Rochelle. The field station is located next to the “Tour St Nicholas” outside the old harbour in La Rochelle.

Chalmers Reproservice

Göteborg, Sweden 2003

## Abstract

### ENVIRONMENTAL ACTIONS ON CONCRETE EXPOSED IN MARINE AND ROAD ENVIRONMENTS AND ITS RESPONSE

- Consequences for the initiation of chloride induced reinforcement corrosion

ANDERS LINDVALL

Department of Building Technology

Building Materials

Chalmers University of Technology

## Abstract

The object of the study presented here has been to describe, further explain and model the influence of the exposure conditions on reinforced concrete structures and the consequences on their expected service life. The focus has been on investigating and quantifying the exposure conditions for structures in marine and road conditions exposed to chloride ions. This has been done by literature studies complemented by field studies, where data on the behaviour of concrete have been gathered and analysed. The literature study has shown that the exposure conditions have a large influence, e.g. due to variations in the severity of exposure to chlorides.

Field studies have been made in both marine and road conditions, where the influence of the exposure conditions has been measured as the environmental response of concrete and mortar. In marine conditions identical concrete specimens, exposed at different submerged locations, have been investigated. The results show that the temperature of the seawater has a large influence on chloride ingress. In road conditions both existing structures and specimens have been investigated. The results show that the exposure to chlorides and the chloride ingress into concrete depend on several factors, e.g. height above and distance to the road and surface orientation towards traffic.

Service life predictions have been made for structures in marine and road conditions, to exemplify the effect of the exposure conditions. The results of the predictions show that the exposure conditions have a large influence on the expected service life. The predictions also showed that the level of the chloride threshold level,  $C_{crit}$ , has a large influence on the predicted service life.

The environmental actions, and their variations, have been found to have a large influence on the chloride ingress into and the service life of reinforced concrete structures. Therefore it is not enough to describe these by rough divisions into exposure classes, but instead the true exposure conditions should be taken into account. Preferably each structure should be treated separately, but this is usually not possible. For these structures the methodology described in this thesis can be used to describe and model the environmental actions.

**Keywords:** Chloride, concrete, corrosion, de-icing salt, environmental actions, marine conditions, moisture conditions, reinforcement, road conditions, service life predictions



## Foreword

The work presented in this doctoral thesis is the outcome of the project “Environmental actions and response of concrete surfaces”. Professor Lars-Olof Nilsson at the Department of Building Materials, Chalmers University of Technology (now professor at the Division of Building Materials, Lund Institute of Technology, Lund), initiated the project. The work has mainly been conducted at the Department of Building Material, Chalmers University of Technology in Göteborg, during the period 1998-2003.

As a part of my work I conducted field exposure programmes, in marine and road conditions. In the marine exposure programme concrete specimens have been exposed at different locations around the world. The marine exposure programme was made possible by the help of the following people, who are all gratefully acknowledged for their kind help and assistance:

- **Banyuls sur Mer**, France. Dr. Antoine Grémare & Mr. Laurent Zudaire. Observatoire Oceanologique de Banyuls-sur-Mer, Laboratoire ARAGO, Banyuls sur Mer.
- **Cascais**, Portugal. Dr. Arlindo Goncalves, Mr. Manuel Vieira & Ms. Angela Machado. Laboratório de Engenharia Civil (LNEC), Lisbon.
- **Dubai**, United Arab Emirate. Mr. Tor H Sandgren & Mr. Odd Moe, Gulf Agency Co., Dubai.
- **Eastern Scheldt**, Netherlands. Mr. Eddie van de Ketterij & Dr. Joost Gulikers, Rijkswaterstaat (RWS), Burgh-Haamstede & Amsterdam.
- **Hirtshals**, Denmark. Dr. Dirch Bager, Aalborg Portland, Aalborg.
- **Hvalfjörður**, Iceland. Mr. Jon Möller, Techn. Lic., ISTAK, Reykjavik.
- **Kjøpsvik**, Norway. Mr. Anders Bergvik & Mr. Erling Kristensen, NORCEM, Kjøpsvik.
- **Källhamn**, Sweden. Mr. Erik Mattson, Göteborg.
- **La Rochelle**, France. Dr. Karim Aït-Mokhtar & Dr. Olivier Poupard, Laboratoire d'Etude des Phénomènes de Transfert Appliqués au Bâtiment (LEPTAB), Université de La Rochelle, La Rochelle.
- **Skanör**, Sweden. Prof. Lars-Olof Nilsson, Department of Building Materials, Chalmers University of Technology, Göteborg (now at the Division of Building Materials, Lund Institute of Technology, Lund).
- **Tasmania**, Australia. Mr. Rod McGee & Mr. Geoff Mulcahy, Department of Infrastructure, Hobart Tasmania.

In the road exposure programme, reinforced concrete road bridges around Göteborg have been investigated, both by taking concrete samples from the bridges and exposing mortar specimens on them. Concrete specimens have also been exposed at the Rv40 field station outside Borås. Mr. Torbjörn Johansson from Gatubolaget in Göteborg assisted in taking

## Foreword

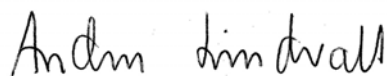
concrete samples from the bridges and exposing the mortar disks on them, for which he is gratefully acknowledged.

The project has been financed by FORMAS, the Swedish Research Council for Environment, Agricultural Sciences and Spatial Planning (earlier called BFR, the Swedish Council for Building Research) and the Swedish National Road Administration (Vägverket). The author would therefore like to acknowledge FORMAS and the Swedish National Road Administration for their financial support. During the first year of my doctoral studies I participated in a Brite EuRam project (financed by the European Union) called DuraCrete, Probabilistic Performance based Durability Design of Concrete Structures (Contract BRPR-CT95-0132 Project BE95-1347).

I wish to thank everyone who has helped me in this work, especially my colleagues at the department of Building Materials, Chalmers University of Technology. In particular I wish to thank Juhan Aavik, M.Sc., Mr. Marek Machowski and Mrs. Nidal Yousif for their help with practical matters and analysis in the laboratory, Bengt Dellming, M.Sc., and Mats Rodhe, M.Sc., for interesting discussions and comments on the work and Ms. Ingela Gustafsson for help with practical matters. I would also like to thank Mr. Tore Andersson and Ms. Carina Forsman, for their help with profile grinding for chloride analysis, Alf Andersen, M.Sc., for interesting discussions and comments on the work and co-operation during parts of the road exposure programme, Professor Lars-Olof Nilsson, for interesting discussions during the work and reading through and commenting the content of this thesis, and Mr. Lewis Gruber, for language editing this thesis.

As a part of my doctoral studies I spent a period of three months during the summer of 2002 at TNO, the Netherlands Organisation for Applied Scientific Research, in Delft. During the stay I worked with a Dutch national research project called DuMaCon, Durable Marine Concrete Structures, in which I participated in an inspection of the Eastern Scheldt storm surge barrier. The stay was a great experience both professionally and privately. I wish to thank Dr. Rob Polder, who was my contact person at TNO, for inviting me to spend the period at TNO and arranging practical matters. I would also like to thank the rest of the staff at TNO for letting me stay there and for arranging a nice flat in Voorburg to live in during the stay. The stay was made financially possible with a scholarship from the fund "Åke och Greta Lissheds stiftelse", which is gratefully acknowledged.

Finally I would like to thank my family for supporting me during my doctoral studies and the writing of this thesis.



Göteborg, November 2003

## Table of Contents

<b>Abstract</b>	<b>I</b>
<b>Foreword</b>	<b>III</b>
<b>Notations and units</b>	<b>VII</b>
<b>1 Introduction</b>	<b>1</b>
1.1 General	1
1.2 Background to research project	2
1.3 Object	3
1.4 Limitations	3
1.5 Disposition of the thesis	4
<b>2 Modelling of service life – theory</b>	<b>7</b>
2.1 Introduction	7
2.2 Service life of reinforced concrete structures	7
2.3 Mathematical models for prediction of chloride ingress into concrete	12
<b>3 Environmental actions and response</b>	<b>17</b>
3.1 Introduction	17
3.2 Environmental actions	18
3.3 Response of concrete	23
3.4 Marine conditions	26
3.5 Road conditions	38
<b>4 Field study – Marine conditions</b>	<b>55</b>
4.1 Background	55
4.2 Exposure programme	56
4.3 Measurement techniques	61
4.4 Results	63
4.5 Analysis and discussion	71
4.6 Conclusions	88
<b>5 Field study – Road conditions</b>	<b>91</b>
5.1 Introduction	91

## Table of Contents

5.2	Exposure programme	92
5.3	Results	102
5.4	Analysis and discussion	109
5.5	Conclusions	128
<b>6</b>	<b>Models for environmental actions</b>	<b>131</b>
6.1	Introduction	131
6.2	Models for environmental actions – general aspects	133
6.3	Models for environmental actions – Marine conditions	147
6.4	Models for environmental actions – Road conditions	151
<b>7</b>	<b>Environmental actions in models of service life</b>	<b>157</b>
7.1	Introduction	157
7.2	Input data – Concrete compositions	158
7.3	Input data – Exposure conditions	159
7.4	Predictions of chloride ingress – general	166
7.5	Predictions of chloride ingress – field conditions	170
7.6	Discussion and analysis – marine and road conditions	178
7.7	Probabilistic predictions	186
7.8	Conclusions	194
<b>8</b>	<b>Final discussion and conclusions</b>	<b>199</b>
8.1	General	199
8.2	Marine conditions	201
8.3	Road conditions	202
<b>9</b>	<b>Future research</b>	<b>205</b>
9.1	Chloride ingress – in general	205
9.2	Marine conditions	206
9.3	Road conditions	208
<b>10</b>	<b>References</b>	<b>211</b>
	<b>Appendix</b>	<b>223</b>
	Meteorological data	223
	Equivalent surface humidity and temperature	228
	Input data – Environmental parameters	230



## Notations and units

Symbol	Unit	Description
$a$	-	Absorption factor for short wave radiation.
$b_e(C_{sa})$	-	Regression parameter for determination of temperature dependency of the surface chloride content.
$b_e(D_a)$	-	Regression parameter for determination of temperature dependency of $D_a$ .
$C$	$\text{kg/m}^3$	Cement content in concrete.
$c_b(T)$	$\text{kg/m}^3$	Content of bound chlorides in concrete as a function of temperature.
$C_{\text{crit}}$	% by weight Cl/binder	Chloride threshold level, i.e. the chloride content at the reinforcement at which reinforcement corrosion is initiated.
$c_f$	$\text{kg/m}^3$	Content of free chlorides in concrete.
$C_{\text{heat}}$	$\text{J}/(\text{m}^3 \text{ K})$	Heat capacity.
$\text{Cl}_c$	% by weight Cl/binder	Chloride content in the concrete.
$\text{Cl}_f$	$\text{g Cl/l}$	Chloride concentration in the exposure solution.
$C'_{s,\text{tot}}$	% by weight Cl/binder	The total chloride content (free and bound chlorides) at the surface of the concrete.
$\text{Cl}_{\text{sol}}$	$\text{kg/m}^3$	Chloride concentration in the exposure solution.
$C_{sa}(T_a)$	% by weight Cl/binder	Surface chloride content at temperature $T_a$ .
$C_{sa,\text{ref}}$	% by weight Cl/binder	Surface chloride content at the reference temperature, $T_{\text{ref}}$ (293 K).
$C_{sc}$	% by weight Cl/binder	Surface chloride content for the diffusion zone.
$C_{\text{SN}}$	% by weight Cl/binder	Apparent surface chloride content.
$C_{\text{SN},\text{eq}}$	% by weight Cl/binder	$C_{\text{SN}}$ measured in equivalent conditions and concrete quality. $C_{\text{SN},\text{eq}}$ is in marine conditions determined in the submerged zone at 1.0 m depth (chloride concentration and temperature of 20g Cl/l and 20°C respectively) and in road conditions at the road surface (vertical surface at 0.0 m distance and height).
$C_{\text{tot}}$	J or kg	Total content of energy or mass.
$c_{\text{tot}}(T)$	$\text{kg/m}^3$	Content of total chlorides in concrete (bound + free) as a function of temperature.

## Notations and units

Symbol	Unit	Description
$C_x$	% by weight Cl/binder	Chloride content at a certain penetration depth.
$D_0$	$m^2/s$	Potential diffusion coefficient, determined at standardized conditions, with a standardized method, e.g. NT Build 492 (1999).
$D_a(t)$	$m^2/s$	Apparent diffusion coefficient for chlorides.
$D_a(T_a)$	$m^2/s$	$D_a$ at temperature $T_a$ .
$D_{a,ref}$	$m^2/s$	$D_a$ at the reference temperature, $T_{ref}$ (293 K).
$d_c$	m	Concrete cover.
$D_{F1}$	$m^2/s$	Diffusion coefficient in Fick's 1 <sup>st</sup> law.
$E_D$	J/mol	Activation energy for chloride diffusion.
$g$	kg/(m <sup>2</sup> s)	Flow rate of condensed water vapour.
$h_e$	kJ/kg	Latent heat of evaporation ( $h_e \approx 2500$ kJ/kg).
$I_{solar}$	W/m <sup>2</sup>	Solar radiation.
$k_c$	-	Constant parameter that accounts for the influence of workmanship on $D_a(t)$ .
$k_{C,Cl}$	-	Parameter that accounts for the influence of chloride concentration in marine submerged conditions on $C_{SN,eq}$ (if the chloride concentration is other than 20 g/l).
$k_{C,conc}$	-	Parameter that accounts for the influence the concrete composition has on $C_{SN,eq}$ .
$k_{C,d}$	-	Parameter that accounts for the horizontal distance to the source of chlorides.
$k_{C,e}$	-	Parameter that accounts for the influence of the exposure environment. To better model the influence of the exposure environment the parameter $k_{C,e}$ is subdivided into the following <b>uncorrelated</b> parameters, $k_{C,Cl}$ , $k_{C,d}$ , $k_{C,h}$ , $k_{C,o}$ and $k_{C,T}$ .
$k_{C,h}$	-	Parameter that accounts for the vertical distance to the source of chlorides.
$k_{C,o}$	-	Parameter that accounts for the orientation towards the source of chlorides.
$k_{C,T}$	-	Parameter that accounts for the influence of temperature on $C_{SN,eq}$ .
$k_{C,test}$	-	Parameter that accounts for the influence of the test method.
$k_{D,c}$	-	Parameter that accounts for the curing conditions.
$k_{D,e}$	-	Parameter that accounts for the environmental conditions. The factor $k_{D,e}$ is proposed to be subdivided into two <b>uncorrelated</b> parameters giving the influence of the RH, $k_{D,RH}$ , and the temperature, $k_{D,T}$ , respectively.
$k_e$	-	Constant parameter that accounts for the influence of environment on $D_a(t)$

## Notations and units

Symbol	Unit	Description
$k_t$ & $k_{D, \text{test}}$	-	Constant parameter that accounts for the influence of test method on $D_a(t)$
$L$	$\text{m}^3/\text{m}^3$ concrete	Air content in the concrete.
$n$	-	Age factor, that accounts for the decrease of $D_a(t)$ with time.
$p$	-	Probability that a certain event occurs.
$P_a$	$\text{m}^3/\text{m}^3$ aggregate	Porosity of the aggregates.
$P_c$	$\text{m}^3/\text{m}^3$	Porosity of the concrete.
$p_f$	-	Failure probability.
$P_p$	$\text{m}^3/\text{m}^3$ cement paste	Porosity of the cement paste.
$p_{\text{sol}}$	-	Porosity of concrete (saturated pore volume that acts as solvent for chloride ions).
$p_{\text{target}}$	-	Target probability.
$q$	J/s or kg/s	Flow of energy or mass.
$q_m$	$\text{kg}/(\text{m}^2 \text{ s})$	Total moisture flow.
$R$	J/(mol K)	Gas constant ( $R=8.314 \text{ J}/(\text{mol K})$ ).
$RH_{\text{air}}$	%	Relative humidity of the air.
$t$	s	Exposure time.
$t_0$	s	Reference time, i.e. time after casting at which $D_0$ is measured.
$T_a$	K	Temperature of the exposure water.
$T_{\text{air}}$	K	Air temperature.
$\bar{T}_r$	K	Sky temperature.
$T_{\text{ref}}$	K	Reference temperature. 293 K.
$T_{s, \text{eq}}$	K	Equivalent surface temperature.
$V_a$	$\text{m}^3/\text{m}^3$ concrete	Volumetric proportion of aggregates in the concrete.
$V_p$	$\text{m}^3/\text{m}^3$ concrete	Volumetric proportion of the cement paste in the concrete.
$v_s(T_{\text{air}})$	$\text{g}/\text{m}^3$	Vapour content of the air at a specific temperature.
$w_e$	$\text{kg}/\text{m}^3$	Amount of evaporable water.
$w_n$	$\text{kg}/\text{m}^3$	Amount of non-evaporable water.
$x$	m	Depth at which the chloride content is determined.
$x_c$	m	Thickness of “convection zone”.
$\alpha$	-	Degree of hydration.
$\alpha_{cv}$	$\text{W}/(\text{m}^2\text{K})$	Convective heat transfer coefficient.
$\alpha_r$	$\text{W}/(\text{m}^2\text{K})$	Radiative heat transfer coefficient.
$\lambda$	$\text{W}/(\text{m K})$	Thermal conductivity.
$\sigma$	$\text{W}/(\text{m}^2\text{K}^4)$	Stefan-Boltzmann constant ( $\sigma=5.6697 \cdot 10^{-8} \text{ W}/(\text{m}^2\text{K}^4)$ ).



# 1 Introduction

## 1.1 General

During the last decades the expenditure on rehabilitation of reinforced concrete structures has increased. Since the value of all structures (infrastructure and built environment) represents a considerable amount of the wealth of a country – in Western Europe the value is approximately 50% of the national wealth - this expenditure represents considerable amounts. Furthermore it is estimated that approximately 50% of the expenditure in the construction industry is spent on repair, maintenance and remediation of existing reinforced concrete structures, Long et al (2001). A large proportion of this expenditure can be related to problems due to lack of durability of the structures, as a result of the influence from exposure conditions for the structure. Thus to reduce this expenditure the performance of the structures should be predicted, where also the influence from the exposure conditions is included, with respect to durability, future maintenance etc. Then future maintenance of the structure can be planned, and based on this the expenditure for repair, maintenance and remediation can be optimised.

There are two principal methodologies to design reinforced concrete structures with respect to durability:

- **Deem-to-satisfy rules.** In a design, based on deem-to-satisfy rules, the service life is predicted by rules of thumb. Examples of rules of thumb are that a sufficiently long service life will be achieved if the concrete is manufactured with a certain w/b and concrete cover. The result will be **sufficiently long but not specified** service lives, which means it is not possible to explicitly plan for future maintenance and optimize the expenditure on repair, maintenance and remediation.
- **Performance based design.** In a performance based design the service life is predicted with respect to the performance of the structure, where the performance is specified with respect to limit states. A difference is made between ultimate limit states (ULS), where the safety of the structure is considered, e.g. risk of collapse, and serviceability limit states (SLS), where the functionality of the structure is considered, e.g. limitation of crack widths and aesthetic appearance. The limit states are defined by for example authorities or the owner of the structure. The performance of the structure is modelled as a function over time with sufficiently realistic mathematical models, where the different behaviour of the concrete structure, e.g. durability, loadbearing capacity etc, is described. The predicted performance is compared with the required performance and once the required performance exceeds the predicted performance (with a certain probability) the service life is ended. With the performance based design the structure has a **sufficiently long and specified** service life, which means it is possible to plan for future maintenance and optimize the expenditure on repair, maintenance and remediation.

The performance of reinforced concrete structures over time is to a large extent influenced by deterioration of the concrete and/or the reinforcement. The deterioration of reinforced concrete structures is mainly influenced by the exposure conditions and it takes place in a number of chemical, electro-chemical and physical processes. These processes change the performance of the structure over time, with respect to user comfort, functionality, aesthetics etc.

In the study presented in this thesis only the initiation of reinforcement corrosion due to chloride ingress has been treated. More information about the other deterioration processes can for example be found in DuraCrete (1998).

Usually the influence of the exposure environment is handled by rough divisions into environmental classes, with only little scientific background, or by using experiences from concrete specimens that have been exposed in environments similar to the one where the structure in question is built or going to be built. This means that the basis for predicting the service life, and thus planning for future maintenance, will be poor.

### 1.2 Background to research project

The research project presented in this thesis was initiated to improve the knowledge of how the exposure conditions influence reinforced concrete structures. The project was initiated on the basis of some of the findings from the DuraCrete project. In the DuraCrete project a design concept for the complete service life of reinforced concrete structures was developed. With the DuraCrete approach the service life is designed with a performance based design methodology, where the service life is related to a required performance, described by a number of limit state functions, the required performance being defined by limit states. The limit state functions are based on (sufficiently) realistic mathematical models where the behaviour of the concrete is (explicitly) modelled. The models include a description of the deterioration of the concrete structures and the structural consequences for the structure, including effects from the exposure environment, concrete properties and load effects.

One of the tasks in the DuraCrete project was to statistically quantify the parameters in the DuraCrete chloride ingress model, DuraCrete (2000a). The quantification was made with data, mainly found in the literature, which were put in a database to get a workable format. Most of the data were in the form of apparent chloride diffusion coefficients and surface chloride contents, analysed from measured chloride ingress profiles. Some of the parameters were analysed from chloride ingress profiles while others were found directly in the literature. No difference was made between these two types of data before they were put in the database.

As part of the statistical quantification the influence of the exposure environment on the chloride ingress was quantified. To achieve sufficiently large amounts of data the data available in the database were classified in appropriate classes. The division of the classes was based on the characteristics of the concrete and exposure, e.g. type of binder (OPC, PFA, GGBS and SF concrete<sup>1</sup>), exposure environment (e.g. marine submerged and tidal zones), curing conditions (curing time) etc. The data were not divided into classes depending on the quality of the data. Examples of data of high quality are when extensive background information regarding the data is known, e.g. detailed information about the

---

<sup>1</sup> OPC – Ordinary Portland Cement, PFA – Pulverized Fly Ash, GGBS – Ground Granulated Blast Furnace Slag and SF – Silica Fume.

concrete composition, exposure conditions and times etc. Examples of data of low quality are when little information regarding the data is known, e.g. about the concrete composition, and if only evaluated parameters are known.

The quantification resulted in large uncertainties, cf. Lindvall & Nilsson (2001a). Further analysis of the cause of the uncertainties showed that one of the major parameters that was found to have an influence was the name of the author of the reference where the data were found. There are many possible reasons for this, e.g. that different authors have used different types of concrete, with various types of cements, aggregates and/or additives, analysis methods or insufficient descriptions of the exposure conditions. Since the quantification was made on parameters analysed from measured chloride ingress profiles, the result is not only influenced by variations between exposure environments but also by concrete properties, resulting from concrete composition and workmanship during construction, and analysis methods. One of the conclusions drawn from the results of the quantification of the environmental parameters in the DuraCrete chloride ingress model was that the influence of exposure conditions on chloride ingress must be better described to enable more accurate quantifications to be made.

### 1.3 Object

The object of this study has been to describe and further explain the influence of the exposure conditions for reinforced concrete structures and the consequences on their expected service life. The focus has been to investigate and quantify the exposure conditions for structures in marine and road conditions exposed to chloride ions originating from seawater and de-icing salt. This has been done by literature and field studies, where data on the behaviour of concrete in different environments have been gathered and analysed. The emphasis has been put on the exposure conditions for reinforced concrete structures exposed in marine (mainly submerged) conditions and road conditions, where the important factors that influence chloride ingress have been identified. Preferably only the environmental actions outside the structures should be taken into account. However, since it is hard to only quantify these actions the response of the concrete, mainly in terms of chloride ingress profiles, has been used as a measure of exposure conditions.

Based on the data collected from literature and field studies, models that describe the exposure conditions of reinforced concrete structures subjected to chlorides have been derived. The models have been developed in such way that it is possible to use them as boundary conditions in models for predictions of chloride ingress into concrete.

### 1.4 Limitations

The study presented in this thesis has been limited to an examination of how the exposure conditions influence chloride ingress into concrete exposed in marine and road conditions. Any effects, which may arise due to material properties, e.g. concrete composition, and workmanship during construction, e.g. compaction, **have not been investigated**. Furthermore only sound concrete has been considered, which means that any effects due to cracks and other defects on the chloride ingress are not taken into account.

The exposure conditions include effects from carbonation, chloride, moisture and temperature conditions, both outside and inside the concrete. In this study mainly the effects from chloride and temperature conditions have been investigated. Carbonation is usually not a problem for correctly designed and constructed reinforced concrete

structures in marine and road conditions, at least not in the Nordic countries, and is therefore not included. The effects of the moisture conditions have only been briefly treated. However, the moisture conditions have been shown to have a significant influence on the chloride ingress in concrete, where transport of chlorides requires a RH above 60%-75%, Saetta et al (1993) and Nilsson et al (1997). However, due to financial and time limitations it was decided not to include the moisture conditions in the study. Instead results from other studies on the influence of moisture conditions have been used, e.g. Saetta et al (1993), Climent et al (2000) and Nielsen and Geiker (2003).

### 1.5 Disposition of the thesis

The thesis has the following disposition:

#### **Chapter 1. Introduction**

In this chapter an introduction is given to the research area and the background to the study presented in this thesis is given. A short description of how reinforced concrete structures deteriorate is given and the object and limitations of the study are stated.

#### **Chapter 2. Modelling of service life – theory**

This chapter describes how the service life of reinforced concrete structures can be predicted, with the focus on modelling of initiation of chloride induced reinforcement corrosion. The propagation period, i.e. when the reinforcement is actively corroding, is only briefly described.

A literature review of different mathematical models to predict the initiation of reinforcement corrosion has been made. The models are briefly described. One of these models, the DuraCrete chloride ingress model, has been chosen as an “example model” to show how the exposure conditions influence the service life predictions, and is therefore described in greater detail.

#### **Chapter 3. Environmental actions and response**

In this chapter the environmental actions on and response of reinforced concrete structures are described. Qualitative models are presented, where the environmental actions are divided into different geographical levels, with different degrees of resolution in space and time. The surface conditions are used as boundary conditions for the description of the deterioration of the concrete.

First a general description of the environmental actions and response is given, where it is shown how the surface conditions can be derived. The response of the concrete, resulting from the surface conditions, is also described and exemplified. Secondly more detailed descriptions of the environmental actions and response for concrete structures exposed in marine and road conditions are given.

#### **Chapter 4. Field study – marine conditions**

This chapter describes a field study where the chloride ingress into concrete specimens exposed at twelve different locations has been studied. Concrete specimens made from a similar concrete composition have been exposed in mostly marine submerged conditions, to get well-defined exposure conditions. Furthermore concrete specimens, similar to ones used in the field exposure, have been exposed in the laboratory in solutions with different chloride concentrations and temperatures. The chloride ingress has been studied through sawn surfaces, to exclude any effects from moulds. In this way it is possible to evaluate



the influence on chloride ingress due to the exposure environment alone. Additionally chloride binding isotherms have been determined for the exposed concrete composition.

In this thesis a general description of the field study is given and the most important results are presented and discussed. A more comprehensive presentation of the field study is given in Lindvall (2003).

### **Chapter 5. Field study – road conditions**

In this chapter field studies made in road conditions are described. The studies include a survey of the chloride ingress and moisture conditions in seven reinforced concrete bridges around Göteborg, a complementary study of the chloride load around two of earlier examined bridges and a study of chloride ingress into three different concretes exposed along the Rv40 field station.

In this thesis general descriptions of the field studies are given and the most important results are presented and discussed. More comprehensive presentations of the studies are given in Lindvall & Andersen (2000), Lindvall (2002) and Lindvall (2003).

### **Chapter 6. Models for exposure conditions**

Quantitative models for exposure conditions for concrete structures exposed in marine and road conditions are described in this chapter. The models are based on the qualitative models described in Chapter 3 together with the results from the literature study in Chapter 3 and the field studies presented in Chapters 4 and 5.

With the models the surface conditions, i.e. the boundary conditions of chloride ingress into concrete exposed in marine and road conditions, can be determined.

### **Chapter 7. Environmental actions in models of service life**

This chapter describes and exemplifies what consequences the models for exposure conditions, described in Chapter 6, have on service life predictions. Predictions of the service life for a number of reinforced concrete structures, exposed in different exposure environments, are made to demonstrate the influence of environmental actions on the service life. The predictions have been made with both deterministic and probabilistic methods.

### **Chapter 8. Conclusions**

This chapter contains conclusions drawn from the results presented in the thesis. A division has been made into general conclusions and more specific conclusions regarding marine and road conditions.

### **Chapter 9. Future research**

In this chapter suggestions are given for future research. The suggestions are based on the earlier presented results and discussion and conclusions.



## 2     Modelling of service life – theory

### 2.1     Introduction

The service life of a structure can be defined as the period of time during which the performance of the structure is fulfilled. Here the performance of a structure is referred to as its ability to satisfy demands and requirements set by the owner, authorities and users. Depending on the type of structure different definitions of the service life are used. In DuraCrete (1997) three different types of service life are defined:

- **Technical service life.** The technical service life is the time in service until a defined unacceptable state of deterioration is reached.
- **Functional service life.** The functional service life is the time in service until the functional performance of the structure becomes obsolete, due to changed requirements from e.g. authorities or the owner.
- **Economic service life.** The economic service life is the time in service until it is more economical to replace the structure than to keep it.

The service life of a structure can be described as a combination of the service lives for the different components of the structure. The component with the shortest service life determines the service life for the structure. With this approach it is possible to obtain information on which component determines the service life of the structure.

### 2.2     Service life of reinforced concrete structures

#### 2.2.1     General

Reinforced concrete structures are usually expected to have a long service life since they often require large investments. This means that it is essential to have an understanding of the interrelations between design, materials, environmental actions, and deterioration and future maintenance.

Traditionally the durability of structures has been estimated by deem-to-satisfy rules, based on rules of thumb derived from experiences from earlier built structures. Examples of rules of thumb are specifications of a certain w/c ratio and/or concrete cover depending on exposure conditions. With the deem-to-satisfy rules the structures will achieve a **sufficiently long** but **not specified** service life.

Recently a performance based design methodology has been developed to predict the service life of concrete structures, cf. DuraCrete (2000b). With the performance based methodology the service life is expressed in terms of performance requirements, e.g. loadbearing capacity or aesthetic appearance. In this way structures can be designed to have a **sufficiently long** and **specified** service life, during which the structure can meet performance requirements with an acceptable level of safety and cost. However, the

performance based design methodology requires mathematical models that predict how the deterioration of concrete takes place in time. For concrete structures subjected to reinforcement corrosion this simple but useful model is proposed by Tuutti (1982), see figure 2.1.

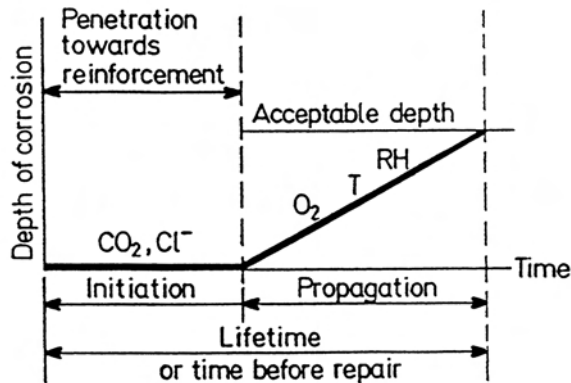


Figure 2.1: Model for reinforcement corrosion, with a division into initiation and propagation periods. Tuutti (1982).

The service life is to large extent dependent on the deterioration of the concrete. The deterioration of reinforced concrete structures is a time dependent process, which takes place as a number of chemical, electro-chemical and physical processes. A common way to model the service life of a reinforced concrete structure is to divide it into different periods. The most common way is to divide into two periods, defined as “initiation” and “propagation” periods, cf. figure 2.1.

During the initiation period changes take place in reinforced concrete, in interaction with the surrounding exposure environment, until a certain limit is reached and damage starts to propagate. These changes initiate deterioration of the concrete and/or the reinforcement, and this takes place in number chemical, electro-chemical and physical processes. In the propagation period the damage propagates until a certain degree of damage is reached. When this degree of damage is reached the service life of the structure is ended or the structure needs to be repaired.

During the initiation period the concrete is carbonating and/or subjected to an ingress of chloride ions. When the carbonation front reaches the reinforcement or the chloride content in the concrete at the reinforcement exceeds the threshold level, reinforcement corrosion is initiated and starts to propagate. There are two principal strategies to deal with service life predictions for concrete structures subjected to reinforcement corrosion:

- **Only initiation period.** In this, conservative, strategy only the initiation period is considered, which means that when reinforcement corrosion is initiated the service life of the structure is ended. This strategy is used when the propagation period is considered to be very short or when the designer does not accept any reinforcement corrosion. The damage that may have occurred usually requires not very extensive repair work, which means that expenditure is probably fairly low.
- **Initiation and propagation periods.** In this strategy both the initiation and propagation periods are considered. The service life is ended when the corrosion has reached a certain level defined by the designer, e.g. a certain loss of cross-sectional area or a certain corrosion – rate, is reached. The damage that may have occurred

usually requires extensive repair work, e.g. removal of the damaged concrete and reinforcement, which may give rise to large expenditure. Furthermore, it is difficult to detect in a reliable way when the reinforcement is corroding and to measure the corrosion rate (general corrosion/pitting corrosion).

In this report **only the initiation period** has been treated.

### 2.2.2 Reinforcement corrosion

The deterioration of reinforced concrete takes place in a number of chemical, electro-chemical and physical processes. The most common in Sweden are reinforcement corrosion, frost attack and chemical attack. In the following section a short description of each of chloride induced reinforcement corrosion is given.

In non-deteriorated concrete the reinforcement is in a passive state regarding corrosion due to the high alkalinity of the pore solution. The reinforcement bars are, in the passive state, protected by a passive layer mainly consisting of insoluble iron oxides ( $\text{Fe}_2\text{O}_3$ ) but also soluble iron oxides (e.g.  $\text{Fe}_3\text{O}_4$ ) and cement hydrates, Sandberg (1998). This passive layer can be deteriorated either by reducing the high alkalinity of the pore solution, e.g. by carbonation, or chloride ingress, where the chloride ions act as a “catalyst” in the degradation of the passive layer. The catalyst effect is intensified when an excess of oxygen is available at the reinforcement, since the chloride attack is then accompanied by an aggressive local acid attack, Sandberg (1998).

Carbonation in concrete is caused by atmospheric carbon dioxide that penetrates into the concrete and reacts with calcium hydroxide in the concrete to form calcium carbonate, which lowers the pH in the pore system (from above 12.5 to 9.0 or below), Möller (1994). The carbonation advances as a front into the concrete and when the front has reached the reinforcement corrosion will be initiated. The rate of transport of carbon dioxide in concrete is mainly dependent of the following three parameters, Neville (1995): (i) Diffusivity of  $\text{CO}_2$  in the concrete, (ii) Environmental conditions (concentration of  $\text{CO}_2$  in the surrounding air) and (iii) Binding capacity of  $\text{CO}_2$  in the concrete.

When chloride ions penetrate into the concrete and when they exceed a certain concentration at the reinforcement, the chloride threshold level,  $C_{\text{crit}}$ , reinforcement corrosion is initiated. The transport of chlorides in concrete takes place in three principal ways, Basheer et al (2001): (i) Permeation of salt solution, (ii) Capillary absorption and (iii) Diffusion of free chloride ions. All three transport processes act simultaneously in the concrete and they have the common property that they require a certain amount of moisture in the pore system of the concrete. This is shown in figure 2.2, where the relation between moisture conditions and the transport of chlorides in concrete is illustrated. The dominating transport mechanisms are diffusion and convection, when the capillary pores are relatively saturated, and absorption, when the capillary pores are relatively dry. The transport rate of chlorides into concrete depends on the following parameters, Neville (1995): (i) The chloride concentration in the surrounding environment, i.e. the driving potential of chlorides, (ii) The chloride transport properties in the concrete and (iii) The chloride binding capacity in the concrete. The driving potential of chlorides is mainly influenced by the exposure environment, while the transport and chloride binding properties are influenced by both the exposure environment and the concrete properties.

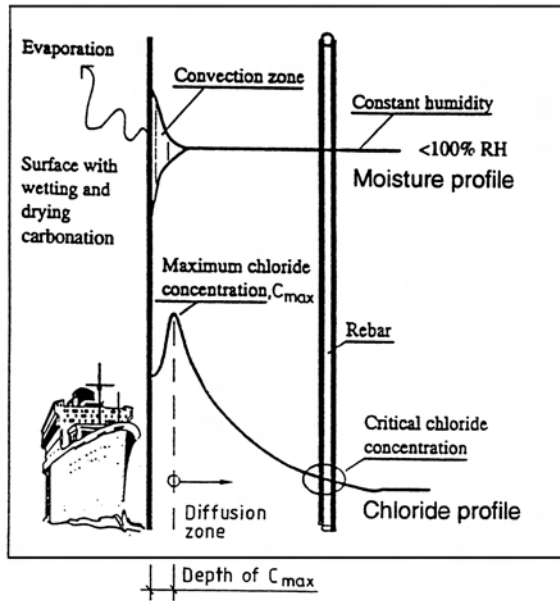


Figure 2.2: Schematic illustration of the moisture and chloride conditions in a high quality concrete. Sandberg (1998).

The initiation of reinforcement corrosion also depends on the chloride threshold level, which is the chloride concentration at which reinforcement is initiated. The magnitude of the threshold level depends on the concrete properties and the exposure conditions. The main influencing factor, however, is the moisture conditions, see figure 2.3. The moisture conditions govern the amounts of the electrolyte and oxygen, which are requirements for reinforcement corrosion.

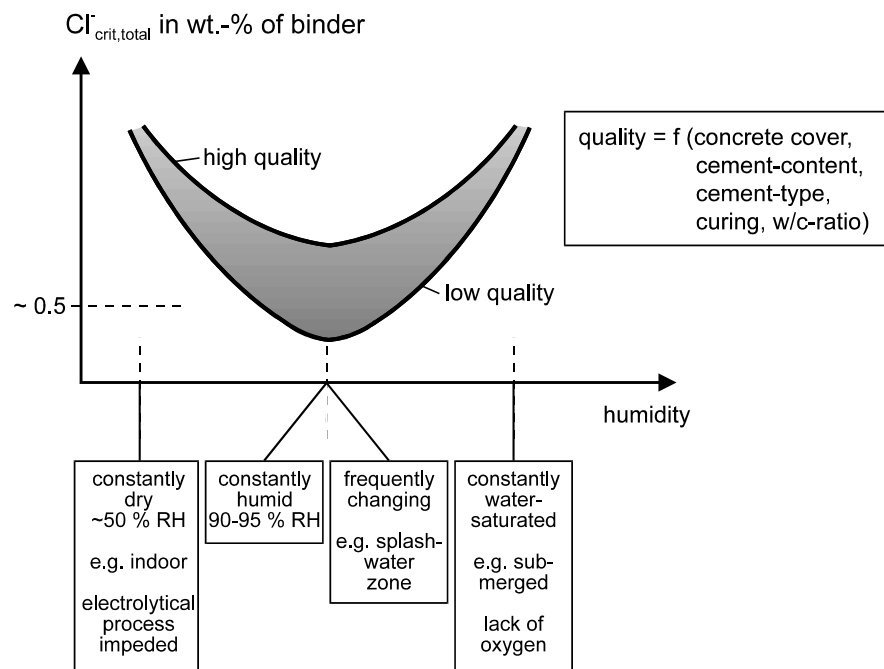


Figure 2.3: Illustration of the relationship between the chloride threshold level and the moisture conditions in the concrete. CEB (1989).

Once reinforcement corrosion has been initiated and the reinforcement is actively corroding, the formation of porous corrosion products is accelerated. Three requirements have to be fulfilled before rust may occur, Broomfield (1997): (i) Availability of oxygen at the cathode, but not at the anode for the initial reaction, (ii) Availability of oxygen at the anode to form ferric oxide and (iii) Availability of water to dissolve ferrous ions and form rust. The extent of formation of porous corrosion products is dependent on the availability of oxygen at the cathode, Sandberg (1998). If enough oxygen is available, solid expansive corrosion products, red-rust, are formed, which may cause the concrete cover to crack and finally spall. If only little oxygen is available, like in submerged conditions, corrosion products that are non-expansive or only slightly expansive are formed, e.g. solid black rust.

A division can be made into uniform corrosion and pitting corrosion, where the latter is usually initiated by chloride ingress. In uniform corrosion the surfaces of the rebars are corroding uniformly, with approximately the same size on the anode and cathode. In pitting corrosion the corrosion takes place in a pit, with a large cathode and a small anode, resulting in a rapid reduction of the cross-section of the rebar. Furthermore pitting corrosion may not give any signs of an ongoing corrosion process, since the corrosion is concentrated to a small area and the corrosion products are soluble in the corrosion pit. In figure 2.4 an illustration of the corrosion in reinforced concrete is shown.

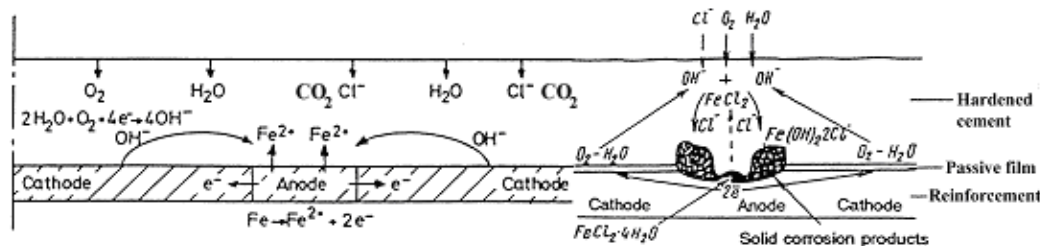


Figure 2.4: Illustration of pitting corrosion in concrete. After Sandberg (1995).

### 2.2.3 Factors influencing deterioration of concrete

The deterioration of concrete can be described as interactions of what takes place at both the surface and inside the concrete. The interactions are governed by the transport properties of the concrete, the chemical composition of the cement paste and aggregates and the exposure conditions. Depending on the type of deterioration these interactions look different. Three main factors can be identified:

- **Material properties.** The material properties can be described as a combination of the properties of the constituent materials in the concrete, i.e. properties of the binders (e.g. chemical composition and fineness of grinding), aggregates (e.g. chemical composition, shape and particle size distribution), mixing water (e.g. chemical composition) and additives (e.g. chemical composition).
- **Workmanship during construction.** The workmanship during construction includes factors related to the construction of the structure, e.g. the compaction of the concrete, the concrete covers, the curing conditions (e.g. moist curing or curing in mould) and the type of formwork (e.g. board or steel).
- **Exposure conditions.** The exposure conditions include moisture and temperature conditions and the exposure to carbon dioxide and chlorides. To get an accurate description of the environmental actions the surface conditions are derived, where the surface properties and the response from the concrete are included.

The material properties and the exposure environment are not constant but vary in time. Thus, to predict how these parameters influence the durability of concrete structures it is necessary to have knowledge of how they change over time. Until now large research efforts have been made to clarify what influences the material properties and to some extent the workmanship during construction have on the performance of reinforced concrete structures. However, there is little reliable information available about the influences of the exposure conditions. This is why the emphasis in this report has been put on the influence of environmental actions on the service life of reinforced concrete structures.

## 2.3 Mathematical models for prediction of chloride ingress into concrete

### 2.3.1 General

There are several models available for the prediction of chloride ingress into concrete. Among the models a division can be made into, Nilsson et al (1997):

- **Empirical models.** The empirical models are based on observations of response, measured on concrete exposed either in laboratory or field conditions. The observations are used to derive the models and quantify the parameters in the models, e.g. by curve fitting of measured chloride ingress profiles. The models are often quite simple and since observations are used to quantify them, the models do not need any extensive validation before they can be used for predictions. Since the models often are quite simple they can be solved without computers. However, due to the simplicity of the models the results may have large uncertainties.
- **Scientific models.** Scientific (or physical) models are based on theories on how transport (separate or combined) and binding of different substances takes place in materials. Together with information about initial and boundary conditions it is possible to make accurate predictions of how different substances are transported into materials. The models are often complex and since they are not directly derived from measurements extensive validations against measured data are necessary before they can be used for practical predictions. Due to the complexity of the models they usually require computers to be solved.

### 2.3.2 Empirical models

It is a common property of empirical models that they predict the chloride ingress from analytical or numerical solutions to Fick's 2<sup>nd</sup> law of diffusion. Fick's 2<sup>nd</sup> law models the chloride ingress with two parameters, an apparent diffusion coefficient,  $D_a$ , and an apparent surface chloride content,  $C_{sa}$ , determined from curve fitting to measured chloride ingress profiles. Usually chloride binding is not separately taken into consideration in the models, i.e. no difference is made between bound and free chlorides in the concrete.

The empirical models can in principle be solved in three different ways, Nilsson (2001):

- The classical  $\text{erfc}^2$  methods, with constant or time-dependant diffusion coefficient,  $D_a$ , and/or surface chloride content,  $C_s$ .
- Analytical solutions to Fick's 2<sup>nd</sup> law with time-dependant  $D_a(t)$  and  $C_s(t)$ .
- Numerical solutions to Fick's 2<sup>nd</sup> law with time-dependant  $D_a(t)$  and  $C_s(t)$  and with chloride binding separately taken into consideration.

---

<sup>2</sup> The complement to the error-function, erf.



Examples of empirical models for determination of chloride ingress into uncracked concrete are:

- **The Selmer chloride ingress model**, presented in Maage et al (1995). This chloride ingress model is based on the error function solution of Fick's 2<sup>nd</sup> law with a time-dependent diffusion coefficient, constant surface chloride content and initial chloride content in the concrete. The principle of the model is to measure potential material properties in the laboratory, correct them to field conditions, with a number of parameters, and make predictions of the chloride ingress in field conditions. The other parameters in the model have been quantified by curve fitting to measured chloride ingress profiles.
- **Mejlbro-Poulsen chloride ingress model**, presented in Mejlbro (1996) and Poulsen (1996). This chloride ingress model is based on an analytical solution of Fick's 2<sup>nd</sup> law with a time-dependent diffusion coefficient and surface chloride content together with initial chloride content in the concrete. The parameters in the model have been quantified by curve fitting to measured chloride ingress profiles.
- **DuraCrete chloride ingress model**, final appearance presented in DuraCrete (2000a). This model is based on the error function solution of Fick's 2<sup>nd</sup> law with a time-dependent diffusion coefficient and a constant surface chloride content. The model has been further developed by Gehlen (2000), where the initial chloride content in the concrete and a possible convection zone are also taken into account. This model has been chosen as an "example model" in chapter 7 to illustrate the consequences of the developed models for environmental actions in predictions of service life.  
The DuraCrete chloride ingress model was originally developed for probabilistic predictions of the chloride ingress. With probabilistic predictions the reliability of a structure can be assessed. The probabilistic predictions require that the parameters in the model are statistically quantified, in terms of mean values, statistical uncertainties and distribution functions.
- **Life-365**, presented in Bentz & Thomas (2001). This chloride ingress model is based on a numerical solution of Fick's 2<sup>nd</sup> law with a time-dependent diffusion coefficient and surface chloride content together with initial chloride content in the concrete. The model also includes the effect of surface treatments on chloride ingress and economic aspects regarding life cycle costs etc. The parameters in the model have been quantified by curve fitting to measured chloride ingress profiles.

### **DuraCrete chloride ingress model**

The background of the DuraCrete chloride ingress model is presented in DuraCrete (1998) and the final appearance of the model is presented in DuraCrete (2000a). The origin of the model is presented in Maage et al (1995 & 1999). To solve the model it is necessary to have knowledge of initial and boundary conditions, which are found by studies, both in laboratory and field conditions. The initial and boundary conditions include information of how the material, workmanship during construction and the exposure environment influence the chloride ingress. The principle of the model is to measure potential material properties in the laboratory, correct them to field conditions, with a number of factors, and make predictions of the chloride ingress in field conditions.

The principal appearance of the model is given in eq. (2.1a).

$$C_x = C_{SN} \cdot \left[ \operatorname{erfc} \left( \frac{x}{2 \cdot \sqrt{D_a(t) \cdot t}} \right) \right] \quad [\% \text{ by weight Cl/binder}] \quad (2.1a)$$

where:

- $C_x$ : the chloride content at a certain penetration depth (environmental and material parameter). [weight-% per binder]
- $C_{SN}$ : the apparent surface chloride content (environmental and material parameter). [weight-% per binder]
- $x$ : the depth at which the chloride content is determined. [m]
- $t$ : the exposure time. [s]
- $D_a(t)$ : the apparent diffusion coefficient for chlorides, see eq. (2.1b). This parameter can be evaluated by curve fitting the error function solution of Fick's 2<sup>nd</sup> law to measured chloride ingress profiles. [m<sup>2</sup>/s]

$$D_a(t) = D_a(t_0) \cdot \left( \frac{t_0}{t} \right)^n = k_c \cdot k_e \cdot k_t \cdot D_0 \cdot \left( \frac{t_0}{t} \right)^n \quad [\text{m}^2/\text{s}] \quad (2.1b)$$

where:

- $k_c$ : constant parameter that accounts for the influence of workmanship (material parameter). [-]
- $k_e$ : constant parameter that accounts for the influence of environment (environmental parameter). [-]
- $k_t$ : constant parameter that accounts for the influence of test method (test-method parameter). [-]
- $D_0$ : potential chloride diffusion coefficient, determined at standardized conditions, with a standardized method, e.g. NT Build 492 (1999) (material parameter). [m<sup>2</sup>/s]
- $t_0$ : reference time, i.e. the time after casting at which  $D_0$  is measured. [s]
- $n$ : age factor (material and environmental parameter). [-]

The advantage of the model is that it is possible to directly measure in the laboratory a material property that describes the chloride transport properties, i.e.  $D_0$ , and then make predictions of the chloride ingress. The model is to a large extent derived from observations of chloride ingress in real structures, which reduces the need for validation. However, values derived from chloride ingress profiles should be used with some caution, especially if not all background information concerning the profiles is known, e.g. exposure environments, sampling spots and analysis methods. A further advantage is that the DuraCrete model considers the decreasing diffusivity of the concrete with increasing age. However, to evaluate this effect it is necessary to have chloride ingress profiles for the same concrete composition exposed in the same environment from at least three different ages. The major drawback of the model is that calculations can end up with doubtful results, e.g. too large chloride penetration depths, if no quality check is made on the data used to quantify the parameters in the model. This is especially the case if data found in literature, from different reference sources, are used in the quantification of the parameters. Examples of quantifications of the parameters in the model and predictions of chloride penetration depths can be found in DuraCrete (2000a).

As mentioned earlier the DuraCrete chloride ingress model was originally developed for probabilistic predictions. These predictions are based on the performance of the structure,

defined by limit states, which define the boundaries between desired and undesired or adverse states. In modern building codes two types of limit states are used, viz. ultimate limit states (**ULS**), which refer to the structural safety of structures, and serviceability limit states (**SLS**), which refer to the comfort and functionality of structures. The limit state function, to model the risk of initiation of chloride induced reinforcement corrosion, has the following appearance, see eq. (2.2).

$$p_f = p \left\{ C_{crit} - C_{SN} \cdot \left[ \operatorname{erfc} \frac{d_c / 1000}{2 \cdot \sqrt{D_a(t) \cdot t}} \right] < 0 \right\} < p_{target} \quad [-] \quad (2.2)$$

where:

- $p_f$ : failure probability. [-]
- $p$ : probability that a certain event occurs. [-]
- $p_{target}$ : target probability. [-]
- $d_c$ : concrete cover. [mm]
- $D_a(t)$  apparent diffusion coefficient determined from eq. (2.1b).

### 2.3.3 Scientific models

In this section a number of scientific (or physical) models which are used to predict the chloride ingress into concrete will be briefly described. It is common to all the models that they predict the chloride ingress based on separate chemical and physical expressions describing the transport of ions (chloride and other ions), and in some cases also the heat and moisture transport, combined with chloride binding. The scientific models are solved by considering the mass balance and flux equations, chloride binding relationship and the influence of characteristics of the exposure conditions and material. The scientific models are based on two different chloride transport models, Nilsson (2001):

- Fick's 1<sup>st</sup> law.
- Nernst-Planck equation.

Examples of physical models for determination of chloride ingress into uncracked concrete are given below. The purpose of the list is just to give the reader brief information on some scientific models available to predict the chloride ingress into concrete. More detailed reviews are given in for example Truc (2000) and Meijers (2003).

- **ClinConc**, first presented in **Tang (1996)**. The ClinConc model predicts the flux of chloride ions into saturated concrete with Fick's 1<sup>st</sup> law and the concentration profiles are calculated by solving mass balance equation for chloride. The chloride binding is described with a Freundlich isotherm, where effects from pH and temperature are included. The transport properties of the concrete are evaluated with a specially developed test, described in NT Build 492 (1999). The chloride ingress is determined with a finite difference method.
- A model by **Samson et al (1999a-c)** predicts the flux of different ions into saturated cement-based materials. In the model the flux is determined by using an extended Nernst-Planck equation, where the electrical coupling between different ions is described with a Poisson equation. A homogenization technique is used to describe the ion diffusion in cement-based materials. In the version described by Samson et al (1999a-c) the chloride binding is not taken into account. The ion diffusion is finally numerically predicted by using a finite element method.

- **MsDiff**, presented in **Truc (2000)**. The MsDiff model predicts the simultaneous flux of several different ions (chlorides, sodium, potassium and hydroxide, which are the major components in pore solution in concrete) into saturated concrete. The flux is modelled with the Nernst-Planck relation, and the chloride binding (described with a Langmuir isotherm) and electroneutrality are taken into account. The transport properties of the concrete are determined with a specially developed test, called the LMDC test method, described in Truc (2000). The resulting ion diffusion is determined by using a finite difference method
- **HETEK Convection model**, first presented in Nilsson et al (1997). An improved version of the model is presented in Nilsson (2000). The model predicts the chloride ingress in non-saturated concrete, where the ingress is described as diffusion and convection of chlorides, following liquid moisture flow in the concrete,. The influence of the water content of concrete, and its variations over time, is taken into account. The model also considers the interaction between chloride and moisture content in the concrete, cf. Hedenblad (1988). Furthermore chloride binding is included in the model and described by a non-linear binding isotherm for non-saturated concrete. The resulting chloride ingress is determined with a forward finite difference method.
- A model for heat, moisture and chloride ion transport in concrete, presented in **Meijers (2003)**. The model predicts the chloride ingress into non-saturated concrete, by three coupled balance equations for heat flow, moisture migration and chloride transport. The chloride transport is modelled both as diffusion (free chloride concentration gradient as driving potential) and convection (water pressure gradient as driving potential). The chloride binding is modelled both with linear and Langmuir isotherms. The chloride ingress, within each time-step, is determined with a finite element method and the time-steps are made with a finite difference method.

### 3 Environmental actions and response

In this section a description is given of the environmental actions on reinforced concrete structures and their response. The focus of the description has been on the conditions for concrete structures subjected to chloride ions and thus subjected to chloride induced reinforcement corrosion.

#### 3.1 Introduction

The environmental actions acting on a structure are mostly determined by processes taking place in the atmosphere. When the processes in the atmosphere are studied scientifically the following division is usually made, Högberg (1998):

- **Meteorology.** Meteorology is the science of physics of the atmosphere, where atmospheric processes are analysed, explained and predicted. There are a number of meteorological elements, viz. air temperature, air moisture, air pressure and air flow (wind), which originate from solar radiation. The current state of air temperature and moisture, precipitation and wind in the nearest atmosphere is called the weather, which can be characterized by movements of air masses, where the boundary between two air masses is called a front.
- **Climatology.** Climatology is the science of how the climate varies between different areas and on different time scales. The climate can be characterized by studying energy and water balances between the atmosphere and the surface of the earth, which means there is a relationship between source (energy flow) and effect (e.g. air temperature change). The climate for a certain location can be described as the weather history for that location and gives a picture of what can be considered normal and the probability of a certain type of weather.

When the climate is described it is convenient to divide it into levels where the climate has different horizontal dimensions and/or time scales. Other possibilities are to divide the climate into the following levels, Högberg (1998): radiation balance; soil-water balance (Thornwaite's model); temperature; precipitation; air and front systems; combination of several climate parameters (e.g. Köppens classification based on temperature and humidity), the influence from the sea etc. However, in this report it has been decided to divide the climate into four different levels based on geographical scale, modified from Oke (1987):

- **Global climate – Macro conditions.** Climate for a larger area. The global climate is influenced by for example geographical latitude/altitude and the distance to an ocean.
- **Regional climate – Meso conditions.** Climate for a certain region (undisturbed by the structure). The regional climate is influenced by for example the topography and distance to bodies of water (seas etc).

- **Local climate.** Climate for a certain part of a region (disturbed by the structure). The local climate is influenced by for example the surrounding terrain, vegetation and the general shape of the structure.
- **Surface climate – Micro conditions.** Climate for a certain part of a structure. The surface climate is influenced by the properties of the structure in greater detail, e.g. the material properties and the response of the material.

More extensive descriptions of the environmental conditions are given in for example Högberg (1998), DuraCrete (1999) or Lindvall (2001).

## 3.2 Environmental actions

### 3.2.1 Qualitative model

The general approach when describing and modelling the environmental actions on a structure is to separate the actions from the response of the structure. With this approach the environmental actions can be described without being dependent on the properties of the structure. When the deterioration of a certain concrete structure is studied the most accurate description of the exposure conditions is given by the surface conditions. In figure 3.1 a qualitative model of the way the surface conditions can be determined is presented. The model is based on the division into four different levels, but the macro conditions have been excluded for simplicity.

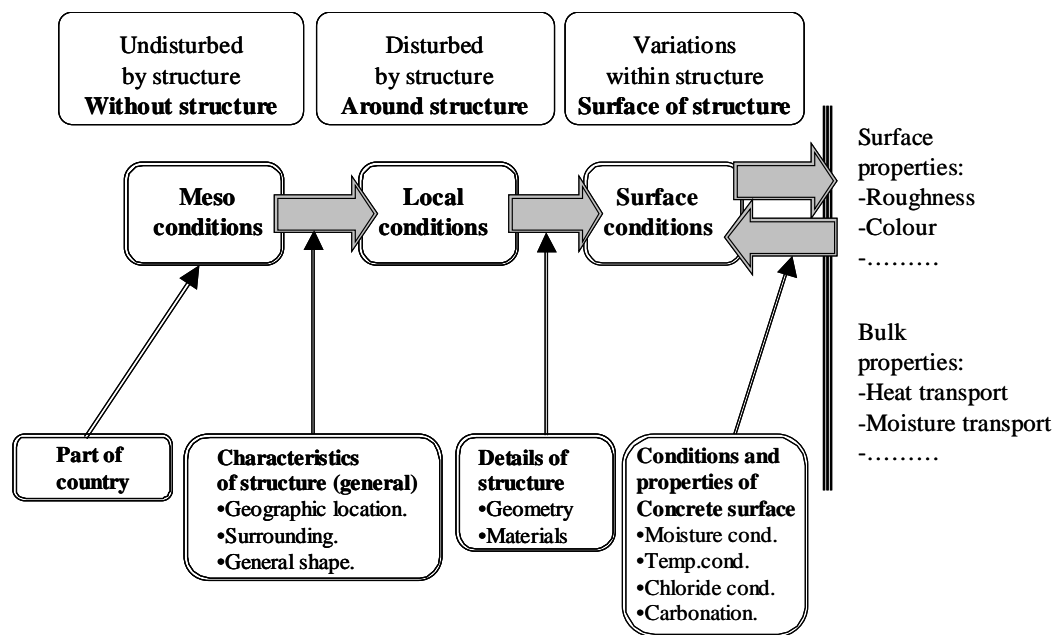


Figure 3.1: Division of the exposure conditions into different geographical scales.

The starting point for the model is knowledge of the exposure conditions (undisturbed by the structure) for the region where the structure is (to be) constructed, i.e. the meso conditions. Data from a nearby meteorological station (e.g. air temperature and humidity, amount of precipitation and wind directions and speeds) can be used to describe the meso conditions (undisturbed by the structure). The meso conditions are then transformed, with information about the location, the surroundings and the general shape of the structure, to achieve the local conditions (disturbed by the structure). Finally the local conditions are converted into surface conditions (variations within structure) with additional information about the structure, e.g. geometry and material properties, and the response of the

concrete, which influences the conditions and properties of the concrete. The conditions and properties of the concrete surface may influence the surface conditions, e.g. surface colour and absorptance, influencing the surface temperature, humidity, and moisture transport properties that influence the uptake of water and consequently the time of wetness (TOW). Furthermore the surface chloride and moisture content influence the leeching of chlorides that affects the chloride concentration at the surface of the concrete.

As seen in figure 3.1 it is not enough to know the environmental actions outside a concrete structure to predict the surface conditions. The surface conditions are also influenced by the response of the concrete, following from the surface and bulk properties.

### 3.2.2 Meso & local conditions

The meso conditions represent a region with fairly similar environmental conditions. They are influenced by the ground properties, e.g. type of terrain and topography, larger bodies of water, e.g. lakes or seas, and urban areas. Individual structures do not influence the meso conditions. Large bodies of water influence the meso conditions by reducing the variations in environmental actions, e.g. temperature conditions, but also by inducing special phenomena, e.g. sea and land breeze. There is also a difference in exposure conditions in urban areas compared with surrounding rural areas, caused by urban changes in the atmosphere and surface properties. Compared with surrounding rural areas the urban climate is usually rougher, warmer and drier. An urban heat island can be identified, where the air temperature in an urban area may be up to 12°C higher than in surrounding rural areas, Oke (1987).

For structures on land data from a nearby meteorological station can be used to represent the meso conditions. Similar data can be used for structures in marine environments with additional information about the chloride conditions. A suitable meteorological station is chosen in such way that the data measured at it are representative for the location for the (future) structure. However, it is not possible to completely find representative data, which means that the data have to be transferred to the location of the (future) structure. Methods for such transformations are presented in for example Kobysheva (1992).

The local conditions follow from the meso conditions, where the large scale geometry of the (future) structure is taken into account, together with surface properties of the ground and structure, shelter against precipitation etc. Influencing factors are radiation exchange between the ground, the structure and the sky, and air streams around the structure.

More comprehensive descriptions of the meso and local conditions are given in e.g. DuraCrete (1999) and Lindvall (2001).

### 3.2.3 Surface conditions

The most accurate way to describe the environmental actions on a structure is to describe them in terms of surface conditions. By doing so, variations in the environmental actions over the structure are considered and severely exposed spots can be identified. The surface conditions can be expressed with the following parameters:

- **Temperature conditions.** The temperature conditions can be expressed as an equivalent surface temperature. In the equivalent surface temperature effects from air temperature, radiation, evaporation, condensation and heat transfer together with geometry of the structure and material and surface properties are lumped together.

- **Moisture conditions.** The moisture conditions can be expressed as an equivalent surface humidity and surface wetness. The equivalent surface humidity can be determined with knowledge of the equivalent surface temperature and the air humidity. The surface wetness can be described with the time of wetness (TOW), which is the total time during which the surface is wet due to condensation, precipitation and running water.
- **Chloride conditions.** The chloride conditions can be expressed as an equivalent chloride surface content, where effects from the exposure environment are lumped together with effects from the geometry of the structure combined with material and surface properties.

In the following sections short descriptions of the temperature, moisture and chloride conditions are given.

### Surface temperature conditions

The surface temperature conditions, in terms of an equivalent surface temperature, can be derived with an energy budget for the surface and a network analysis, illustrated in figure 3.2 (the complete network is shown to the left and the reduced network to the right).

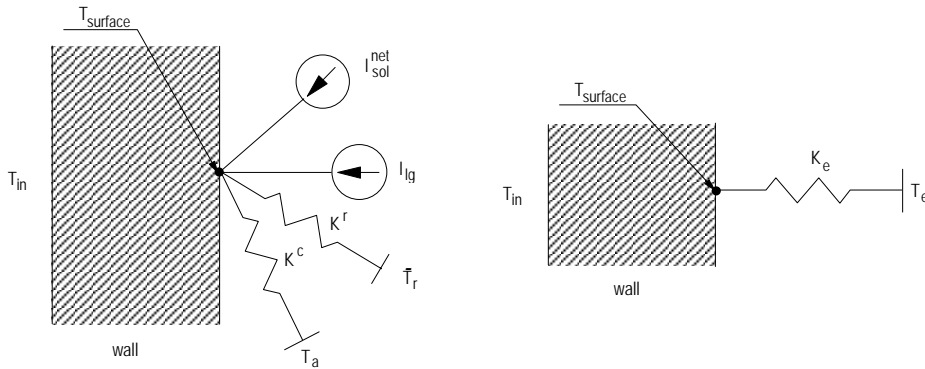


Figure 3.2: Left: The complete network for the heat exchange between a surface and its surroundings. Right: The reduced network with the equivalent temperature. Picture from Högberg (1996).

Based on the network analysis and network reduction rules, Hagentoft (2000), an expression for the equivalent surface temperature can be established, see eq. (3.1).

$$T_{s,eq} = T_{air} + \frac{1}{\alpha_r + \alpha_{cv}} \cdot (I_{solar} \cdot a + g \cdot h_e + \alpha_r \cdot (\bar{T}_r - T_{air})) \quad [K] \quad (3.1)$$

where:

- $T_{air}$ : air temperature. [K]
- $\alpha_r$ : radiative heat transfer coefficient. [ $W/m^2K$ ]
- $\alpha_{cv}$ : convective heat transfer coefficients. [ $W/m^2K$ ]
- $I_{solar}$ : solar radiation. [ $W/m^2$ ]
- $a$ : absorption factor for short wave radiation. [-]
- $g$ : flow rate of condensed water vapour. [ $kg/m^2s$ ]
- $h_e$ : latent heat of evaporation ( $h_e \approx 2500$  kJ/kg).
- $\bar{T}_r$ : “sky temperature”. [K]



The convective heat transfer coefficient,  $\alpha_{cv}$ , depends on the surface wind speed,  $u$ , according to eq. (3.2a). The radiative heat transfer coefficient,  $\alpha_r$ , depends on the surface and sky temperatures and the surface emissivity,  $\varepsilon$ . With the assumption that the surface temperature is equal to the air temperature  $\alpha_r$  can be determined with eq. (3.2b), Hagentoft (2000).

$$\begin{cases} \alpha_{cv} = 6 + 4 \cdot u & u \leq 5 \text{ m/s} \\ \alpha_{cv} = 7.41 \cdot u^{0.78} & u > 5 \text{ m/s} \end{cases} \quad [\text{W/m}^2\text{K}] \quad (3.2a)$$

$$\alpha_r \approx 4 \cdot \varepsilon \cdot \sigma \cdot \left( \frac{T_{sky} + T_{air}}{2} \right)^3 \quad [\text{W/m}^2\text{K}] \quad (3.2b)$$

where:

$\sigma$ : Stefan-Boltzmann constant ( $\sigma=5.6697 \cdot 10^{-8} [\text{W}/(\text{m}^2\text{K}^4)]$ )

If all influencing parameters in eq. (3.1), and their variations, are considered the determination of the equivalent surface temperature requires computer methods. Examples of computer methods to determine the equivalent surface temperature are given in Borlinger (1996) and Bentz (2000). In the model described in Bentz (2000) the consequences for the surface moisture conditions are also included.

In figure 3.3 an example is given of the differences between the air and the surface temperature. The measurements are made on a structure in Holzkirchen in the southern part of Germany. The figure is based on data representing five-day averages.

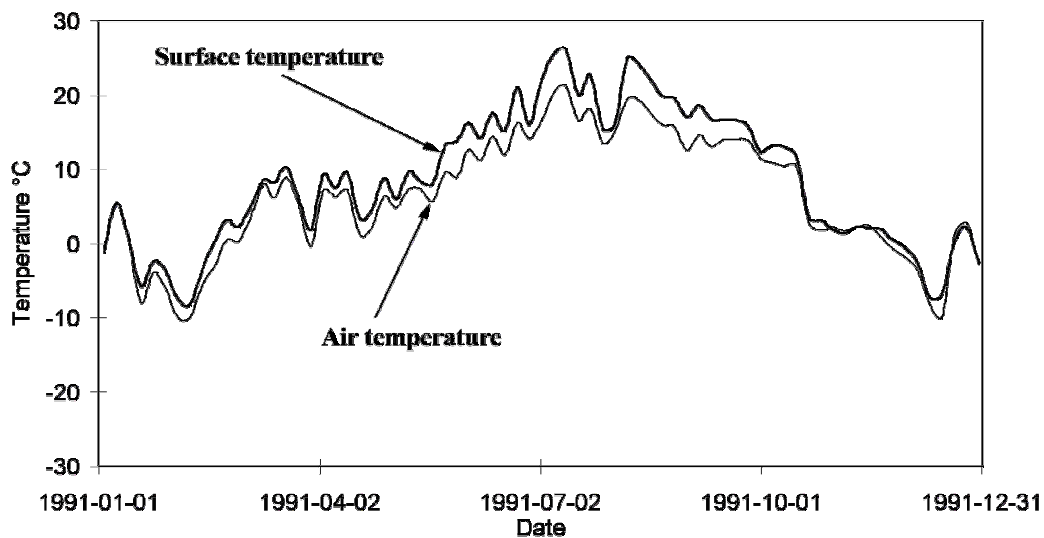


Figure 3.3: The air and surface temperature for a structure in Holzkirchen. CEB (1997). Based on data from IBP Holzkirchen (1995).

### Surface moisture conditions

The surface moisture conditions can be expressed in terms of an equivalent surface humidity and surface wetness. The equivalent surface humidity can be expressed as a function of the equivalent surface temperature and moisture conditions in the surrounding air, see eq. (3.3).

$$RH_{s,eq} = \frac{RH_{air} \cdot v_s(T_{air})}{v_s(T_{s,eq})} \quad (3.3)$$

where:

$RH_{air}$ : relative humidity of the air. [%]

$v_s(T_{air})$ : vapour content of the air at saturation at a specific temperature. [ $g/m^3$ ]

$T_{air}$ : air temperature. [K]

$T_{s,eq}$ : equivalent surface temperature. [K]

If the equivalent surface humidity exceeds 100% RH, i.e. if the equivalent surface temperature is below the dew point temperature of the air, surface condensation occurs.

In figure 3.4 an example of the differences between the air and the surface humidity is shown. The measurements are made on a structure in Holzkirchen in the southern part of Germany. The figure is based on data representing five-day averages. The difference between the five-day average air and surface humidity can be up to 5% RH. If hourly average values are studied the difference between air and surface humidity can be over 20% RH.

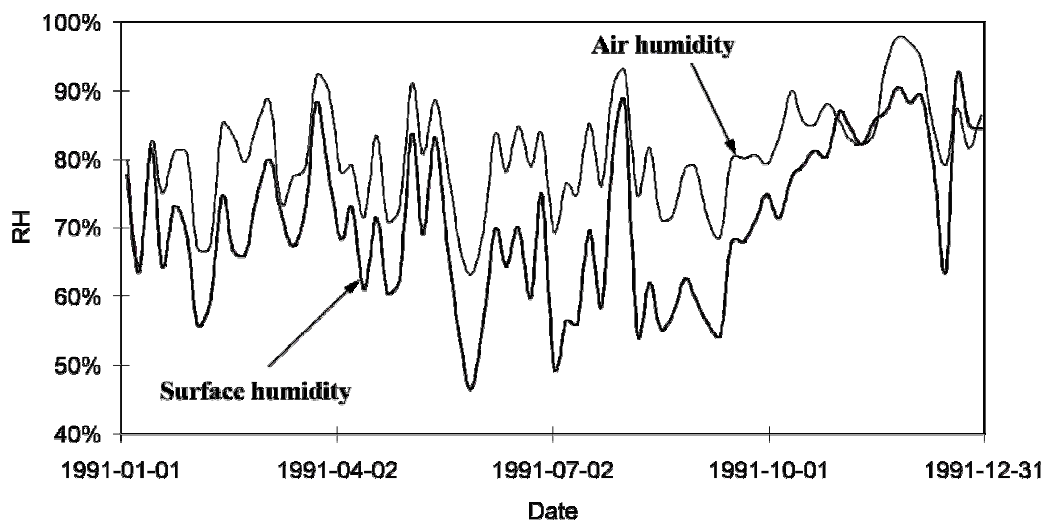


Figure 3.4: The air and surface humidity for a structure in Holzkirchen. CEB (1997). Based on data from IBP Holzkirchen (1995).

The surface wetness can be described in terms of TOW, which is the total time the surface is wet due to rain, surface condensation and running water from higher up on the structure. The surface wetness has been thoroughly studied by Svennerstedt (1989), where a methodology to quantify the time of wetness for a surface is presented. It is shown that TOW for a vertical surface is not equal to the time of rain, surface condensation and/or running water. This is explained by the fact that it takes a certain time for a moisture film to be formed and removed from the surface.

### Chloride conditions

The chloride conditions should be described as the chloride concentration at the surface of the concrete and also include effects from temperature and moisture conditions. Preferably only the influence of the exposure environment should be considered. However, in empirical models the chloride conditions are modelled as surface chloride

content, which is a combination of the exposure environment and the response of the material. This means that the material properties should also be included in the description of the chloride conditions in empirical models.

A possible approach to determine the surface chloride content in empirical models can be the following. The surface chloride content,  $C_s$ , can be predicted from an equivalent chloride concentration in the surrounding environment,  $C_{env}$ , and the chloride binding capacity of the concrete (influenced by amount and type of binder, w/b, the chloride concentration and temperature). This is summarised in a general formula, see eq. (3.4).

$$C_s = C'_{s,tot} (C_{env}, w/b, \text{type of binder}, T) \quad (3.4)$$

where:

$C'_{s,tot}$  : total chloride content (free and bound chlorides) at the surface of the concrete.  
[% by weight Cl/binder]

The relation between free and bound chloride content follows from chloride binding isotherms. Today chloride binding isotherms are available for most binders. The equivalent chloride concentration,  $C_{env}$ , follows from the type of exposure environment. The simplest case is when the concrete is exposed in marine submerged conditions, where  $C_{env}$  is equal to the chloride concentration of the seawater. For other environments where chlorides are present, the distance, height and orientation of the chloride source also have to be taken into account, which makes the description too complicated.

### 3.3 Response of concrete

#### 3.3.1 General

In Nilsson (1996) an overview is given of the interaction between the exposure environment and the response of concrete structures. In this paper the interactions between environmental actions outside a concrete and the response of the concrete are described. If the surrounding conditions are different from the conditions inside the concrete, the result will be flow processes that equilibrate these differences. Generally, these processes can be described by the law of conservation of energy or mass, which in one dimension can be written as eq. (3.5), Nilsson (1996).

$$\frac{\partial C_{tot}}{\partial t} = - \frac{\partial q}{\partial x} \quad (3.5)$$

where:

$C_{tot}$ : total content of energy or mass.  
t: time.  
q: flow of energy or mass.

In the following sections the response of the concrete is further described.

#### 3.3.2 Temperature conditions

The temperature conditions in a concrete are decisive for many deterioration processes. They influence both the flow rate and binding of various substances and chemical reactions in the concrete. The temperature conditions in concrete are mainly influenced by solar and long wave radiation, but also to some extent by cement hydration (at young

ages), evaporation and condensation and freezing and thawing. Examples of processes that are influenced by the temperature conditions are freeze/thaw actions, transport and binding of chlorides and cracking of the concrete.

The fundamental relationship to determine the temperature conditions in a concrete is the “law of energy conservation”, cf. eq (3.5). Together with the heat capacity, which gives the relationship between the energy transport and the corresponding change in temperature, the temperature conditions in the concrete can be determined. The heat transport takes place by convection, conduction and radiation. In low porous material, like concrete, conduction is dominant. The heat conduction in concrete can be modelled with the Fourier law, see eq. (3.6a).

$$q = -\lambda \cdot \frac{\partial T}{\partial x} \quad [\text{W/m}^2] \quad (3.6a)$$

where:

$\lambda$ : thermal conductivity.  $[\text{W}/(\text{m K})]$

$T$ : temperature.  $[\text{K}]$

By establishing a heat balance equation the temperature conditions in the concrete can be determined, see eq. (3.6b).

$$-\frac{\partial}{\partial x} \left( \lambda \cdot \frac{\partial T}{\partial x} \right) = -C_{\text{heat}} \cdot \frac{\partial T}{\partial t} \quad (3.6b)$$

where:

$C_{\text{heat}}$ : heat capacity.  $[\text{J}/(\text{m}^3 \text{ K})]$

The boundary conditions for the temperature inside the concrete are the surface temperature, most accurately expressed as equivalent surface temperature. The resulting temperature distribution in the concrete is to a large extent influenced by the fact that concrete is an excellent heat conductor, which means that temperature gradients in the concrete disappear rapidly. Thus a reasonable first approach could therefore be to assume the temperature conditions in the concrete to be similar to the surface temperature conditions. More complex solutions to eq. (3.6b) are presented in for example DuraCrete (1999).

### 3.3.3 Moisture conditions

The moisture conditions have, like the temperature conditions, decisive effects on many deterioration processes. They influence both the hardening of the concrete and transport and reactions of different substances in the concrete. Regarding the influence on the rate of transport, moisture will be an obstacle to transport of gas, e.g. carbon dioxide, and solids while it is a requirement for transport of ions, e.g. chlorides, and water. An illustration of the effects of moisture on rate of reaction and flow are shown in figure 3.5.

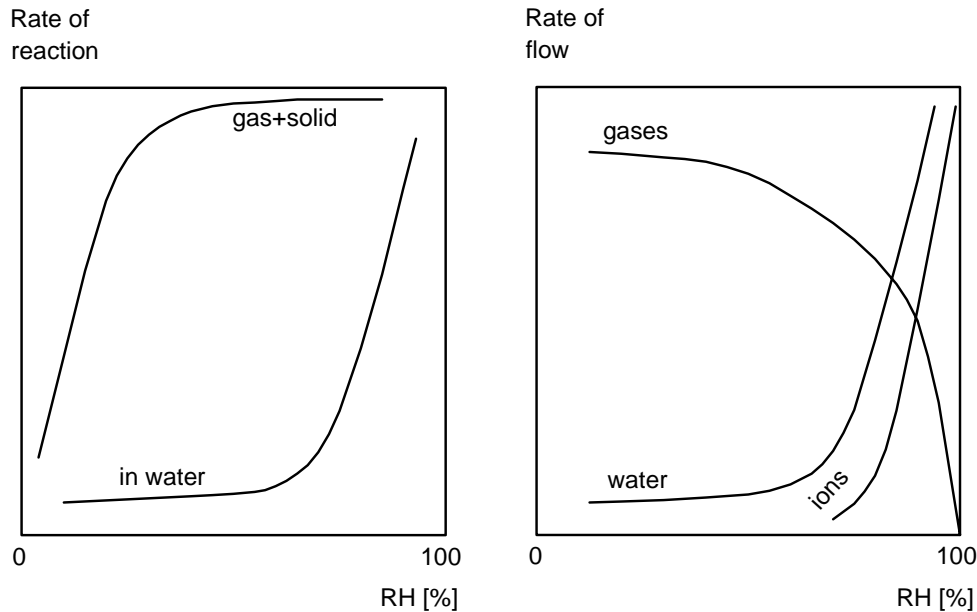


Figure 3.5: The effect of moisture conditions in the concrete on rate of reaction (left) and flow (right). Nilsson (1996).

An obvious example of a deterioration process influenced by the moisture conditions is freeze/thaw actions, where a certain amount of moisture is required for the reactions to take place. Another example is alkali-aggregate reactions, where moisture is required to transport alkalis to the aggregate and for the reactions to take place. Reinforcement corrosion is influenced by the moisture conditions during both the initiation and propagation periods. During the initiation period moisture acts as an obstacle to carbonation but is a requirement for transport of chloride ions. Once corrosion has been initiated the moisture conditions largely influence the corrosion rate by limiting the amount of oxygen and electrolyte. This means that in dry or wet conditions the corrosion rate is low while it is high in between.

Moisture in a concrete can be either chemically or physically bound. The physical binding of moisture takes place in the pores of the concrete. The binding is influenced by the pore size distribution, where moisture in small pores is more firmly bound than in large pores. Water menisci are established in pores and since there is a relationship between the water pressure in the menisci and the RH in the air above, RH is used as a measure of the moisture conditions. The relationship between the amount of physically bound moisture and the RH in the pore system is given by sorption isotherms. The shape of the isotherms is influenced by several factors, e.g. cement hydration, carbonation and chloride and temperature conditions. The chemical binding of moisture mostly takes place when the concrete is young, when the moisture reacts with binder. However, the moisture effects from the early chemical binding, so-called self-desiccation, may influence the moisture conditions in the concrete several years after casting. The moisture conditions are also influenced by the chloride content of the concrete, due to the hygroscopic properties of salt, cf. Nilsson et al (1997).

The moisture conditions in a material follow from an interaction between the surface conditions, most accurately described as equivalent surface conditions, and the conditions inside the concrete. The main driving force for moisture transport is a difference in moisture conditions at the surface and inside the concrete, but the temperature conditions also have an influence. The moisture distribution in a concrete can be determined by

solving the “law of mass conservation”, cf. eq. (3.5). In one dimension this is described with eq. (3.7).

$$\frac{\partial w_e}{\partial t} = -\frac{\partial q_m}{\partial x} - \frac{\partial w_n}{\partial t} \quad (3.7)$$

where:

- $w_e$ : amount of evaporable water. [kg/m<sup>3</sup>]
- $q_m$ : total moisture flow. [kg/(m<sup>2</sup> s)]
- $w_n$ : amount of non-evaporable water. [kg/m<sup>3</sup>]

The resulting moisture distribution is influenced by several factors, e.g. chemical and physical fixation of water and if the concrete is drying or getting wetter. Examples of models to predict the moisture conditions are presented in DuraCrete (1999).

### 3.3.4 Chloride conditions

The chloride conditions in concrete are decisive for the occurrence of chloride induced reinforcement corrosion. Since the emphasis of this study has been on chloride ingress and initiation of chloride induced reinforcement corrosion in marine and road conditions, the exposure conditions and the chloride ingress in these conditions are presented separately in the following sections. However, some general comments on observations of the chloride ingress into concrete are given here.

The age of the concrete at first exposure to chlorides has a large influence on the chloride ingress. If the first exposure to chlorides takes place at young age of the concrete the chloride ingress will be significantly larger than on first exposure at an older age. Additionally the chloride ingress has been found to almost stop after a certain exposure time, at least for structures in the marine atmospheric zone and in road conditions, cf. Andersen (1997) and de Rooij & Polder (2002). These phenomena can be explained by the fact that the pore structure of the concrete is not so dense at younger ages, since the cement hydration has not reached its final level. The longer the hydration can continue before exposure to chlorides the denser the concrete gets, and thus chloride ingress is the smaller. The effect of age on first exposure to chlorides has been indicated in road structures, e.g. Lindvall (2002b), and it seems reasonable to assume that a similar effect should be observed on marine structures, at least above the water surface.

## 3.4 Marine conditions

In the following section the exposure conditions in marine conditions are described. The exposure conditions are summarised in qualitative models, which are based on the general model presented in figure 3.1.

### 3.4.1 General

Marine conditions are characterized by vicinity to an ocean or sea, including coastal areas. Coastal areas are influenced some kilometres from the coastline, due to wind-blown salt mist. However, on special occasions, e.g. during severe storms, the area influenced by salt from the sea may reach several 100 km from the coastline, Gustafsson & Franzén (2000). In CEB (1989) it is proposed to divide the marine conditions into four different exposure zones. The basis for the division is the position in relation to the water surface and tidal and wave actions. The following exposure zones can be identified:

- **Submerged zone.** The submerged zone is the zone below the water level, where the surface of the concrete is constantly exposed to seawater.
- **Tidal zone.** The tidal zone is the zone between low and high tide, which means that the concrete is subjected to an alternating moist and dry environment (with an approximately 12 hour cycle). The surface of the concrete is cyclically exposed to seawater or air corresponding to the tidal cycle.
- **Splash zone.** The splash zone is the zone above the tide level influenced by the waves, which means that the concrete is subjected to randomly alternating moist and dry environments due to wave – action. The surface of the concrete is randomly exposed to splash from seawater or air.
- **Atmospheric zone.** The atmospheric zone is the zone above the splash zone and the concrete is exposed to humid marine air with airborne chlorides that follow spray from breaking waves.

The exposure conditions in the splash and atmospheric zones are to a large extent influenced by the characteristics of the waves hitting the structure. Waves are characterised by their heights, period and direction, which are functions of wind speeds and fetch lengths, Concrete in coastal structures (1998). There is a relationship between the wind speed and the maximum fetch length, which means that if the wind blows over a sufficiently long distance the total fetch length is reached and no further development of the waves takes place. The wave height is also influenced by the water depth, where the characteristics of the waves change in shallow waters.

In the splash and atmospheric zones a surface is exposed to splash and spray from breaking waves. When waves are breaking at sea or along the coastline droplets of seawater are produced and thrown up in the air. Depending on the size of the droplets and the wind speed the droplets will either be directly deposited (splash) or follow airstreams (spray) and be deposited either on structures in the sea or on land, (marine aerosols). Since the marine aerosols are following airstreams they can also be deposited on surfaces not directly exposed to a marine environment.

A division can be made of the marine aerosols (spray from breaking waves), where large droplets (diameter  $>10\ \mu\text{m}$ ) will be deposited close to the coast and small droplets (diameter  $<10\ \mu\text{m}$ ) are deposited over larger areas. A number of factors, e.g. height above and distance to the sea, topography of the land and wind directions and velocities, influence the transport of marine aerosols over land. Morcillo et al (2000) found that at certain wind directions, which are defined as “saline winds”, the transport of marine aerosols over land was significantly increased, and that the critical wind speed for the transport is as low as 3 m/s. Marine aerosols may be transported over long distances from the coastline, during severe storms several hundred kilometres. In a study by Gustafsson & Franzén (2000) it was found that the concentration of marine aerosols 50 km from the coastline was approximately 20% of the concentration at the coastline. Gustafsson & Franzén also found that the influence of wind speed is high close to the coastline and decreases with increasing distance from the coastline.

### 3.4.2 Temperature and moisture conditions

The temperature and moisture in marine conditions are to large extent influenced by the position in relation to the water level. In the submerged zone a surface is constantly moist and the surface temperature is equal to the water temperature. Surfaces in the tidal and splash zones are periodically exposed to seawater and randomly exposed to splash from seawater, and consequently the surface temperature and moisture conditions can be

described as a combination of the conditions in the seawater and the air. In the atmospheric zone the temperature and moisture conditions are mainly influenced by the conditions in the air. The temperature and moisture conditions for surfaces exposed in the air are influenced by for example radiation conditions and exposure to rain. Thus to correctly model the exposure conditions for these surfaces they should be expressed as equivalent surface temperature and humidity, cf. eq (3.1) and (3.2), and surface wetness.

The temperature in seawater varies between  $-2^{\circ}\text{C}$  (around the poles – freezing point of seawater) and  $+36^{\circ}\text{C}$  (Arabian gulf), according to Concrete in coastal structures (1998). The yearly variations are generally not that large, usually some  $10\text{--}15^{\circ}\text{C}$ , but at some locations they can be up to  $30^{\circ}\text{C}$  (east of Nova Scotia and north east of Japan) due to periodic changes in cold and warm currents. There is also a temperature gradient with water depth, where the temperature decreases rapidly and reaches a steady-state value of  $2\text{--}5^{\circ}\text{C}$  at depths larger than 100 m.

### 3.4.3 Chloride conditions

The chloride conditions are, in the same way as the temperature and moisture conditions, influenced by the position in relation to the water level. In the submerged zone a surface is constantly exposed to seawater and thus also to chlorides. Surfaces in the tidal and splash zones are periodically exposed to seawater and randomly exposed to splash of seawater, which results in a periodic and random exposure to chlorides. In the atmospheric zone surfaces are exposed to chloride-contaminated spray that is following air streams.

The chloride concentration in seawater is in most seas approximately 20 g/l. However, in seas with limited access to larger seas or close to river deltas, the chloride concentration can be significantly lower. Stratification may also occur, where water of different densities (and chloride concentrations) is not fully mixed, as illustrated in figure 3.6.

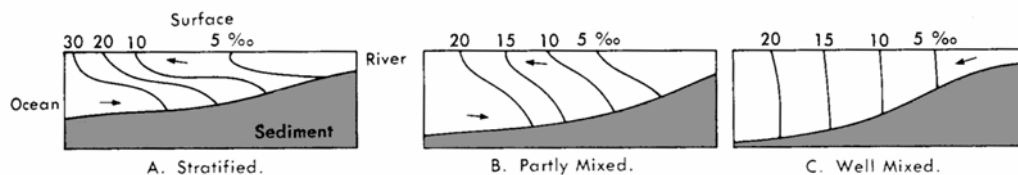


Figure 3.6: Illustration of the variations of salinity (‰) in the water close to a river delta. McCormick & Thiruvathukal (1981).

### 3.4.4 Response by marine concrete structures

#### General

From the presentation above it is obvious that the exposure of marine structures to chlorides takes place with a number of mechanisms. One way to determine the significance of these mechanisms is to study the response, as chloride ingress profiles, measured on existing structures or concrete specimens. In the following section some examples of measured response from marine concrete structures found in literature are presented.

#### Chloride conditions

Examples of measured chloride ingress profiles from concrete specimens exposed in the harbour of Träslövsläge are presented in figure 3.7. More comprehensive presentations of



the results from the Träslövsläge field station are given in for example Andersen et al (1998) and Tang (2003). The profiles with index **S** come from the submerged zone and those with index **A** from the atmospheric zone.

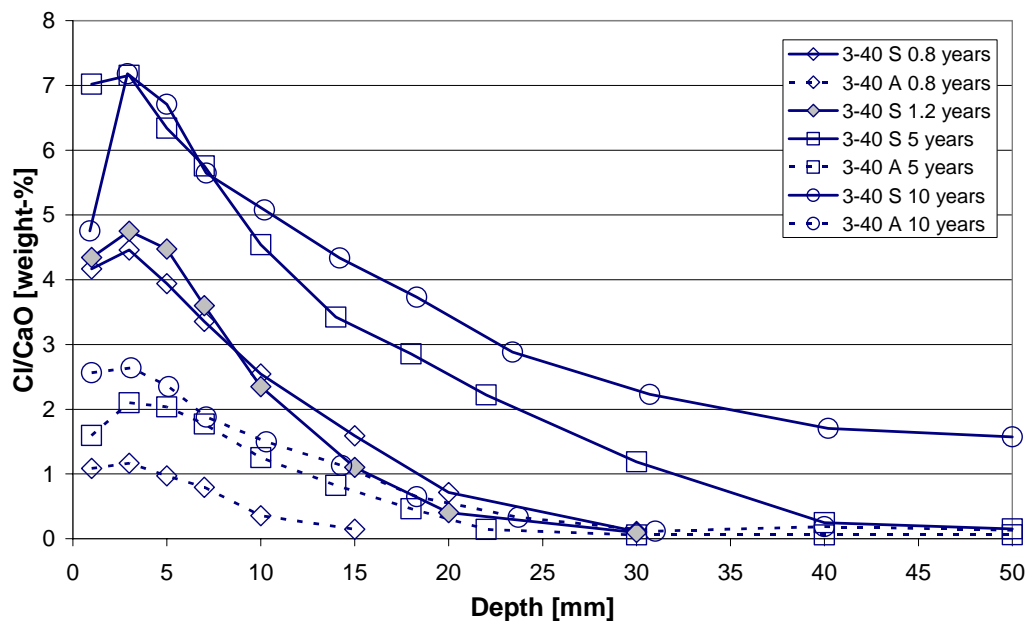


Figure 3.7: Examples of measured chloride ingress profiles at different ages (up to ten years exposure) from concrete specimens, made from one concrete composition, exposed at the field station in Träslövsläge. Concrete 3-40<sup>3</sup>. Data from Tang (2003).

In figure 3.7 it can be seen that in the submerged zone the chloride ingress continues over time, while in the atmospheric zone the chloride ingress seems to stop after the first years of exposure. The corresponding evaluated age factors, in the DuraCrete chloride ingress model, are 0.63 in the submerged zone and 0.59 in the atmospheric zone.

One of the concrete compositions exposed in Träslövsläge (concrete composition Ö<sup>4</sup>) has also been exposed in the Baltic Sea (at the location of the Öland bridge), where the latter has significantly lower salinity. In figure 3.8 examples of measured chloride ingress profiles from exposure in the Baltic Sea and Träslövsläge are presented. The profiles with index #2 and #13 come from the atmospheric zone, those with index #17 and #20 from the splash zone and those with index #31 and #33 from the submerged zone at the location of the Öland bridge. The profiles with index **Su** and **At** come from the submerged and atmospheric zones in Träslövsläge respectively. The exposure times have been 1387 days for the specimens at the Öland bridge and 1862 days for the specimens in Träslövsläge.

<sup>3</sup> Swedish OPC (CEM I 42.5) + 5% Silica fume w/b=0.40

<sup>4</sup> 100% Swedish SRPC (CEM I 42.5 BV/SR/LA) w/b=0.40.

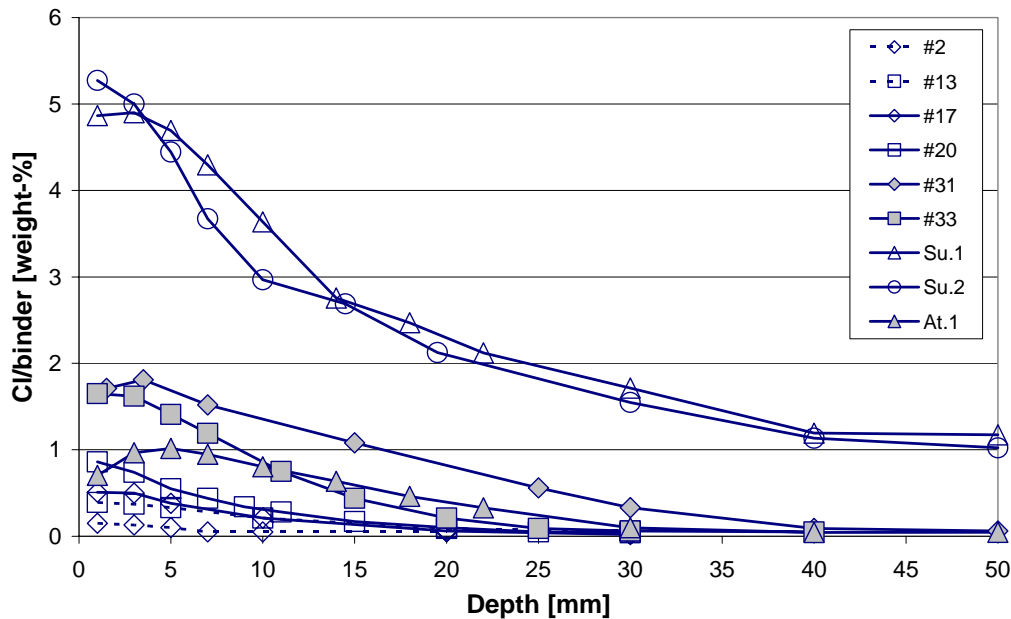


Figure 3.8: Measured chloride ingress profiles from exposure in the Baltic Sea (four years exposure) and at the field station in Träslövsläge. Data from Tang (1997) and Andersen et al (1998).

In figure 3.8 it can be seen that the largest chloride ingress was found in the concrete exposed in submerged conditions in Träslövsläge, which can be partly explained by the longer exposure time, but is mainly due to higher chloride content in the seawater.

Kompen et al (1997) made an extensive investigation of the chloride conditions on the Gimsøystraumen bridge in the northern part of Norway. The bridge is a box girder bridge with a total length of 840 m divided into nine spans. The exposure conditions have been monitored at a meteorological station on the bridge and the response of the concrete has been measured in terms of chloride ingress and reinforcement corrosion. The chloride ingress has been measured in the columns and the box girder at over 1000 locations. It was found that the chloride conditions varied significantly over the bridge. The data from the investigation of the Gimsøystraumen bridge have been used for further analysis by several authors, e.g. Fluge (1997), Grefstad & Grindland (1997) and Maage et al (1997). In the investigation of the Gimsøystraumen bridge, among other things, the variations in chloride ingress along the box girder have been investigated. Examples of these variations are presented in figure 3.9 where the average chloride content in the outer 10 mm of concrete along the box girder is shown. The chloride content was found to increase significantly close to the columns, where the box girder walls have maximum heights and thus present a larger obstacle to the wind. This effect was especially clear around column 2, where the box girder is also closest to the sea (in the vertical direction).

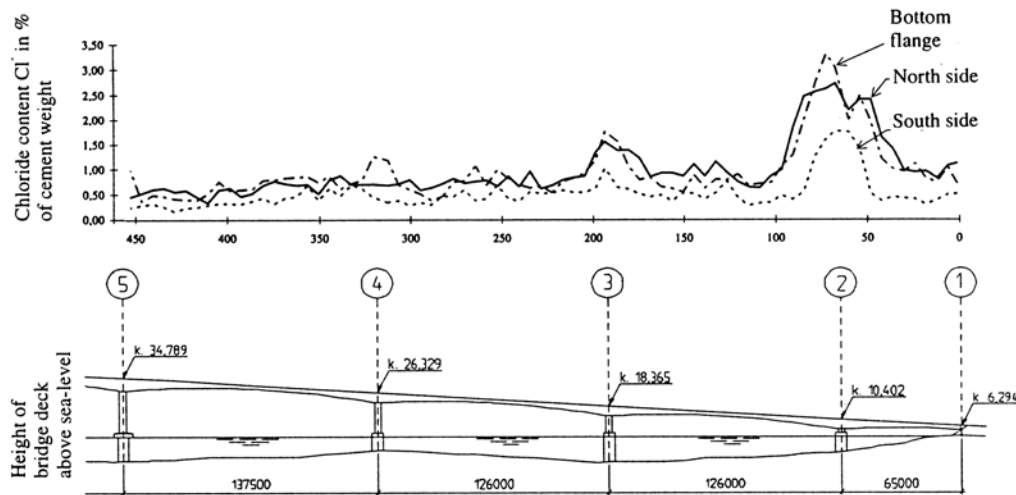


Figure 3.9: Average chloride content in the outer 10 mm of the concrete along the box girder on the Gimsøystraumen bridge. Fluge (1997).

In Sørensen & Maahn (1982) one column (atmospheric zone), on a bridge in the Danish Store Belt area, was sampled for chloride ingress at different heights above the water surface. The results showed that chloride ingress is height – dependent. Izquierdo et al (2000) found a similar behaviour when they investigated the chloride ingress in a column (atmospheric zone) and a beam (tidal and splash zones). A correlation was found between surface chloride content and the height above the water surface. Wood & Crerar (1997) found similar results, where chloride ingress into a bridge column, on a bridge on the Scottish east coast, was analysed up to a height of 16 m above the water surface. The surface chloride content could be correlated with the height above the water surface.

The results from Sørensen & Maahn (1982), Fluge (1997), Tang (1997), Wood & Crerar (1997) and Izquierdo et al (2000) are summarized in figure 3.10. In Fluge (1997) the combined effect of height and orientation on the chloride ingress has also been investigated (results presented with filled symbols, where each observation is a mean value of two or three measurements). The data from Fluge represent the chloride content in the outer 15 mm of the concrete while the other data are represented by an apparent surface chloride content,  $C_{sa}$ , evaluated from measured chloride ingress profiles. It should be noticed that the examined bridges are not constructed with similar concrete compositions, which means that the results cannot be directly compared.

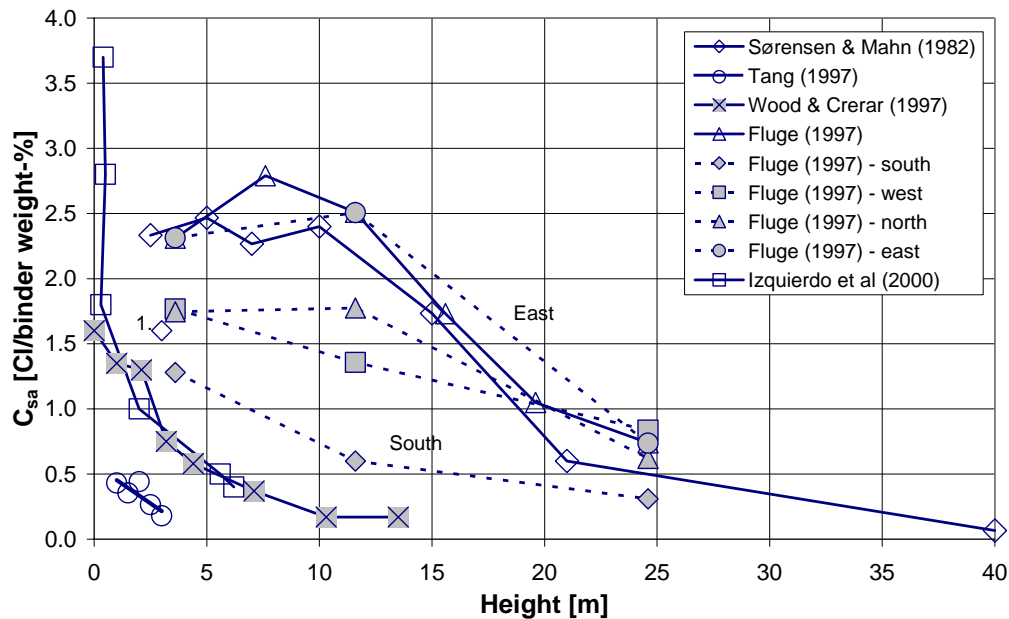


Figure 3.10: Variations in  $C_{sa}$  as a function of the height above the water surface. The sample with index 1 is taken from a sheltered area. Data from Sørensen & Maahn (1982), Fluge (1997), Tang (1997), Wood & Crerar (1997) and Izquierdo et al (2000).

From figure 3.10 it can be seen that the chloride ingress is not only a function of the height above the sea but is also influenced by the orientation of the surface. The orientation effect, observed by Fluge (1997), is explained by deposition of airborne chlorides on the side of the column that is not exposed to wind driven rain, i.e. the eastern side. The other sides of the column are exposed to wind driven rain resulting in a washout of chlorides. The washout of chlorides is most significant on the southern side of the column, which is also the part of the column that has the heaviest exposure to wind driven rain.

From the results in figure 3.9 and 3.10 it can be observed that the exposure to chlorides in the marine atmospheric zone varies a lot not only between different structures but also within one single structure. In Kompen et al (1997) it is concluded that the chloride load in the marine atmospheric zone depends on height above sea, windward/ leeward effects and size and shape of exposed surfaces which influence the exposure to chlorides and rain.

Similar observations are reported by Polder et al (2003), where chloride ingress data from a bridge structure on the Eastern Scheldt storm surge barrier, along the Dutch North Sea coast, are presented. The barrier crosses the Eastern Scheldt in a north-south direction. The chloride ingress was found to vary depending on orientation of the surface and sheltering effects, see figure 3.11. In this figure measured chloride ingress profiles from two types of concrete, gravel and lightweight concrete, and two sides of the bridge structure, facing towards the Eastern Scheldt and the North Sea respectively, are presented. The broken lines in figure 3.11 denote the standard deviation of the measured chloride ingress profiles. The coefficient of variation for the measured chloride ingress profiles, COV determined according to eq. (4.1), is up to 0.60.

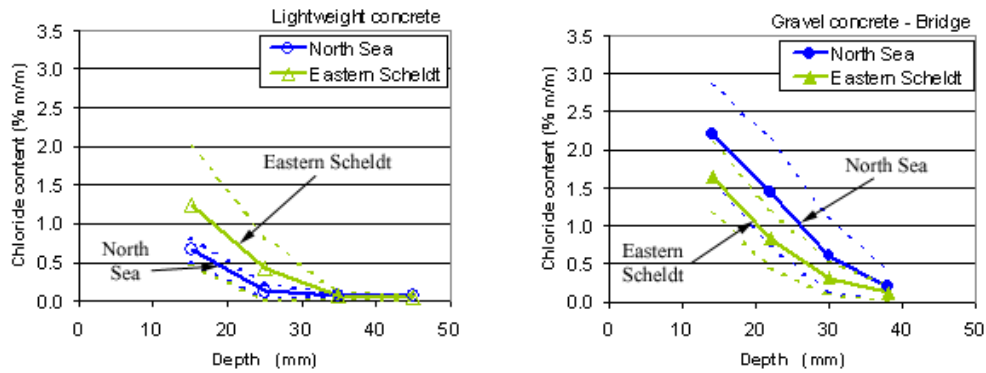


Figure 3.11: Chloride ingress data from the bridge structure of the Eastern Scheldt storm surge barrier. Data from Polder *et al* (2003).

From figure 3.11 it can be seen that the measured chloride ingress depends on the surface orientation. The chloride ingress measured in lightweight concrete is larger on the Eastern Scheldt side, and that in gravel concrete on the North Sea side. The larger chloride ingress on the Eastern Scheldt side measured in the lightweight concrete can be attributed to deposition of airborne chlorides on the leeward side of the structure, i.e. Eastern Scheldt side. The larger chloride ingress on the North Sea side measured in the gravel concrete can be explained by sheltering effects from sliding doors on the North Sea side of the structure, which reduce the deposition of chloride on the leeward side of the structure.

Similar results were found by Andersen (1996), where the chloride ingress in the splash zone on a road bridge column on the east coast of Jutland in Denmark has been investigated. The column has been investigated in different orientations to determine the effect of orientation on the chloride ingress. The largest chloride ingress was found on the eastern side of the column, which is the side that is also most exposed to splash from waves.

There is also a certain extension of the marine atmospheric zone over land at different distances from the coastline. In a study presented in McGee (2000), the chloride ingress into concrete structures at different distances from the coastline has been determined. Takewaka & Mastumoto (1988) have studied the surface chloride content on structures at different distances from the coastline, where they found that the marine atmospheric zone reaches up to three km from the coastline. In figure 3.12 the relation between  $C_{sa}$  at different distances from coastline and  $C_{sa}$  at the coastline is presented, based on data from Takewaka & Mastumoto (1988) and McGee (2000). McGee (2000) also found that the apparent diffusion coefficient evaluated from measured chloride ingress profiles<sup>5</sup>,  $D_{F2}$ , did not vary with the distance from the coastline.

<sup>5</sup> The apparent diffusion coefficient,  $D_{F2}$ , is similar to  $D_a(t)$  in the DuraCrete chloride ingress model, defined in eq. (2.1a) and (2.1b).

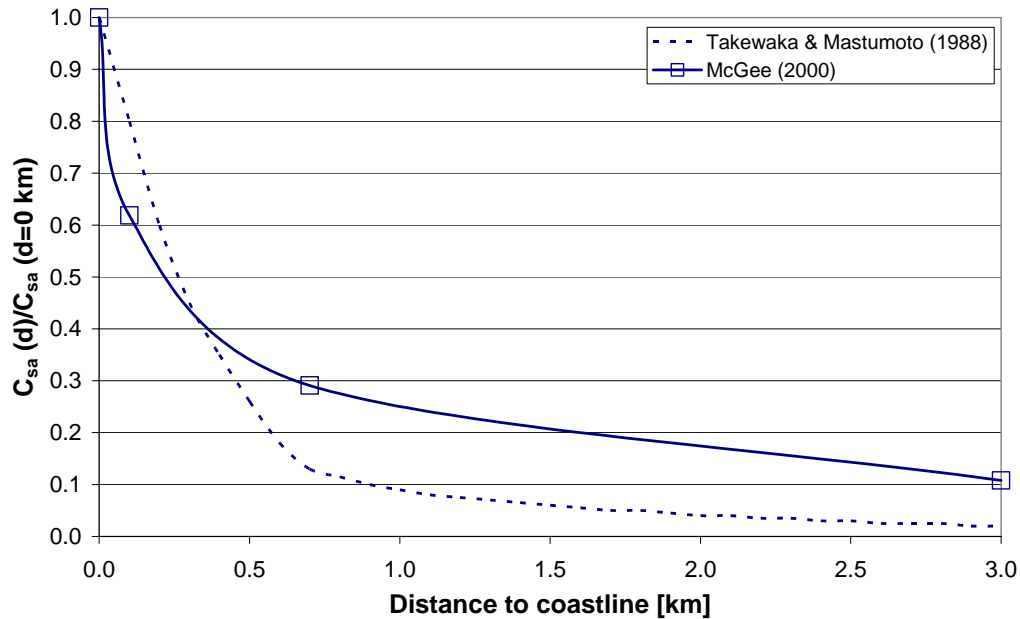


Figure 3.12: Correlation between  $C_{sa}$  and the distance from the coastline. Based on data from Takewaka & Mastumoto (1988) and McGee (2000).

As seen in figure 3.12  $C_{sa}$  decreases with increasing distance from the coastline. For distances over 3 km from the coastline McGee (2000) found that  $C_{sa}$  was generally below 10% of the level at the coastline. Similar results were found by Takewaka & Mastumoto (1988), but the decrease in  $C_{sa}$  with increasing distance from the coastline was even larger than McGee (2000) reported. For structures close to the coastline a height dependency in  $C_{sa}$  was also observed. In a study by Fitzpatrick (1996) similar results were reported, where concrete structures in Florida, up to two km from the coastline, were found to be exposed to chlorides from seawater.

### Moisture conditions

In a Swedish national research project called BMB (Durability of Marine Concrete Structures), some 40 types of concrete specimens have been exposed in the harbour of Träslövsläge on the Swedish west coast. The concrete compositions include Swedish and Danish cements, with different w/b, additives and admixtures. The concrete specimens have been periodically sampled for chloride ingress and moisture conditions in the marine submerged, splash and atmospheric zones for exposure times up to ten years. In figures 3.13a (RH) and 3.13b ( $S_{cap}$ ) examples of measured moisture profiles from the marine submerged (filled symbols) and atmospheric (non-filled symbols) zones are presented.

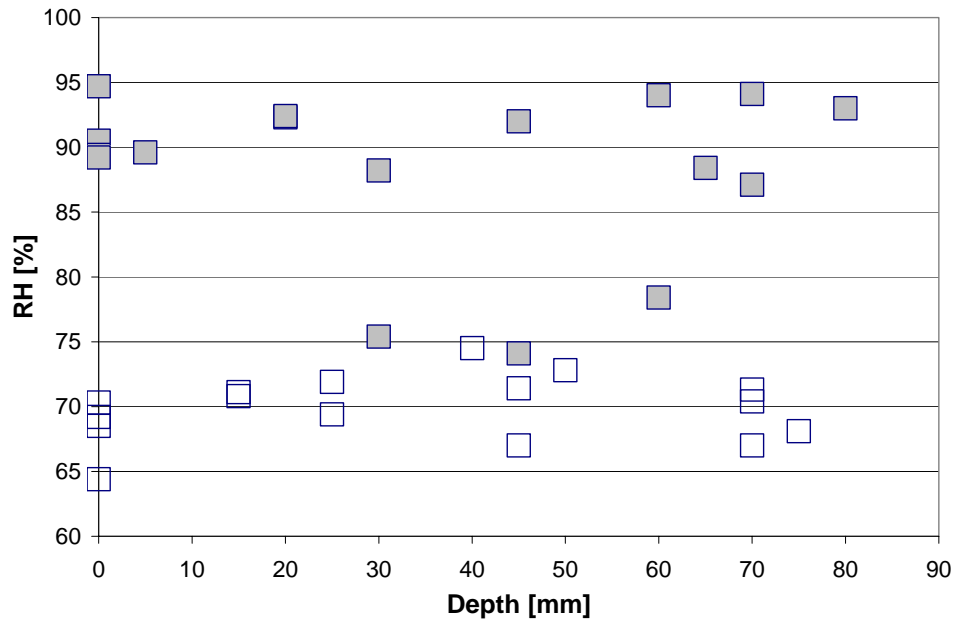


Figure 3.13a: Examples of measured moisture profiles ( $RH$ ) from the marine submerged (filled symbols) and atmospheric (non-filled symbols) zones. The exposure time has been 5.5 years. Concrete with  $w/b=0.40-0.50$ . Unpublished data.

In figure 3.13a it can be seen that there is a significant difference in  $RH$  between the submerged and atmospheric zones.  $RH$  is generally around 90% ( $\pm 5\%$ ) in the submerged zone and 70% ( $\pm 5\%$ ) in the atmospheric zone. The low values of  $RH$  in the submerged zone are probably caused by either defects in the concrete or leakage during the measurements.

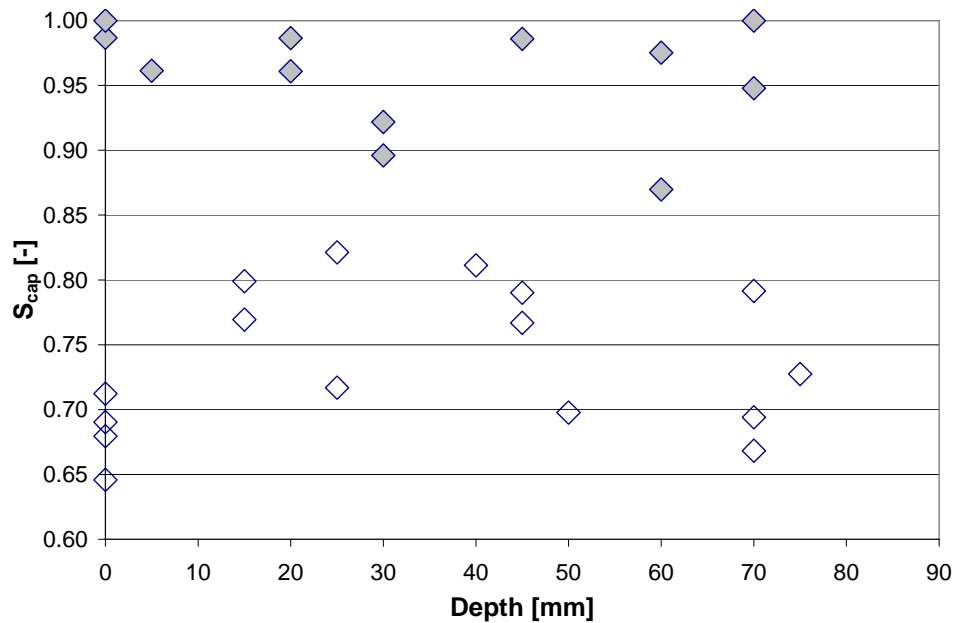


Figure 3.13b: Examples of measured moisture profiles ( $S_{cap}$ ) from the marine submerged (filled symbols) and atmospheric (non-filled symbols) zones. The exposure time has been 5.5 years. Concrete with  $w/b=0.40-0.50$ . Unpublished data.

As in the case of RH, there is a significant difference in  $S_{cap}$  between the submerged and atmospheric zones.  $S_{cap}$  is 0.85-1.00 in the submerged zone and 0.65-0.80 in the atmospheric zone.

### 3.4.5 Qualitative models

#### General

From the description of the marine environment it is obvious that the environmental conditions and their variations on structures are not trivial. The actions are influenced by a number of factors, e.g. tidal actions and wave heights, height above the water level and distance from coastline.

The environmental conditions in marine exposure zones have been summarised in qualitative models. The models are based on the general model presented in figure 3.1. Since the exposure environments are rather different for the different marine exposure zones, three different models have been developed, for the submerged zone, for the tidal and splash zones and for the atmospheric zone.

#### Submerged zone

In the marine submerged zone the surface conditions mainly follow from the characteristics of the seawater (temperature and the chemical composition), since the structure is constantly exposed to seawater. A qualitative model that describes the environmental actions in the submerged zone is presented in figure 3.14.

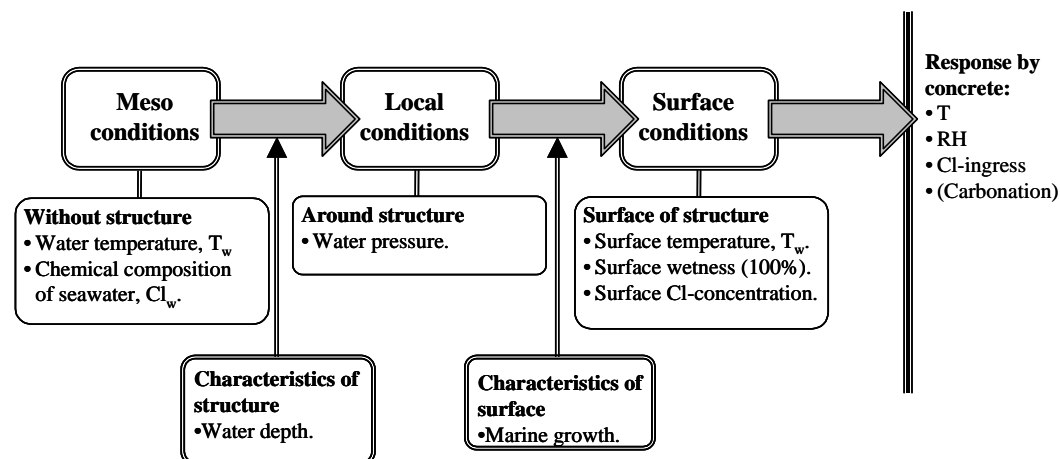


Figure 3.14: Qualitative model for environmental actions on structures exposed in marine conditions – submerged zone.

The starting point for the model in figure 3.14 is information about the meso conditions, described in terms of temperature and chemical composition of the seawater. The local conditions can be derived on the basis of information about the water depth. Finally the surface conditions can be derived with knowledge of the extent of marine growth. The response by the concrete has very small influence on the surface conditions in the submerged zone and is therefore omitted in figure 3.14.

#### Tidal and splash zones

The exposure conditions in the tidal and splash zones follow from the conditions in the submerged zone together with information on tidal and wave actions and location in relation to the water surface. A qualitative model that describes the environmental actions in the tidal and splash zones is presented in figure 3.15.



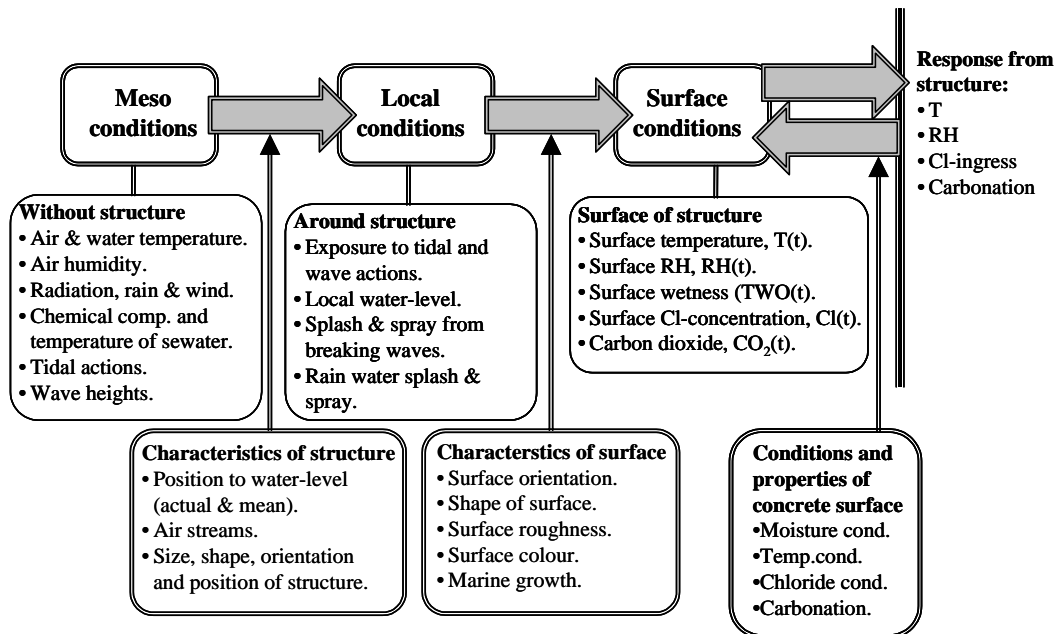


Figure 3.15: Illustration of qualitative model for environmental actions on structures exposed in marine conditions – tidal and splash zones.

The starting point for the model described in figure 3.15 is information about the meso conditions, described in terms of temperature and chemical composition of the seawater, the temperature and humidity of the air, radiation, rain and wind conditions, chemical composition and temperature of the seawater and tidal actions and wave heights. The local conditions can be derived on the basis of information about the position in relation to the water level, the way air streams are moving around the structure, and shelter against rain. In the local conditions variations in exposure due to tidal actions, splash and spray from breaking waves and rain are taken into account. Finally the surface conditions can be derived if the effects due to orientation, shape, surface roughness and marine growth together with the conditions and properties of the concrete surface (in terms of moisture, temperature and chloride conditions and carbonation) are taken into account. The conditions and properties of the concrete surface may for example influence the surface roughness, due to frost action (following from temperature conditions), or surface colour, due to variations in moisture conditions etc.

### Atmospheric zone

The exposure conditions in the atmospheric zone follow from the exposure conditions in the submerged, tidal and splash zones together with information about the height above the water surface, the distance from the coastline (both inland and over sea) and movements of airstreams. A qualitative model that describes the environmental actions in the atmospheric zone is presented in figure 3.16.

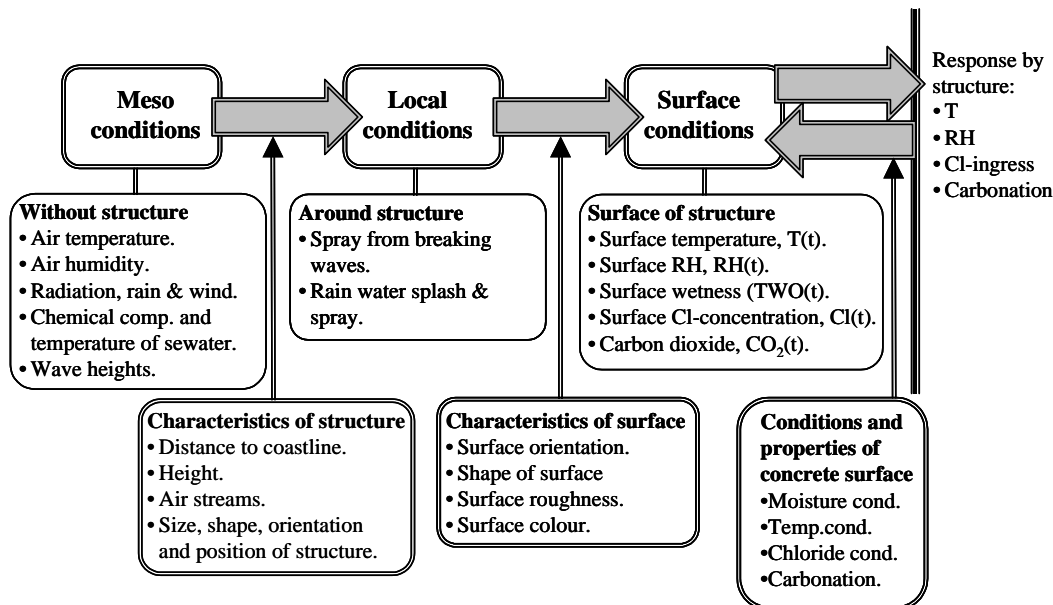


Figure 3.16: Illustration of qualitative model for environmental actions on structures exposed in marine conditions – atmospheric zone.

The starting point for the model in figure 3.16 is information about the meso conditions, described in terms of air temperature and humidity, radiation, rain and wind conditions, chemical composition and temperature of seawater and wave heights. The local conditions can be derived on the basis of information about the distance from the coastline, height, movements of airstreams and shelter against rain. In the local conditions effects of exposure to spray from breaking waves and rain are taken into account. Finally the surface conditions can be derived on the basis of information about orientation, shape and surface roughness together with the conditions and properties of the concrete surface (in terms of moisture, temperature and chloride conditions and carbonation). The conditions and properties of the concrete surface may for example influence the surface roughness, due to frost action (following from temperature conditions), or surface colour, due to variations in moisture conditions etc.

## 3.5 Road conditions

### 3.5.1 General

As for most outdoor structures, the exposure conditions for concrete structures in road conditions are characterized by rapid changes in temperature and moisture conditions and exposure to carbon dioxide. However, what distinguishes road structures from other outdoor structures is the exposure to chlorides originating from de-icing salt spread to prevent slippery road conditions. If de-icing salt is not spread, the road structures are not exposed to chlorides and can be treated as just any outdoor structure, by considering the variations in equivalent surface temperature and moisture conditions. There is also a transport of chlorides to the surroundings of the road, due to drainage, ploughing, splash and spray, which means that the road conditions have a certain extension from the road itself.

In the following section the road conditions for roads where de-icing salt is spread is described. The focus of the description is on how the exposure to chlorides, originating from spreading de-icing salt, takes place. The exposure conditions are summarised in qualitative models, which are based on the general model presented in figure 3.1.

### 3.5.2 Temperature and moisture conditions

The temperature and moisture conditions on road structures may vary significantly both between different parts of the structure and from the temperature and moisture conditions in the air. Examples of surfaces where there can be significant differences between moisture and temperature conditions on the surface and in the air are horizontal surfaces during clear nights, and surfaces facing towards the south during sunny days. A horizontal surface, e.g. a bridge slab, may have a significantly lower surface temperature than the air temperature due to cooling from the radiation exchange with the sky. Examples of large variations in moisture and temperature conditions in road structures are described in Alavizadeh-Farhang & Paulsson (1997), where measurements of temperature and moisture conditions outside and inside a concrete bridge slab in Stockholm, Sweden, are presented. There may also be significant effects from the orientation of a surface, where a surface facing towards the south, e.g. an edge beam, may have a surface temperature and humidity significantly different from the temperature and humidity of the air and also of other surfaces, Paulsson-Tralla (2001). This difference is mainly a result of radiation effects (solar and long wave radiation).

### 3.5.3 Spread of de-icing salt

The main reason to spread de-icing salt on roads is to prevent slippery road conditions, due to ice and snow. De-icing salt has been spread on roads in Europe since the Second World War. However, in Sweden and Denmark de-icing salt (NaCl) has been spread on roads since the mid 1960s, Bäckman (1980) & Randrup & Pedersen (1996). Before the 1960s sand was used to prevent slippery road conditions in these countries. Since ice and snow is only present on roads during approximately half the year, de-icing salt is also only spread during half the year. For example, in the southern parts of Sweden de-icing salt is spread from October to April, i.e. 6-7 months during the year.

There are many types of de-icing salts available on the market, e.g. sodium chloride (NaCl), potassium chloride (KCl), calcium chloride ( $\text{CaCl}_2$ ), magnesium chloride ( $\text{MgCl}$ ), but different types of agents without salt, e.g. alcohols, are also used. The most common type of de-icing salt used on roads is NaCl, due to its low price. Furthermore, NaCl has high activity, is readily available and easy to store. Theoretically a saturated NaCl solution freezes at  $-21^\circ\text{C}$  and  $\text{CaCl}_2$  solution freezes at  $-52^\circ\text{C}$ . However, for practical use NaCl can be used down to temperatures of  $-8^\circ\text{C}$  and  $\text{CaCl}_2$  down to temperatures of  $-15^\circ\text{C}$  to  $-20^\circ\text{C}$  – at lower temperatures  $\text{CaCl}_2$  still melts ice, while NaCl is immobilized, OECD (1989). An important difference between the two types of salt is that  $\text{CaCl}_2$  emits heat when dissolved while NaCl requires heat to be dissolved. In Sweden it is recommended to use NaCl on main roads at temperatures above  $-12^\circ\text{C}$  and on regional roads at temperatures above  $-8^\circ\text{C}$ , Blomqvist (1998). This means that other types of de-icing salts must be used, e.g.  $\text{CaCl}_2$  or  $\text{MgCl}$ , at lower temperatures. In especially sensitive environments with high risk of corrosion, e.g. airports, de-icing salts may not be used since they contain chlorides, which means that for example an alcohol-based agent must be used instead.

There are three principal sources for de-icing salt, sea salt which is extracted from the sea, rock salt which is extracted from the soil, and vacuum salt, Randrup & Pedersen (1996). Vacuum salt is extracted from the ground by pumping water through salt deposits to the surface and then extracting the salt from the water. A de-icing salt is characterized by its water content and particle size distribution. Sea salt has large irregular particles, rock salt has varying particle size and vacuum salt has mainly small particles. The particle size has an influence on the ability to melt ice on the road, where small salt particles are more

rapidly dissolved and thus have a rapid effect. Larger salt-particles stay longer on the road and can melt thicker layers of ice. The particle size distribution of the de-icing salt also has an influence on the amount of salt spread on the road, where the amount of salt is larger with a wide particle size distribution than with a more narrow, and optimised, distribution, Dobson (1991).

Once de-icing salt is spread on a road surface it works in three steps to remove the snow and ice, Salt Institute (1995). In the first step the de-icing salt melts through the layer of ice and snow forming a brine. The remaining snow and ice floats on the brine breaking the bond with the road surface. Finally the vehicular traffic breaks through the snow and ice, reducing the layer of snow and ice to a ploughable slush, which can be moved to the side of the road. Usually de-icing salt is spread from special vehicles, e.g. tractors or trucks, but there are ongoing experiments where automatic spreading devices are tested on especially exposed locations, e.g. bridges.

There are two reasons for spreading de-icing salt: (i) to fight ice and snow on the road or (ii) to prevent slippery road conditions. In general there are two different methods to determine when to spread de-icing salt on a road, Paulsson & Andersen (1997):

- **Active method (ice and snow control).** The active method is based on meteorological observations and testing of the actual road conditions. The vehicles used for spreading de-icing salt are used to test the friction at critical locations on the road. If the friction is too low de-icing salt will be spread on the road. De-icing salt is spread to **fight** slippery road conditions.
- **Preventive method (prevention of slippery road conditions).** The preventive method is based on meteorological observations and information about the temperature of the road surface. If the surface temperature is below a certain level de-icing salt will be spread, regardless of whether the road is slippery or not. De-icing salt is spread to **prevent** slippery road conditions.

There are five methods to spread de-icing salt on a road, Paulsson & Andersen (1997):

- **Dry salt.** The salt is spread on the road surface as dry salt. Each time 12-20 g/m<sup>2</sup> of NaCl is spread.
- **Wetted dry salt.** The salt is spread on the road as dry salt slightly wetted with a 24% NaCl solution. Each time 10 g/m<sup>2</sup> of NaCl is spread with this method.
- **Salt solution.** A salt solution with 24% NaCl is sprayed on the road surface. Each time 20 g/m<sup>2</sup> of salt solution, i.e. approx. 4 g/m<sup>2</sup> of NaCl, is spread.
- **Sand mixed with salt.** Sand is mixed with 3% by weight of NaCl. The sand is added to achieve better friction between the tyres and road surface when the temperature is too low for the salt to work. Each time 200-250 g/m<sup>2</sup> of the sand mix is spread, i.e. 6-7.5 g/m<sup>2</sup> of NaCl.
- **Crushed aggregate and sand mixed with salt.** By mixing crushed aggregate into the sand salt mix the amount of NaCl can be reduced to 1% by weight. Furthermore the friction between the tyres and the road surface is increased. Each time 200-250 g/m<sup>2</sup> of the mix is spread, i.e. 2-2.5 g/m<sup>2</sup> of NaCl.

In Sweden de-icing salt is usually spread as wetted dry salt or salt solution, Paulsson & Andersen (1997). However, the number of vehicles used to spread the de-icing salt in these ways is limited, which means that sometimes de-icing salt must be spread in other forms as well. Usually de-icing salt is spread during the night or early morning, when the

amount of traffic is low, to let the salt be properly melted. However, if needed, de-icing salt may also be spread at other times during the day.

In urban areas the spread of de-icing salt correlates fairly well with occasions when the air temperature passes 0°C, Paulsson & Andersen (1997). The amount of de-icing salt that is spread depends on the characteristics of the road, e.g. the amount of traffic and the topography, where the amount of salt is higher on roads with a lot of traffic than with less traffic. Furthermore the amount of de-icing salt is dependant on the temperature of the road surface, where the required amount of de-icing salt increases with decreasing temperature. If the temperature decreases from 0°C to -10°C the required amount of NaCl to melt ice increases by a factor seven (46.3 kg ice/kg NaCl and 6.3 kg ice/kg NaCl respectively), Salt Institute (1999). This has consequences on the amount of de-icing salt that is spread on roads. For example in Denmark it is recommended to use 5-10 g/m<sup>2</sup> de-icing salt at road temperatures above 0°C, 10 g/m<sup>2</sup> de-icing salt at road temperatures below 0°C (preventive method) and 15-20 g/m<sup>2</sup> de-icing salt at heavy snowfall (ice and snow control), Jacquet et al (1992). The amount of de-icing salt spread on the road is also influenced by the type of equipment used to spread the de-icing salt on the road. Examples of spreading equipment are roller spreaders, disc-wheel spreaders and fluid spreaders, Jacquet et al (1992). The type of spreading equipment that is used depends on the characteristics of the road and the availability of the equipment.

There are differences between countries in the amount of de-icing salts that are spread. In Sweden de-icing salt is spread up to 200 times per season, which means that if 10 g/m<sup>2</sup> of salt is spread each time, a total amount<sup>6</sup> of up to 2.0 kg/m<sup>2</sup> (20 ton/km) and year may be spread, Nilsson et al (2000) and Löfgren (2000). In other countries the amount of de-icing salt spread on a main road is reported to vary between 2.3-4.5 kg/m<sup>2</sup> and year (23-45 ton/km), Norway, Åstebøl et al (1996), 3.8 kg/m<sup>2</sup> and year (38 ton/km), Germany, Golwer (1991), 1.25 kg/m<sup>2</sup> and year (12.5 ton/km), USA, Salt Institute (1999), 1.3-2.0 kg/m<sup>2</sup> and year (13-20 ton/km), Denmark, Jacquet et al (1992), and 3.0-5.0 kg/m<sup>2</sup> and year (30-50 ton/km), England, Bradshaw et al (1995).

### 3.5.4 Transport of chlorides from the road surface

There is a transport of chlorides spread on the road surface to the surroundings of the road, which means that the road environment has a certain extension from the road itself. The transport can be divided into two stages, Blomqvist (1998): (i) Initial loss and (ii) Loss over time.

The initial loss is mainly dependent on the spreading method and the prevailing weather conditions. A factor that has a decisive influence on the initial loss is the moisture conditions on the road surface where a moist surface has small initial losses but larger loss over time, while a dry surface has large initial losses but smaller loss over time.

The loss over time takes place in four principal processes, described below. It is to a large extent influenced by precipitation, where the decrease of chlorides on the road surface increases during times with precipitation. The transport of chlorides to the surroundings of the road takes place in four principal transport processes, Andersen & Paulsson (1997) and Blomqvist (1998):

---

<sup>6</sup> Assuming a road width of 10 m (motorway with four lanes).

- **Drainage.** De-icing salt is soluble in water and the brine which is formed on the road is forced to the side by gravitation and/or traffic movements. In Åstebøl et al (1996) it is described that the amount of chlorides that is transported from the road by drainage during a winter may be 35%-75%, of the chlorides spread on the road.
- **Ploughing.** When the road is ploughed, salt-laden snow is pushed to the roadside.
- **Splash.** Splash is produced by the drainage system of vehicle tyres. It consists of both water and snow-slush. The splash is largely directed from the car towards the side of the road. It is characterized by relatively large droplets that are not so easily caught by wind streams around vehicles, which means that they are deposited fairly close to the road, usually maximum 4 m from the road surface, Frederiksen (2001).
- **Aerosols (Spray).** Aerosols, like splash, originate from the drainage system of tyres. The aerosols are formed when water is thrown outwards by centrifugal action tangentially from the tyre tread and it breaks down into small droplets when it hits other parts of the vehicle. In this way a wake with fog of water and dirt from the road surface is formed behind the vehicle, with an extension of up to 120 m behind the vehicle, Sandberg (1980). The amount of aerosols formed is dependent on the type and speed of the vehicles. The main cause of spray is heavy vehicles (e.g. trucks) – the amount of spray behind a passenger car is 25% of that behind a truck, Sandberg (1980). Since the spray consists of small drops it may be transported long distances from the road, distances over 100 m from the road surface have been reported, Kelsey & Hootman (1992).

The exposure of road structures to chlorides is mainly due to splash and spray from the road. The amount of splash and spray depends on the following factors, Sandberg (1980): (i) characteristics of road (texture, etc), (ii) amount of water and pollutants on the road surface, (iii) wind direction and speed, (iv) characteristics of traffic (type of vehicles, speed etc) and (v) characteristics of vehicles (tyres, spray protectors etc).

The amount of chlorides in the splash and spray can be correlated to the chloride concentration in the water on the road surface. The chloride concentration in the surface water is mainly a function of the precipitation and the spread of de-icing salt, Paulsson & Andersen (1997). During periods with precipitation the chloride concentration decreases (especially during rainy periods) and during dry periods there is an accumulation of chlorides in the surface water.

#### **Transport to the surroundings**

Several investigations have been made on how de-icing salt spread on a road is transported (horizontally and vertically) to the surroundings. The spread can be assessed by collecting deposited chlorides in containers or materials (e.g. filters, concrete etc), snow sampling, soil sampling and analyses of vegetation, Blomqvist & Johansson (1999).

Chlorides from de-icing salt spread on a road can be detected over 100 metres from the road in open landscapes with few trees surrounding the road, Eliasson (1996) and Kelsey & Hootman (1992). The transport of chlorides from roads surrounded by lots of trees is significantly smaller, since the trees “filter” chlorides from the air. In two studies it was found that around 20% of the de-icing salt spread on the road will be deposited within 3 m from the road surface, Dragstedt (1980), and 25% will be deposited within 7 m from the road surface, Pedersen & Fostad (1996). In Blomqvist & Johansson (1999) it was found that 20%-63% of the de-icing salt spread on a road is transported by air and deposited 2-40 m from the road. Blomqvist & Johansson (1999) also found that the

deposition of chlorides was influenced by the wind conditions, where the deposition was larger on the eastern side of the road with westerly winds, cf. figure 3.17.

McBean & Al-Nassri (1987) have studied how chlorides are dispersed as de-icing salt on a road is spread to the surroundings as a function of the speeds of traffic. The study was made by taking snow samples at different distances from the road surface near roads with different speed limits (50, 60, 70, 80 and 100 km/h). The snow samples have been analysed for chloride content. These results are supported by Langille (1976), who has studied chloride content in soil samples at different distances from a highway in USA. Langille (1976) also found that there is an increase in chlorides in the soil during a salting season. In an investigation by Burton (1992) the transport of chlorides from the roadway was found to depend on the speed of the traffic. Burton found that at speeds of 50-60 km/h and 80-100 km/h the maximum amount of salt was deposited within 1.5-2 m and 8-10 m from the road surface respectively. However, no information is given about the traffic intensity.

The results from the study of McBean & Al-Nassri (1987) are presented in figure 3.17 together with data from Blomqvist & Johansson (1999). The data from McBean & Al-Nassri (1987) are labelled with speeds (50 km/h, 60 km/h etc) and the data from Blomqvist & Johansson (1999) with “Älgviken” and “Bankekind”. The indexes **E** (east) and **W** (west) denote on which side of the road the sample has been taken. In the investigation by Blomqvist & Johansson (1999) the speed limit has been 90 km/h on the studied roads.

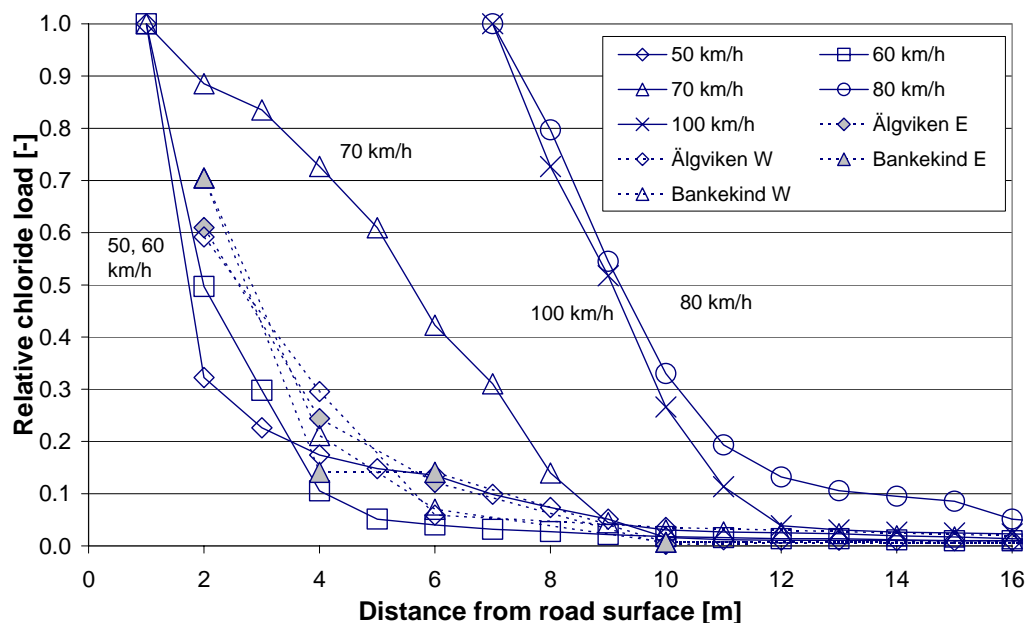


Figure 3.17: Transport of chlorides along roads with different speed limits. Based on data from McBean & Al-Nassri (1987) (continuous lines), Blomqvist & Johansson (1999) (broken lines).

From figure 3.17 it can be seen that at low speeds (<60 km/h) more than 90% of the salt is deposited within 4 metres from the road. At higher speeds (>60 km/h) the salt is transported longer distances from the road. The reason that no data for speeds of 80 km/h and 100 km/h are available for distances less than eight metres from the road surface is that McBean & Al-Nassri only made measurements for larger distances. Furthermore it

can be observed that the chloride load, up to distances of sixteen metres from the road surface, is larger for speeds of 80 km/h than for speeds of 100 km/h. However, at longer distances from the road surface the relative chloride load is larger for speeds of 100 km/h. The larger relative chloride load at speeds of 80 km/h can be probably be explained by differences in the exposure conditions (e.g. weather conditions) and measurement uncertainties.

The influence of traffic intensity has been studied by Pedersen & Fostad (1996). Pedersen & Fostad found that a high traffic intensity and a speed limit of 90 km/h resulted in a transport of salt 12-16 m from the road, while a low traffic intensity and a speed limit of 80 km/h resulted in a transport of salt 8 m from the road surface.

Thus there is a horizontal transport of chlorides from the road to the surroundings. It has been shown that the extent of the transport depends on the speeds and intensity of the traffic, the characteristics of the road and the weather conditions around the road. It seems reasonable to differentiate the transport of chlorides from roads depending on the traffic intensity and speeds.

The transport in the vertical direction from the road surface has been studied by Tang & Utgennant (1998) and Wirje & Offrell (1996). Tang & Utgennant have collected salt water from aerosols in plastic containers at different heights above the roadway and analysed the water for chloride content. Wirje & Offrell have studied the absorption of chlorides in mortar specimens exposed at different heights above the roadway. Both exposures have been made approximately 3 m from the traffic. The speeds on the motorway are above 100 km/h, which means that the exposure has been made in a zone with high chloride load, cf. figure 3.18. The results from these studies are presented in figure 3.18, where the experimental setup used by Tang & Utgennant is also shown.

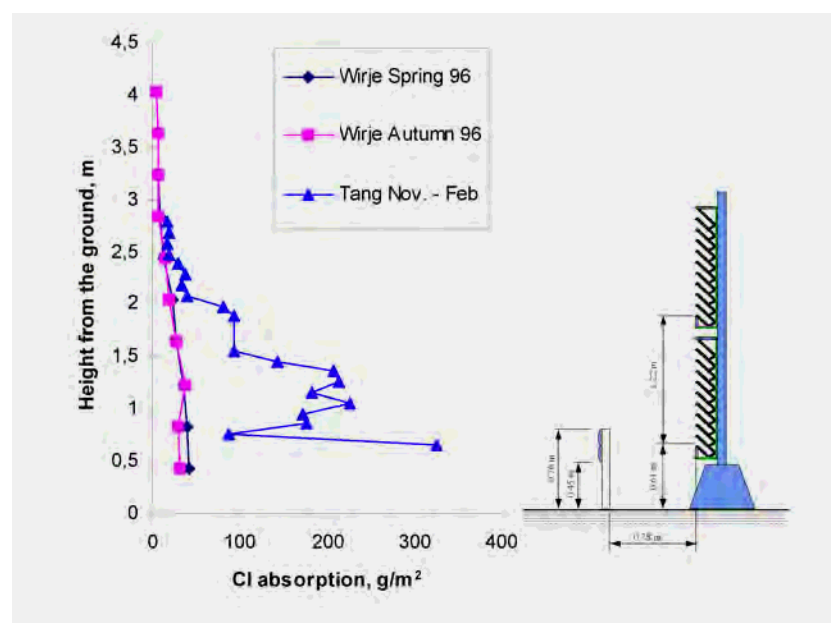


Figure 3.18: Chloride exposure on a vertical surface along the motorway Rv40 outside Borås. During the winter 1995-1996 1432g/m<sup>2</sup> of sodium chloride spread on the road (869g/m<sup>2</sup> chlorides). Data from Wirje & Offrell (1996) and Tang & Utgennant (1998).



From figure 3.18 a clear height-dependency in the exposure to chlorides can be observed. Chlorides are present up to a height of some 3 m above the roadway. The sheltering effect from the collision barrier can be observed from the measurements by Tang & Utgenannt, where a reduction in the chloride concentration can be observed at a height of approximately 0.7 m above the road surface. Furthermore the available amount of chlorides (as splash and spray from the traffic) and the amount of chlorides that actually has been absorbed by the mortar can be observed if the measurements by Tang & Utgenannt (1998) and Wirje & Offrell (1996) are compared. The chlorides that have not been absorbed by the mortar has been washed away, either directly or during the parts of the year when no de-icing salt is spread.

### 3.5.5 Response by concrete structures along roads

#### General

It is clear that the exposure of bridges to chlorides takes place with a number of different mechanisms. One way to determine the significance of these mechanisms and the most exposed parts of bridges is to study where damage, due to deterioration of the concrete, has occurred on existing structures. This has been done in a study by Wallbank (1989), where 200 motorway bridges in Great Britain have been examined with respect to degradation, due to reinforcement corrosion, freeze/thaw actions, AAR etc. It was found that exposure to chlorides takes place in three principal exposure mechanisms:

- Leakage of chlorides through joints. Chloride-contaminated slush on the road surface may leak through joints and reach for example the underside of a slab.
- Splash from passing traffic. Splash from the road may hit surfaces on structures that are facing towards the traffic.
- Spray from passing traffic. Spray from the road may follow air streams and be deposited on structures along the road. Since the spray follows air streams this means that chlorides may reach surfaces on the structure that are not directly facing towards the traffic.

Wallbank (1989) also found differences in deterioration between bridges in the northern and southern part of Great Britain. This difference was supposed to occur due to differences in the environmental conditions between different parts of Great Britain, with the result that more de-icing salts were spread in the northern part than in the southern part. Wallbank summarizes that the chloride ingress into a road bridge depends on several factors, e.g. geographical location of the bridge, the history of maintenance for the bridge, exposure to rain, the amount traffic on the road and the amount of de-icing salt spread on the road.

#### Chloride conditions

In Frederiksen (2001) it is proposed to divide the exposure environment for a road bridge into two environments: (i) **dry**, which are sheltered from rain and direct splash from the road surface, and (ii) **wet**, which are exposed to rain and direct splash from the road surface. These environments are further divided into three principal exposure zones:

- **Dry splash zone (DRS).** This zone is closer than 4 m to the traffic and sheltered from rain. Exposure to chlorides mainly takes place in the form of splash from passing traffic. Examples of structural parts exposed in this zone are columns.
- **Wet splash zone (WRS).** This zone is closer than 4 m to the traffic and exposed to rain. Exposure to chlorides mainly takes place in the form of splash from passing traffic. Examples of structural parts exposed in this zone are edge beams.

- **Distant road atmosphere (DRA).** This zone is more than 4 m from the traffic and is both exposed and sheltered against rain and direct splash from the traffic. Exposure to chlorides mainly takes place in the form of spray from passing traffic.

A similar division is proposed in Svenska Betongföreningen (2003), see figure 3.19. This report gives guidance for the use of the new concrete standard EN 206-1, in Sweden called SS-EN 206-1. In figure 3.19 surfaces in zone I are exposed to splash while surfaces in zone II are exposed to spray from the road. The indexes within brackets show the exposure classes in EN 206-1. The division presupposes that the structure is constructed and maintained in a proper way, e.g. without leakage in the drainage system etc.

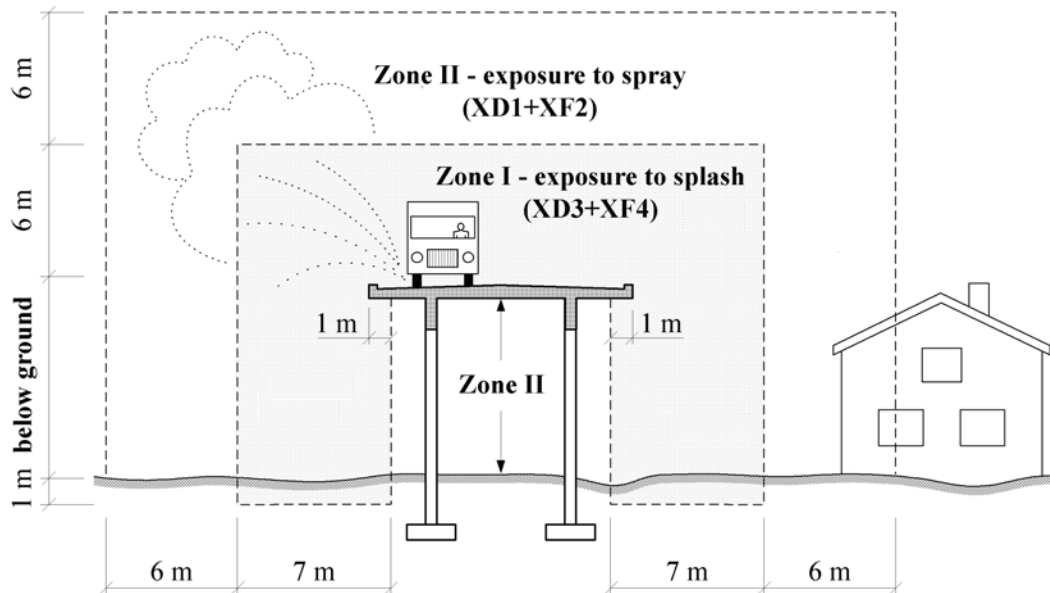


Figure 3.19: Division of the road environment into different exposure zones. Svenska Betongföreningen (2003).

Two of these zones, viz. dry and wet splash zones, can be identified in data from Wirje & Offrell (1996), where the amounts of chlorides absorbed in mortar specimens exposed at different heights above the road have been studied, see figure 3.20. The specimens have been exposed along a motorway on an edge beam (wet splash zone) and on a column between two lanes (dry splash zone). It should be noticed that the data in figure 3.20 come from only one winter season of exposure (winter 1995-1996) and one location, which means that other parameters, e.g. car speeds and type of traffic, are kept constant.

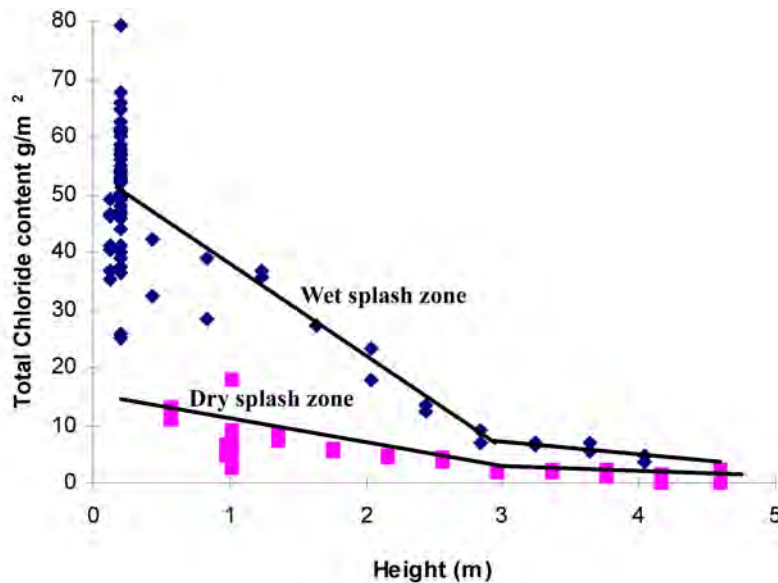


Figure 3.20: The amount of chloride absorbed in mortar specimens close to highway Rv40 in Sweden during the winter 1995-1996 as a function of height above the road for dry and wet road structures. Data from Wirje & Offrell (1996).

In figure 3.20 the height dependency in the absorption of chlorides can clearly be seen. The mortar disks analysed by Wirje & Offrell (1996) have been exposed during five additional seasons to investigate the time dependency of the chloride penetration, results are presented in Fagerlund & Svärd (2001). Some of the findings of Fagerlund & Svärd (2001) are presented in figure 3.21. The chloride penetration into the mortar disks has been analysed at three different exposure times: (i) after one winter, (ii) after one year (winter + summer) and (iii) after five years (five years + half summer).

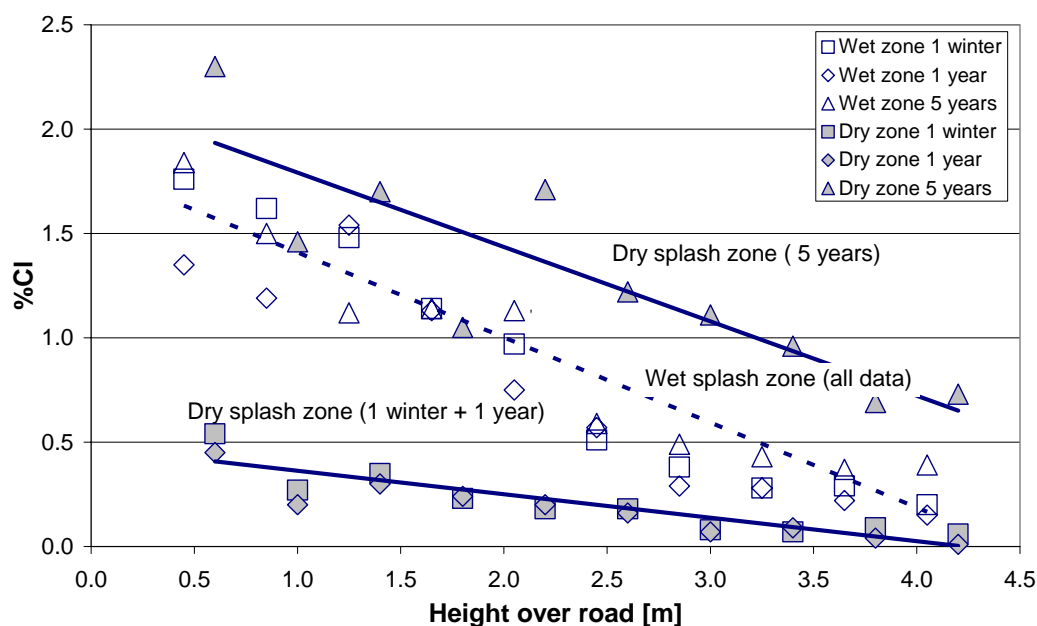


Figure 3.21: The total amounts of chlorides absorbed in the mortar disks at different exposure times. Based on data from Fagerlund & Svärd (2001).

From figure 3.21 a difference in the chloride ingress in the dry and wet zones can be observed. The height dependency in chloride ingress can also clearly be seen. The mortar disks exposed in the wet zone show no increase in total amount of penetrating chlorides and maximum chloride concentration. However, the depths at which the maximum chloride concentration can be observed have increased with time, which means that chlorides have been transported into the disks. On the contrary, the mortar disks exposed in the dry zone show an increase in chloride concentration with time. These latter findings are supported by Weber (1982).

### Dry road environment

Surfaces in the dry road environments are, as mentioned earlier, not exposed to direct rain. Sometimes the relative humidity may be lower than in the surrounding air due to radiation effects from sun at low altitude.

The exposure to chlorides in the dry road environment takes place mainly as splash and spray from the traffic. Since de-icing salt is spread during the night or early morning the most exposed surfaces are usually the ones facing towards the lanes with the heaviest traffic in the morning. However, this is not always the case as described by Volkwein et al (1986), Andersen (1997) and Lindvall & Andersen (2000). Instead high chloride loads have been found on surfaces facing away from the lanes with heavy traffic in the morning or on the leeward side. This is illustrated in figure 3.22, where chloride ingress profiles from a motorway bridge north of Copenhagen, reported by Andersen (1997), are shown. The profile with index S faces towards the traffic leaving Copenhagen (high speeds in the morning) and the profiles with index N face towards the traffic to Copenhagen (low speeds in the morning). The profiles indexed with diamonds should be compared, since these are taken from the same height above the roadway (1.3 m), but in different orientation directions. All profiles have been taken in May, i.e. just after the season when de-icing salt is spread.

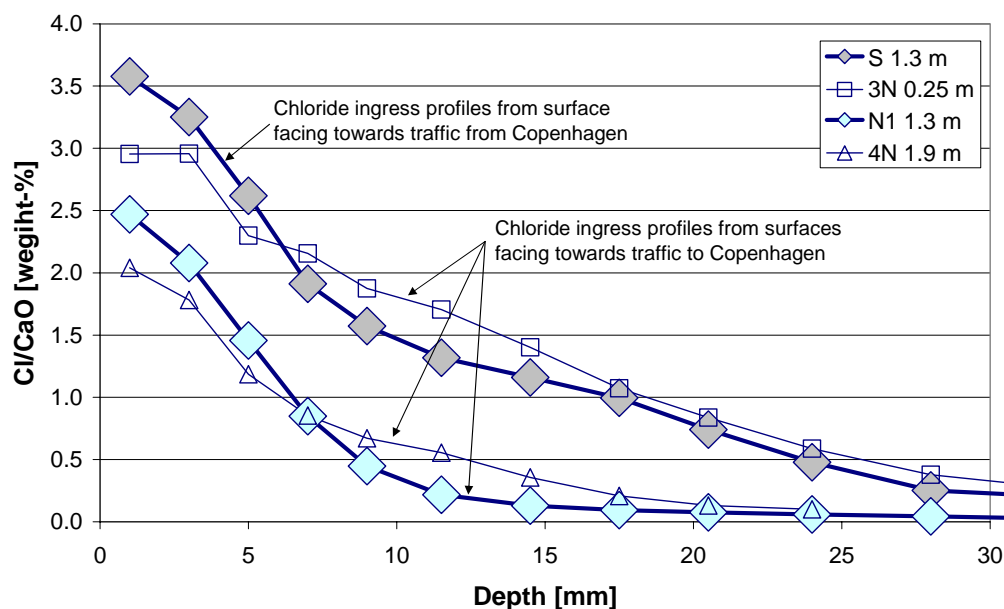


Figure 3.22: Chloride ingress measured on two opposite sides of column. Based on data from Andersen (1997).

From figure 3.22 it can be seen that the chloride ingress into the surface facing towards the traffic leaving Copenhagen (index S) is significantly higher compared with the surface facing towards the traffic to Copenhagen (index N). One explanation for this is that the car speeds in the lanes with heaviest traffic in the morning are low (commuter traffic towards Copenhagen), due to congestions, resulting in little splash and spray and thus low chloride ingress into surfaces facing towards this traffic. However, on surfaces facing towards the lanes in the opposite direction, with high car speeds but less traffic, the chloride ingress is significantly higher. Airborne chlorides may also be deposited on the leeward side of for example columns, where they will not be washed away, since the surface is sheltered from wind-driven rain.

### **Wet road environment**

Structural parts in the wet road environment are, as mentioned earlier, exposed to direct rain. However, there may also be large variations in the temperature and moisture conditions due to radiation effects. During clear nights the equivalent surface temperature, especially for horizontal surfaces, may be significantly lower than the air temperature, and thus the equivalent surface humidity higher than the surrounding air humidity. There may also be differences in temperature and humidity conditions between surfaces depending on the orientation of the surfaces.

The exposure to chlorides on surfaces in wet road environments takes place as a combination of ploughed salt-contaminated slush from the road surface and splash and spray from the traffic. Since some surfaces may be horizontal, e.g. on edge beams, ponding of salt solution may occur on the surface, resulting in high chloride load. Furthermore surfaces in the wet road environment are often fairly close (at least in the vertical direction) to the roadway, which means that the wet parts of a structure often have the most severe chloride exposure. However, the surfaces are also exposed to direct rain, which means that the chlorides may also be washed away. This can be seen on the shape of measured chloride ingress profiles, if profiles from the dry and wet road environment on the same bridges are compared, see figure 3.23. The maximum chloride contents in the profiles have been shaded grey. The profiles have been taken in November or December, i.e. just before or in the beginning of the season when de-icing salt is spread.

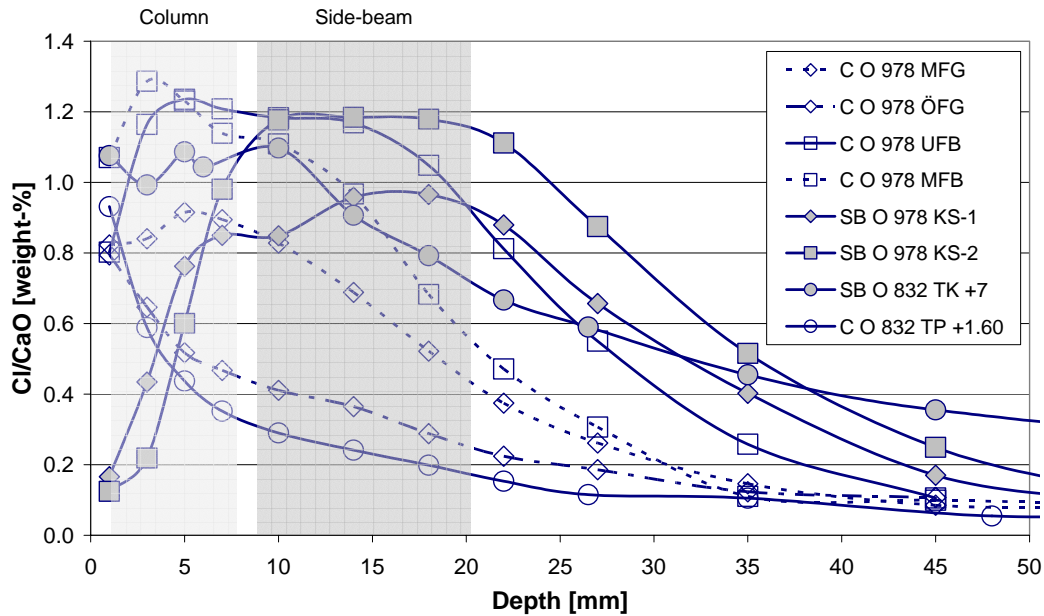


Figure 3.23: Measured chloride ingress profiles from columns (C – non filled symbols) and edge-beams (SB – filled symbols). Lindvall & Andersen (2000).

As seen in figure 3.23 the maximum chloride contents in the profiles are found at a depth of 1-8 mm (columns) and 9-20 mm (edge beams). Furthermore in the outer parts of the profiles from edge beams on bridge O 978 the chloride content decreases rapidly. This indicates that the washout of chlorides from the surface near region of the concrete is larger from edge beams than from columns. The larger depth for the maximum chloride content indicate a more severe exposure to chlorides, e.g. due to ponding of salt solution on horizontal surfaces.

### Moisture conditions

The moisture conditions in concrete structures on roads have been studied by Andersen (1997) and Lindvall & Andersen (2000). In figure 3.24a (RH) and 3.24b ( $S_{cap}$ ) some measurements of the moisture conditions in concrete structures along roads in Denmark and Sweden are presented. The non-filled symbols represent data from edge beams (wet road environment) and filled symbols represent data from the columns supporting bridge slabs (dry road environment). It should be noticed that the shape and level of the moisture profiles depend on the exposure conditions (varying over the year), which means that the time for sampling has an influence. In figure 3.24a and 3.24b the Swedish profiles (index N and O etc) are taken in November and December and the Danish profiles (index 10-, 14-, 20- and 30- etc) are taken in July.

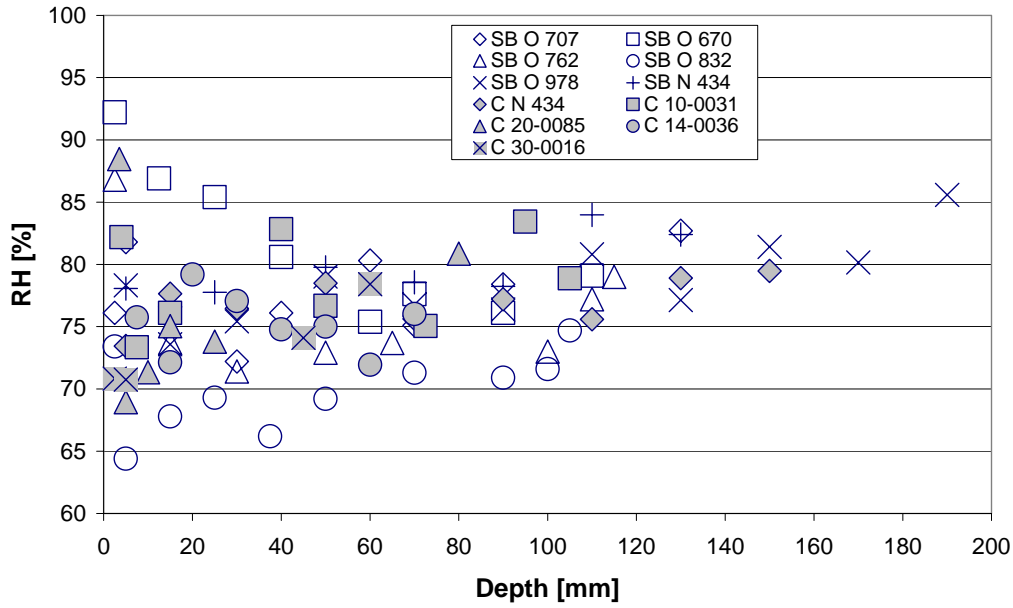


Figure 3.24a: Moisture conditions (RH) in columns (filled symbols) and side-beams (non-filled symbols). Data from Andersen (1997) and Lindvall & Andersen (2000). OPC-concrete  $w/b=0.40-0.50$ .

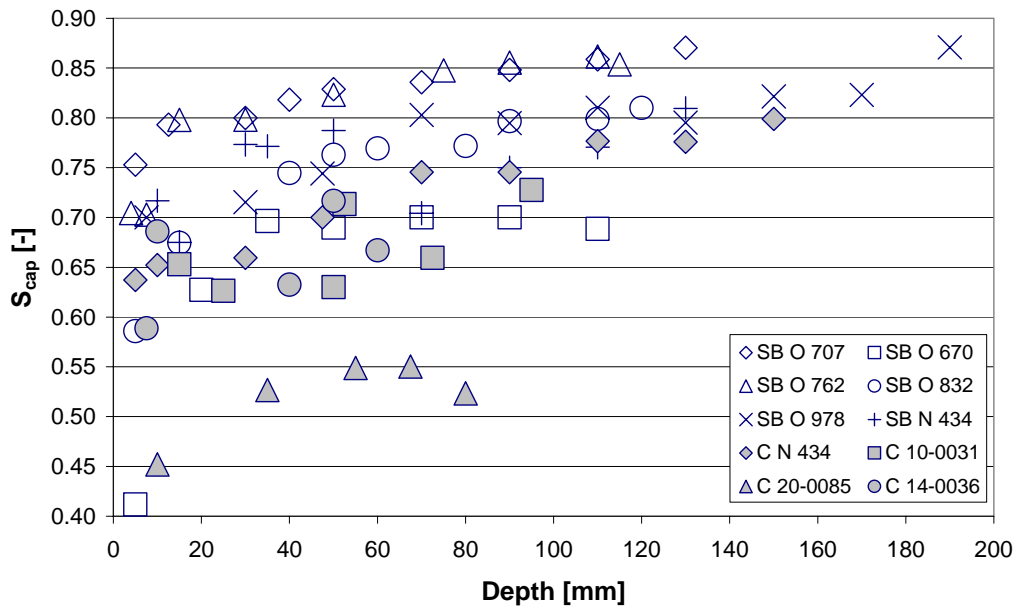


Figure 3.24b: Moisture conditions ( $S_{cap}$ ) in columns (filled symbols) and side-beams (non-filled symbols). Data from Andersen (1997) and Lindvall & Andersen (2000). OPC-concrete  $w/b=0.40-0.50$ .

From figures 3.24a and 3.24b it can be seen that the moisture conditions are fairly stable in the concrete, except in the surface near region (0-40 mm), where the RH varies between 70-85 and  $S_{cap}$  varies between 0.65-0.85. The low values of  $S_{cap}$  for profile C 20-0085 can be explained by the fact that this structure is constructed with a concrete with higher  $w/b$  than the other structures ( $w/b \approx 0.70$ ).

### 3.5.6 Qualitative model

From the description of the road environment it is obvious that the environmental conditions and their variations on structures built along roads are not trivial. The actions are influenced by a number of factors, e.g. characteristics of traffic, distances from and orientations towards roadways. Thus, to take all these factors into account and consider the variations in a proper way the environmental actions should be expressed as surface conditions.

The environmental conditions in road environments have been summarised in a qualitative model, see figure 3.25. The model is based on the general model presented in figure 3.1.

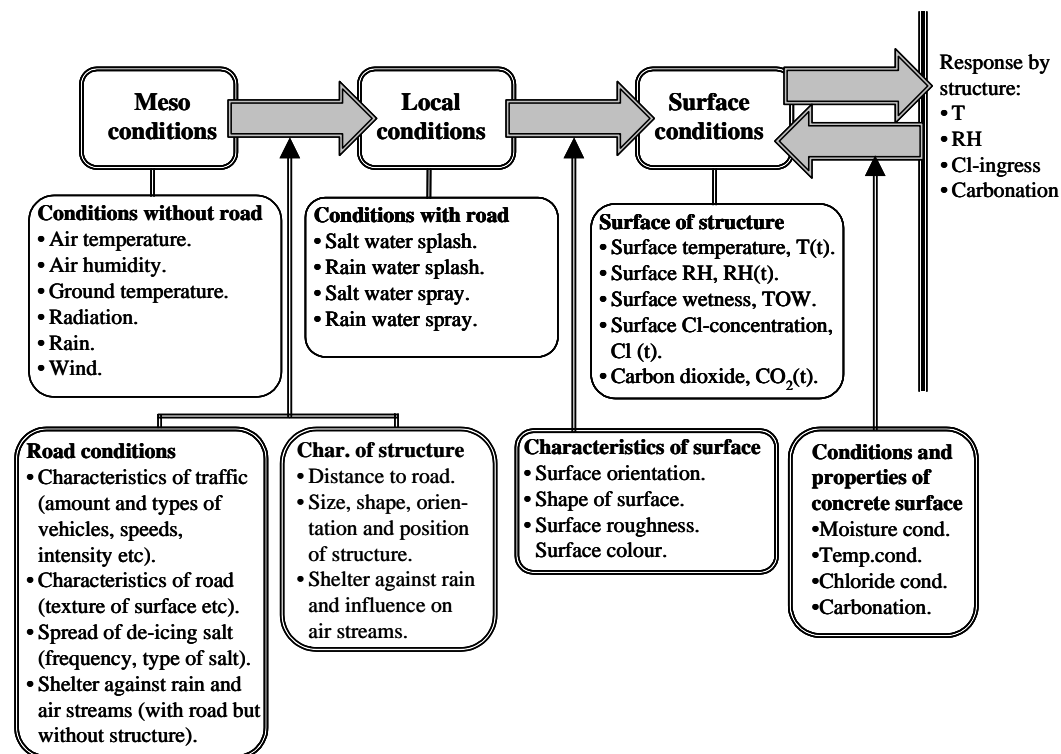


Figure 3.25: Qualitative model for environmental actions on concrete structures exposed in road conditions.

The starting point for the model in figure 3.25 is information about the meso conditions, without any influence from the road. These conditions can be described in terms of air temperature and humidity, ground temperature, radiation, rain and wind conditions. The influence of the road is incorporated in the description of the local conditions, together with the influence of the structure. The influence of the road can be described in terms of characteristics of the traffic (amount and type of vehicles, traffic speeds and intensity etc), characteristics of the road (texture of road surface etc), spread of de-icing salt (frequency, type of salt, prevailing weather conditions etc) and information about the surroundings of the road (with road but without structure – e.g. shelter against rain and air streams etc). The influence of the structure can be described in terms of distance from the road, size, shape and orientation of the structure and possible shelter against rain and influence on airstreams. Finally the surface conditions can be derived on the basis of information about the surface characteristics (orientation, shape and roughness) together with the conditions and properties of the concrete surface (moisture, temperature and chloride conditions and carbonation). The conditions and properties of the concrete surface may for example



## Chapter 3    Environmental actions and response

influence the surface roughness, due to frost action (following from temperature conditions), or surface colour, due to variations in moisture conditions etc.



## **4    Field study – Marine conditions**

In this chapter a field study, where the environmental response to chloride ingress into identical concrete specimens exposed in different marine environments has been studied, is presented. The background to the programme is given, the programme is briefly described, the results are presented and discussed and finally conclusions are drawn. A complete presentation of the exposure programme and the results is given in Lindvall (2003).

### **4.1    Background**

Usually studies of the environmental response to chloride ingress into concrete, of a certain composition, are made by investigating concrete exposed at one, and in some rare cases two, locations. The chloride ingress is measured in concrete, which means the results are not only influenced by the exposure conditions but also by the concrete properties, resulting from the composition and manufacture of the concrete. Additionally the method used to measure the chloride ingress may influence the results, where the measured chloride ingress may be different with different methods. Thus it is difficult to compare chloride ingress measured in different concretes exposed at different locations, since the chloride ingress will be influenced by an interaction of the concrete properties and the exposure conditions and the analysis method. Furthermore the chloride ingress is usually only determined at single points, which means no assessment of the scatter in chloride ingress can be made.

Based on this an exposure programme has been made to investigate differences in exposure conditions between different marine exposure locations. The purpose of the exposure programme has been to determine how different exposure environments influence the environmental response to chloride ingress into concrete exposed in marine conditions. This has been done by exposing concrete specimens made from one single concrete composition at twelve different locations around the world and, at the end of the exposure period, analysing the chloride ingress into the concrete. The exposure conditions have been registered as chloride concentrations and temperatures in the seawater and if appropriate the position in relation to the mean water level and the extent of tidal actions. Parallel with the field exposure specimens have been exposed in the laboratory in salt solutions of two different chloride concentrations and two different temperatures.

In the exposure programme, the concrete specimens have been exposed in submerged conditions at all locations. The submerged conditions have been chosen to get a well-defined exposure, where only the chemical composition and the temperature of the seawater vary. In other marine conditions other parameters, e.g. position in relation to the surface of the water and effects from splash from breaking waves, will also significantly influence the resulting chloride ingress. However, at one location specimens have also been exposed in tidal conditions so that submerged and tidal conditions may be

compared. Thus, in total specimens have been exposed in thirteen different field and four different laboratory environments. Between four and six specimens have been exposed in each exposure environment to enable statistical analysis of the measured chloride ingress to be performed.

## 4.2 Exposure programme

### 4.2.1 Materials and specimens

The concrete composition used in the exposure programme is presented in table 4.1. To minimise any effects due to variations in the materials used for the concrete all castings have been made with cement from only one delivery from the cement factory, aggregates from the same two deliveries (sand and gravel) and air entraining agent from only one bottle.

Table 4.1: The concrete composition used in the exposure programme.

Material	Amount [kg/m <sup>3</sup> ]	Density [kg/m <sup>3</sup> ]	Volume proportion [-]
Cement (CEM I 42.5 BV/SR/LA)	450	3105	0.143
Sand 0-8 mm	938	2650	0.354
Stone 8-16 mm	745	1650	0.281
Water <sup>+</sup>	180	1000	0.180
Air <sup>*</sup>	-	-	0.045

CEM I 42.5 BV/SR/LA – Swedish SRPC (Sulphate Resistant Portland Cement – Anläggningscement Portland Degerhamn). The chemical composition of this cement can for example be found in Sandberg et al (1998) in TABLE 1 – “*Sulfate resisting Portland cement (SRPC)*”.

<sup>+</sup> : w/b=0.40.

<sup>\*</sup> : The air content in the concrete is regulated by adding AEA (Cementa L 14) – dosage 0.030 % of cement weight.

The concrete specimens used in the exposure programme measure 150x150x75 mm<sup>3</sup>. The specimens were cast in moulds used to cast standard cubes measuring 150x150x150 mm<sup>3</sup>, without the partition walls. This means that beams measuring 150x150x470 mm<sup>3</sup> (each partition wall is approximately 10 mm thick) were cast. After casting the concrete was cured for three days in the moulds, before de-moulding, and then wrapped in a plastic cover and stored in a controlled climate room (+20°C and 50%RH) to an age of at least 28 days. After the curing, the concrete beams were sawn into specimens, with a water-cooled diamond saw, and then finally stored in the controlled climate room (+20°C), under a plastic cover to prevent drying, before exposure. During transport to the exposure locations the specimens were also wrapped in plastic to prevent drying. Consequently the initial conditions before exposure of the concrete were self-desiccation for at least a month

### 4.2.2 Field exposure

The specimens have mainly been exposed in marine submerged but also at one location in marine tidal conditions (La Rochelle). The concrete specimens were exposed at twelve locations around the world. Generally the exposure started and ended in late summer or autumn at all locations, i.e. August-November in Europe and January-April in Tasmania. However, in Kjøpsvik the exposure started and ended in late October and early November

respectively. The exposure at all location was started in 2000 and ended in 2001. The exact dates for the beginning and end of the exposure at each location are given in Lindvall (2003). The geographical locations of the different exposure locations are shown in the map in figure 4.1.



Figure 4.1: The geographical locations of the exposure locations in the exposure programme. Map downloaded from Texas University (2003).

The exposure locations Dubai (3) and Isle of the dead (7) are outside the map in figure 4.1.

Information about each exposure location is given in the following list (each location is listed with the name of the closest town, country, name of the ocean/sea and exposure time):

1. **Banyuls sur Mer**, France. Exposure in the Mediterranean. Ten specimens have been exposed in submerged conditions in an aquarium (water taken from 8 m depth in the sea) and at sea (depth 24.5 m) – five specimens at each location. Unfortunately one specimen disappeared during the exposure in the aquarium. The exposure time has been 376 days.

2. **Cascais**, Portugal. Atlantic Ocean. Ten specimens have been exposed in submerged conditions in an old lobster farm at a depth of approximately 1 m. The exposure time has been 378 days.
3. **Dubai**, United Arab Emirate. Exposure in the Persian Gulf. Five specimens have been exposed in submerged conditions in a harbour at a depth of approximately 1 m. The exposure time has been 370 days.
4. **Eastern Scheldt**, the Netherlands. Exposure in the English Channel/North Sea. Five specimens have been exposed in submerged conditions in a harbour hanging from a floating pontoon at approximately 1 m depth. The exposure time has been 378 days.
5. **Hirtshals**, Denmark. Exposure in the North Sea. Two specimens have been exposed in submerged conditions in a harbour at a depth of approximately 1 m. Originally five specimens were exposed but unfortunately three specimens disappeared during the exposure. The exposure time has been 391 days.
6. **Hvalfjörður**, Iceland. Exposure in the Atlantic Ocean. Five specimens have been exposed in submerged conditions in a harbour at a depth of approximately 1 m. The exposure time has been 358 days.
7. **Isle of the dead**, Australia. Exposure in the Pacific Ocean. Three specimens have been exposed in submerged conditions at a depth of approximately 1 m and one specimen has been exposed in the lower part of the tidal zone. Originally five specimens were exposed in submerged conditions but currents moved one specimen to the tidal zone and one specimen disappeared during the exposure. The exposure time has been 403 days.
8. **Kjøpsvik**, Norway. Exposure in the Norwegian Sea/Atlantic Ocean. Five specimens have been exposed in submerged conditions in a harbour at a depth of approximately 1 m. The exposure time has been 372 days.
9. **Källhamn**, Sweden. Exposure in the Baltic Sea. Five specimens have been exposed in submerged conditions in the sea at a depth of approximately 1 m. The exposure time has been 364 days.
10. **La Rochelle**, France. Exposure in the Bay of Biscay/Atlantic Ocean. Ten specimens have been exposed in two harbours – five specimens have been exposed in submerged conditions hanging from a floating pontoon at a depth of approximately 1 m and five specimens have been exposed in tidal conditions. The exposure in the tidal conditions has been approximately at the mean sea level, which means that specimens have been exposed to seawater approximately 12 hours per day. The exposure time has been 379 days.
11. **Skanör**, Sweden. Exposure in Öresund. Five specimens have been exposed in submerged conditions at a depth of approximately 1 m. The exposure time has been 377 days.
12. **Träslövsläge**, Sweden. Exposure in Kattegat. Six specimens have been exposed in submerged conditions at a depth of approximately 0.5 m. The exposure time has been 387 days.

The specimens in marine submerged conditions have been exposed either in baskets or buckets with holes, to ensure good water circulation, or on the seabed. The baskets and buckets have been wrapped in net and fastened with ropes to jetties or similar. The baskets (one at each location) have been used in Cascais and Eastern Scheldt and the buckets (two at each location) at all other locations, except in Källhamn and La Rochelle (tidal exposure) and in the aquarium in Banyuls sur Mer, where the specimens were placed directly on the seabed and the bottom of the aquarium respectively. The buckets and baskets used in the exposure programme are shown in figure 4.2.



*Figure 4.2: The buckets (left) and baskets (right) used to expose the concrete specimens.*

During the exposure the surfaces of the concrete specimens were not cleaned from marine growth. The severity of the growth varies between the different exposure sites, but generally specimens exposed in locations with high water temperatures had more marine growth than the specimens exposed in locations with low water temperatures. After the exposure the specimens were cleaned from marine growth before they were sent to the laboratory.

#### **4.2.3 Laboratory exposure**

Parallel with the field exposure specimens have been exposed in the laboratory. The exposure has been in submerged conditions in salt solutions prepared with de-ionised water and sodium chloride (NaCl). The salt solutions had two different chloride concentrations, 8.3 g NaCl/l (5 g Cl<sup>-</sup>/l), representing the conditions in the Baltic Sea, and 33.0 g NaCl/l (20 g Cl<sup>-</sup>/l), representing the conditions in the Atlantic Ocean. The salt solutions had two temperatures: +7°C and +20°C. The specimens were exposed in plastic containers holding four specimens each, filled with 15 litres of salt solution. The pH in the exposure solutions was monitored and when it exceeded pH 11 in any of the containers the solution was changed in all containers.

#### **4.2.4 Exposure conditions – field study**

The exposure conditions have been investigated in terms of chemical composition and temperature of the exposure water. In figures 4.3a and 4.3b the temperature and chloride concentrations of the seawater are presented for the different exposure sites. The names of the locations have been abbreviated due to limitations of space. The water temperatures are given as monthly mean values at the different exposure locations at the water surface, i.e. depth 0.0 m. Data on the water temperatures have been taken from the Levitus seasonal database. The water temperature varies with depth, the temperatures being generally slightly higher close to the surface, due to warming from solar radiation.

The chloride concentration in the seawater has been analysed from water samples taken from each exposure site. Each column in figure 4.3b represents a measurement from one water sample taken during the exposure. The time intervals for the water samples are not the same for the different exposure sites, which means that the variations in chloride content between the different locations cannot be directly compared. The seawater also contains other substances, e.g. sulphates, magnesium etc, Mehta (1991). The concentrations of these substances can be related to the concentration of chlorides in the seawater, Andersson (2001), where high concentrations of chlorides also imply high concentrations of other substances in the seawater, like sulphates etc.



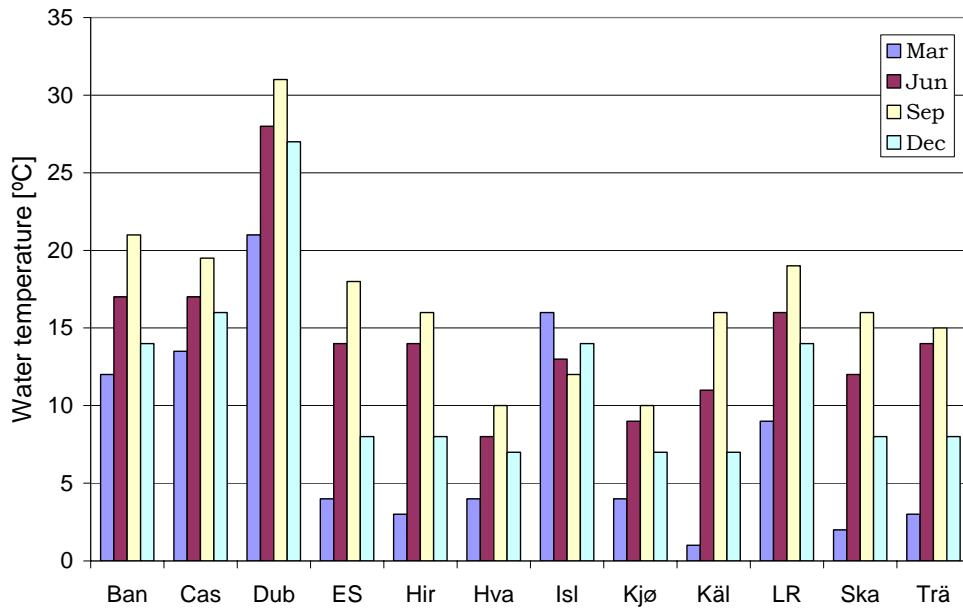


Figure 4.3a: Yearly variations in water temperatures for the exposure locations. Data from Levitus seasonal database.

From figure 4.3a it is clear that the temperature of the seawater varies over the year, with the temperatures high during the summer and low during the winter.

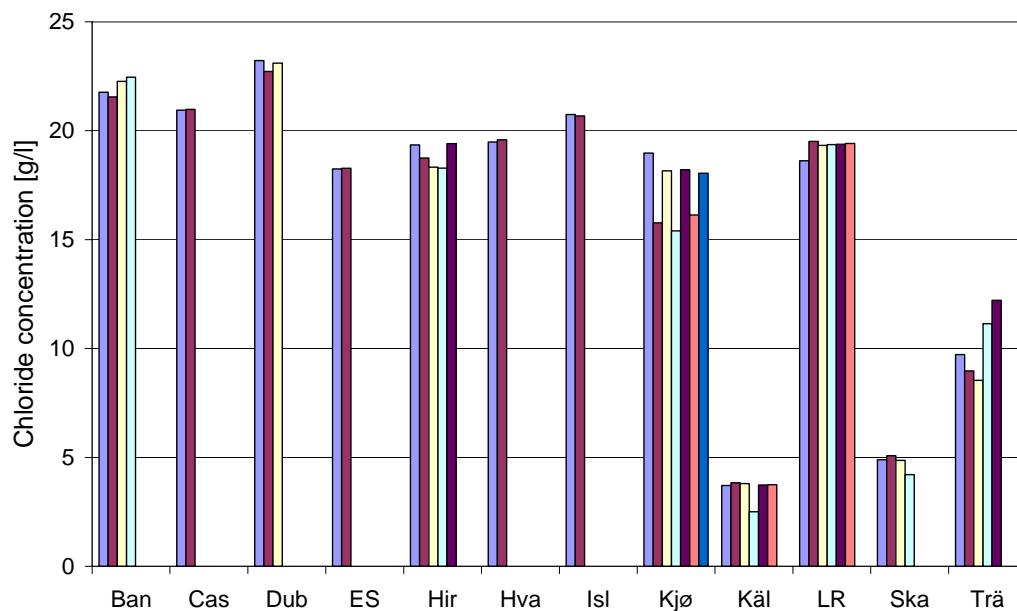


Figure 4.3b: Variations in chloride concentration in the seawater at the exposure locations.

In figure 4.3b it can be seen that the measured chloride concentrations in the seawater are fairly constant for most of the exposure locations. In the oceans, the chloride concentration is approximately 20 g/l. However, in confined seas, e.g. the Baltic Sea (Källhamn), Öresund (Skanör) and Kattegat (Träslövsläge), the chloride concentration may vary depending on the direction of currents and winds and the time of year (effects from melting of snow in springtime etc). Furthermore in fjords, with limited access to the



open sea, as in Kjølpsvik, the chloride concentration varies over the year, with the concentration lower during the spring due to melting water from snow. This is further discussed in section 4.5.4.

### 4.3 Measurement techniques

The environmental response has been determined in terms of chloride ingress profiles where the quotient of chloride and cement content is given as a function of depth. The calcium content can be correlated to the cement content in the concrete, since Swedish concretes usually do not contain aggregate containing calcium. The chloride and calcium content has been determined by wet chemical analysis on dust samples from profile grinding.

#### 4.3.1 Preparation of samples

To get a well-defined surface, without any effects from the type of mould etc, only chloride ingress through sawn surfaces on the specimens has been studied. Since the specimens have been sawn from beams almost all specimens have two exposure surfaces.

After the exposure all specimens were cleaned from marine growth and transported to the laboratory. Before the transport the specimens were dried in the air, to let surface water dry away, and then packed in plastic bags which were sealed to prevent uncontrolled drying and an adverse transport of chlorides. In the laboratory, cores (diameter 75 mm) were drilled from the centre of each sawn surface and powder samples were collected from the cores at different distances from the exposure surface by means of thorough profile grinding. The profile grinding was carried out in a modified lathe equipped with a drilling machine and a diamond drill. The schematic set-up of the equipment is shown in figure 4.4. The powder was collected on a sheet of paper below the drill. The sampling intervals increase with increasing depth from the surface, i.e. small intervals in the surface-near region (0-10 mm) and larger intervals further in from the surface. The depth of each sampling point was measured with an accuracy of 0.5 mm.

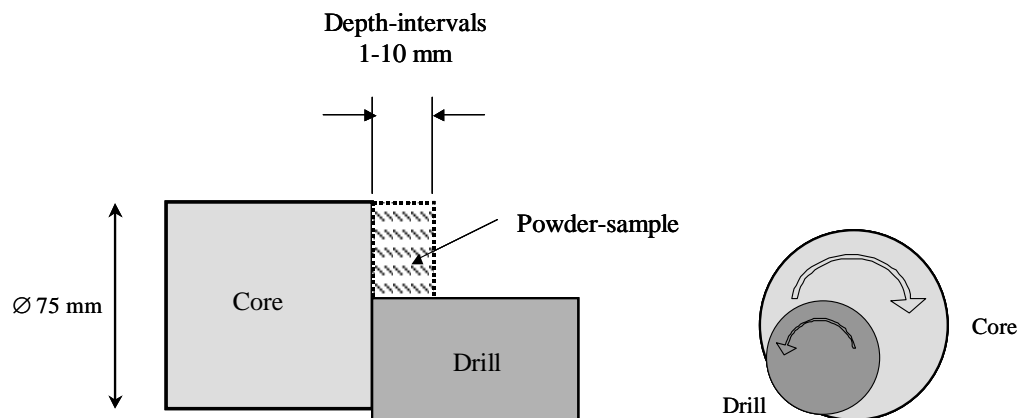


Figure 4.4: Schematic set up of the equipment used for profile grinding (drilling machine).

The powder samples from the cores were collected on sheets of paper and crushed until they passed through a 0.125 mm sieve. After that the powder was placed in paper envelopes and dried at 105°C for at least 24 hours. Finally the powder samples were stored in airtight containers with desiccants to prevent them absorbing moisture before the chemical analysis.

### 4.3.2 Laboratory analysis

The powder samples were analysed for acid-soluble chlorides and calcium. A sample of approximately 1 g was taken from each envelope and weighed to an accuracy of  $\pm 0.001$  g. The sample was diluted in 50 ml hot (boiling) de-ionised water and 5 ml concentrated nitric acid ( $\text{HNO}_3$ ) and agitated frequently for a period of 20 minutes. Finally the solution was filtered on a pre-wetted filter, which was washed 4-6 times with de-ionised water until the total volume of the filtrate was 100-110 ml. The chloride and calcium contents were analysed with potentiometric titration. The method is similar to the one presented in AASHTO T 260-84 (1984), except that the sample was around 1 g. This has been done to facilitate the parallel analysis of calcium content that was performed on the same samples. The chloride content has been measured by using a chloride ion selective electrode and a 0.01 N silver nitrate ( $\text{AgNO}_3$ ) solution.

After the chloride titration the pH value was corrected to  $\text{pH} > 12$  with sodium hydroxide ( $\text{NaOH}$ ) and finally 5 ml 1:2 diluted triethanolamine was added to neutralize the solution and avoid interactions from other ions. The calcium content was measured by using a calcium ion selective electrode and a 0.100 N EDTA solution. The chloride and calcium contents were determined by evaluating the endpoints for the potential differences during the titration. The binder content in each sample was determined from the analysed calcium content, since the acid soluble calcium content in the aggregate used in the concrete is negligible. The calcium content in the binder used in the concrete has been 64.9%.

### 4.3.3 Chloride binding isotherms

The chloride binding isotherms for the exposed concrete composition have been determined in two different ways: free-bound and free-total. The relationship between free and bound chloride has been determined with the equilibrium method, further described in the following. The relation free-total chlorides has been determined on concrete disks exposed in the same plastic containers as the concrete specimens exposed in the laboratory.

#### Free – bound (equilibrium method)

The relationship between free and bound chlorides has been determined on crushed concrete samples, according to a method by Tang (2002), modified from Tang & Nilsson (1993). The crushed concrete was put in test tubes and exposed to solutions with different chloride concentrations (0.01 mol/l, 0.05 mol/l, 0.10 mol/l, 0.50 mol/l and 1.00 mol/l). During the preparation the samples were protected from carbonation. After a certain time (about two weeks or longer), when equilibrium had been reached in the test tubes, the chloride concentration in the solution was measured and the contents of free and bound chlorides were determined.

#### Free – total

The relationship between the free chloride content in the surrounding exposure solution and the total chloride content in the concrete has been determined. This was done on concrete disks exposed in the same plastic containers as the concrete specimens exposed in the laboratory. The exposure was of sufficiently long duration to enable equilibrium to be reached between the concrete and the exposure solution. Under the assumption that equilibrium is reached, a relationship between the free (in the solution) and bound (in the concrete discs) chlorides can be established.

For this purpose concrete disks, measuring 150x150x30 mm, have been exposed in salt solutions between 413 and 422 days (similar exposure conditions and times as for the concrete specimens). After exposure the chloride ingress into concrete disks was analysed at two depth intervals in a similar way as for the concrete specimens. Since the concrete disks were exposed in solutions with different temperatures and chloride contents the effect of these parameters can be examined.

## 4.4 Results

The results are presented as measured chloride ingress profiles, where the quotient between the chloride and binder content is presented in depth intervals. The binder content has been estimated from the analysed calcium content in each sample, since the amount of acid soluble calcium in the aggregate used in the exposed concrete is negligible. The cement used in the exposed concrete has a CaO content of 64.9% by weight.

### 4.4.1 Field exposure

#### Measured chloride ingress

In figures 4.5a and 4.5b the measured chloride ingress profiles from the field exposure are presented. For clarity a division has been made into a “cold” part (Eastern Scheldt, Hirtshals, Hvalfjörður, Kjøpsvik, Källahamn, Skanör and Träslövsläge), where the annual mean water temperature is below +14°C, and a “warm” part (Banyuls sur Mer, Cascais, Dubai, Isle of the Dead and La Rochelle), where the annual mean water temperature exceeds +14°C. Since in total 69 chloride ingress profiles have been analysed, for the sake of clarity mean profiles from each exposure location are presented in figures 4.5a and 4.5b. The exposure times were around one year for all exposure locations.

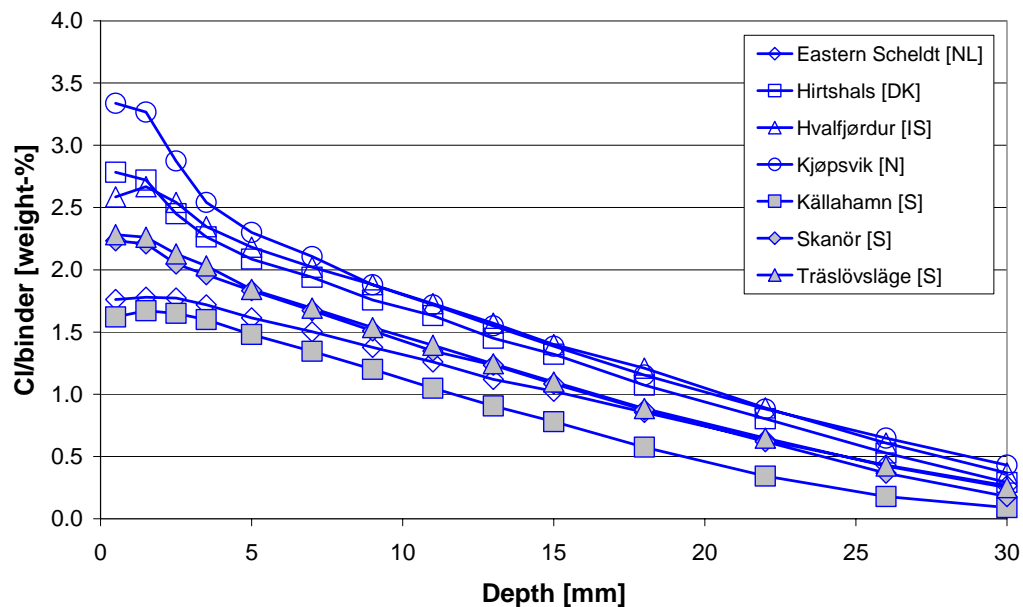


Figure 4.5a: Chloride ingress profiles from the field exposure – cold exposure conditions. Mean profiles from each exposure location.

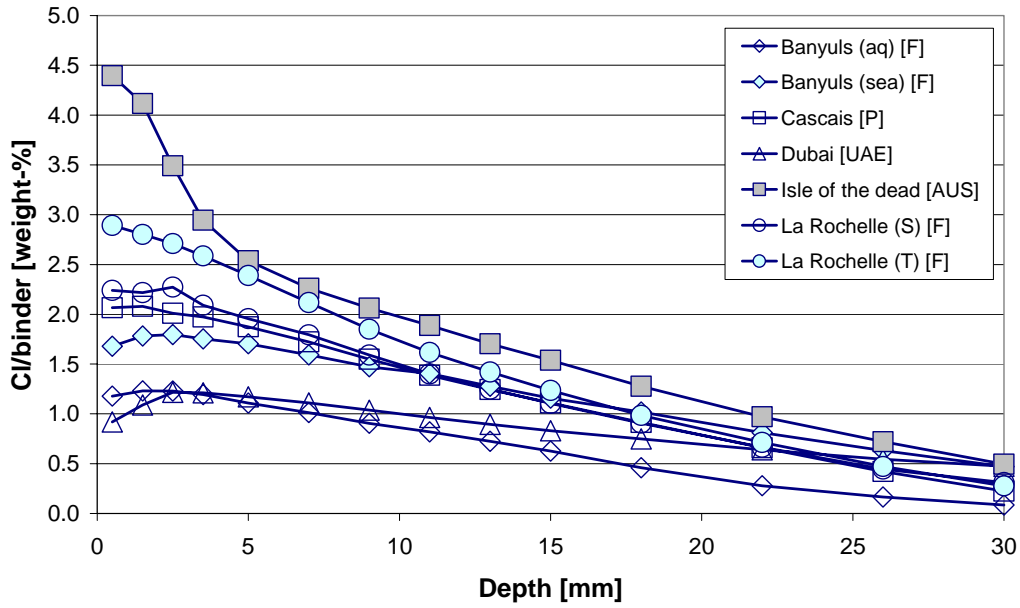


Figure 4.5b: Chloride ingress profiles from the field exposure – warm exposure conditions. Mean profiles from each exposure location.

To get a measure of the variations in the measured chloride ingress profiles the coefficient of variation (COV) has been determined for each depth of the measured chloride ingress profiles. In figures 4.6a and 4.6b COV for each depth in the chloride ingress profiles, given in figures 4.5a and 4.5b, is presented. COV has been determined according to eq. (4.1).

$$\text{COV} = \frac{\sigma}{\mu} \quad (4.1)$$

where:

- $\mu$ : mean value of the measured chloride ingress (4-6 profiles) at one depth in the profile.
- $\sigma$ : standard deviation of the measured chloride ingress (4-6 profiles) at one depth in the profile.

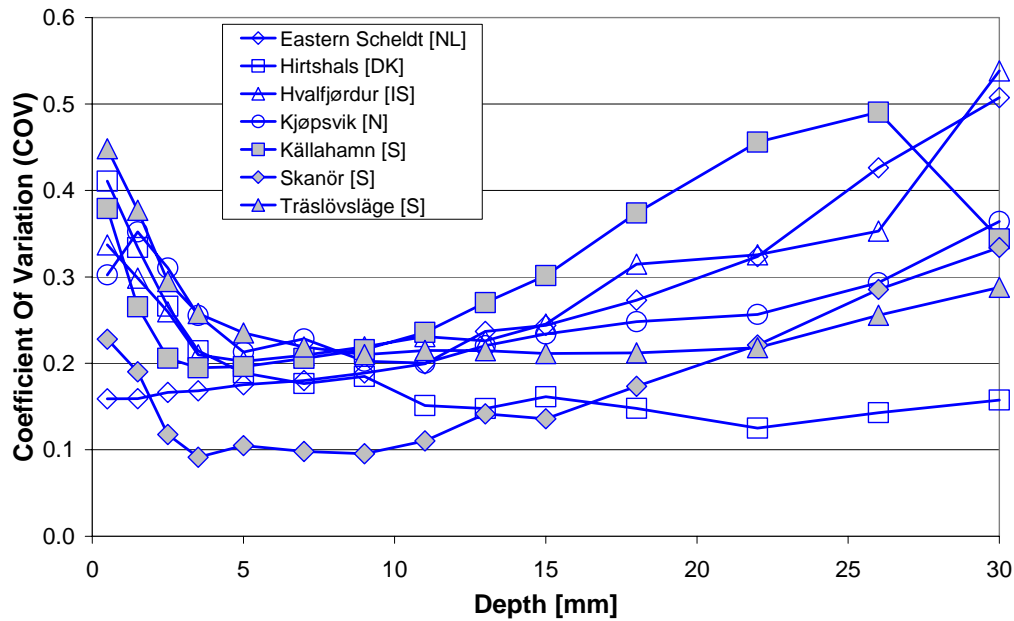


Figure 4.6a: The coefficient of variation (COV) for each depth in the measured chloride ingress profiles – cold exposure conditions.

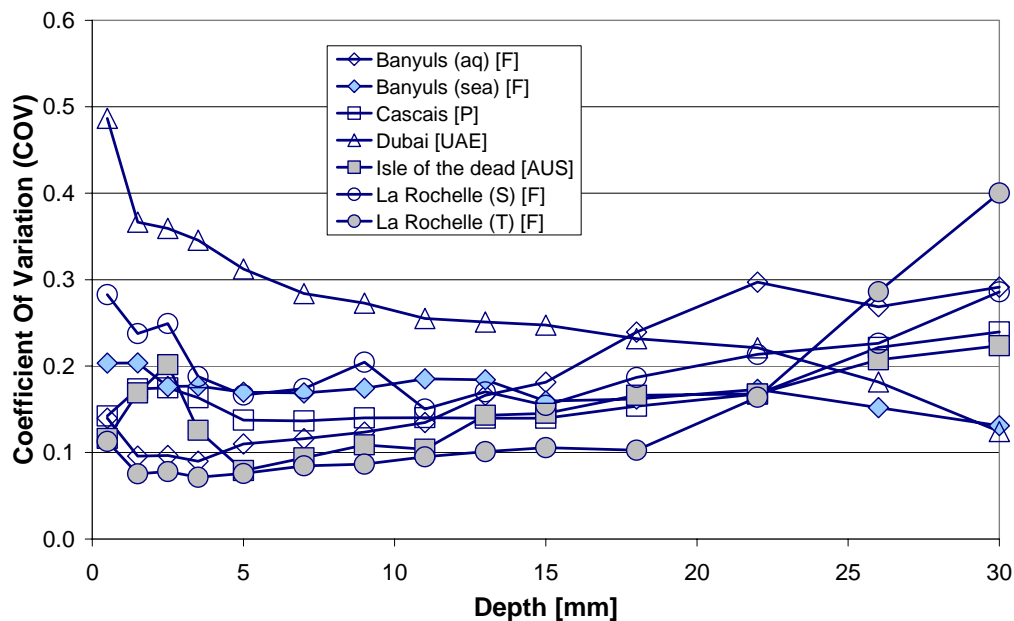


Figure 4.6b: The coefficient of variation (COV) for each depth in the measured chloride ingress profiles – warm exposure conditions.

As seen in figures 4.6a and 4.6b the coefficient of variation varies over depth. Close to the surface (up to depth of 5 mm) COV is large due to surface effects, which give variations in the chloride ingress. At depths over 20 mm COV is large since the measured chloride contents are small and thus have large relative uncertainties. Between 5 and 20 mm COV is generally between 10% and 20% for all locations. These calculated COVs should reflect the accuracy in the determination of the chloride content in the concrete with the method used in this study, since the exposure conditions should not vary significantly at one exposure location. However, variations in the concrete composition may have an influence on the calculated COVs. The results in figures 4.6a and 4.6b correspond to what

is reported in Tang (2003), where the reproducibility of parallel determination of chloride and calcium contents in concrete was found to be 0.90% by weight of sample. This means that if the measured chloride content is low, the corresponding uncertainties are large, which also can be observed at depths 0-5 mm and 20-30 mm in figures 4.5a and 4.5b.

The slightly different shape of the measured chloride ingress profiles from Kjøpsvik, with high chloride content close to the surface, can be explained by the fact that the exposure started in late October 2000 and ended in early November 2001. At all other locations the exposure was started and ended in late summer.

### Discussion of variations in chloride ingress

As seen in figures 4.5a-4.5b and 4.6a-4.6b, the variations between the measured chloride ingress profiles are large, both between the different locations but also within one single location (indicated by large COV for the profiles), which is somewhat surprising. Examples of this are shown in figure 4.6c where chloride ingress profiles from Cascais (continuous profiles with index Cas) and Källahamn (dotted profiles with index Käl) are presented. The exposure times have been 378 (Cas) and 364 (Käl) days.

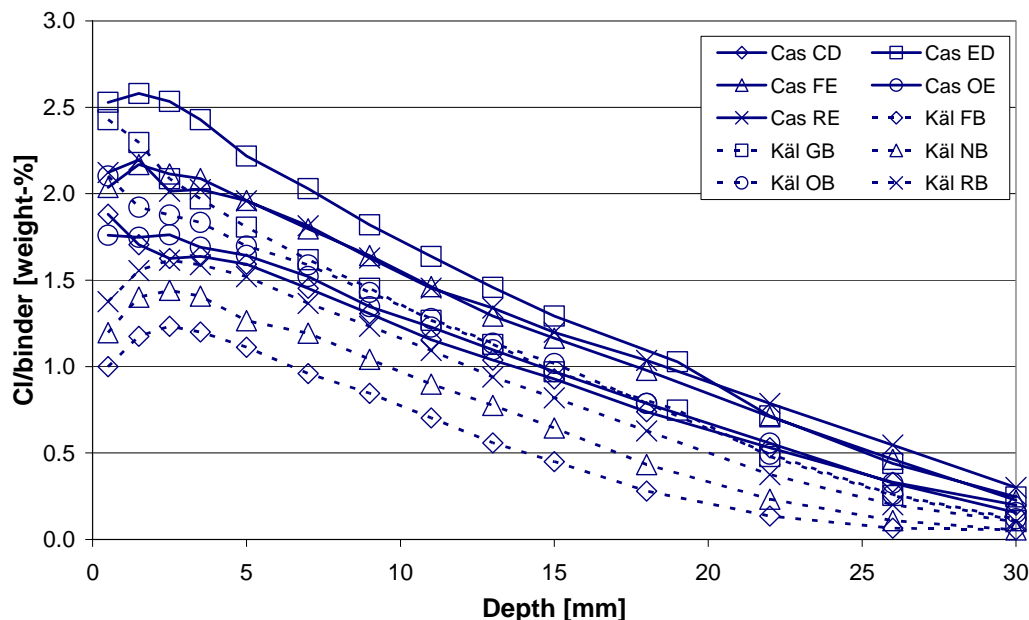


Figure 4.6c: Chloride ingress profiles from Cascais and Källahamn.

From figure 4.6c it can be seen that the profiles from Cascais are fairly close together, while the profiles from Källahamn show fairly large variations. The mean coefficient of variation (COV) for the measured chloride ingress profiles is approximately 16% for Cascais and 30% for Källahamn. Another interesting feature can be observed in the surface- near region, at least in the profiles from Källahamn, where the profiles tend to either decrease or increase when the chloride concentration at a depth of 3-4 mm from the surface exceeds or drops below a “critical” chloride content of around 2.0% by weight (Cl/binder). The reason for this is not known.

Another interesting feature that can be observed in figure 4.6c is that the measured chloride ingress profiles almost never cross each other, i.e. high surface chloride contents result in large chloride contents further into the concrete. Similar observations have been made on the measured profiles from almost all exposure locations, cf. Lindvall (2003).

Thus, the variations in chloride ingress at one exposure location can be attributed mainly to variations in the surface chloride content and only to a small extent to the chloride transport properties in the concrete.

The concrete specimens were exposed in either buckets or baskets, which were suspended from jetties or similar or placed on the seabed, at most of the exposure locations. To ensure good circulation of water, holes were made in the buckets – the design of the baskets ensured good water circulation without modifications of the baskets. All five specimens in the baskets (one basket was used at each exposure location) were exposed separated from each other, standing on one of the short sides, which means that the exposure to chlorides has been studied through vertical surfaces. The specimens in buckets were exposed in two buckets at each location, with three specimens in one bucket and two specimens in the other bucket. The specimens in the buckets were exposed either standing on one of the short sides or lying on two specimens (one specimen at each location, where buckets were used). This means that the exposure to chlorides has been studied through either vertical or horizontal surfaces. The placement of the specimens in the baskets (left – only four specimens shown) and buckets (right – buckets with three and two specimens) is illustrated in figure 4.7. The holes in the buckets, drilled to ensure good water circulation, are also illustrated in figure 4.7.

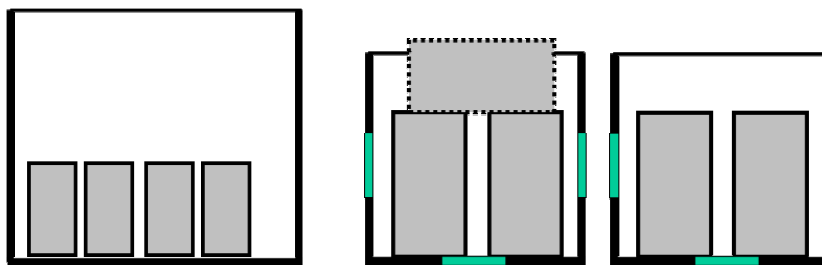


Figure 4.7: Illustration of the placement of concrete specimens in baskets (left) and buckets (right).

Although the concrete specimens in the buckets have different surface orientations they are still subjected to the same water pressure, which should mean that they should have similar exposure conditions. No systematic differences in the measured chloride ingress profiles have been found between horizontal and vertical exposure. However, at some exposure locations the surface orientation may have an influence on the chloride ingress. At some locations where buckets have been used, the lower parts of the standing specimens became partly covered with sediment. This effect was especially significant in the submerged exposure at La Rochelle, where the water contains large amounts of sediment originating from tidal actions. Furthermore the specimens with horizontal exposure surfaces in Skanör (two specimens) were also found to be covered with sediment when the exposure was finished. However, the extent and significance of the influence of the sediment on chloride ingress into concrete at these exposure locations is not known. Furthermore at some locations the standing specimens in the buckets had merged together – at these locations the chloride ingress has been studied through the free surfaces.

The extent of marine growth on the specimens may also influence chloride ingress into the concrete. Information about the extent of marine growth when the exposure was finished is given in Lindvall (2003). Unfortunately this information is not known for all exposure locations. However, at the exposure locations where information about the

extent of marine growth is known, the marine growth has not been found to have any significant influence on the chloride ingress.

Thus parts of the observed variations in measured chloride ingress at one single exposure location can be explained by variations in the concrete compositions and uncertainties in the determination of the calcium and chloride contents. Furthermore the surface orientation, effects due to sediment and marine growth, as discussed above, may have an influence on the measured chloride ingress. However, the remainder of the variations must depend on variations in the exposure conditions, i.e. chloride concentration and temperature of the seawater.

#### 4.4.2 Laboratory exposure

In figure 4.8 the measured chloride ingress profiles from the laboratory exposure are presented. In total sixteen chloride ingress profiles have been analysed, so for the sake of clarity mean profiles from each exposure environment are given. The exposure times have been between 413 and 422 days.

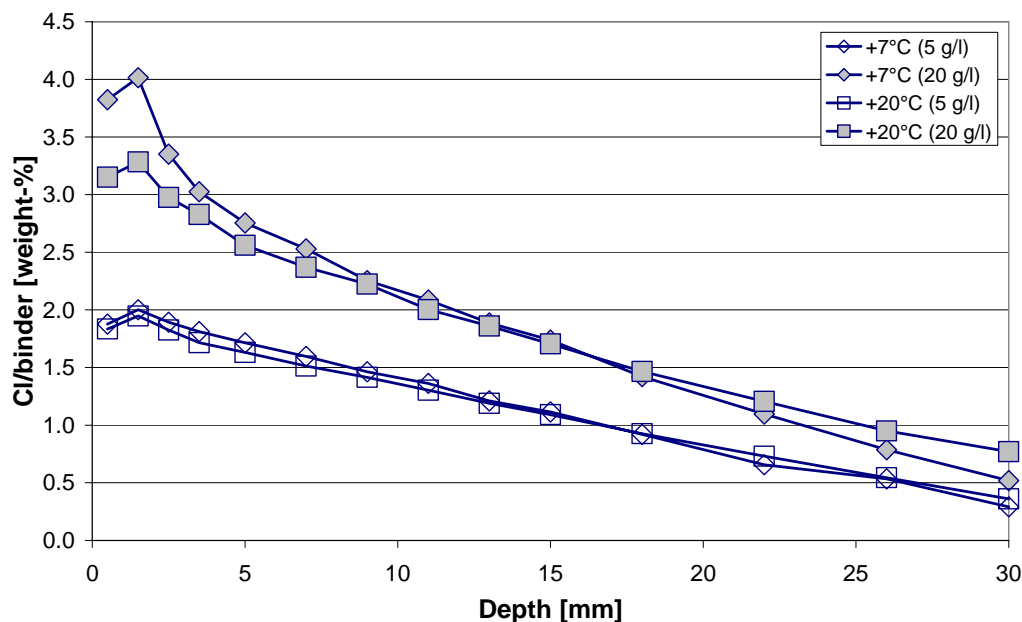


Figure 4.8: Chloride ingress profiles from the laboratory exposure. Mean profiles from each exposure location.

From figure 4.8 it can be seen that the level of the profiles seems mainly to be a function of the chloride concentration in the exposure solution. The temperature of exposure solution seems to have only a subordinate influence.

To get a measure of the variations in the measured chloride ingress profiles the coefficient of variation (COV) has been determined for each depth of the measured chloride ingress profiles, according eq. (4.1), see figure 4.9.



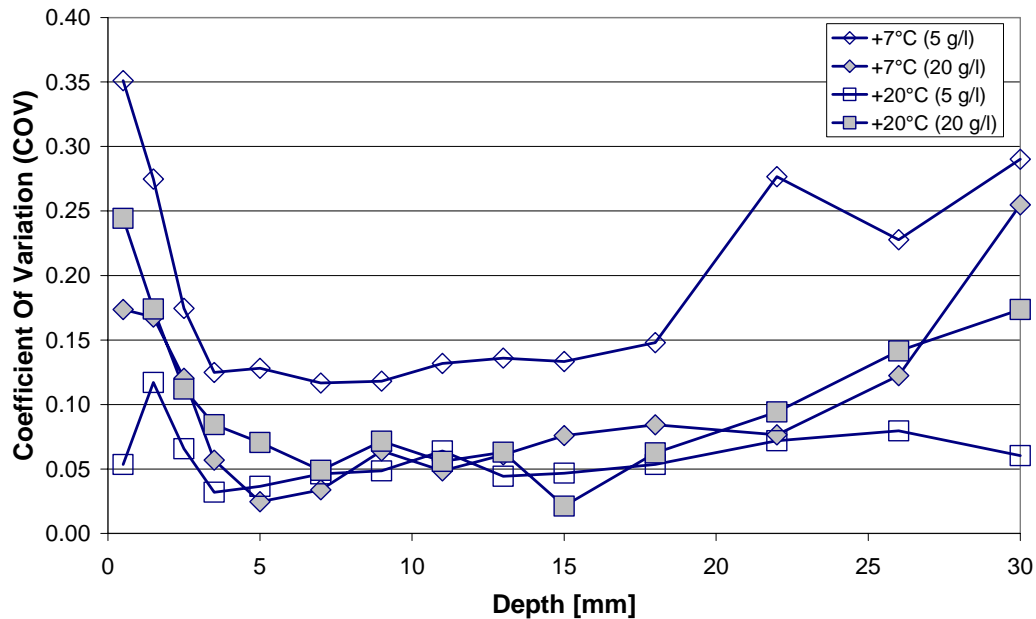


Figure 4.9: The coefficient of variation (COV) for each depth in the measured chloride ingress profiles – laboratory exposure.

The shapes of the COV profiles from the laboratory exposure are similar to COV profiles from the field exposure, with large COV close to the surface and in the inner part. This is explained by the fact that the chloride contents in the concrete are low, which means that the uncertainty arising from the analysis method has a large impact on the uncertainties of the results.

#### 4.4.3 Chloride binding isotherms

The chloride binding, where the relation between the free and bound chloride content in the concrete is given, has been determined with the equilibrium method. Three different analyses of chloride binding have been made with the equilibrium method, where during the first two analyses the concrete samples were exposed to the chloride solutions under vacuum. These analyses yielded incorrect results, especially for the high chloride concentrations (0.5 mol/l and 1.0 mol/l) where even negative chloride binding was measured, which of course is not realistic. Therefore it was decided to make a complementary analysis for these chloride concentrations but without vacuum. This analysis gave more realistic results and combined with the results from the second analysis (for 0.01 mol/l, 0.05 mol/l and 0.10 mol/l) a chloride binding isotherm has been established. The chloride binding has been determined in laboratory conditions with a temperature ranging between 20°C and 22°C.

Measured chloride binding data (free-bound), describing the adsorption of chlorides, are shown in figure 4.10a. The points which have been measured without the vacuum are marked. Each point in figure 4.10a is a mean value of two measurements. The scatter was fairly large, especially for the high chloride concentrations.

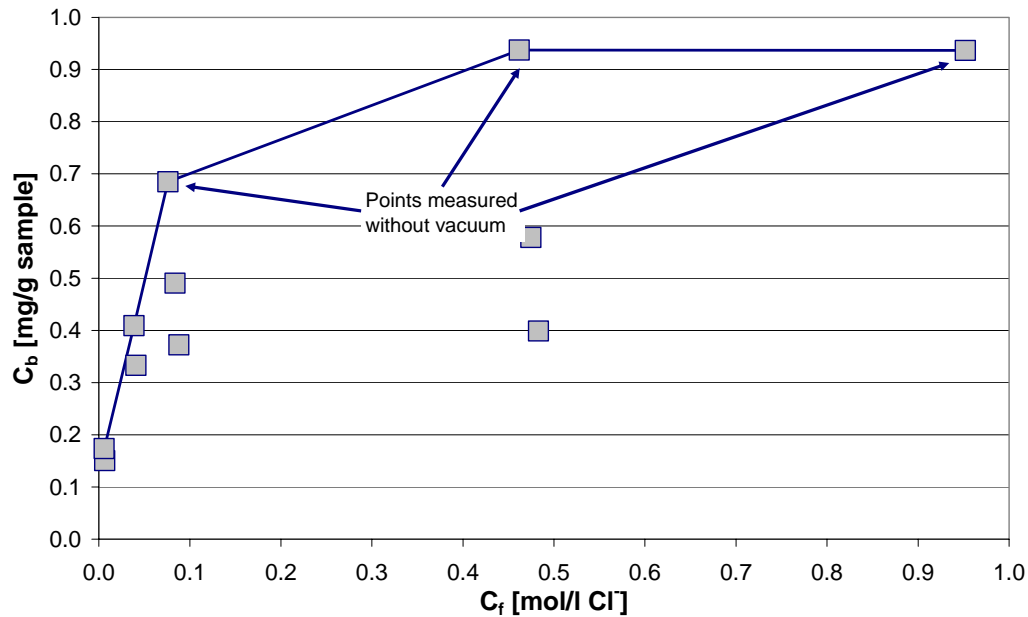


Figure 4.10a: Chloride binding isotherm (free-bound), for the concrete composition used in the exposure programme.

The chloride binding, where the relation between the chloride concentration in the exposure solution and total chloride content in the concrete is given, has been determined on concrete disks exposed in chloride solutions, with different chloride concentrations and temperatures, in the laboratory. In figure 4.10b the chloride binding isotherm (free-total), describing the adsorption of chlorides, is shown. An exponential trend line has been added to show the trend in chloride binding with increasing chloride concentration in the exposure solution. The diamonds and squares denote the temperature of the exposure solutions, +20°C and +7°C respectively.

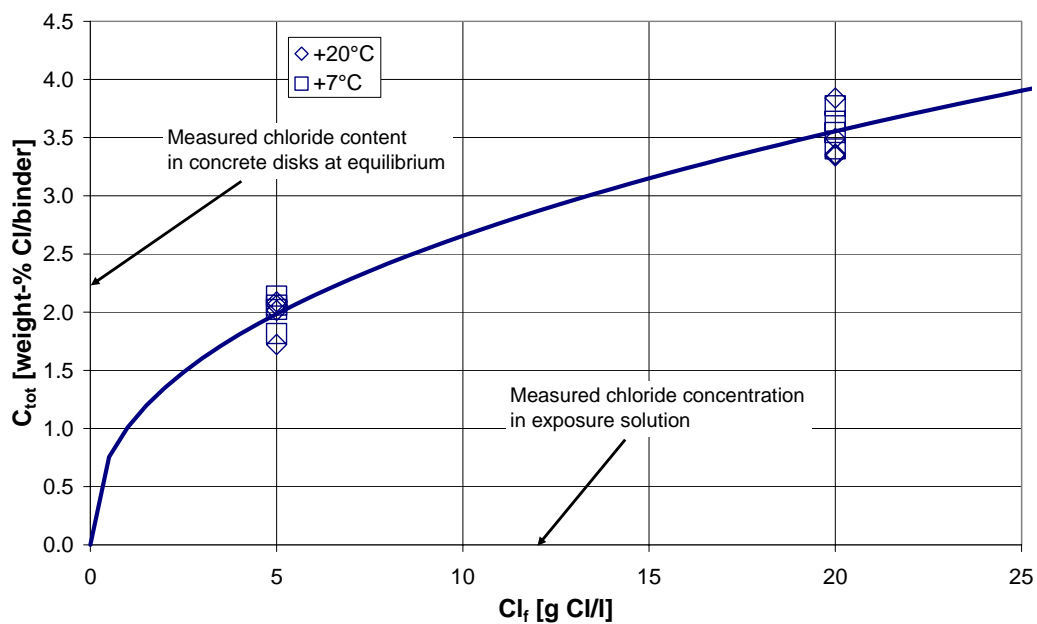


Figure 4.10b: Chloride binding isotherm (free-total), for the concrete composition used in the exposure programme.

If the data in figures 4.10a and 4.10b are combined the relation between the chloride concentration in the exposure solution and the free chloride content in the concrete can be determined, see figure 4.10c. According to figure 4.10b the difference between the chloride binding measured at +7°C and +20°C is very small and cannot be considered significant. Therefore only the relation between the chloride concentration in the exposure solution and the chloride content in the concrete (as total and bound chloride content) has been evaluated by curve fitting, where all data independent of exposure temperature have been included, see eq. (4.2).

$$\begin{cases} C_{\text{tot}} = 1.01 \cdot Cl_f^{0.42} \\ C_{\text{bound}} = 0.1344 \cdot \ln(Cl_f) + 0.3609 \end{cases} \quad [\% \text{ by weight Cl/binder}] \quad (4.2)$$

where:

$Cl_f$ : chloride concentration in the exposure solution. [g Cl/l].

In figure 4.10c the amount of free chlorides in the concrete (dotted line) has been determined by subtracting the bound chloride content from the total chloride content in the concrete. Since the temperature has been found to be insignificant for chloride binding, the chloride binding isotherms are only expressed as functions of the chloride concentration in the exposure solution.

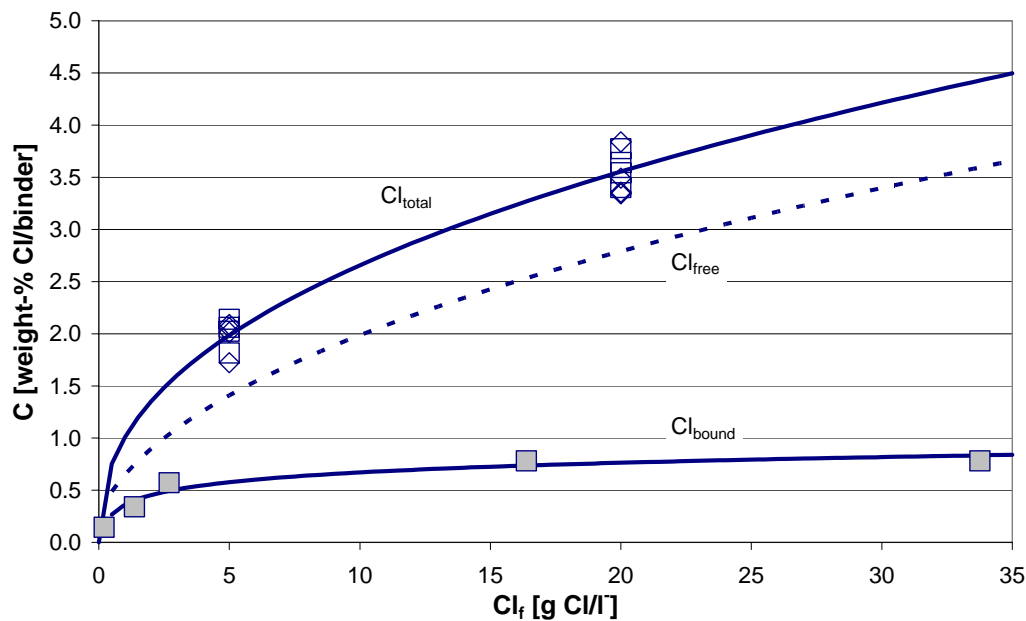


Figure 4.10c: Chloride binding isotherms (total, free and bound chloride content in concrete as a function of the chloride concentration in the exposure solution).

## 4.5 Analysis and discussion

In this section the following topics will be analysed and discussed:

- Evaluation of measured chloride ingress profiles.
- Effect on chloride ingress of chloride concentration and temperature of exposure water.

- Chloride ingress in submerged and tidal conditions.
- Chloride concentration in seawater in Kjøpsvik and Träslövsläge.
- Influence of chloride binding.

#### 4.5.1 Evaluation of measured chloride ingress profiles

The measured chloride ingress profiles have been evaluated by curve fitting to the error function solution of Fick's 2<sup>nd</sup> law. The curve fitting has been done in such a way that the inner parts of the profiles are fitted where the correlation between the measured and fitted profiles has a maximum. Curve fitting has been performed in accordance with a procedure described in Nilsson et al 2000 and resulted in two regression parameters, namely an apparent diffusion coefficient,  $D_{F2}$ , and an apparent surface chloride content,  $C_{sa}$ . Two additional parameters have been determined,  $x_c$ , showing the thickness of the "convection zone", where measured profiles do not fit the error function, measured from the surface, and a surface chloride content for the convection zone,  $C_{sc}$ . For each profile the curve fitting has first been made with all points in the profile and then points have been omitted from the surfaces until the coefficient of correlation,  $R$ , exceeded 0.980.

The area below each chloride ingress profile (% by weight Cl/concrete) has been determined to get a measure of the total amount of chlorides that have penetrated into each specimen. The reason for not using the chloride ingress profiles, with % by weight Cl/binder, is that the binder content (correlated with the CaO content) is not constant over depth in the profile, due to variations in aggregate content in each sample. This is illustrated in figure 4.11, where profiles with the measured CaO content in the concrete exposed in Cascais and Källahamn are presented. The theoretical CaO content in the concrete, calculated to 13.3<sup>7</sup> [% by weight], has also been added to the figure.

---

<sup>7</sup> Determined as the quotient between the CaO content in the concrete (CaO content in the cement, since the aggregate does not contain calcium) and the dry density of the concrete (aggregate, cement and chemically bound water –  $0.25 \cdot \alpha \cdot C$ , where  $\alpha$  is the degree of hydration and  $C$  is the cement content). The concrete composition is given in table 4.1 and  $\alpha \approx 0.6$  (corresponding to  $w/c=0.40$ ), according to Nilsson (1980).

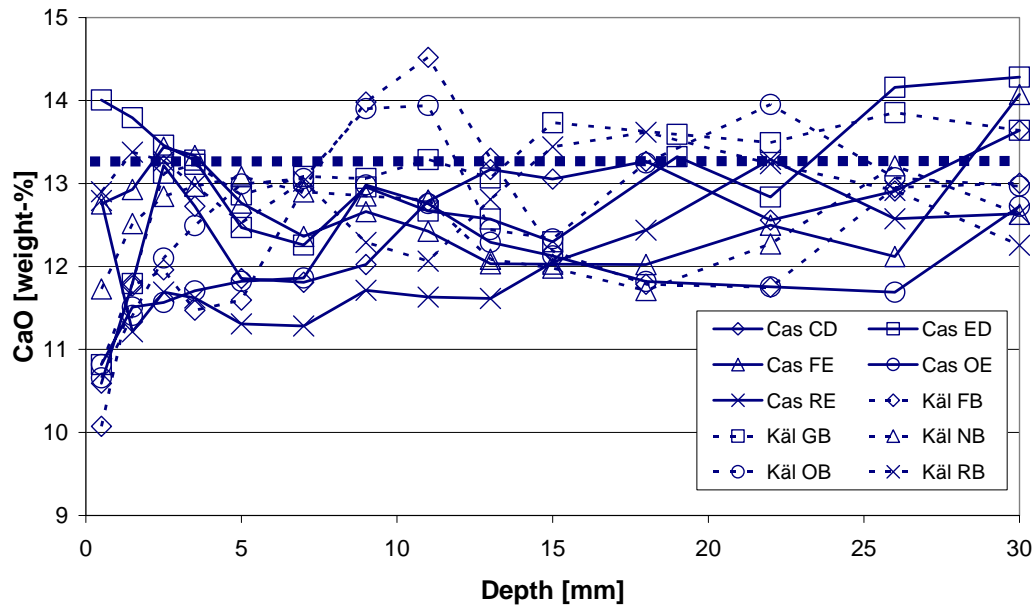


Figure 4.11: Measured CaO-content in the concrete exposed in Cascais and Källhamn.

As seen in figure 4.11 the CaO content in the concrete samples varies between 10.0 and 14.5 [% by weight]. The mean CaO content in the profiles varies between 12.0 and 13.2 [% by weight] the overall mean CaO content for the profiles was 12.6 [% by weight]. The largest variations in CaO content can be observed in the profile with index Käl FB. The measured CaO contents are mostly lower than the theoretically calculated CaO content, which may indicate that leaching of calcium takes place or that the concrete is not completely homogeneous. However, the concrete specimens used in the marine exposure programme are special, since the chloride ingress has been measured through sawn surfaces, without any effects from moulds etc. This can also be seen in figure 4.11, where the CaO content is fairly stable over depth. Examples of variations in CaO content in concrete, where the chloride ingress has been studied through ordinary concrete surfaces (concrete cast in steel moulds), are given in e.g. Nilsson et al (2000).

The results from the evaluation of the chloride ingress profiles from the marine exposure programme are presented in Lindvall (2003). The statistical uncertainties in the evaluated parameters have also been determined, in terms of coefficients of variation (COV), since at least four profiles have been evaluated from each exposure location. For the field exposure COV has been found to vary for  $D_{F2}$  between 8.6% (at sea in Banyuls sur Mer) and 34.9% (Dubai) and for  $C_{sa}$  between 7.3% (tidal zone in La Rochelle) and 33.0% (Dubai).

#### 4.5.2 Effect on chloride ingress of chloride concentration and temperature of exposure water

The effect on chloride ingress of the chloride concentration and temperature of the seawater has been investigated. For clarity the different exposure locations have been grouped into classes, based on the chloride concentration in the seawater:

- **BS+ÖS.** Exposure made in the Baltic Sea and in Öresund with an annual mean chloride concentration in the seawater of approximately 3-5 g/l.

- **KG.** Exposure made in Kattegat with an annual mean chloride concentration in the seawater of approximately 10 g/l.
- **KV.** Exposure made in Kjøpsvik with an annual mean chloride concentration in the seawater of approximately 17 g/l.
- **Rest.** Exposure made at the rest of the exposure locations with an annual mean chloride concentration in the seawater of approximately 18-23 g/l.
- **LR(T).** Exposure in the tidal zone at La Rochelle with an annual mean chloride concentration in the seawater of approximately 19 g/l.
- **Lab.** Exposure made in the laboratory in two different exposure solutions with chloride concentrations of approximately 5 g/l and 20 g/l.

The reason that Kjøpsvik is shown separately is that the chloride concentration in the seawater varies significantly over the year due to effects from melting water in the springtime. This is further discussed below.

In figure 4.12a effects of the temperature of the seawater on  $D_{F2}$  are shown. Exponential trend lines (for chloride concentrations of 5, 10 and 20 g/l in the seawater) have been added to the figure to show the influence of the temperature.

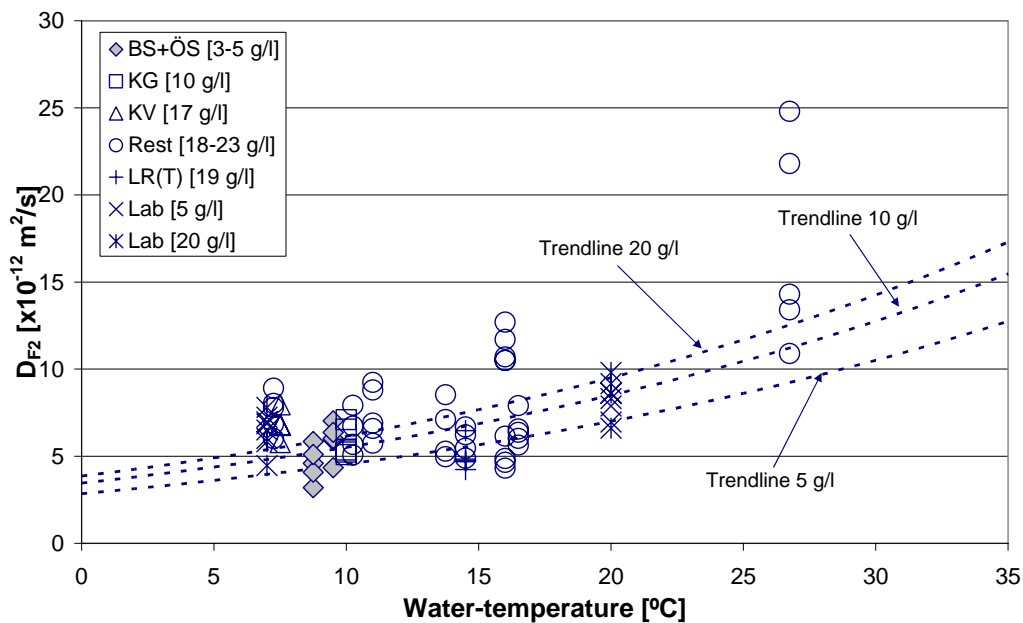


Figure 4.12a: The effect of the chloride concentration and temperature of the exposure water on  $D_{F2}$ . Exponential trend lines have been added for clarity.

From figure 4.12a it can be seen that the temperature of the exposure water seems to have a significant effect on  $D_{F2}$ , with  $D_{F2}$  increasing with increasing temperature. The chloride concentration in the seawater seems to have only a small effect on  $D_{F2}$ , with  $D_{F2}$  showing a slight decrease with decreasing chloride content.

The effects of the temperature of the seawater on  $C_{sa}$  are shown in figure 4.12b. Exponential trend lines (for chloride concentrations of 5, 10 and 20 g/l) have been added to the figure to show the influence of the temperature.

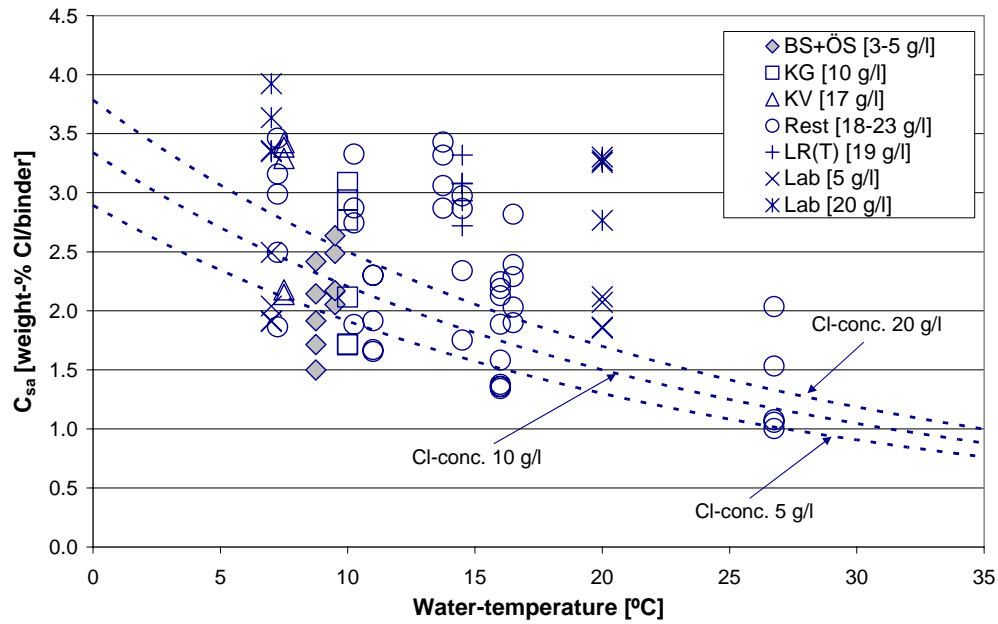


Figure 4.12b: The effect of the chloride concentration and temperature of the exposure water on  $C_{sa}$ . Exponential trend lines (dotted lines) have been added for clarity.

From figure 4.12b it can be seen that the temperature has an effect on  $C_{sa}$ , with  $C_{sa}$  decreasing with increasing temperature. The chloride concentration in the seawater has a fairly large effect on  $C_{sa}$ , with  $C_{sa}$  increasing with increasing chloride concentration.

The effect of temperature on the total amount of chlorides that have penetrated into the concrete is shown in figure 4.12c, where the areas below each of the measured chloride ingress profiles are plotted as a function of the water temperature. Exponential trend lines (for chloride concentrations of 5, 10 and 20 g/l) have been added to the figure to show the influence of the temperature.

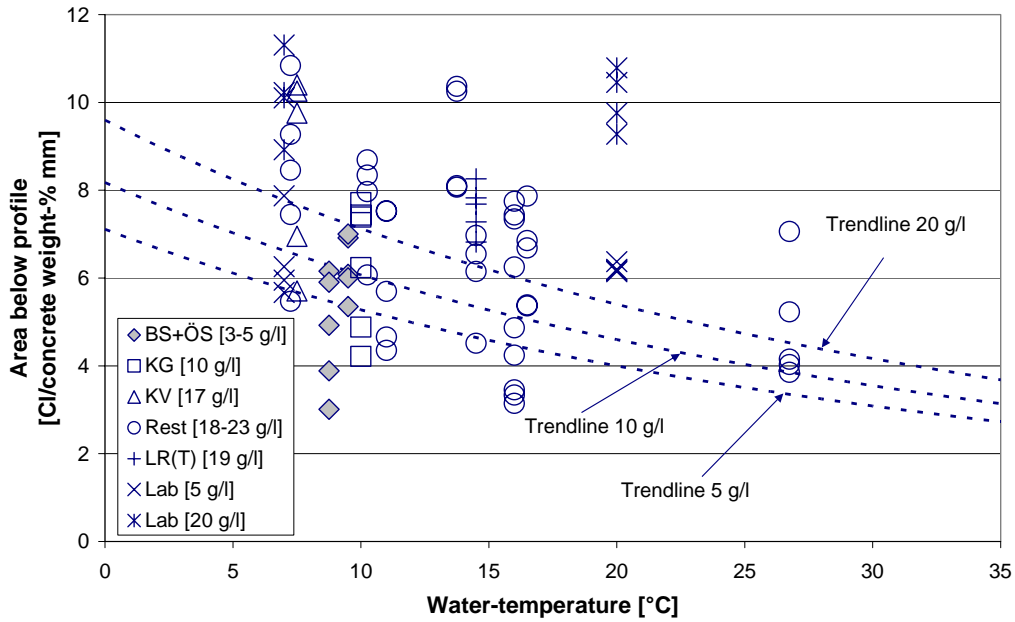


Figure 4.12c: The effect of the chloride concentration and temperature of the exposure water on the areas below the measured chloride ingress profiles. Exponential trend lines have been added for clarity.

From figure 4.12c it can be observed that the total amount of chlorides that have penetrated into the concrete decreases with increasing temperature. It can also be seen that more chlorides have penetrated into the specimens exposed in laboratory conditions than in field conditions, though the chloride concentrations and temperatures of the exposure solutions used in the laboratory exposure have been similar to what has been measured at the locations used for the field exposure. This can also be seen in the evaluated  $C_{sa}$ , where the laboratory exposure resulted in higher  $C_{sa}$  than the field exposure, cf. figure 4.12b. However,  $D_{F2}$  seems not to be affected by the site of the exposure, cf. figure 4.12a.

The effects of the temperature and chloride concentration in the seawater are further discussed in the following sections.

### Temperature effect

Page et al (1981) proposed to model the increase in chloride diffusivity with temperature with the Arrhenius relationship. Similar proposals have been made by for example Tang (1996), Boddy et al (1999), Gehlen (2000) and Mejlhede-Jensen (1998). Based on these references the following relationship is proposed to model the effect of temperature on the diffusion coefficient measured in the exposure programme, eq. (4.3a).

$$\frac{D_a(T_a)}{D_{a,ref}} = e^{\left[ b_e(D_a) \cdot \left( \frac{1}{T_{ref}} - \frac{1}{T_a} \right) \right]} \quad [-] \quad (4.3a)$$

where:

$D_a(T_a)$ :  $D_a$  at temperature  $T_a$ . [ $m^2/s$ ]

$D_{a,ref}$ :  $D_a$  at the reference temperature,  $T_{ref}$  (293 K). [ $m^2/s$ ]

$b_e(D_a)$ : regression parameter for determination of temperature dependency of  $D_a$ . [-]

$T_a$ : temperature of the exposure water. [K]



$T_{ref}$ : reference temperature. 293 [K]

The regression parameter,  $b_e(D_a)$ , is equal to the quotient between the activation energy for chloride diffusion,  $E_D$ , and the gas constant,  $R$ , according to eq. (4.3b), Tang (1996). In Page et al (1981)  $E_D$  was found to vary between 32.0 and 41.8 [kJ/mol] depending on the w/b (corresponding to variation in  $b_e$  between 3848 and 5028 [K]), where  $E_D$  decreases with increasing w/b.

$$b_e = \frac{E_D}{R} \quad [-] \quad (4.3b)$$

where:

$E_D$ : activation energy for chloride diffusion. [J/mol]

$R$ : gas constant ( $R=8.314$  [J/(mol K)]).

Based on the data in figure 4.12a the regression parameter,  $b_e(D)$ , can be quantified. If the diffusion coefficient at the reference-temperature (+20°C),  $D_{ref}$ , is assumed to be  $9.5 \cdot 10^{-12}$  [m<sup>2</sup>/s] the regression parameter,  $b_e$ , is equal to 3700 [K]. This value is slightly low compared with that reported by Page et al (1981) and Gehlen (2000), where  $b_e$  is equal to 4800 [K], based on data from Page et al (1981). This difference can (partly) be explained by the fact that the water temperatures in figure 4.12a are mean values with yearly variations, while the water temperatures in Page et al (1981) are constant over time (laboratory conditions). Since the water temperatures vary over the year, and the chloride ingress increases exponentially with increasing temperature,  $b_e$  quantified from the data in figure 4.12a should be higher if the variations of the water temperature were taken in consideration. However, the variations in water temperature have not been continuously measured at the exposure locations and are therefore not taken into account. Instead, the yearly mean temperatures have been used for the sake of simplicity.

Several authors have studied the temperature effect on chloride diffusivity. In the study by Page et al (1981), the chloride diffusivity in cement paste exposed in different temperatures has been determined. Sørensen (1992 & 1993) and Polder (1996) have studied chloride ingress into concretes exposed in chloride solutions with different temperatures. The results from these studies are presented, together with the trend lines from the field study presented above, in figure 4.13, where the evaluated apparent diffusion coefficients,  $D_{F2}$ , are shown as a function of the temperature of the exposure solution.  $D_{F2}$  measured when the water temperature is +20°C equals 1.0, the continuous line is given by eq (4.3a). For comparison the model by Gehlen (2000) has been added to the figure, dotted lines.

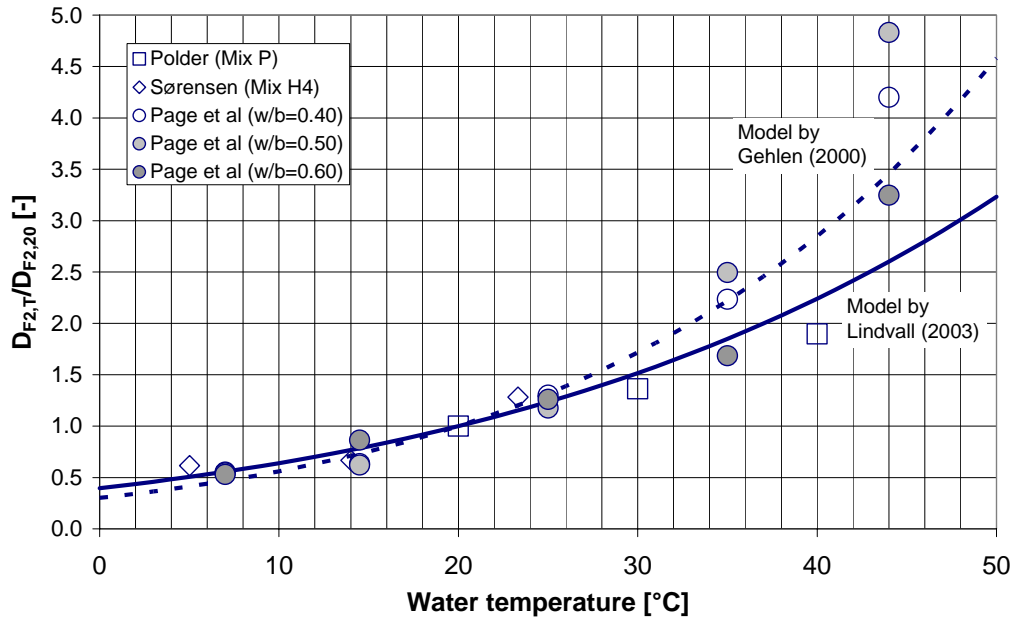


Figure 4.13: Temperature effect on  $D_{F2}$ . Data from Page et al (1981), Sørensen (1993 and Polder (1996).

As seen in figure 4.13 there is an agreement between the data, from Page et al (1981), Sørensen (1992 & 1993) and Polder (1996), and the model for the temperature dependency. The results in figure 4.13 are also in accordance with the findings by Mejlhede-Jensen (1998), where the chloride ingress into cement paste and mortar with different compositions and exposure conditions has been studied. In this study it was concluded that the main influencing factors on chloride diffusion are w/b, additives (silica fume) and the temperature. However, the influence of the temperature was found to be higher, with an increase in temperature of 10°C resulting in an increase of  $D_{F2}$  by a factor 2.

The chloride ingress into concrete can be described as a combination of chloride transport (convection and diffusion) and chloride binding. The temperature effect on the chloride binding (free-total) can be observed in figures 4.10b and 4.10c, where the chloride ingress seems mainly to be influenced by the chloride concentration in the exposure solution and only to a small extent by the temperature. Thus the observed temperature effect on the chloride ingress seems to be mainly an effect on the chloride transport and only to a small extent on the chloride binding. However, in figure 4.12b  $C_{sa}$ , evaluated from measured chloride ingress profiles, shows a clear temperature dependency. Both  $C_{sa}$  and  $D_{F2}$  are regression parameters that also are correlated, where high  $C_{sa}$  gives low  $D_{F2}$  and vice versa. This means that the observed temperature effect on  $C_{sa}$  can be attributed to a temperature effect on the chloride transport properties, described by  $D_{F2}$ , where an increase in  $D_{F2}$ , due to increasing temperature, consequently gives a decrease in  $C_{sa}$ .

In figure 4.12b it can be seen that the temperature of the seawater has an effect on  $C_{sa}$ , with  $C_{sa}$  decreasing with increasing temperature. The effect of the chloride concentration in the exposure water is larger compared with  $D_{F2}$ , with  $C_{sa}$  decreasing with decreasing chloride concentration. In a similar way as for  $D_{F2}$  the temperature dependency of  $C_{sa}$  can be modelled with the Arrhenius relation, see (4.4).

$$\frac{C_{sa}(T_a)}{C_{sa,ref}} = e^{\left[ b_e(C_{sa}) \left( \frac{1}{T_a} - \frac{1}{T_{ref}} \right) \right]} \quad [-] \quad (4.4)$$

where:

- $C_{sa}(T_a)$ : surface chloride content at temperature  $T_a$ . [% by weight Cl/binder]  
 $C_{sa,ref}$ : surface chloride content at the reference temperature,  $T_{ref}$  (293 K). [% by weight Cl/binder]  
 $b_e(C_{sa})$ : regression parameter for determination of temperature dependency of the surface chloride content. [-]  
 $T_a$ : temperature of the exposure water [K].

Similar to  $b_e(D_a)$  the regression parameter,  $b_e(C_{sa})$  should be equal to the quotient between the activation energy for chloride diffusion,  $E_D$ , and the gas constant,  $R$ , cf. eq. (4.3b). Based on the data in figure 4.12b  $b_e(C_{sa})$  can be quantified. If the surface chloride content at the reference temperature,  $C_{sa,ref}$ , is assumed to be 1.70 [% by weight Cl/binder],  $b_e(C_{sa})$  is equal to 3200 [K].

In Nilsson et al (1996) the observed temperature effect on  $D_{F2}$ , illustrated in figure 4.12a, is mainly explained by a temperature effect on the chloride binding. This relation is shown in eq. (4.5), where the  $D_{F2}$  is expressed as a function of  $D_{F1}$  and the chloride binding isotherm.

$$D_{F2}(T) = \frac{D_{F1}}{p_{sol} \cdot \left( 1 + \frac{\partial c_b(T)}{\partial c_f} \right)} = \frac{D_{F1}}{p_{sol} \cdot \left( \frac{\partial c_{tot}(T)}{\partial c_f} \right)} \quad [m^2/s] \quad (4.5)$$

where:

- $D_{F1}$ : diffusion coefficient in Fick's 1<sup>st</sup> law. [ $m^2/s$ ]  
 $p_{sol}$ : porosity of concrete (saturated pore volume that acts as solvent for chloride ions). [-]  
 $c_b(T)$ : content of bound chlorides in concrete as a function of temperature. [ $kg/m^3$ ]  
 $c_f$ : content of free chlorides in concrete. [ $kg/m^3$ ]  
 $c_{tot}(T)$ : content of total chlorides in concrete (bound + free) as a function of temperature. [ $kg/m^3$ ]

From eq. (4.5) it is clear that  $D_{F2}$  does not have a temperature dependency of its own, but it can be attributed to the temperature dependency of  $c_{tot}$  (or  $c_b$ ), where  $c_{tot}$  has been observed to decrease with increasing temperature, Larsen (1998). Furthermore the temperature effect on  $c_{tot}$  can also explain the temperature dependency of  $C_{sa}$ , where  $C_{sa}$  consequently should decrease with increasing temperature. This is supported by the data presented in figure 4.12b, where  $C_{sa}$  decreases with increasing temperature.

However, in the chloride binding isotherms, measured as part of the exposure programme, the influence of temperature on chloride binding was found insignificant. Instead, the chloride binding was found to be mainly influenced by the chloride concentration of the exposure solution. This is further discussed in section 4.5.5.

**Effect of chloride concentration in exposure water**

From figures 4.12a-4.12c the effect of the chloride concentration in the exposure water seems to be small for the concrete specimens exposed in field conditions. However, for the concrete specimens exposed in the laboratory a significant influence due to the chloride concentration in the exposure solution has instead been observed, shown in figure 4.14, where the total amount of chlorides in the concrete is shown (results from laboratory exposure are highlighted). The temperature effects on  $D_{F2}$  and  $C_{sa}$  analysed from the chloride ingress measured in the laboratory are also small, cf. figure 4.12a and 4.12b.

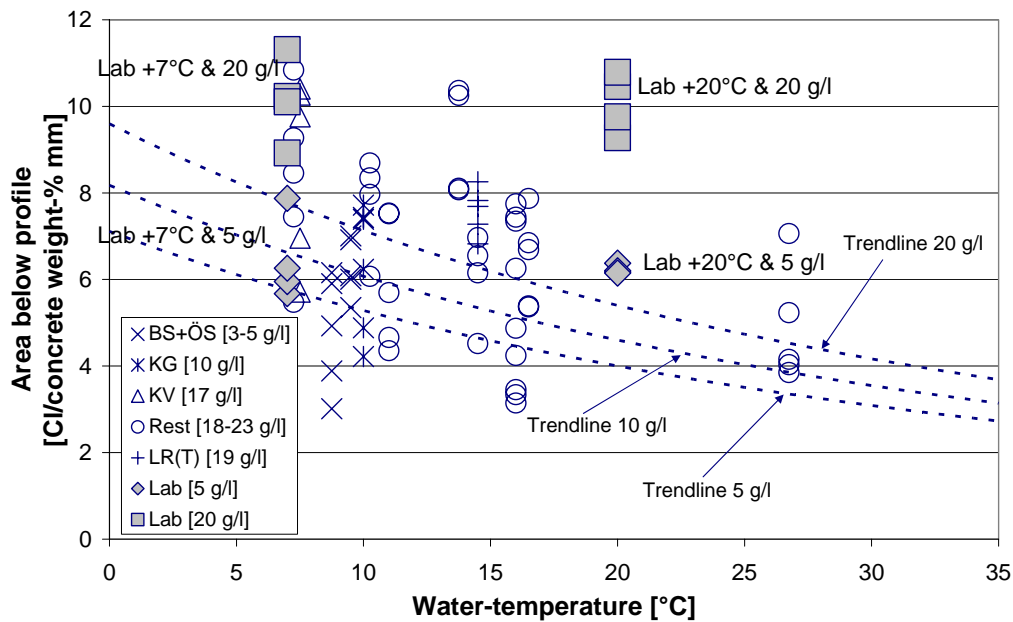


Figure 4.14: The effect of chloride concentration in the exposure water on the chloride ingress.

The results from the laboratory exposure have been compared with the results from a study presented in Tang & Sandberg (1996) and Tang (1997). In the study by Tang & Sandberg the effects of chloride concentration and temperature of the exposure solution on the chloride ingress have been studied. For this purpose concrete specimens have been exposed in both field and laboratory conditions. The field exposure has been made in seawater, continuously pumped from the sea, with a chloride content of 7.6-10.4 g/l. The exposure in the laboratory has been either in artificial seawater, prepared according to ASTM D 1141-86, with a chloride content of 10.3 g/l or in sodium chloride solution with a chloride content of 12.1 g/l. The temperatures of the exposure solutions are  $13 \pm 8^\circ\text{C}$  for the field exposure and  $20 \pm 8^\circ\text{C}$  for the laboratory exposure. For some of the tests in the laboratory the pH in the exposure solution has been regulated by adding nitric acid. In figure 4.15 some of the chloride profiles from the field and laboratory exposure by Tang are presented (Portland cement concrete  $w/b=0.35$ ). The temperature of the exposure solution has been  $20 \pm 3^\circ\text{C}$  for all exposures except A1, where the water temperature has been  $13 \pm 8^\circ\text{C}$ .

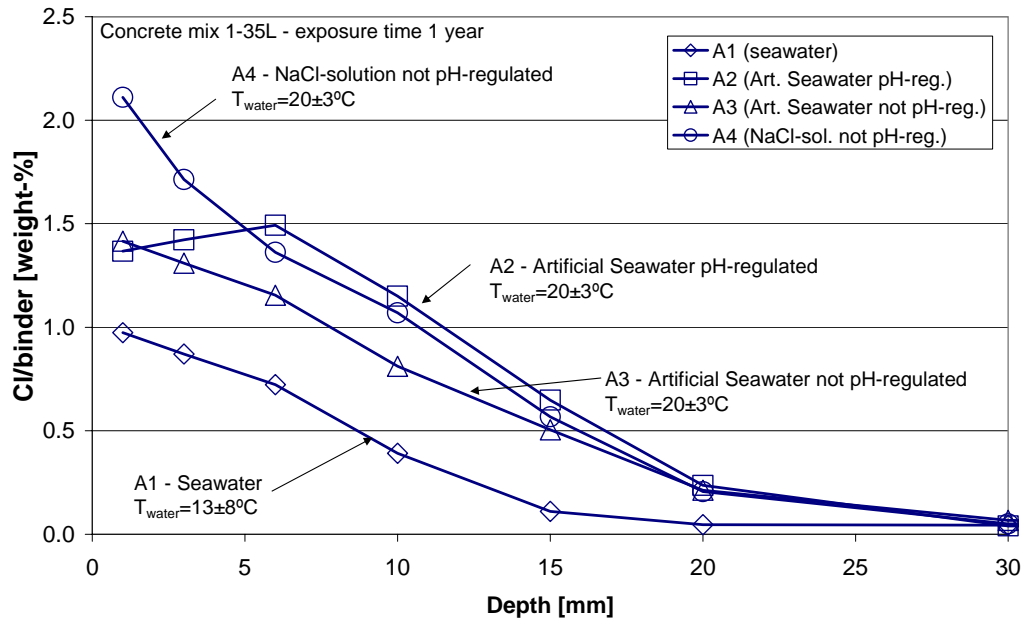


Figure 4.15: Measured chloride ingress profiles from the field and laboratory exposure by Tang (1997).

The profiles in figure 4.15 have been evaluated with the error function solution to Fick's 2<sup>nd</sup> law, and the corresponding  $D_{F2}$  are  $1.71 \cdot 10^{-12} \text{ m}^2/\text{s}$  for the field exposure and  $2.63\text{--}3.46 \cdot 10^{-12} \text{ m}^2/\text{s}$  for the laboratory exposure. Thus the amounts of chloride that have penetrated into the concrete are larger for concrete exposed in the laboratory than in field conditions. Tang & Sandberg (1996) explained this by the higher temperature and chloride concentration in the exposure solution used in the laboratory exposure. There seems to be a temperature effect on the evaluated  $D_{F2}$  where the higher temperature of the exposure solution in the laboratory (approximately 20°C) compared with the field (approximately 13°C), results in higher  $D_{F2}$ . Furthermore, the results from the laboratory exposure show that the type of exposure solution (artificial seawater or NaCl solution), and whether the pH of the solution was regulated or not, seem to have only a small effect on the measured chloride ingress.

The findings by Tang & Sandberg can be used to explain some of the results from the study in marine conditions presented in this thesis. Similar to Tang & Sandberg the larger chloride ingress in laboratory conditions compared with field conditions can be explained by a higher water temperature in laboratory conditions. Furthermore the water temperature in the laboratory is fairly constant during the complete exposure, which is not the case for the field exposure. Since  $D_{F2}$  increases exponentially with increasing temperature, cf. figure 4.12a and eq. (4.3a), the chloride ingress will be proportionally higher with a constant than with a varying temperature, even if the mean temperatures are similar.

#### 4.5.3 Chloride ingress in submerged and tidal conditions

The differences in chloride response in submerged and tidal conditions have been studied at La Rochelle, where specimens have been exposed both in the marine submerged and tidal zones. In figure 4.16a the measured chloride ingress profiles from La Rochelle and in figure 4.16b,  $D_{F2}$  and  $C_{sa}$ , evaluated from the profiles, are plotted against the position in relation to the mean water level. Linear trend lines have been added to the figure to make to effect of the position relative to the mean water level clearer. The profile with index

DB in the tidal zone has a slightly different shape compared with the other profiles from the tidal zone, which results in a higher  $D_{F2}$  but an unchanged  $C_{sa}$ . In figure 4.16a the profiles from the submerged zone (continuous lines) are denoted with an “S” and the profiles from the tidal zone (broken lines) with a “T”.

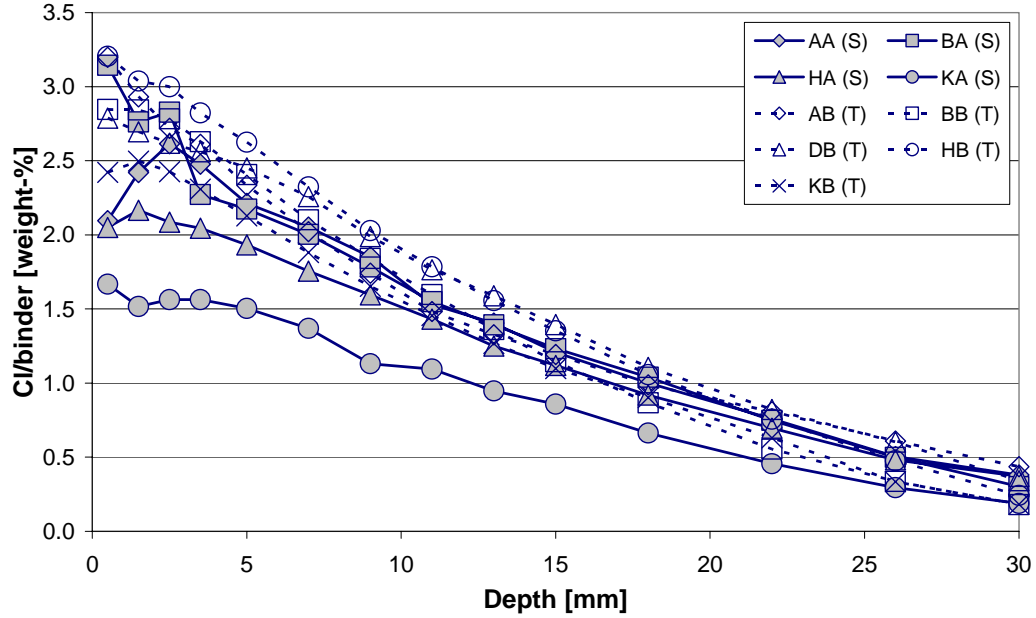


Figure 4.16a: Measured chloride ingress profiles from La Rochelle.

In figure 4.16a it can be seen that the profiles are fairly close together independent of the exposure zone, especially at depths over 15-20 mm. There is even a slight increase in the amount of chlorides that have penetrated into the concrete exposed in the tidal zone.

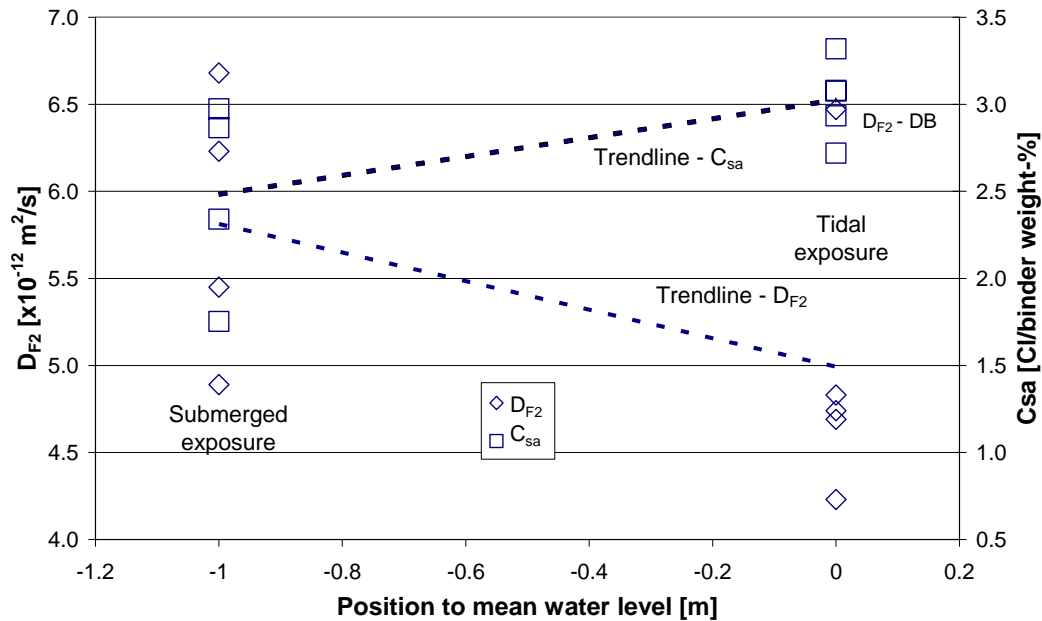


Figure 4.16b: The effect of position relative to the mean water level on  $D_{F2}$  and  $C_{sa}$ .

From figure 4.16b it can be seen that  $D_{F2}$  decreases and  $C_{sa}$  increases when the concrete is exposed in the tidal zone compared with the submerged zone. This behaviour can also be

observed in the profiles, see figure 4.16b, where the profiles from the submerged zone are flatter, i.e. higher  $D_{F2}$ , and lower  $C_{sa}$ , than the profiles from the tidal zone.

A possible explanation for the fairly similar chloride content in the concrete exposed in the tidal exposure compared with the submerged exposure could be differences in the temperature of the concrete specimens. The submerged specimens have the same temperature as the surrounding seawater during the complete exposure period. The specimens in the tidal exposure have the same temperature as the seawater for approximately 12 hours per day, when they are covered with water, while during the rest of the time when the specimens are exposed to the air and solar and long-wave radiation they will have a different, probably higher, equivalent surface temperature, giving larger  $D_a(T)$ , according to eq. (4.3a). However, since the specimens in the tidal zone are exposed to seawater some 12 hours, the time of exposure to chlorides is shorter in the tidal zone (but longer than 12 hours since the specimens are wet and thus exposed to chlorides also a certain time after the tide has withdrawn). Furthermore there is a time delay in the drying of the specimens exposed in the tidal zone when the tide goes back, which means that chloride may be transported also when the concrete is exposed to the air. This means that the resulting chloride content in the concrete exposed in the tidal exposure will be fairly similar to the chloride ingress in the submerged conditions, despite the shorter time of exposure to chlorides, cf. figure 4.16a.

The influence of the depth of water on the chloride ingress has been examined on the specimens exposed at Banyuls sur Mer, where specimens have been exposed both in an aquarium, with water taken from approximately 8 m depth at sea, and at sea at a depth of 24.5 m. However, the specimens exposed in the aquarium have been exposed at a depth of approximately 0.3 m, i.e. the specimens have not been subjected to any water pressure.

In figure 4.17a the measured chloride ingress profiles and in figure 4.17b the effects of the water depth on  $D_{F2}$  and  $C_{sa}$  are shown. Linear trend lines have been added to make the effect of the position relative to the water level clearer. In figure 4.17a the profiles with index “aq” and “sea” come from exposure in the aquarium and in the sea respectively.

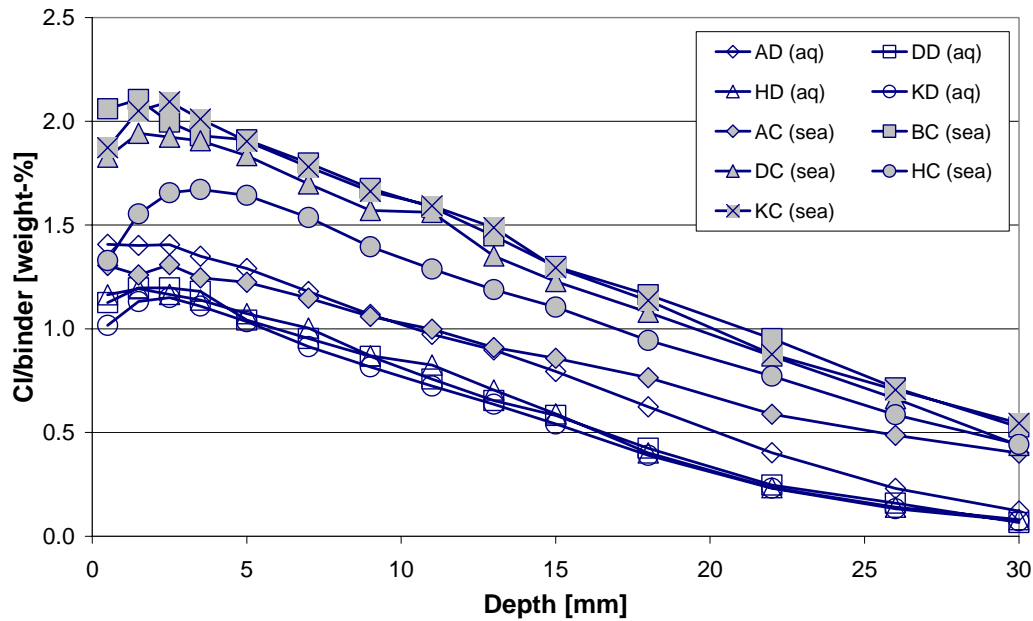


Figure 4.17a: Measured chloride ingress profiles from Banyuls sur Mer.

In figure 4.17a it can be seen that the chloride content in the concrete is significantly higher in the sea than in the aquarium, except for depths up to 15-20 mm in the profile with index AC (sea). However, at larger depths the chloride contents in the profiles, measured in concrete exposed both in the aquarium and at sea, are fairly close together.

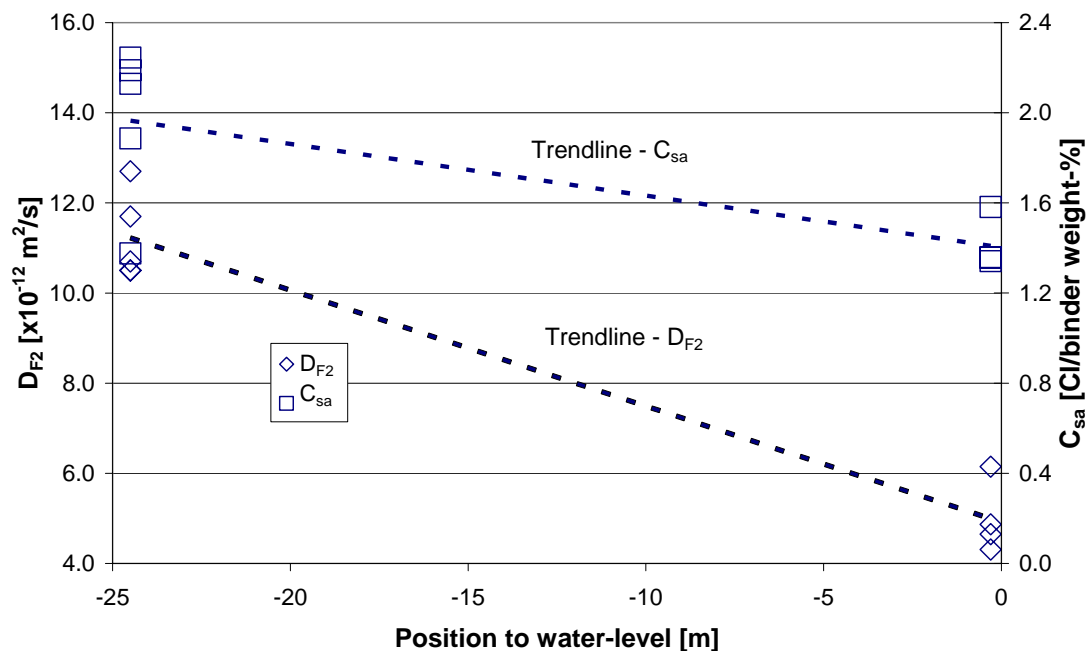


Figure 4.17b: The effect of water depth on  $D_{F2}$  and  $C_{sa}$ .

From figure 4.17b it can be observed that the position in relation to the water level has a clear effect on the chloride ingress into concrete. Both  $D_{F2}$  and  $C_{sa}$  are higher for the exposure at sea than in the aquarium, which means that the transport rate of chlorides increases with increasing water depth. There are several possible explanations for this,



e.g. effects due to increasing water pressure and differences in chloride concentrations and/or temperature of the seawater with increasing depth.

#### 4.5.4 Chloride concentration in seawater at Kjøpsvik and Träslövsläge

The chloride concentration in the seawater at Kjøpsvik is of special interest since the exposure is made in a fjord with only a narrow passage to the open sea. This means that the water exchange between the fjord and the surrounding sea is limited. The fjord is surrounded by high mountains that are covered with snow during the winter and when the spring comes the snow on the mountains melts and runs into to the fjord and since salt water is heavier than fresh water, a layer of water with lower chloride concentration will be formed, “floating” above the salt water deeper down. Since the concrete specimens have been exposed 1-4.5 m below the water surface (depending on the tide level), the exposure has been made in this layer of fresh water mixed with salt water. The seasonal variations in Cl concentration in the seawater have been studied by taking frequent water samples for chloride analysis during the spring and summer.

Similar exposure conditions occur at Träslövsläge and to some extent at Skanör as well, where the chloride concentration in the seawater varies depending on the direction of currents and winds. With currents and winds from the north the chloride concentration in the seawater increases and vice versa with winds and currents from the south. The results of the analyses of the chloride concentrations in the seawater, from water samples taken at different times during the year, at Kjøpsvik and Träslövsläge are shown in figure 4.18.

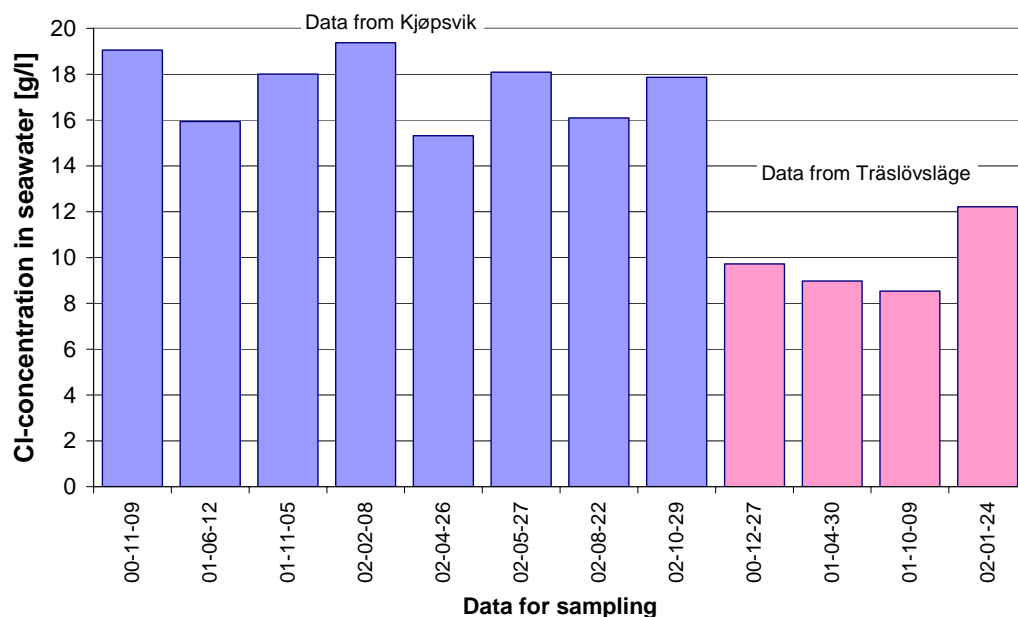


Figure 4.18: Seasonal variations in chloride concentration in the seawater at Kjøpsvik and Träslövsläge.

In figure 4.18 it can be seen that chloride concentration in the seawater at Kjøpsvik is significantly lower each spring (samplings 01-06-12 and 02-04-26) than during the rest of the year. At Träslövsläge the chloride concentration in the seawater on 02-01-24 is significantly higher than on the other occasions. This latter measurement is made after a period with heavy winds from northwest, bringing seawater with high chloride concentration, from the North Sea, towards Träslövsläge. These results show that it is not enough to only have one measurement of the chloride concentration in the seawater, at

least not for locations along the Norwegian and Swedish coastlines. Instead the chloride concentration should be measured on a number of occasions, preferably during a yearly cycle.

#### 4.5.5 Influence of chloride binding

The chloride binding isotherms for the exposed concrete composition have been determined both as bound-free, with the equilibrium method, and free-total, by exposing concrete disks in salt solution in the laboratory. The resulting chloride binding isotherms (free-bound, free-total and free-free) are presented in figure 4.19 together with surface chloride contents,  $C_{sa}$  (circles), evaluated from measured chloride ingress profiles from the different exposure locations (submerged exposure). The filled and unfilled circles denote  $C_{sa}$  evaluated from profiles in figure 4.5a (cold exposure) and 4.5b (warm exposure) respectively. The amount of bound chlorides has been recalculated as Cl content per binder (assuming that the Ca content in the concrete is 12.0%<sup>8</sup> and the binder 64.9%), from the results presented in figure 4.19.

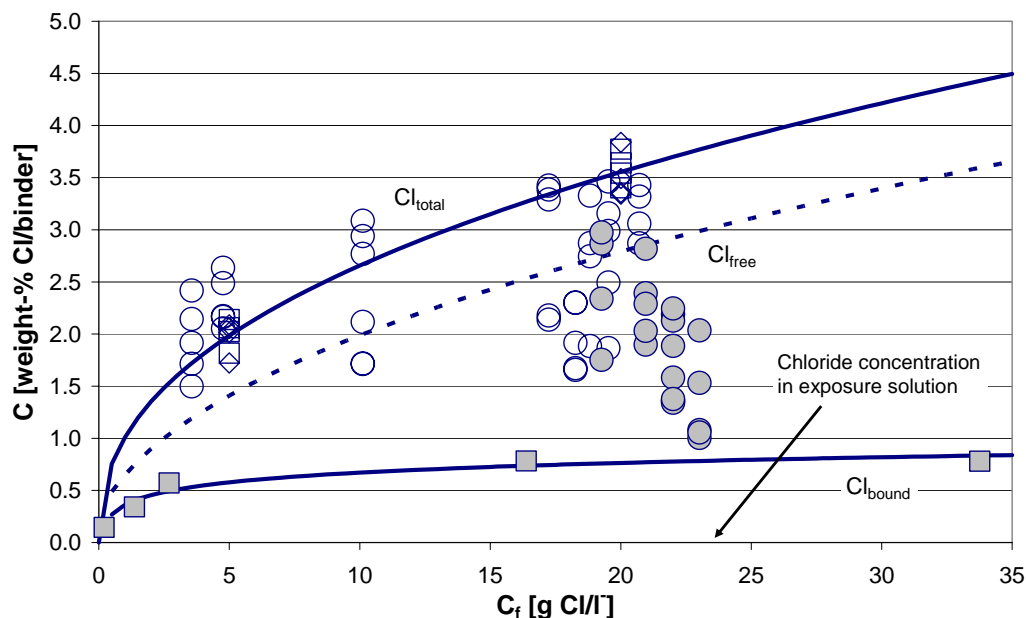


Figure 4.19: Chloride binding isotherm (free-total, free-free and free-bound), for the concrete composition used in the exposure programme together with evaluated  $C_{sa}$  (circles) from all exposure locations.

The chloride binding isotherms in figure 4.19 are mainly influenced by the chloride concentration and to a very small extent the temperature of the exposure solution. This is opposite to what has been reported by Larsen (1998), where the amount of bound chlorides in the concrete, and thus also the total chloride content in the concrete, increases with decreasing temperature (if the free chloride content is unchanged). However, a clear temperature dependency can be observed in  $C_{sa}$  evaluated from measured chloride ingress profiles, with  $C_{sa}$  decreasing with increasing temperature, cf. also figure 4.12b.

Since the total chloride content has been determined on concrete disks, where chlorides have diffused into the concrete, the temperature influences both the chloride binding and

<sup>8</sup> Average CaO content from all measured ingress profiles. This value is somewhat low compared with the CaO data presented in figure 4.11.

the transport properties in the concrete. Thus the measured total chloride content in the concrete follows from a combination of the chloride concentration and the temperature of the exposure solution, where the effects on chloride binding and transport seem to balance each other. This “balancing-effect” may explain the apparent temperature independency in the binding isotherms in figure 4.19.

In figure 4.19 the measured chloride binding can be compared with  $C_{sa}$  evaluated from measured chloride ingress profiles. At low chloride concentrations in the seawater, up to 10 [g Cl/l], the evaluated  $C_{sa}$  correlates fairly well with the measured chloride binding isotherm (free-total), while at higher chloride concentrations in the seawater the evaluated  $C_{sa}$  is lower than the measured chloride binding isotherm (free-total – at chloride concentrations over 20 [g Cl/l] even free-free). Thus the measured chloride binding seems to overestimate the chloride content in the concrete. Some of these differences can be explained by the observed temperature dependency of  $C_{sa}$ , where  $C_{sa}$  decreases with decreasing temperature of the seawater, cf. figure 4.12b, while the chloride binding was found to be very little influenced by temperature.

The measured chloride binding isotherms have been compared with the theoretically possible maximum chloride content in the concrete. The theoretically possible maximum chloride content in the pore solution of the concrete (saturated pore system), i.e. free chloride content, at a certain chloride concentration in the exposure solution can be determined with eq. (4.6a).

$$Cl_c = \frac{Cl_{sol} \cdot P_c}{C} \cdot 100 \quad [\% \text{ by weight Cl/binder}] \quad (4.6a)$$

where:

- $Cl_c$ : chloride content in the concrete. [% by weight Cl/binder]
- $Cl_{sol}$ : chloride concentration in the exposure solution. [kg/m<sup>3</sup>]
- $P_c$ : porosity of the concrete, see eq. (4.6b) – only valid for Portland cement concrete.
- $C$ : cement content in concrete. [kg/m<sup>3</sup>]

$$P_c = P_a \cdot V_a + P_p \cdot V_p = P_a \cdot V_a + \frac{C}{1000} \cdot (w/c - 0.19 \cdot \alpha) + L \quad [m^3/m^3] \quad (4.6b)$$

where:

- $P_c$ : porosity of the concrete. [m<sup>3</sup>/m<sup>3</sup>]
- $P_a$ : porosity of the aggregates. [m<sup>3</sup>/m<sup>3</sup> aggregate]
- $V_a$ : volumetric proportion of aggregates in the concrete. [m<sup>3</sup>/m<sup>3</sup> concrete]
- $P_p$ : porosity of the cement paste. [m<sup>3</sup>/m<sup>3</sup> cement paste]
- $V_p$ : volumetric proportion of the cement paste in the concrete. [m<sup>3</sup>/m<sup>3</sup> concrete]
- $\alpha$ : degree of hydration (assumed to be equal to 0.7)
- $L$ : air content in the concrete. [m<sup>3</sup>/m<sup>3</sup> concrete]

Normally  $P_a=0$ , i.e. the aggregate is not porous, which means that the porosity of the concrete only depends on the porosity of the cement paste, which means that the first term in eq. (4.6b) disappears. The concrete used in the exposure programme has a cement content of 450 [kg/m<sup>3</sup>],  $w/b=0.40$  and  $L=0.045$  [m<sup>3</sup>/m<sup>3</sup> concrete], which means that the porosity of the concrete can be determined according to eq. (4.6c).

$$P_c = \frac{C}{1000} \cdot (w/b - 0.19 \cdot \alpha) + L = \frac{450}{1000} \cdot (0.40 - 0.19 \cdot 0.7) + 0.02 = 0.14 \quad (4.6c)$$

In figure 4.20 the theoretical maximum free chloride content, determined with eq. (4.6a), is presented together with the measured chloride binding isotherms. The theoretical chloride content has been determined for the actual porosity in the concrete,  $P_c=0.14$ .

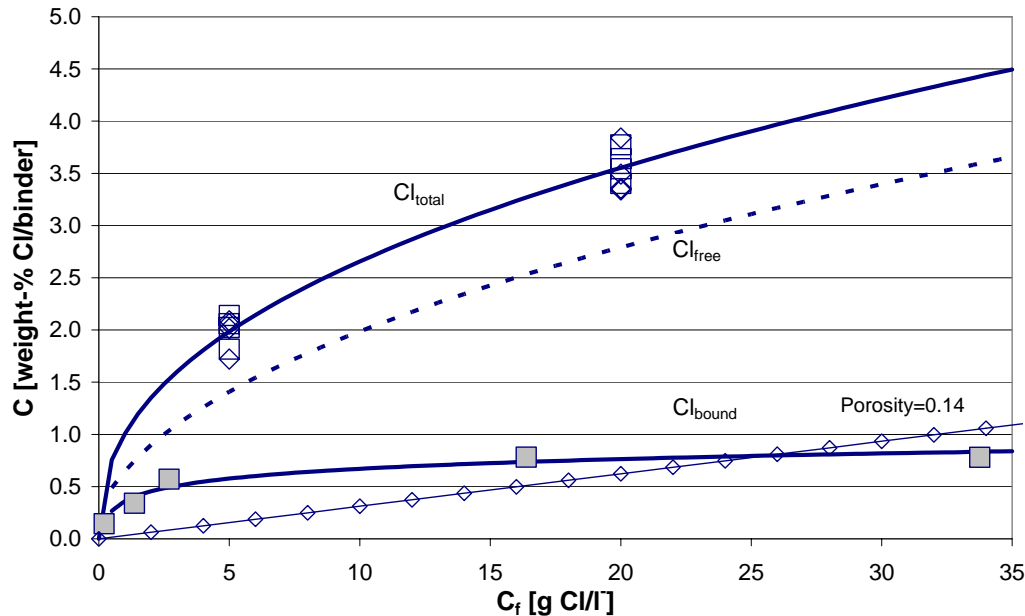


Figure 4.20: Measured chloride binding isotherms together with theoretically determined chloride binding.

In figure 4.20 it can be observed that the measured chloride binding (free chloride content in concrete – dotted line) is larger than the theoretically possible free chloride content. Thus the chloride binding isotherm (free-free) overestimates the chloride content in the pore solution and consequently the chloride transport into concrete will also be overestimated. However, the reason for this is not known.

## 4.6 Conclusions

Based on the results and analyses presented in this chapter the following conclusions have been drawn regarding the marine field exposure:

- Influence of the exposure conditions.** The presented marine exposure programme illustrates how the exposure conditions influence the chloride ingress into concrete. The measured chloride ingress shows fairly large variations between different locations. Since all measurements have been made in identical concretes exposed during approximately similar times, the measured variations should mainly depend on differences in the exposure conditions between the locations. Furthermore the exposure conditions at one location are not constant but vary over time, both periodically and randomly, which also influence the chloride ingress. Thus, it is not possible to model, in a realistic way, the chloride ingress into concrete without taking the exposure conditions, and their variations, into consideration.
- Effect of chloride concentration and temperature of exposure water.** The measured chloride ingress is influenced both by the chloride concentration and the

temperature of the exposure water. In field conditions the main influencing factor was the temperature of the seawater, while in laboratory conditions the chloride concentration of the exposure solution was the main influencing factor. However, it should be kept in mind that these conclusions have been drawn from measurements of the total chloride content in concrete, which means that they reflect the combined effect of the chloride concentration and temperature on the chloride binding and transport. If the effects on the bound or free chloride content had been studied instead, the results may have been different.

- **Factors affecting chloride binding.** Chloride binding isotherms have been established for the concrete composition used in the exposure programme, and the results show that the isotherms are non-linear. The chloride binding is mainly influenced by the chloride concentration in the exposure solution and only to a small extent by the water temperature. However, the temperature effect has only been studied on concrete into which the chlorides have been diffusing and the corresponding total chloride content has been measured, which means that the temperature influences both the chloride binding and transport properties. To better clarify the temperature effect on chloride binding, the effect should be investigated in tests where the bound and free chloride contents are measured at different temperatures, e.g. in the equilibrium test.
- **Effect of position relative to mean water level.** For exposure in submerged conditions the chloride ingress has been found to increase with increasing depth below the water surface. If the depth increases from 0.0 m to 24.5 m  $D_{F2}$  increases by a factor 2.5 and  $C_{sa}$  by a factor 1.4. The chloride ingress in submerged and tidal (exposure at the mean water level giving approximately 12 hours daily exposure to seawater) conditions has been found similar. This is mainly explained by the higher temperature of the concrete in tidal conditions than in submerged conditions. However, for concrete in other positions in the tidal zone, the chloride ingress may be different. Thus, when the chloride ingress is studied in tidal conditions it is important to specify where, in relation to the mean water level and the tidal actions, the exposure takes place.
- **Variations in exposure conditions (chloride concentration and temperature).** The exposure conditions, in terms of chloride concentration and temperature of the seawater, vary, both periodically and randomly, at the different exposure locations in the exposure programme. Generally the chloride concentration in the seawater only shows small variations for the exposure locations. However, along the Swedish coasts, in particular the west coast, the chloride concentration in the seawater varies randomly, depending on the direction of currents and winds, and in fjords, where the chloride concentration in the surface near water is influenced by melting water in the spring. However, the temperature of the seawater varies with a yearly cycle for all exposure locations. This means that to get a correct description of the exposure conditions it is not enough to use only yearly mean values, at least not for the water temperature. Instead, the variations, primarily periodically and if possible also randomly, should be taken into account. This can be done by frequent measurements, or logging, of the water temperature during the exposure. Furthermore the chloride concentration in the seawater for locations in or close to inland seas, e.g. the Baltic Sea, and in fjords, has been found to vary significantly (both periodically and randomly) and should therefore preferably be monitored over the year to be properly described.



## 5 Field study – Road conditions

This chapter describes field studies in which measurements have been made of chloride ingress, moisture conditions and resistance to frost damage for concrete structures exposed along thaw-salted roads. However in this report only measurements of the environmental response such as chloride ingress are presented. The field study has been made as three separate investigations, which are fully presented in Lindvall & Andersen (2000), Lindvall (2001), Lindvall (2002a) and Lindvall (2002b).

### 5.1 Introduction

A field study has been made to investigate the exposure conditions along thaw-salted roads. The purpose of the field study has been to determine how the exposure conditions vary between different locations along thaw-salted roads and how the corresponding chloride ingress into concrete structures exposed along the roads varies. The exposure conditions have been registered in terms of the amount of de-icing salt spread on the roads, characteristics of roads (number of lanes etc), characteristics of traffic (amount of traffic, speeds etc) and meteorological data for the roads (air temperature etc). The field study has been made as three separate investigations:

- **Investigation of chloride ingress in seven reinforced concrete bridges around Göteborg.** The investigation was made during 1998 and 1999 on columns, side beams and the underside of a bridge slab. The following parameters influencing the chloride ingress have been studied: type of structural element (column or side beam), orientation of surface, distance to road, speed of traffic, height above the road and orientation towards the traffic. Detailed presentations of the study are given in Lindvall & Andersen (2000) and Lindvall (2001).
- **Mapping of the exposure to chlorides around two Swedish reinforced concrete bridges.** Two of the bridges examined in the first investigation have been further studied, by exposing mortar disks on bridge columns (at different heights and orientations). The mortar disks have been exposed between February 2001 and May 2001 and after exposure the absorption of chlorides in the disks has been determined. The effects of height above the road and orientation towards the traffic have been examined. A detailed presentation of this investigation is given in Lindvall (2002a).
- **Five years of chloride ingress data from exposure in a Swedish road environment.** Chloride ingress data measured in concrete blocks, made from three different concrete compositions, exposed for five years at the Rv40 field station outside Borås. Two exposure series have been made, where the first was started in 1996 and the second in 1997. The concrete blocks were periodically sampled for chloride ingress (in the first exposure series on four and in the second exposure series on six occasions). A detailed presentation of this investigation is given in Lindvall (2002b).

In the following sections first the three different field studies are described, then the results from each of the studies are presented and analysed and finally conclusions are drawn.

## 5.2 Exposure programme

### 5.2.1 Investigation of chloride ingress in seven reinforced concrete bridges around Göteborg

#### Introduction

Seven reinforced concrete bridges around Göteborg have been investigated with the purpose to produce input data for mathematical prediction models and to study how the exposure environment influences the service life of reinforced concrete structures. The aim of the study has not been to perform complete assessments of the current state of the bridges, but to acquire additional information about the physical processes that govern deterioration of reinforced concrete. The study has been limited to structural parts of bridge structures where published (quality) data are missing. For this purpose side beams and columns on different bridges have been investigated. The following has been included in the study: (i) Survey of the exposure conditions for the examined bridges, (ii) Measurements of the response of the concrete, in terms of chloride ingress and moisture conditions, (iii) Survey of visible corrosion damage, i.e. no measurements of corrosion activity, and (iv) Visual survey of substandard workmanship and maintenance. Detailed presentations of the study are given in Lindvall & Andersen (2000) and Lindvall (2001).

#### Examined bridges

Seven bridges have been included in the investigation. The bridges have been chosen in such a way that they represent typical Swedish reinforced concrete bridges, with an age between 25 and 35 years. The term typical Swedish reinforced concrete bridge means here that the bridge was designed and constructed according to valid Swedish concrete codes. All bridges have been constructed with K400 concrete, with a cement content varying between 300-360 kg/m<sup>3</sup> and a w/c of approximately 0.45-0.50. All bridges are motorway bridges, where the motorway crosses, either above or below, another road.

The following seven bridges have been investigated in the study:

- **Bridge N 434.** Bridge, built in 1972, south of Göteborg, over the motorway E6 (four lanes with hard shoulders on each side and exit and entry roads to the motorway), where E6 crosses the road between Kungsbacka and Onsala. The bridge is orientated in the north-south direction.
- **Bridge O 670.** Bridge, built in 1968, north of Göteborg, where the motorway E6 (four lanes with hard shoulders on each side) crosses the river Nordre Älv. The bridge is orientated in the north-south direction.
- **Bridge O 707.** Bridge, built in 1968, in Göteborg, with exit and entry road to the motorway E6 (four lanes with hard shoulders on each side). The exit and entry road is on a bridge formed as a 180° curve over a local road and a car park.
- **Bridge O 762.** Bridge, built in 1974, east of Göteborg, where the motorway Rv40 (five lanes with hard shoulders on each side) crosses the road between Landvetter and Partille. The bridge is orientated in the east-west direction. Bridge O 762 is situated approximately 2 km west of bridge O 978 along the same motorway.
- **Bridge O 832.** Bridge, built in 1972, east of Göteborg, with exit and entry road to the motorway E20 (six lanes with hard shoulders on each side). The bridge is a part of a roundabout over E20. The bridge is orientated in the east-west direction.



- **Bridge O 951.** Bridge, built in 1972, south of Göteborg, where a local road crosses the motorway E6 (four lanes with hard shoulders on each side). The bridge is orientated in the east-west direction.
- **Bridge O 978.** Bridge, built in 1974, east of Göteborg, where a local road crosses the motorway Rv40 (four lanes with hard shoulders on each side) in Landvetter. The bridge is part of a roundabout over Rv40 together with bridge O 979. Bridge O 978 is situated approximately 2 km east of bridge O 762.

### Exposure conditions

The environmental conditions for the examined bridges have been assumed equal to the regional conditions in Göteborg with variations in the road environment for each bridge. The monthly mean air temperature varies between -1.7°C (February) and +16.2°C (July), and the monthly mean RH varies between 72% RH (May) and 87% RH (January and December). The road environment for each of the bridges is given in table 5.1.

Table 5.1: The road environment for the examined bridges. Data from Nilsson (2000).

Bridge	Built	Traffic		De-icing kg/m <sup>2</sup> year	Lanes	
		Amount <sup>9</sup> [ÅDT]	Speed limit [km/h]		Number	Hard shoulder
N 434*	1972	27000	110	2,8	3+3 <sup>10</sup>	Yes
N 434 <sup>+</sup>	1972	♦	70	♦	1+1	No
O 670*	1968	40000	110	3,1	2+2	Yes
O 670 <sup>†</sup>	1968	-	-	-	2+2	Yes
O 707 <sup>-</sup>	1968	♦	50	2,3	1+1	No
O 707 <sup>+</sup>	1968	2400	50	♦	1+1	No
O 762*	1974	32000	110	3,0	3+2	Yes
O 762 <sup>+</sup>	1974	♦	70	♦	1+1	No
O 832*	1972	50000	90	2,7	3+3	Yes
O 832 <sup>+/-</sup>	1972	13200	50	♦	2	No
O 951*	1972	34000	110	2,8	2+2	Yes
O 978*	1974	26000	110	3,0	2+2	Yes
O 978 <sup>+</sup>	1974	♦	50	♦	1	Yes

\* : Motorway.

+ : Local road.

- : Exit/entry on motorway

† : Underside bridge slab.

ÅDT : Mean traffic during a day.

♦ : Data not known

<sup>9</sup> The data on the amounts of traffic are only valid for the motorways. Data on the amount of traffic on the local roads and exits/entries on the motorway are not known, except for bridge O 707 and bridge O 832.

<sup>10</sup> Two lanes in each direction on the motorway and entry lanes.

### Field study

The bridges have been investigated for chloride ingress, moisture conditions and resistance to frost damage, during the autumns of 1998 and 1999. In this report only the results from the investigation of chloride ingress are presented. The measured moisture conditions and resistance to frost damage are presented in Lindvall & Andersen (2000).

Cores have been drilled from the bridges in selected positions. A water-cooled drilling machine was used. Fresh water was used as cooling water and at temperatures below 0°C an anti-freezing agent (alcohol) was added to prevent the water from freezing. After coring the cores were brought to the laboratory for further analysis. The cores have been drilled from the bridges as set out below:

- **Bridge N 434.** Two columns (middle and side column), along the motorway, and one of the side beams, along a local road, have been investigated.
- **Bridge O 670.** One of the side beams, along the motorway, and the underside of the bridge slab have been investigated.
- **Bridge O 707.** One of the side beams, along the exit and entry road, and one side column, along the local road, have been investigated.
- **Bridge O 762.** One side beam, along the motorway, and one side column, along a local road, have been investigated.
- **Bridge O 832.** One side beam, along the entry lane, and one side column, along the motorway, have been investigated.
- **Bridge O 951.** One of the middle columns, along the motorway, has been investigated.
- **Bridge O 978.** One side beam, along a local road, and one middle column, along the motorway, have been investigated.

The exact locations where the samples were taken are described in detail in Lindvall & Andersen (2000) and Lindvall (2001).

The chloride ingress into the columns on bridges N 434, O 951 and O 978 has been investigated more thoroughly, where cores have been drilled from the columns at three levels and four directions to investigate the effects of height above the road and orientation towards the traffic on the chloride ingress. An illustration showing the sampling positions is given in figure 5.1. The heights above the road are denoted by U (0.00-0.50 m), M (1.05-1.55 m) and Ö (2.20-2.70 m) and the distances to the traffic have been between 2.10 m and 3.05 m.

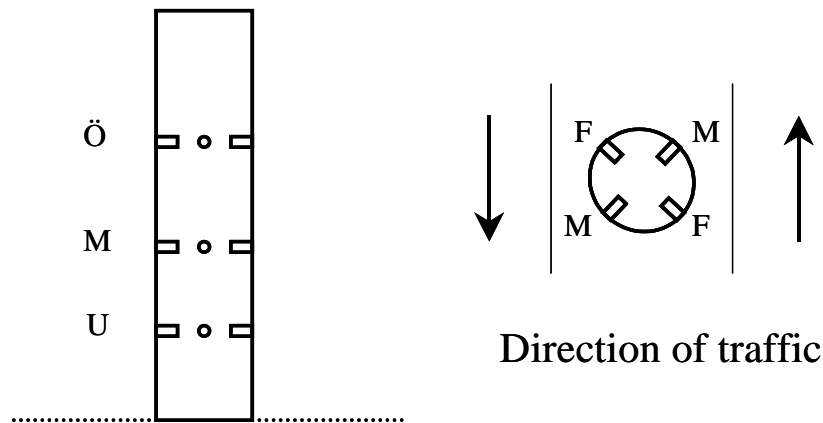


Figure 5.1: Illustration of sampling positions on columns on bridges N 434, O 951 and O 978.

On the other bridges the columns have been investigated at heights between 0.40 m and 2.50 m and distances to the traffic between 2.30 m and 5.00 m. The side beams have been investigated mainly on horizontal surfaces except on bridges N 434 and O 978 where vertical surfaces have also been investigated. The distances between the side beams and the traffic have been between 0.80 m and 4.20 m. A more comprehensive description of where the columns have been investigated is given in Lindvall & Andersen (2000) and Lindvall (2001).

### 5.2.2 Mapping of the exposure to chlorides around two Swedish reinforced concrete bridges

#### Introduction

Based on the results from the study presented in Lindvall & Andersen (2000) and Lindvall (2001) two of the bridges, bridge O 951 and O 978, were chosen for further studies. The results from these bridges showed large variations in the measured chloride response, both between the bridges but also within one single bridge. Since the chloride ingress measured in concrete is influenced both by the environmental actions and the material properties it is hard to quantify the influence due only to the exposure environment. Therefore mortar disks, with similar paste composition, were exposed in this study, to exclude any effects from variations in material properties. The mortar disks were exposed on the bridges during the period February-May 2001. The disks were exposed at different heights above the road and orientations towards the traffic on the earlier examined columns on bridges O 951 and O 978. In this way the results from Lindvall & Andersen (2000) could be further explained and the exposure conditions for the two bridges could be better understood.

#### Materials and exposure environment

The composition of the mortar used in the disks is given in table 5.2.

Table 5.2: The mortar composition used in the mortar disks.

Material	Content [kg/m <sup>3</sup> ]	Density [kg/m <sup>3</sup> ]
CEM I 42,5 BV/SR/LA*	525	3100
Sand (fine)	525	2650
Sand (medium)	525	2650
Sand (coarse)	525	2650
Water (tap water)	236	1000
AEA <sup>^</sup>	0.26	-

\* : Swedish SRPC (Cementa Anläggningcement Degerhamn)

<sup>^</sup> : Cementa L 14 has been used as air entraining agent (AEA). A dosage of 0.05% AEA of cement weight has been used, producing 10.5 % air by volume in the mortar.

All disks have been cast on the same occasion, in cylindrical moulds (100 mm in diameter), and then cured in the moulds for four days and 23 days in water. After curing, the cylinders were sawn into disks (30–40 mm thick). The boundary surfaces on the disks were sealed with asphalt tape and vulcanising tape to enable exposure to chlorides in only one direction. Finally, the disks were glued to steel plates which had been fastened to the concrete columns with stainless screws. The mortar disks are shown in figure 5.2 (left) and as mounted on steel plates in figure 5.2 (right).

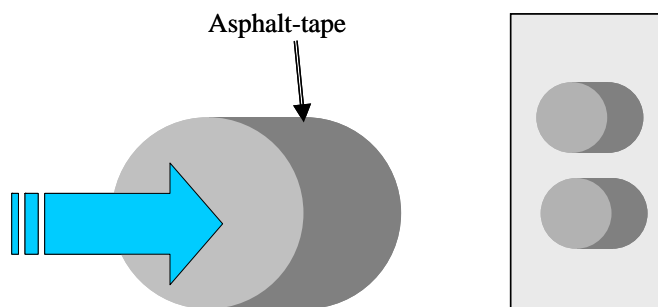


Figure 5.2: The appearance of the mortar disks (left) and as mounted on steel plates (right).

The exposure conditions for bridge O 951 and O 978 are given in section 5.2.1.

### Field study

On bridge O 951 the mortar disks have been exposed on the southern of the middle columns at two different heights above the road and in four/six different directions towards the traffic, see figures 5.3a and 5.3b. In figure 5.3a, the examined column is marked with grey.

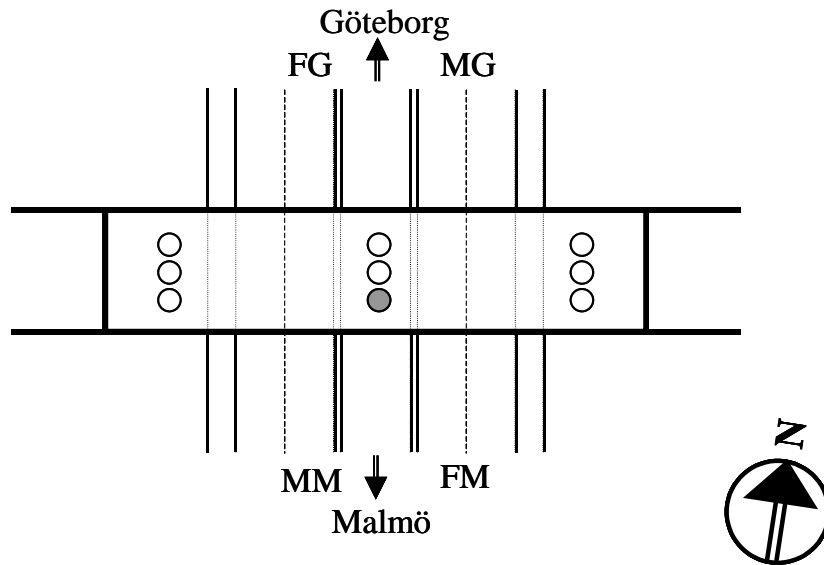


Figure 5.3a: The location of mortar disks on bridge O 951. The examined column is marked with grey.

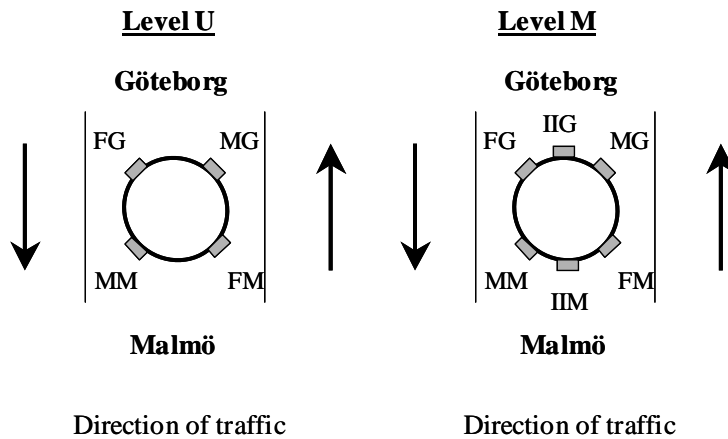


Figure 5.3b: The positions of the mortar disks on the southern of the middle columns on bridge O 951.

The lower level on bridge O 951 is approximately 0.20 metre above the road and the middle level is approximately 1.40 metres above the road. The horizontal distance between the road and the column is approximately 2.00 m.

In the study made in autumn 1999 the westerly of the columns between the carriageways on the motorway and the western side beam on the bridge slab have been examined. The mortar disks were exposed on the column at three different heights above the road and in four/eight different directions towards the traffic. The distance between the road and the column is approximately 3.05 m. The positions of the mortar disks on bridge O 978 are shown in figures 5.4a and 5.4b. In figure 5.4a the examined column is marked with grey.

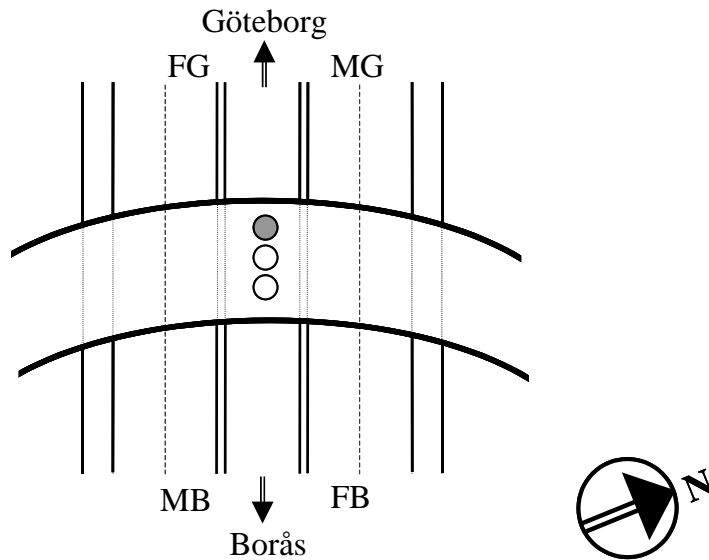


Figure 5.4a: The locations of the mortar disks on bridge O 978. The examined column is marked with grey.

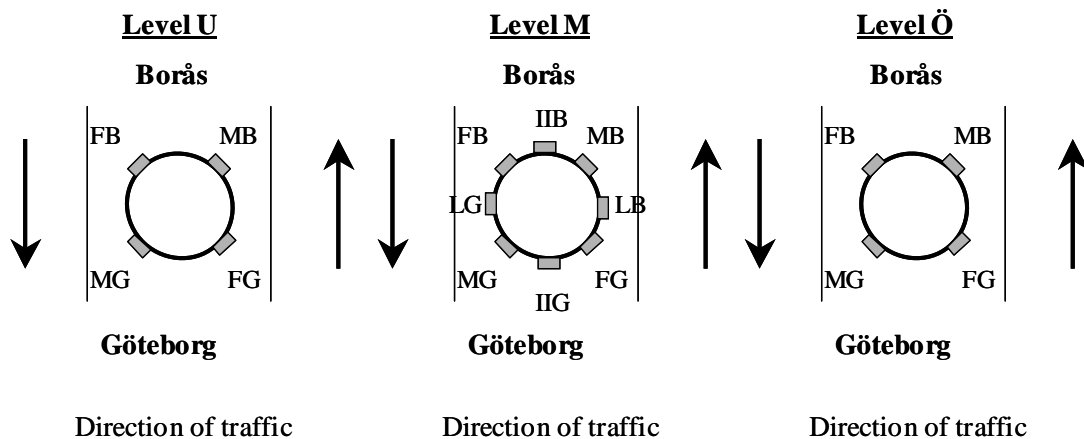


Figure 5.4b: The positions of the mortar disks on the western of the middle columns on bridge O 978.

The lower level on bridge O 978 is approximately at the same level as the road, the middle level is approximately 1.05 metres above the road, and the higher level is approximately 2.20 metres above the road. The horizontal distance to the traffic is approximately 3.05 metres for all mortar disks.

### 5.2.3 Five years of chloride ingress data from exposure in a Swedish road environment

#### Introduction

In an ongoing Nordic research project, Durability of Concrete structures exposed to de-icing salts (*BTB – Beständighet hos Tösaltad Betong*), a number of concrete compositions are exposed in a road environment. The concrete compositions have been made from a number of Nordic cements, with different w/b, binders (Portland cement, fly ash and silica fume) and admixtures. Blocks made from these concrete compositions have been exposed at a field station along the motorway Rv40 west of Borås, some 60 km from the Swedish west coast.

The concrete blocks have been periodically investigated for chloride ingress, frost and salt attack, moisture content and reinforcement corrosion. This report presents the chloride ingress measured for three of the exposed concrete mixes, with w/b=0.40 and 0.75 made from Portland cement and for one of the mixes with an addition of silica fume, up to five years exposure. The results from the other investigations are presented elsewhere, e.g. Nilsson et al (2000) and Utgenannt & Petersson (2001).

### Materials and exposure environment

Three different concrete compositions have been studied in this investigation. The exposure took place at the Rv40 field station with concrete blocks that have been cast and put in place at the field station on two different occasions. The compositions of the exposed concretes are presented in table 5.3. In table 5.3 the contents of cement and aggregates are presented as kg/m<sup>3</sup> concrete.

Table 5.3: The studied concrete mixes exposed at the Rv40 field station.

Concrete mix		Cement	Aggregates [kg/m <sup>3</sup> ]		Water	w/b	Additives [%]	
No.	Block	[kg/m <sup>3</sup> ]	0-8 mm	8-16 mm	[kg/m <sup>3</sup> ]	[-]	AEA	Plasticizer
201	D, E	420.0	886.4	851.6	168.0	0.40	0.028	0.97
206	D, E	399.0*	860.0	860.0	168.0	0.40	0.040	1.20
236	C, D	260.0	1007.4	791.6	195.0	0.75	0.012	-

\* 5% of the amount of binder in concrete mix 206 is silica fume, i.e. 21.0 kg/m<sup>3</sup>. This means that the total amount of binder in the concrete is 420 kg/m<sup>3</sup>.

The cement used in all concrete mixes has been a Swedish SRPC cement *Degerhamn Anläggningscement* (CEM I 42.5 BV/SR/LA). Air entraining agent (AEA) and plasticizer *Cementa L14* and *Melcrete* respectively have been used.

The concrete blocks measure 300x300x400 mm<sup>3</sup> and have been cast in steel moulds. The blocks have been slightly tilted away from the road in such a way that the upper surface has a slight tilt to simulate the upper surface of side beams on a bridge. The blocks have been placed on gravel to avoid capillary suction from the ground. Nevertheless, this has not always been avoided.

The field station is located along the northern side of the motorway Rv40 west of Borås. The concrete blocks have been placed approximately 0.70 m from the road surface behind a collision barrier. The motorway Rv40, which goes in an east-west direction, is the main road between Borås and Göteborg and during the wintertime de-icing salt is spread to prevent slippery road conditions. This means that the concrete blocks during the wintertime have been exposed to chlorides from de-icing salt spread on the road. In figure 5.5 the field station with concrete blocks exposed along the motorway Rv40 is shown.



Figure 5.5: The Rv40 field station. Concrete blocks placed along the northern side of motorway Rv40. Picture taken towards the east.

The exposure environment has been monitored at a meteorological station placed at the field station. The meteorological station has monitored, among other parameters, the air temperature and humidity. Furthermore the amount of de-icing salt and the days when it is spread on the road have been registered. The amounts of snow, ice and water around the concrete blocks have been visually inspected continuously during the exposure. In figure 5.6 an example of the variations in air temperature and humidity during a winter are shown (the winter 1999/2000).

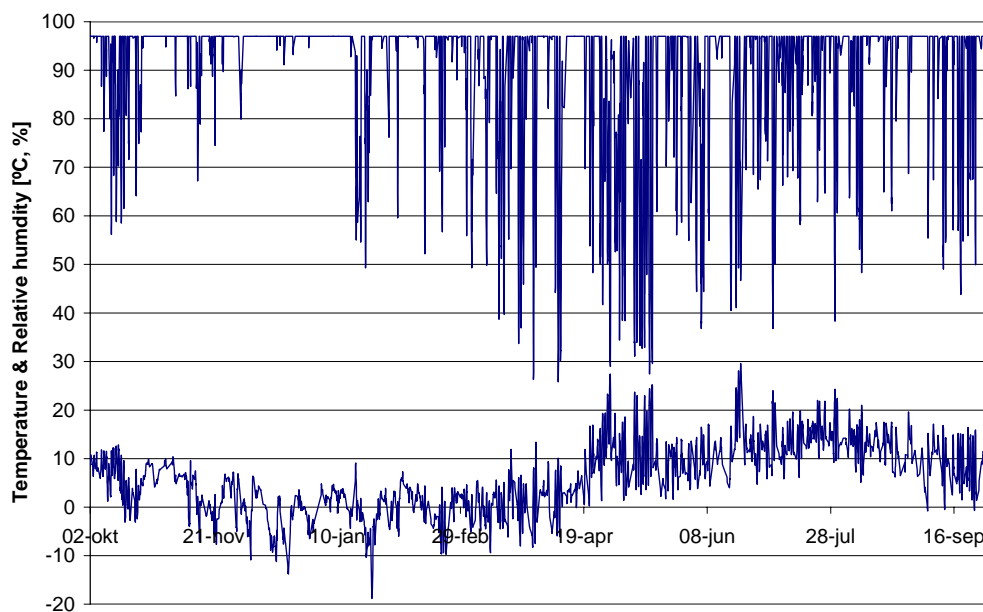


Figure 5.6: The air temperature and humidity during the winter 1999/200. Based on unpublished meteorological data measured at the Rv40 field station.



As mentioned in chapter 3 de-icing salt is spread either to prevent slippery road conditions or to clear snow. To prevent slippery road conditions a salt solution is used with 24% salt (each time approx.  $10 \text{ g/m}^2$  solution is spread – meaning that  $0.24 \cdot 10 = 2.4 \text{ g/m}^2$  salt is spread). Snow is cleared with pure salt (NaCl), where each time approximately  $15 \text{ g/m}^2$  salt are spread. The occasions when de-icing salt has been spread on the road during the winters 1996/1997-2000/2001 are given in table 5.4. Both spreading methods have been used during all the studied winters. Information on when the two spreading methods have been used is only known for the winter 2000/01, where occasions of snow clearance are given within brackets. The road width on which de-icing salted is spread, in each direction, is approx. 8 m.

*Table 5.4: The occasions when de-icing salt has been spread on Rv40 at the field station during the winters 1996/1997-2000/2001. Data from Utgenannt (2002).*

Month	1996/97	1997/98	1998/99	1999/00	2000/01
October	0	13	4	1	0
November	22	29	25	15	0
December	34	30	34	42	15 (11)
January	35	28	27	38	29 (12)
February	23	18	29	27	16 (16)
Mars	8	23	27	16	10 (4)
April	4	16	5	2	1 (3)
<b>Total</b>	<b>126</b>	<b>157</b>	<b>151</b>	<b>141</b>	<b>71 (46)</b>

Unfortunately it is not known on how many occasions each of the two spreading methods have been used, except for the winter 2000/2001, consequently the amounts of de-icing salt spread each year are not known either, except for the winter 2000/2001. However, traditionally de-icing salt has been spread as pure salt (snow clearance) and the use of salt solutions (preventive spreading) has become more common during the last years, which means it can be assumed that the use of salt solution has become more common only during the last years. Based on this some assumptions have been made concerning the amounts of de-icing salt spread on the road, where the assumed usage of the different methods is shown within brackets: During the winter 1997/1998  $1.76 \text{ kg/m}^2$  de-icing salt was spread (assuming that 30% was preventive spreading and 70% was for snow clearance) and during the winter 2000/2001  $0.86 \text{ kg/m}^2$  de-icing salt was spread.

### Field study

As mentioned earlier two exposure series of concrete blocks have been included in the study. The first series has been exposed since December 1996 and the second series since November 1997. The blocks in the first exposure series have been sampled on four different occasions, after approximately 0.5, 1.0, 1.5 and 4.5 years of exposure. The blocks in the second exposure series have been sampled at six different occasions, after 90, 120, 150, 180, 223-224 and 330 days of exposure.

Cores have been drilled from the blocks both from horizontal and vertical surfaces, facing towards the traffic. The cores have been drilled in such a way that chloride ingress is only studied in one dimension, i.e. cores have not been drilled close to corners etc. The blocks

have been brought to the laboratory for coring. After the coring the drilled holes were repaired and the blocks were brought back to the field station for further exposure.

### 5.3 Results

The results from the field study are presented as measured chloride ingress profiles. The profiles from each of the three investigations are given separately. In this section only a selection of the results is presented. Complete presentations of the results are given in Lindvall & Andersen (2000), Lindvall (2001), Lindvall (2002a) and Lindvall (2002b).

#### 5.3.1 Measuring techniques

The chloride conditions in the concrete have been determined as chloride ingress profiles where the quotient between the chloride and calcium contents has been determined at different depths from the surface. For this purpose cores have been drilled from the concrete in the bridges or from the centre of the exposed specimens. The cores have been drilled in the exposure direction perpendicular to the exposure surface. The cores have been divided into depth intervals by means of profile grinding. The profile grinding has been carried out in a modified lathe equipped with either a cutting wheel, with set-up shown in figure 5.7, or a drilling machine, with set-up shown in figure 4.4.

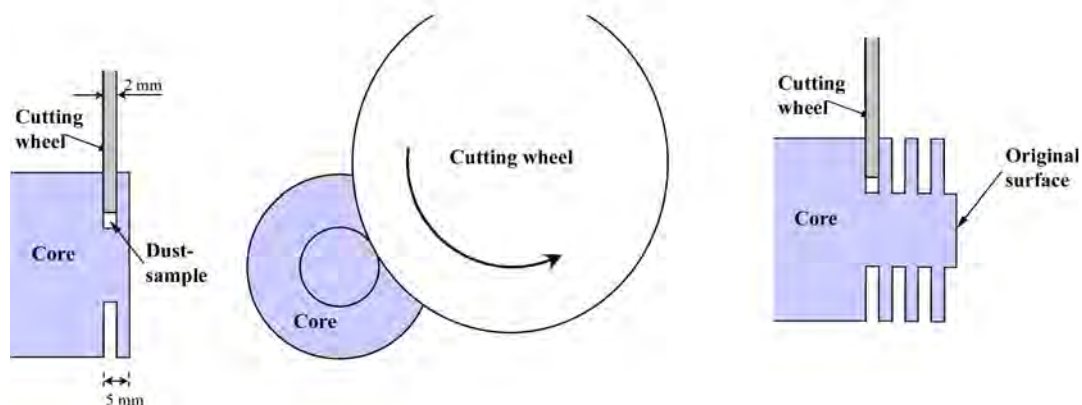


Figure 5.7: The setup of the equipment used for profile grinding (cutting wheel).

The advantage of using the drilling machine instead of the cutting wheel is that the amount of collected powder is significantly higher with the drill. Furthermore it is possible to take powder samples at smaller depth intervals with the drill, since the cutting wheel has a thickness of 2 mm, which sets the minimum limit for the depth intervals. However, an advantage with the sawing blade is that samples can be taken from large depths without having to remove all concrete up to that depth. The method with the cutting wheel has been used for all cores ground before July 2001.

The powder samples have been analysed for acid-soluble calcium and chlorides. The analyses have been made as in the marine exposure programme (described in chapter 4).

#### 5.3.2 Measured chloride ingress

##### Chloride ingress into reinforced concrete bridges around Göteborg

A selection of the measured chloride ingress profiles from the examined bridges is presented in figures 5.8a (columns) and 5.8b (side beams). The chloride ingress is

presented as the quotient between the contents of chlorides and calcium in the concrete, since neither the cement content nor the calcium content in the cement used in the concretes are known.

In figure 5.8a the indexes for profiles from bridges N 434, O 951 and O 978 show the height above the road and the orientation towards the traffic. Furthermore the profiles with indexes O 707 OP +40 and O 762 SPOB +2.0 have been taken along local roads and the profile with index O 832 TP +1.60 along a motorway. In figure 5.8b all profiles have been taken from horizontal surfaces, except N 434 Sida1-3 and O 978 KU-1. The profile with index O 670 KK +RH has been taken along a motorway, the profile with index O 707 OKO has been taken along an exit road from a motorway and the profiles from bridges N 434 and O 978 and the profile with index O 832 TK +7 have been taken along local roads. The exposure times have been between 24 and 30 years.

It should be noticed that the chloride conditions in a concrete bridge vary over the year due to variations in the environmental actions, especially due to the fact that de-icing salt only is spread during the cold part of the year. This means that the presented chloride ingress profiles only indicate the current state at the time of sampling. The variations in chloride ingress over the year are exemplified in e.g. Nilsson et al (2000) and Gaal et al (2003).

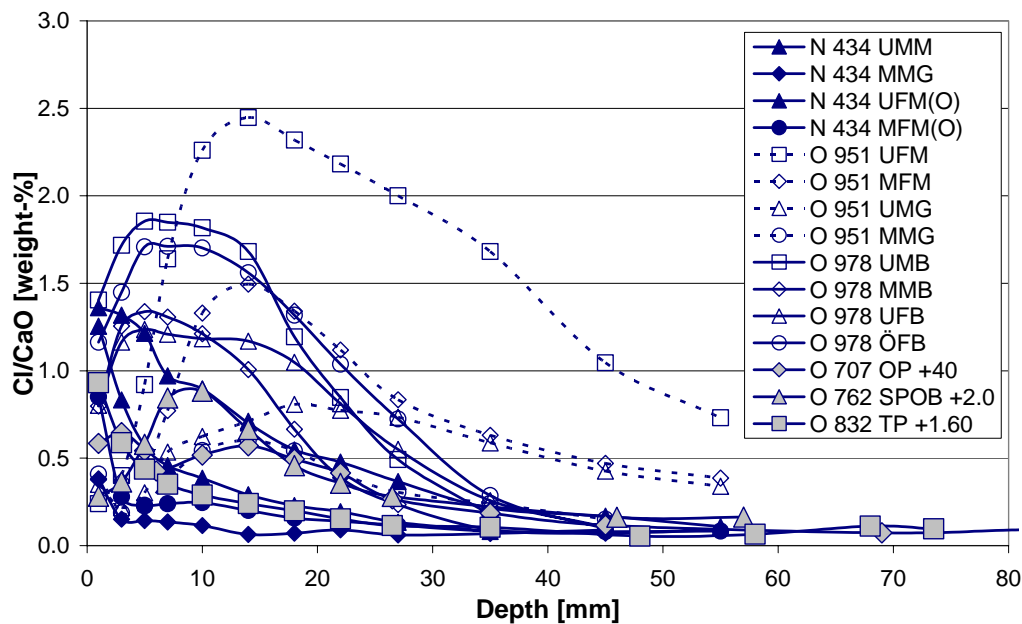


Figure 5.8a: Selection of chloride ingress profiles from columns.

In figure 5.8b the chloride ingress in the side beams has been measured in horizontal (index: N 434 ovansida, O 978 KU-1, O 670 KK+RH, O 707 OKO and O 832 TK+7) and vertical (index: N 434 Sida2 & Sida 1 and O 978 KS-1 & KS-2) surfaces.

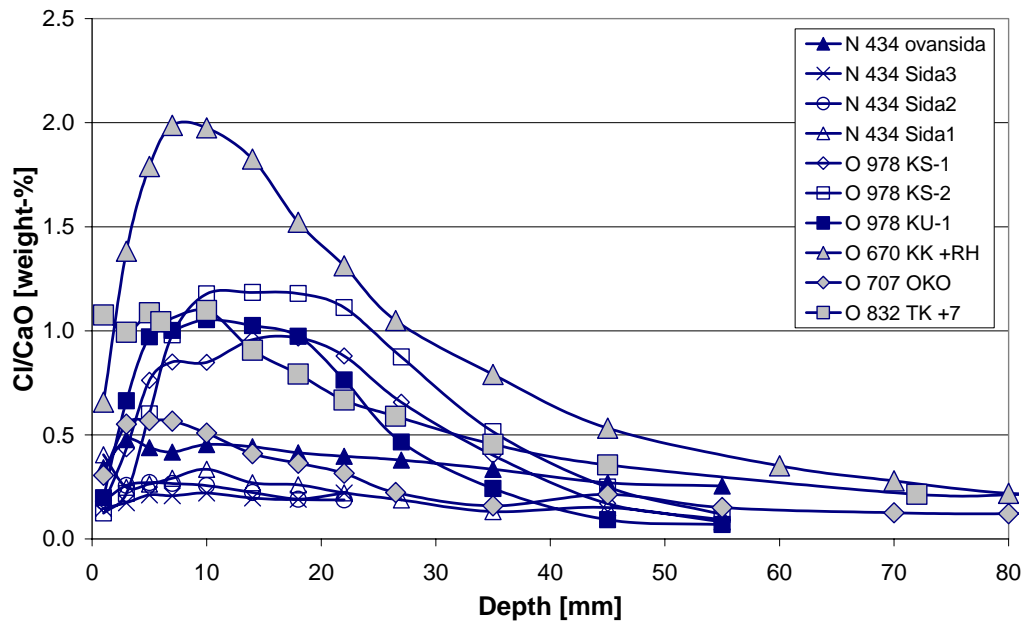


Figure 5.8b: Selection of chloride ingress profiles from side beams.

In figures 5.8a and 5.8b it can be seen that the measured chloride ingress profiles vary significantly not only between different bridges, but also within one single bridge. These variations can mainly be attributed to where on the structure, in relation to the road (height and distance) and the traffic (orientation), the chloride ingress has been measured. Furthermore the exposure to chlorides is influenced by the characteristics of the traffic and spread of de-icing salt. Generally surfaces close to the road and the traffic and orientated towards the traffic have the severest exposure to chlorides. These factors are further discussed in section 5.4.

As mentioned earlier the chloride ingress into columns on bridges N 434, O 951 and O 978 has been studied at different heights above the road and orientations towards the traffic. In figure 5.8c measured chloride ingress profiles from the examined column on bridge O 978, along the motorway Rv40 between Göteborg and Borås, are shown. In figure 5.8c the first letter in the index indicates the height above the road, according to figure 5.1, and the last two letters the orientation towards the traffic (FB –towards the traffic to Göteborg, FG – towards the traffic to Borås, MB – from the traffic to Borås and MG – from the traffic to Göteborg). For clarity the chloride ingress data in figure 5.8c are presented with a scale different from that in figures 5.8a and 5.8b.

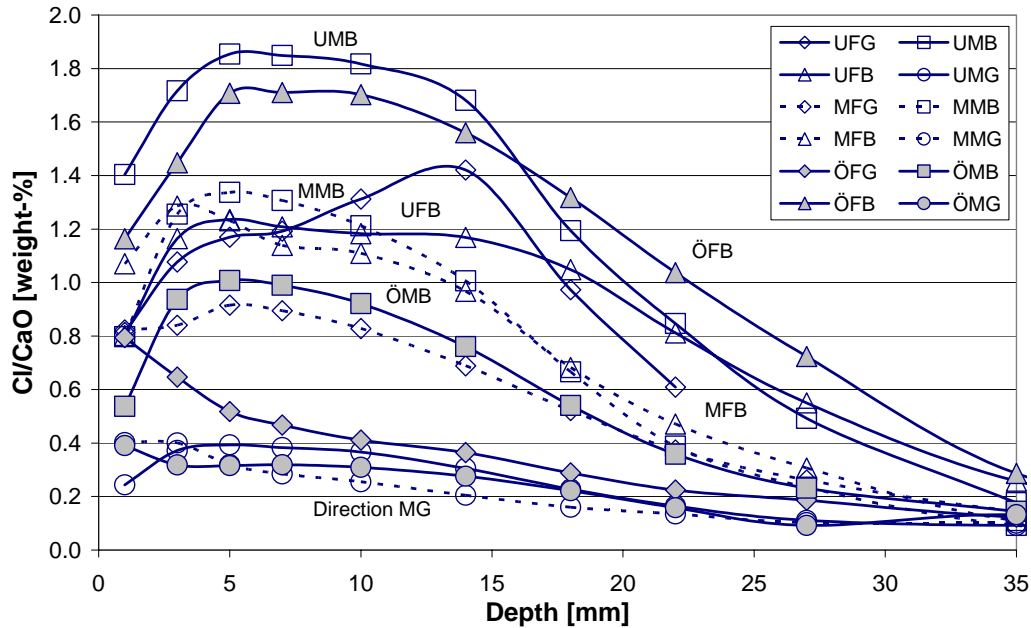


Figure 5.8c: Chloride ingress profiles from the concrete in the column on bridge O 978.

From figure 5.8c it can be seen that the measured chloride ingress may vary significantly on one single column. The largest chloride ingress was measured on a surface at the level of the road orientated towards the traffic (index UMB). However, large chloride ingress was also measured on the surface with index (ÖFB), i.e. 2.2 m above the road facing towards the traffic from Borås. The chloride ingress on bridge O 978 is further discussed in section 5.4.

#### Mapping of the chloride load around two Swedish reinforced concrete bridges

The results from the mapping of the chloride load around two Swedish reinforced concrete bridges are presented in figures 5.9a (bridge O 951) and 5.9b (O 978), as measured chloride ingress profiles from the mortar disks exposed on the bridges.

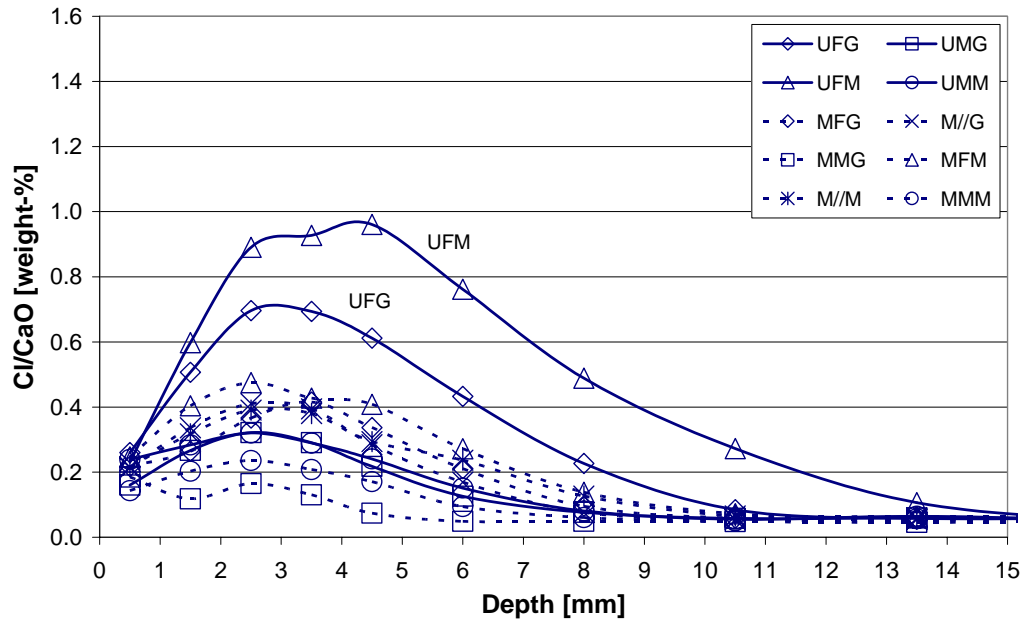


Figure 5.9a: Chloride ingress profiles from mortar disks exposed on bridge O 951.

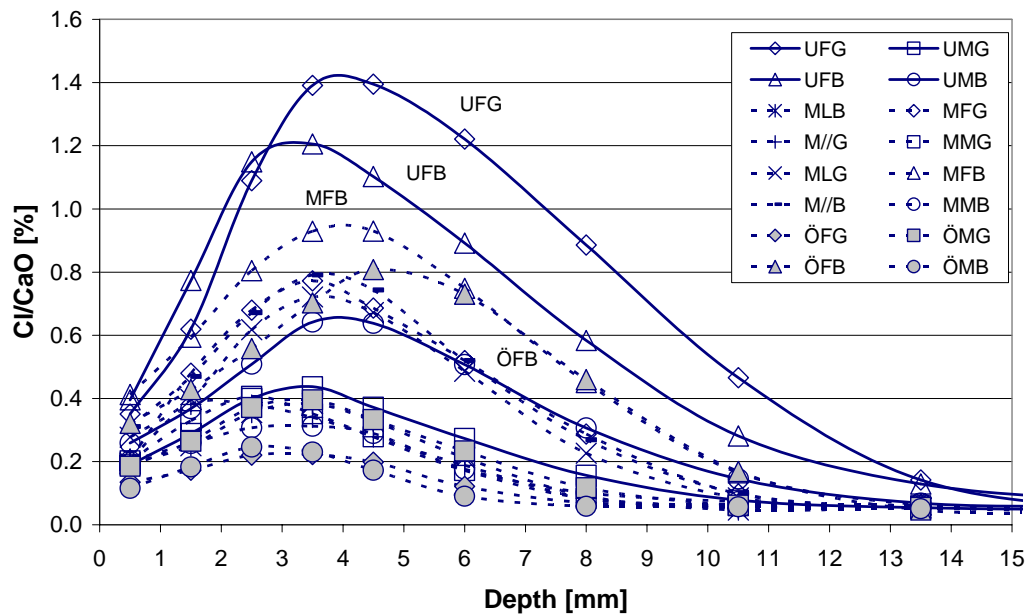


Figure 5.9b: Chloride ingress profiles from mortar disks exposed on bridge O 978.

The measured chloride ingress profiles presented in figures 5.9a and 5.9b demonstrate the influence of height above the road and orientation towards traffic. The largest chloride ingress, on both bridges, was measured on surfaces at the level of the road facing towards the traffic (disks index UFG and UFM on bridge O 951 and UFB and UFG on bridge O 978). Noticeable is the relatively large chloride ingress measured in the disk with index ÖFB. This confirms the findings from the measurements of chloride ingress into concrete on bridge O 978, see figure 5.8c. The results in figures 5.9a and 5.9b are further discussed in section 5.4.

### Chloride ingress in a Swedish road environment – Five years' exposure for three concrete compositions

A selection of the results from the investigation of chloride ingress in a Swedish road environment are shown in figures 5.10a (first exposure series) and 5.10b (second exposure series), where chloride ingress profiles measured in concrete 201 (w/c=0.40) after different exposure times are presented. The chloride ingress is presented as the quotient between the chloride and calcium contents in the concretes, to facilitate comparisons with the chloride ingress profiles presented in figures 5.8a and 5.8b. In figures 5.11a (first exposure series) and 5.11b (second exposure series) chloride ingress profiles measured in concrete 236 (w/c=0.75) are presented. All profiles have been taken from horizontal surfaces.

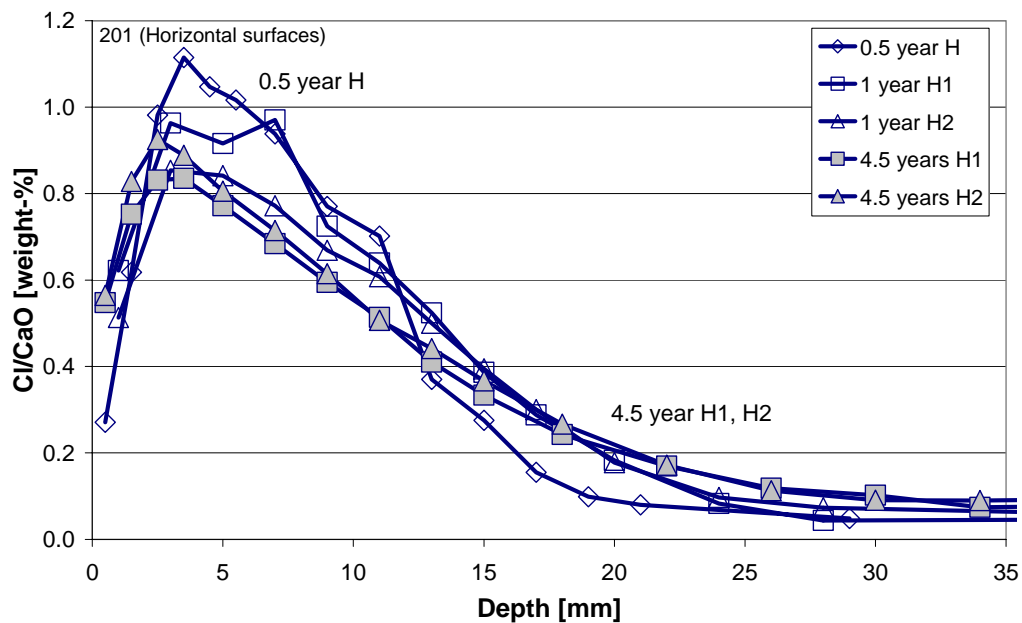


Figure 5.10a: The measured chloride ingress profiles from the first exposure series measured at different exposure times (0.5-4.5 years) on concrete 201.

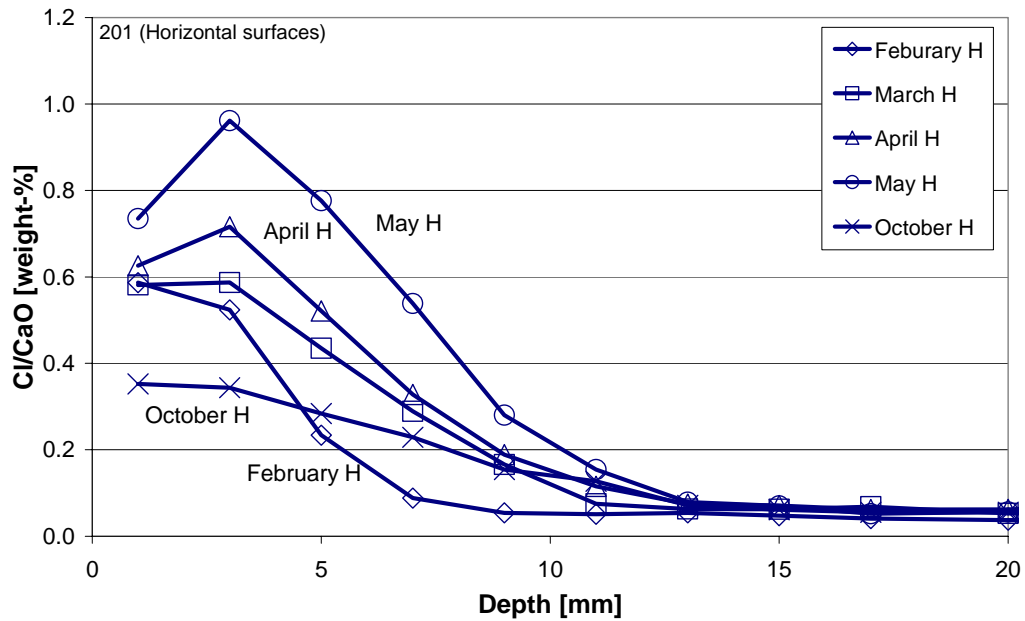


Figure 5.10b: The measured chloride ingress profiles from the second exposure series measured at different exposure times during the first year of exposure (1998) on concrete 201.

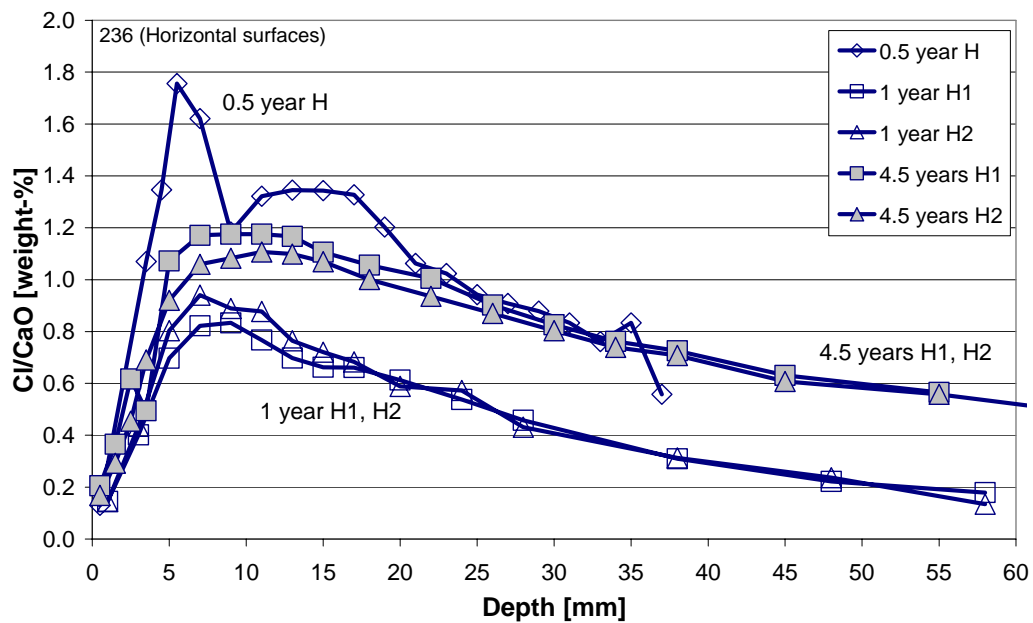


Figure 5.11a: The measured chloride ingress profiles from the first exposure series measured at different exposure times (0.5-4.5 years) on concrete 236.



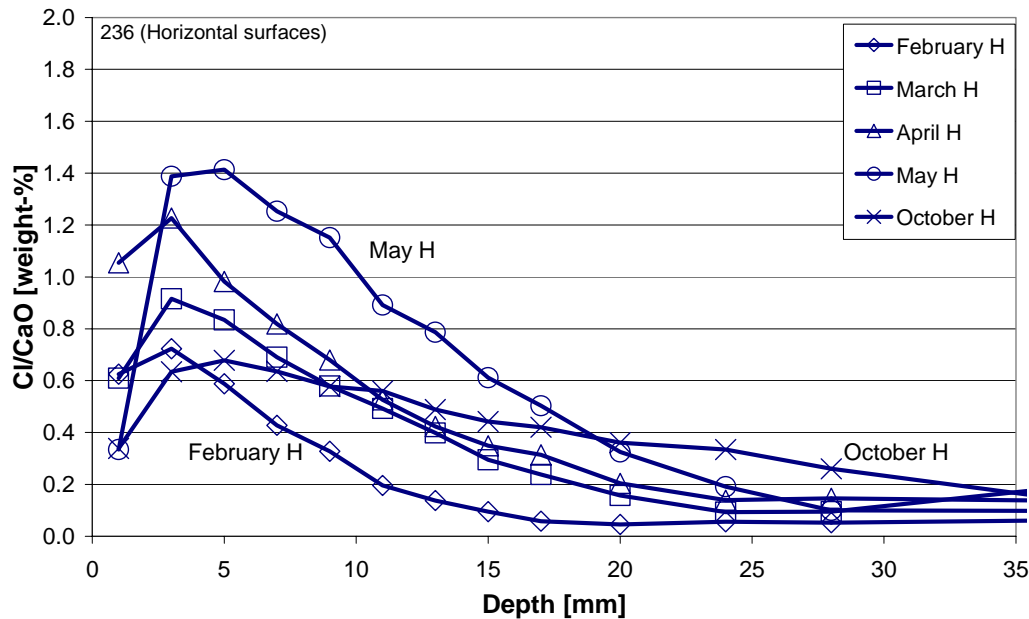


Figure 5.11b: The measured chloride ingress profiles from the second exposure series measured at different exposure times during the first year of exposure (1998) on concrete 236.

From figures 5.10a and 5.11a it can be seen that the main part of the chloride ingress takes place during the first winter and during the following winters there is only a slight increase in chloride content in the concrete. The profiles measured after 1 year of exposure of concrete 236 are lower than the other profiles for this concrete. This is obviously wrong, since it would mean that chlorides disappear from the concrete during exposure. However, the reason for this is not known.

In figures 5.10b and 5.11b a build-up of chlorides during the winter can be observed, with the highest chloride content measured in May. During the summer (profile measured in October) the chlorides have been redistributed, with a chloride transport into the concrete, and washout of chlorides, with the chloride content decreasing close to the surface.

## 5.4 Analysis and discussion

Obviously it is possible to make extensive analyses of the results from the investigations made in road conditions. However, due to limitations of space in this thesis the following topics will be analysed and discussed:

- Evaluation of measured chloride ingress profiles.
- Effect of height above road and orientation towards traffic.
- Chloride ingress over time in road conditions.
- Comparison of chloride ingress measured in concrete and mortar disks.
- Comparison of chloride ingress into columns and side beams.

More extensive analyses of the results from the investigations are given in Lindvall & Andersen (2000), Lindvall (2001), Lindvall (2000a) and Lindvall (2000b).

### 5.4.1 Evaluation of measured chloride ingress profiles

The chloride ingress profiles measured in concrete have been evaluated by curve fitting to the error function solution of Fick's 2<sup>nd</sup> law. The curve fitting has been performed in such a way that the inner parts of the profiles are fitted where the correlation between the measured and fitted profiles has a maximum. The curve fitting has been carried out in accordance with a procedure described in Nilsson et al 2000 and resulted in two regression parameters, namely an apparent diffusion coefficient,  $D_{F2}$ , and an apparent surface chloride content,  $C_{sa}$ . Two additional parameters have been determined,  $x_c$ , showing the thickness of the "convection zone", where measured profiles do not fit the error function, measured from the surface, and a surface chloride content for the diffusion zone,  $C_{sc}$ . For each profile curve fitting was first made with all points in the profile and then points were omitted from the surfaces until the coefficient of correlation,  $R$ , exceeded 0.980.

The chloride ingress profiles measured in mortar have been evaluated by integrating the area below each profile. In this way the amount of chlorides that have penetrated into each of the mortar disks can be determined, which gives a measure of the severity of the exposure to chlorides.

#### Chloride ingress into reinforced concrete bridges around Göteborg

The parameters evaluated from the measured chlorides profiles presented in figures 5.8a-5.8c are set out in tables 5.5a-5.5c.

Table 5.5a:  $D_{F2}$ ,  $C_{sa}$ ,  $x_c$  and  $C_{sc}$  evaluated from chloride ingress profiles in figure 5.8a (except profiles from the column on bridge O 978)

Profile	Age [years]	$D_{F2}$ [ $\times 10^{-13} \text{ m}^2/\text{s}$ ]	$C_{sa}$ [wt-% Cl/CaO]	$x_c$ [mm]	$C_{sc}$ [wt-% Cl/CaO]
N 434 UMM	27	2.23	0.65	5	0.57
N 434 MMG	27	12.90	0.132	3	0.15
N 434 UFM (O)	27	2.96	1.39	1	1.36
N 434 MFM (O)	27	7.80	0.27	3	0.28
O 951 UFM	27	12.70	3.32	14	2.45
O 951 MFM	27	7.13	2.08	14	1.50
O 951 UMG	27	15.70	1.13	18	0.81
O 951 MMG	27	14.50	0.74	22	0.49
O 707 OP +40	30	3.93	0.92	14	0.57
O 762 SPOB+20	24	2.16	1.38	10	0.88
O 832 TP+1.60	26	1.92	0.45	5	0.44

From table 5.5a large variations in the evaluated parameters from the examined columns can be seen, both between bridges, but also within one single bridge. Examples of factors that influence the evaluated parameters are characteristics of concrete (composition, age etc), traffic on road (speeds, amount of traffic, types of vehicles etc), spread of de-icing salt (frequency, type of salt etc), orientation towards traffic and height above and distance to the road. This is further discussed in section 5.4.2.

In table 5.5b the parameters have been evaluated from chloride ingress data from horizontal (index: N 434 ovansida, O 978 KU-1, O 670 KK+RH, O 707 OKO and O 832 TK+7) and vertical (index: N 434 Sida2 & Sida 1 and O 978 KS-1 & KS-2) surfaces.

*Table 5.5b:  $D_{F2}$ ,  $C_{sa}$ ,  $x_c$  and  $C_{sc}$  evaluated from chloride ingress profiles in figure 5.8b*

Profile	Age [years]	$D_{F2}$ [ $\times 10^{-13} \text{ m}^2/\text{s}$ ]	$C_{sa}$ [wt-% Cl/CaO]	$x_c$ [mm]	$C_{sc}$ [wt-% Cl/CaO]
N 434 ovansida	27	42.20	0.48	3	0.48
N 434 Sida3*	27	-	-	-	-
N 434 Sida2	27	9.19	0.30	5	0.27
N 434 Sida1	27	10.20	0.37	10	0.34
O 978 KS-1	25	5.70	1.64	14	0.96
O 978 KS-2	25	5.08	2.34	18	1.18
O 978 KU-1	25	3.40	1.98	14	1.03
O 670 KK+RH	30	7.80	2.36	7	1.99
O 707 OKO	30	9.98	0.57	5	0.60
O 832 TK+7	26	10.80	1.13	5	1.09

\* : Evaluated data from the profiles with index N 434 Sida3 are obviously wrong and therefore not presented in table 5.5b.

In table 5.5b large variations in the evaluated parameters from the examined side beams can be seen. The orientation of the examined surface (horizontal/vertical) seems not to have any significant effect on the evaluated parameters. This is further discussed in section 5.4.5.

Table 5.5c:  $D_{F2}$ ,  $C_{sa}$ ,  $x_c$  and  $C_{sc}$  evaluated from chloride ingress profiles in figure 5.8c (profiles from the column on bridge O 978). The exposure time has been 25 years.

Profile	$D_{F2}$ [ $\times 10^{-13}$ m <sup>2</sup> /s]	$C_{sa}$ [wt-% Cl/CaO]	$x_c$ [mm]	$C_{sc}$ [wt-% Cl/CaO]
UFG	1.50	3.82	14	1.42
UMB	1.88	3.94	14	1.68
UFB	4.19	1.86	10	1.18
UMG	4.02	0.48	5	0.39
MFG	3.35	1.16	5	0.92
MMB	2.06	1.98	7	1.31
MFB	3.24	1.51	3	1.29
MMG	3.80	0.39	1	0.40
ÖFG	3.76	0.63	3	0.65
ÖMB	2.80	1.32	5	1.01
ÖFB	3.56	2.67	10	1.70
ÖMG	5.56	0.38	1	0.39

From table 5.5c large variations in the evaluated parameters from the examined column on bridge O 978 can be seen. These variations can be attributed to differences in orientation towards traffic and height above the road.  $D_{F2}$  seems not be significantly influenced by the position on the column, except for the profiles with indexes UFG and UMB where  $D_{F2}$  is lower than for the other profiles.  $C_{sa}$  is high for surfaces facing towards the traffic at the level of the road (index UFG and UMB) and decreases with increasing height above the road. However, it should be noticed that  $C_{sa}$  evaluated from the profile with index ÖFB (2.20 m above the road facing towards the traffic from Borås) does not conform to this. This is further discussed in section 5.4.2.

#### Chloride ingress in a Swedish road environment – Five years' exposure for three concrete compositions

In tables 5.6a (concrete 201) and 5.6b (concrete 236)  $D_{F2}$ ,  $C_{sa}$ ,  $x_c$  and  $C_{sc}$  evaluated from the measured chloride profiles presented in figures 5.10a-5.10b and 5.11a-5.11b, are presented.

Table 5.6a:  $D_{F2}$ ,  $C_{sa}$ ,  $x_c$  and  $C_{sc}$  evaluated from chloride ingress profiles in figures 5.10a and 5.10b (concrete 201).

Profile	Age [days]	$D_{F2}$ [ $\times 10^{-12}$ m <sup>2</sup> /s]	$C_{sa}$ [wt-% Cl/CaO]	$x_c$ [mm]	$C_{sc}$ [wt-% Cl/CaO]
H	150	5.28	1.56	3.5	1.12
H1	390	2.30	1.65	7.0	0.97
H2	390	3.03	1.28	7.0	0.77
H1	1663	0.93	0.99	2.5	0.83
H2	1663	0.89	1.06	2.5	0.93
February	90	1.00	1.15	0.0	1.15
March	120	2.31	0.89	1.0	0.59
April	150	1.10	1.21	1.0	0.72
May	180	1.20	1.57	1.0	0.96
October	330	6.27	0.52	3.0	0.34

Table 5.6b:  $D_{F2}$ ,  $C_{sa}$ ,  $x_c$  and  $C_{sc}$  evaluated from chloride ingress profiles in figures 5.11a and 5.11b (concrete 236).

Profile	Age [days]	$D_{F2}$ [ $\times 10^{-12}$ m <sup>2</sup> /s]	$C_{sa}$ [wt-% Cl/CaO]	$x_c$ [mm]	$C_{sc}$ [wt-% Cl/CaO]
H	150	34.5	2.97	5.5	2.41
H1	390	22.8	0.98	9.0	0.83
H2	390	18.1	1.10	7.0	0.94
H1	1663	14.0	1.34	7.0	1.17
H2	1663	19.0	1.22	11.0	1.11
February	90	4.95	1.00	3.0	0.72
March	120	9.18	1.12	3.0	0.92
April	150	6.49	1.42	3.0	1.23
May	180	8.11	1.81	3.0	1.39
October	330	14.0	0.77	5.0	0.68

In tables 5.6a and 5.6b it can be seen that both  $C_{sa}$  and  $D_{F2}$  decrease over time, if the chloride ingress over 4.5 years of exposure is studied. This is a result of the fact that the chloride ingress almost stops after the first winter of exposure. If  $C_{sa}$  and  $D_{F2}$  during the first winter of exposure are studied it can be seen that  $C_{sa}$  increases as long as chlorides are available at the surface of the concrete, i.e. when de-icing salt is spread, and decreases during the summer, when there is a washout of chlorides from the surface of the concrete.  $D_{F2}$  is fairly stable as long as chlorides are available on the road, but increases significantly during the summer, as a result of the transport of chlorides into the concrete that takes place during the summer. The parameter  $x_c$  is fairly constant over time, with a slight increase with increasing exposure, indicating that the extent of the convection zone increases.  $C_{sc}$  is fairly constant over time, if the chloride ingress over 4.5 years is studied. However, if the first winter of exposure is studied  $C_{sc}$  increases as long as chlorides are available at the surface of the concrete, and then decreases during the summer. The decrease in  $C_{sc}$  during the summer can be attributed to the washout of chlorides from the

surface of the concrete. The chloride ingress over time is further discussed in section 5.4.3.

#### Mapping of the chloride load around two Swedish reinforced concrete bridges

In figures 5.12a (bridge O 951) and 5.12b (bridge O 978) the results are presented. In figure 5.12a results from the lower level (level U – 0.20 m above the road) and the middle level (level M – 1.40 m above the road) are shown to the left and right respectively. In figure 5.12b the results from the lower level (level U – 0.00 m above the road), the middle level (level M – 1.05 m above the road) and the higher level on bridge O 978 (level Ö – 2.20 m above the road) are shown to the left, in the middle and to the right respectively.

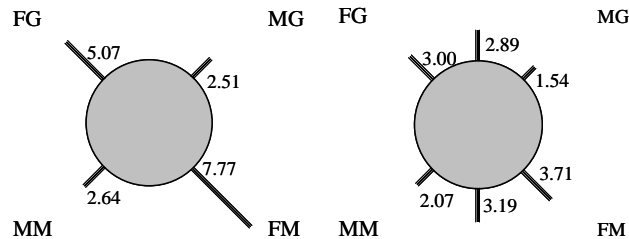


Figure 5.12a: The amounts of chlorides that have penetrated into the mortar disks on bridge O 951 (left – lower level, U, and right – middle level, M).

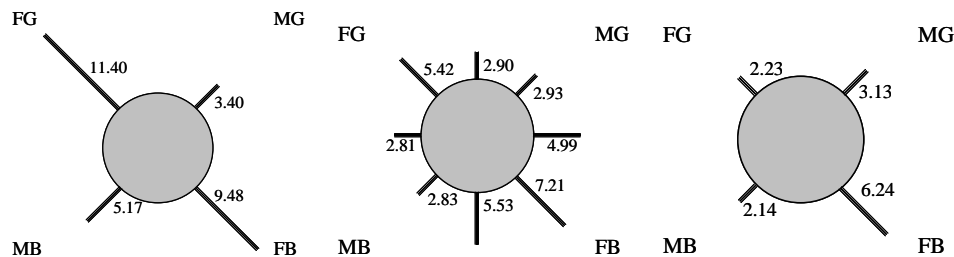


Figure 5.12b: The amounts of chlorides that have penetrated into the mortar disks on bridge O 978 (left – lower level, U, middle – middle level, M, and right – higher level, Ö).

From figures 5.12a and 5.12b it can be seen that the amounts of chlorides that have penetrated into the mortar disks, indicating the severity of exposure to chlorides, vary significantly. The most severe exposure to chlorides is found on surfaces close to the road facing towards the traffic (index O 951 UFG & UFM and O 978 UFB & UFG). The severity of exposure to chlorides decreases with increasing height, except for the surface with index O 978 ÖFB (as discussed earlier). Furthermore the effect of orientation towards the traffic becomes less significant with increasing height above the road. These effects are further discussed in section 5.4.2. The severity of exposure to chlorides measured with the mortar disks has also been compared with the chloride ingress measured in concrete – this comparison is made in section 5.4.4.

#### 5.4.2 Effect of height above road and orientation towards traffic

The effect of height and orientation towards the traffic on the chloride ingress has been studied, by plotting  $D_{F2}$  and  $C_{sa}$ , evaluated from measured chloride ingress profiles from bridges N 434, O 951 and O 978. In figures 5.13a and 5.13b the height – dependence of  $D_{F2}$  and  $C_{sa}$  is presented and exponential trend lines have been added to the figures. The indexes FT and TT indicate surfaces facing away from and towards the traffic respectively.

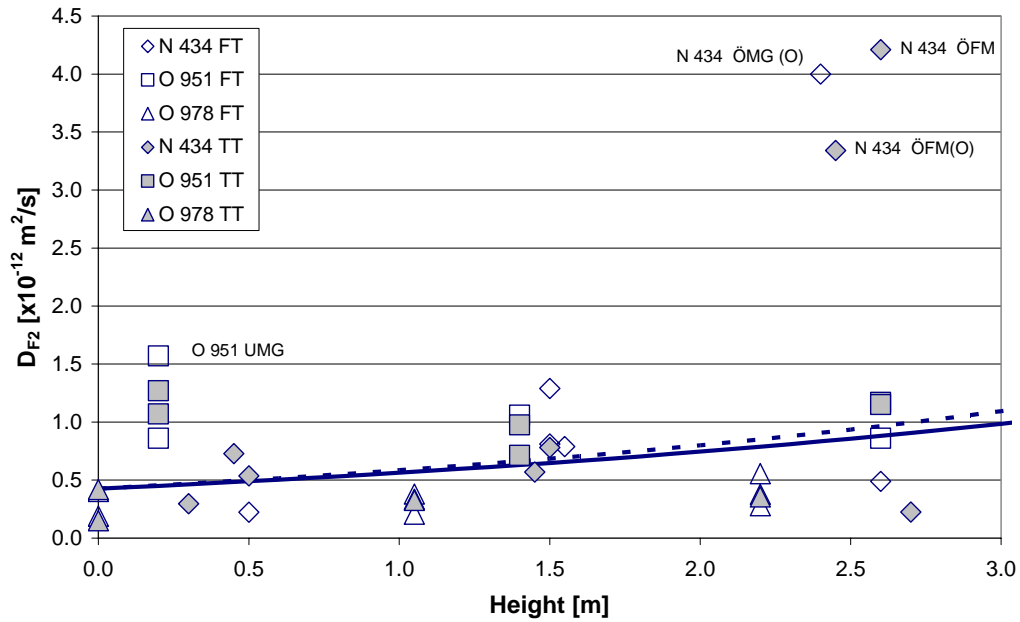


Figure 5.13a: The height dependence of  $D_{F2}$  evaluated from chloride ingress data from the concrete in bridges N 434, O 951 and O 978.

From figure 5.13a it can be seen that  $D_{F2}$  has no height dependence. This behaviour seems realistic, since  $D_{F2}$  should not be influenced by the exposure to chlorides, but by the transport properties in the concrete, following mainly from the moisture conditions in the concrete. The high values of  $D_{F2}$  from bridge N 434 at 2.0-3.0 m above the road, can (partly) be explained by the strange shapes of the chloride ingress profiles from bridge N 434, cf. figures 5.8a and 5.8b.

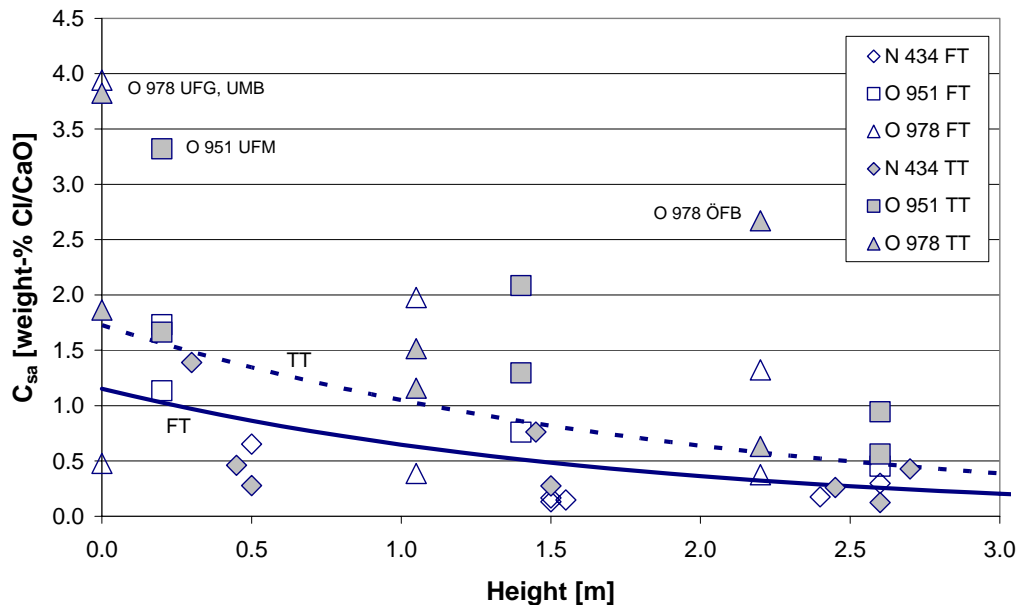


Figure 5.13b: The height dependence of  $C_{sa}$  evaluated from chloride ingress data from the concrete in bridges N 434, O 951 and O 978.

In figure 5.13b it can be seen that  $C_{sa}$  is dependent on height and orientation, with  $C_{sa}$  decreasing with increasing height. Furthermore  $C_{sa}$  is higher for surfaces facing towards

the traffic (TT) than for surfaces facing away from the traffic (FT). This seems realistic since splash and spray from the traffic should hit surfaces facing towards the traffic more frequently than surfaces facing away from the traffic.

Similar results are achieved if the amounts of chloride that have penetrated into the mortar disks, exposed in the complementary study, are plotted against the height above the road. This is done in figures 5.14a and 5.14b, where the amounts and maximum levels of chlorides that have penetrated into the mortar disks exposed on bridges O 951 and O 978 are presented. For clarity exponential trend lines have been added to the figures. These data are compared with the amount of chlorides that have penetrated into the concrete in section 5.4.4.

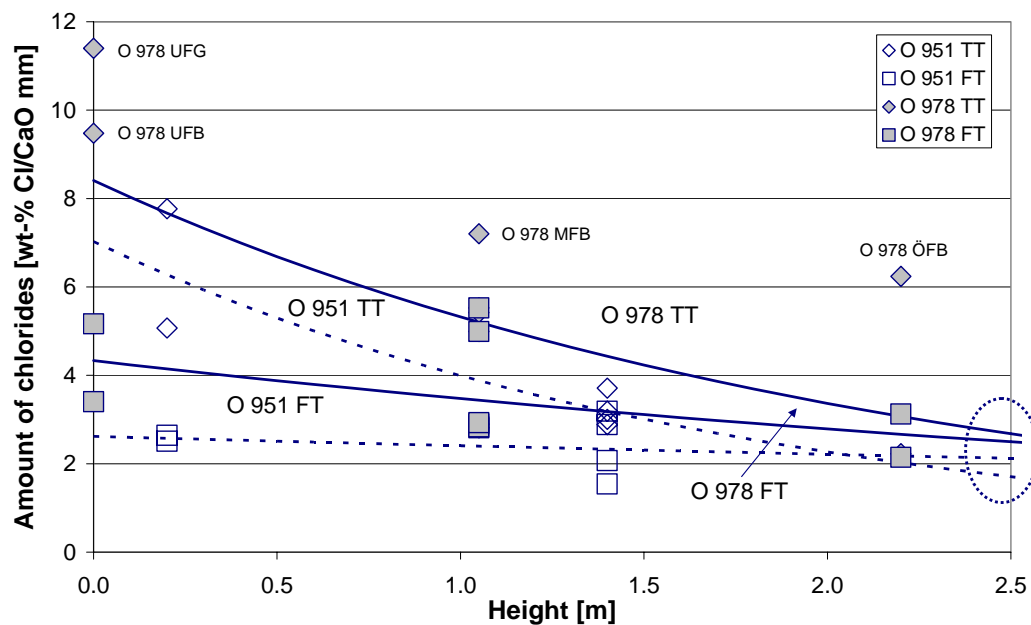


Figure 5.14a: The height dependence in the amount of chlorides that have penetrated into the mortar disks.

The results in figure 5.14a support the fact that the exposure to chlorides, and thus also  $C_{sa}$ , decreases with increasing height above the road. It can also be seen that surfaces that are facing towards the traffic have a higher chloride load than surfaces facing away from the traffic at the same height above the road. Furthermore the magnitude of the chloride load at different heights above the road follows from the chloride load at the level of the road (height 0 m). However, the shapes of the curves showing the decrease with increasing height are almost the same regardless of the exposure direction and bridge.



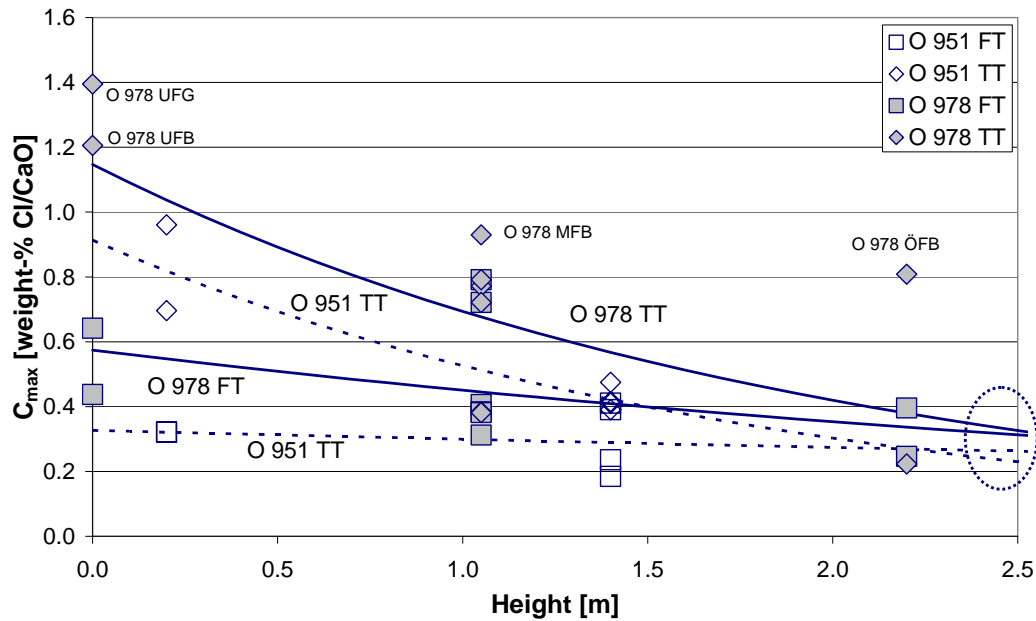


Figure 5.14b: The height dependence in the maximum chloride content in the mortar disks.

In the same way as the chloride load, the maximum chloride content in the mortar disks decreases with increasing height and the magnitude of the chloride content follows from the content at the level of the road (height 0 m). Thus it seems reasonable to describe the height dependence of the chloride load with the chloride load at the level of the road and a decrease with height. The chloride load at the level of the road is different for surfaces facing away from and towards the traffic. The difference for surfaces facing away from and towards the traffic is approximately 0.40 (based on data from bridges O 951 and O 978).

Another interesting feature can be observed if the measured chloride ingress profiles from the column on bridge O 951 are studied, see figure 5.15 where measured chloride ingress profiles from levels U and M (height 0.2 m and 1.4 m) on bridge O 951 are shown. In this figure surfaces with index FM, facing towards the traffic from Malmö (morning commuter traffic towards Göteborg), have higher chloride ingress than the other surfaces. The amount of traffic, passing under bridge O 951, is high towards Göteborg in the morning and from Göteborg in the afternoon. This can be explained by the fact that de-icing salt is normally spread during the night or early in the morning, which means that surfaces facing towards the lanes with the heaviest (moving) morning traffic also have the heaviest exposure to chlorides.

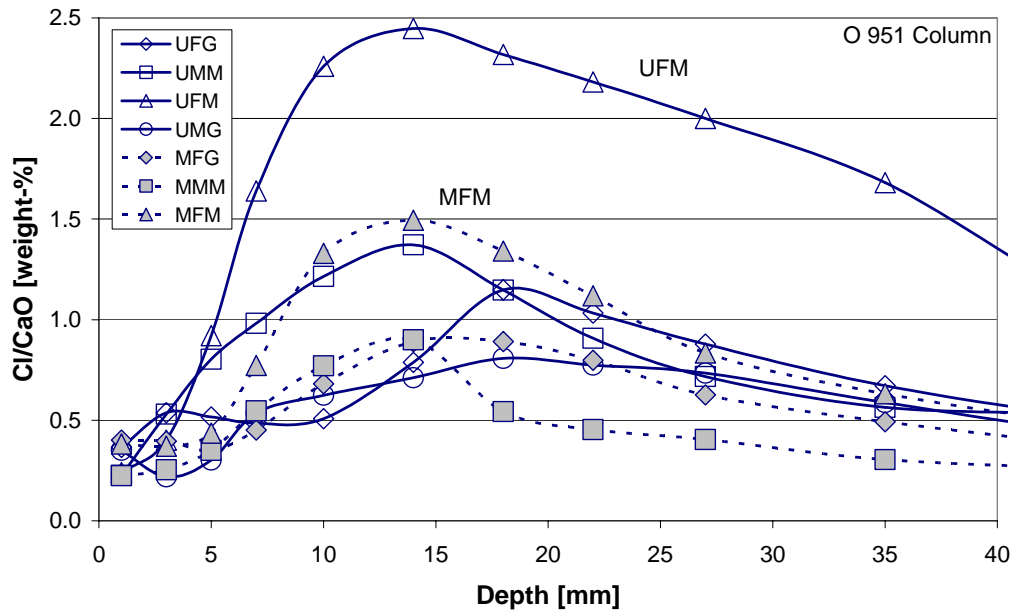


Figure 5.15: Chloride ingress profiles (concrete) from levels U and M (0.2 m and 1.4 m above the road respectively) on bridge O 951.

From the data presented in figure 5.15 it is obvious that the orientation towards the traffic and the lanes that have the heaviest (moving) traffic in the morning have an effect on the exposure to chlorides. Similar behaviour can be found in the results from the exposure of mortar disks on bridges O 951 and O 978, cf. figures 5.12a and 5.12b. The results are supported by an investigation of chloride ingress into Danish concrete road bridges presented in Andersen (1997), cf. figure 3.22.

Based on the results and analyses presented above a relation to describe the height dependence of the exposure to chlorides in road conditions has been developed. This is illustrated in figure 5.16, where the relative exposure to chlorides at the level of the road is set to 1.0 and the decrease with increasing height is described with a linear trend line. The filled and unfilled symbols denote surfaces facing away from and towards the traffic respectively.

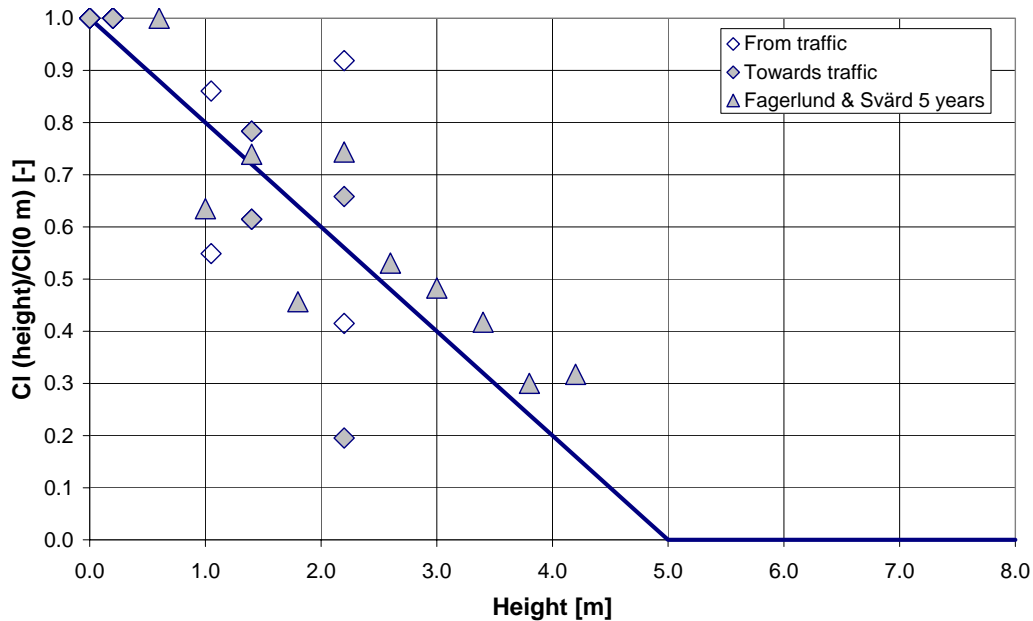


Figure 5.16: Illustration of the model showing how the chloride load decreases with increasing height above the road. Data from Lindvall (2002a) Fagerlund & Svärd (2001).

However, the height dependence of the chloride load does not always follow this pattern. This can for example be seen in figure 5.8c where chloride ingress profiles (measured in concrete) from the investigated column on bridge O 978 are shown. These profiles have been evaluated with the error function solution to Fick's 2<sup>nd</sup> law and the corresponding  $C_{sa}$  and  $D_{F2}$  evaluated from the chloride ingress data from bridge O 978, presented in figure 5.8c, are shown in figure 5.17, based on data from table 5.5c.

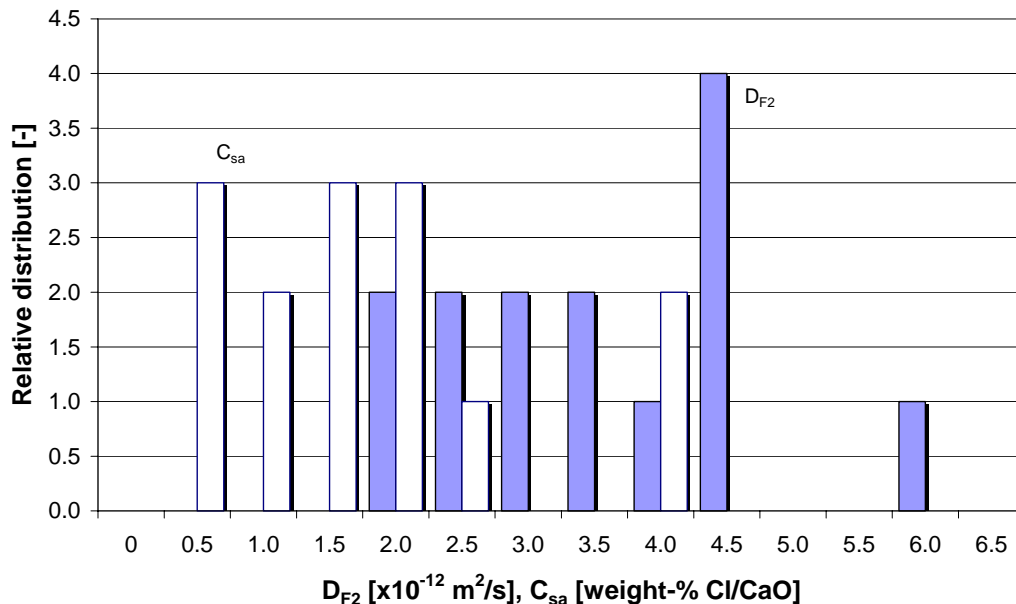


Figure 5.17:  $C_{sa}$  and  $D_{F2}$  evaluated from chloride ingress data presented in figure 5.8c. The exposure time has been 25 years.

In figure 5.17 fairly large variations can be seen both for  $C_{sa}$  and  $D_{F2}$  evaluated from chloride ingress profiles measured in the examined column on bridge O 978. As mentioned earlier the variations in  $D_{F2}$  cannot be attributed to the position on the column while the variations in  $C_{sa}$  have been found to depend both on the orientation towards the traffic and the height above the road.

From figure 5.8c it can be seen that there are large variations in the chloride ingress into the concrete in the column, with the chloride ingress into the surfaces with index MG significantly lower than for the other surfaces. The largest chloride ingress has been measured into a surface at the level of the road (index UMB, i.e. a surface facing away from the traffic towards Borås). Large chloride ingress has also been measured into the surface 2.2 m above the road (index ÖFB, i.e. a surface facing towards the traffic from Borås). Similar results have been obtained from the complementary investigation with the mortar disks. A possible explanation for the large chloride ingress into the surface with index ÖFB can be found if the airstreams around the column are studied. The predominant wind direction is from the west and airborne chlorides (spray from passing traffic) that are following the airstreams are deposited on the leeward side of the column. Since this surface is protected from rain the chloride is not washed away, but instead the chloride concentration increases over time. Furthermore it has been observed during wintertime that snow, ploughed from the road, gets stuck to the lower parts of the column in direction FB, acting as a shelter against exposure to chlorides.

Obviously to get an accurate description of the exposure conditions along thaw-salted roads, and to include movements of air streams etc, each structure should be considered separately. Furthermore the model for exposure to chlorides needs to be further developed, to e.g. include statistical uncertainties, which requires further research about the exposure conditions along thaw-salted roads.

### 5.4.3 Chloride ingress over time in road conditions

The chloride ingress over time has been studied by combining chloride ingress data from the specimens at the Rv40 field station with the investigation of seven reinforced concrete bridges around Göteborg. In figures 5.18a and 5.18b the variations over time in  $D_{F2}$  and  $C_{sa}$ , evaluated from the measured chloride ingress data from the investigated bridges and the Rv40 field station, are presented. The indexes denote: C – data from columns, SB – data from side beams, OPC – Ordinary Portland Cement and SF – Addition of silica fume. For clarity the data are presented in a log-log scale. For clarity the data in figure 5.18a are plotted in a log-log diagram and a trend line has been added to the data measured in side beams (index SB) made from OPC, i.e. Ordinary Portland Cement (CEM I).

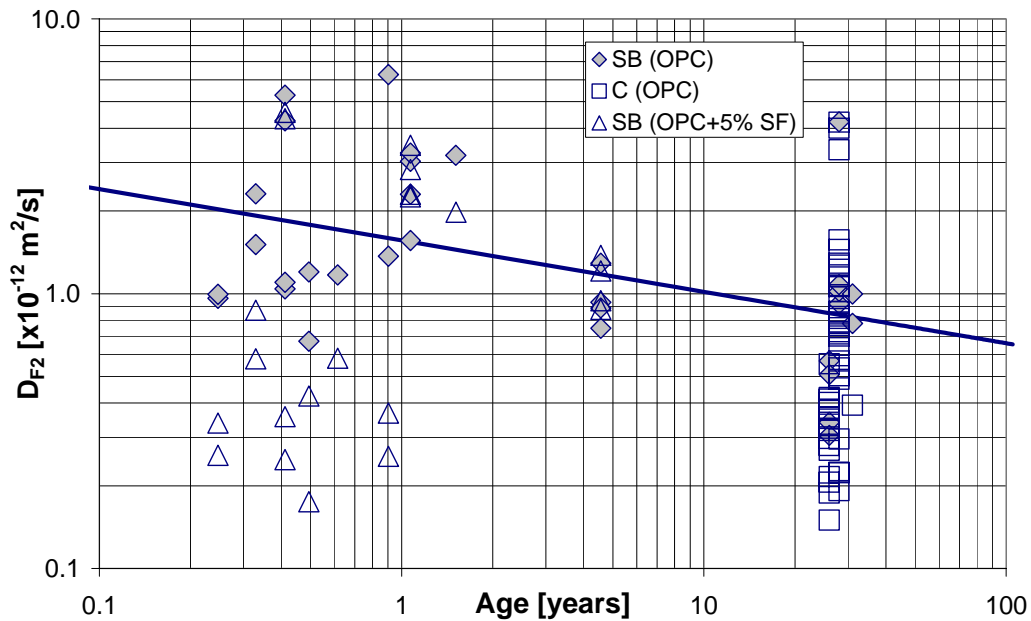


Figure 5.18a:  $D_{F2}$ , evaluated from measured chloride ingress data, as a function of time.

From figure 5.18a it can be seen that  $D_{F2}$  decreases with increasing age. However, there is large scatter in the data. The corresponding age factor for the trend line is 0.19 evaluated with the DuraCrete chloride ingress model.

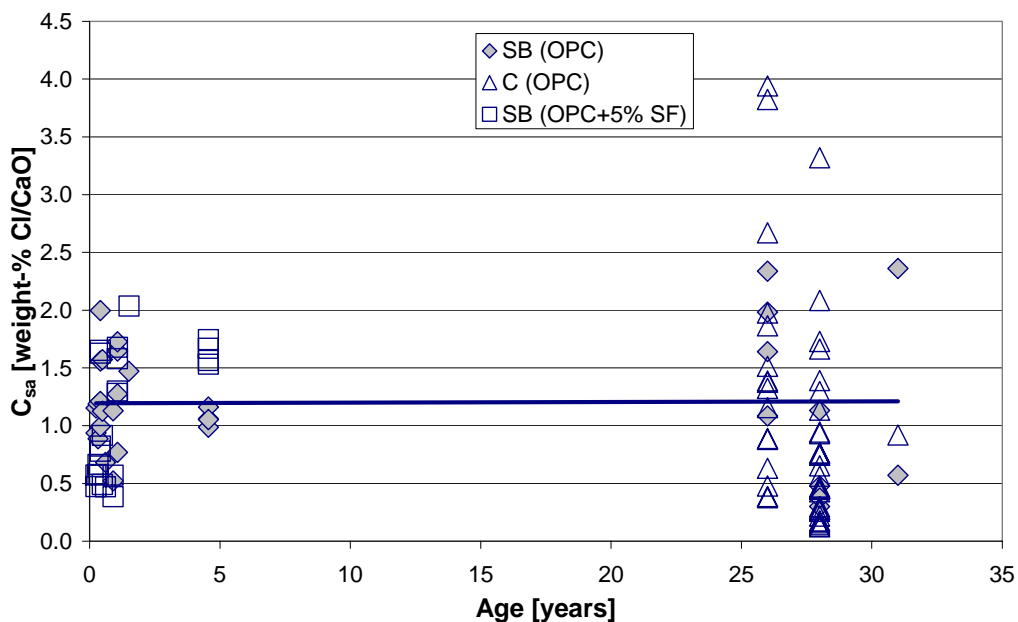


Figure 5.18b:  $C_{sa}$ , evaluated from measured chloride ingress data, as a function of time.

From figure 5.18b it can be seen that  $C_{sa}$  does not vary over time. However, there is large scatter in the data ( $COV^{11}=0.72-0.92$ ).

<sup>11</sup> Coefficient of variation determined according to eq. 4.1.

The differences in chloride ingress during two different winters have been studied by comparing chloride ingress profiles measured on the concrete specimens at the Rv40 field station, in May 1997 (first exposure series) and May 1998 (second exposure series). The exposure times have been approximately the same (six months for both exposure series), which means that they should give a measure of the severity of the two winters. In figure 5.19a the chloride ingress profiles from concrete 236 measured in May 1997 (unfilled symbols) and May 1998 (filled symbols) are presented. The broken profiles denote horizontal surfaces and the continuous profiles vertical surfaces. Winter 1 denotes the winter 1996/1997 and winter 2 denotes the winter 1997/1998.

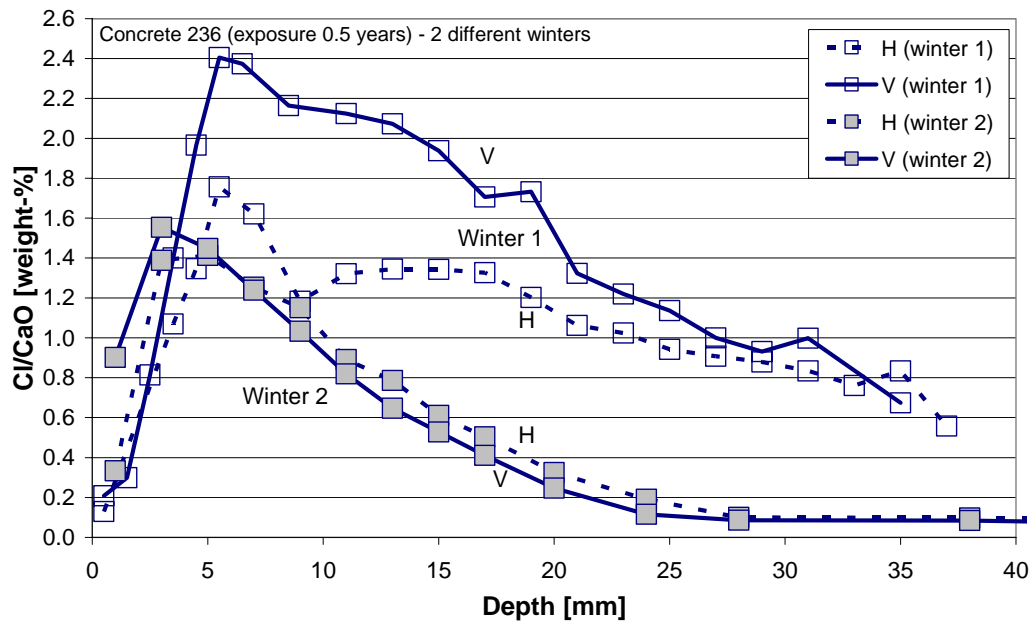


Figure 5.19a: The chloride ingress profiles from concrete 236 measured in May 1997 and May 1998.

In figure 5.19a it can be seen that the chloride ingress is significantly larger and the chloride levels are much higher after winter 1 than after winter 2. The amounts of chlorides that have penetrated into concrete have been determined as the areas below the chloride ingress profiles (Cl/concrete), see figure 5.19b. In figure 5.19b the continuous line shows the line of conformity for areas from winter 1 and 2, while the dotted line is the trend line for the measured areas.

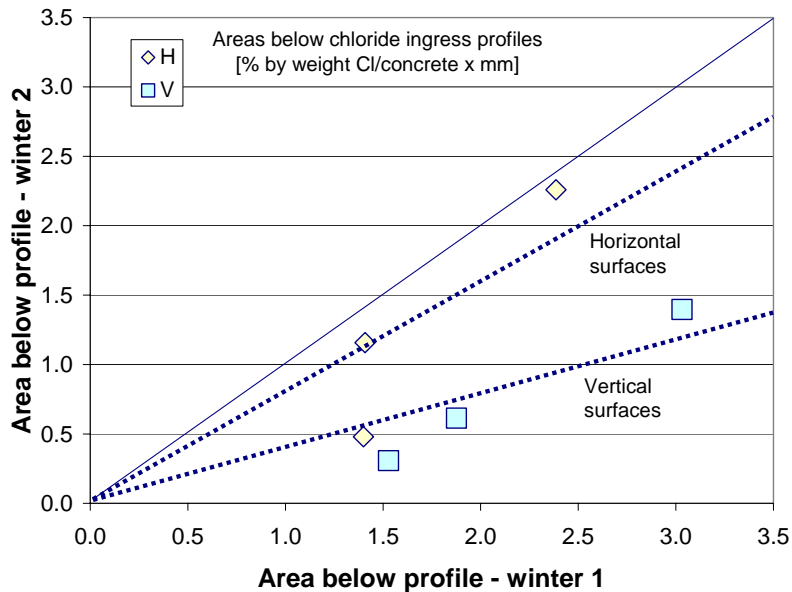


Figure 5.19b: The areas below the chloride ingress profiles from all concretes measured in May 1997 (first exposure series – winter 1) and May 1998 (second exposure series – winter 2). Chloride ingress data from concretes 201, 206 and 236.

From figure 5.19b it can be seen that the amounts of chlorides that have penetrated into horizontal surfaces are almost similar for the two winters, while for vertical surfaces the amounts of chlorides that have penetrated into the concrete were significantly larger for winter 1. Furthermore it can be seen that the amounts of chlorides that have penetrated into the concrete are generally larger for winter 1 than for winter 2. This is somewhat surprising since the amount of de-icing salt spread during the winter 1997/1998 is higher than that in the winter 1996/1997, cf. table 5.4. The measured air temperature and humidity are comparable, which means that if only the amount of chlorides spread on the road is studied, the exposure to chlorides during the winter 1997/1998 should be more severe than during the winter 1996/1997.

One explanation can be found if the age of the concrete on first exposure to chlorides is studied. The concrete blocks from the first exposure series have been exposed since December 19<sup>th</sup> 1996, while the concrete blocks from the second exposure series have been exposed since November 6<sup>th</sup> 1997. All blocks were around 40 days old when they were put out. It can be assumed that the blocks in the first exposure series almost immediately were exposed to chlorides, since de-icing salt had been spread since November, cf. table 5.4. However, the blocks from the second exposure series may not immediately have been exposed to chlorides, since de-icing salt is not spread that frequently in the beginning of November.

This means that blocks from the first exposure series are exposed to chlorides for the first time at a younger age than the blocks from the second exposure series. The exposure to chlorides at younger ages should also be more frequent for the blocks from the first series than the second series. If the exposure starts when the concrete is young and a lot of chlorides are available, e.g. in December, the result will also be large chloride ingress. On the other hand if the exposure starts when the concrete is young and not that much chlorides are available, e.g. in early November, the result will be less chloride ingress. A

possible explanation for this is that the pore structure of the concrete is not so dense at younger ages, since the cement hydration has not reached its final level. The longer the hydration can continue before exposure to chlorides the denser the concrete gets. Thus the observed differences in chloride ingress between the two winters could be caused by differences in the age of the concrete on first exposure to chlorides.

From the data presented above it is obvious that chloride ingress data from two winters measured on concretes with different histories (manufacturing and exposure) cannot be compared directly, although they have the same concrete composition. The chloride ingress is influenced both by the history of the concrete, e.g. curing and first exposure to chlorides, and the characteristics of the spread of de-icing salt, e.g. spreading occasions and spreading method. The most important factor seems to be the age of the concrete on first exposure to chlorides, where a young concrete has a significantly larger chloride ingress than an old concrete. Even an age difference of only a few weeks seems to have a large effect here on the chloride ingress. Thus, it is important to state both when the concrete was cast and when it was first exposed to chlorides. Furthermore definition of the exposure time for concrete along a thaw-salted road is not trivial – is the exposure time the total time of exposure or the time of exposure to chlorides? The difference between these two times can be up to six months, depending on whether the exposure of the concrete starts during the spring or autumn.

### **5.4.4 Comparison between chloride ingress measured in concrete and mortar disks**

The amounts of chlorides that have penetrated into the mortar disks have been compared with amounts of chlorides that have penetrated into concrete investigated in the original study of bridges O 951 and O 978. The results from this comparison are presented in figure 5.20a, where the amounts of chlorides are plotted against the height above the road, and figure 5.20b, where the data in figure 5.20a are combined. Since the mortar disks have similar material composition and the bridges should have almost similar concrete compositions it should be possible to estimate the effects on chloride ingress due to the formwork used for the concrete. The broken trend lines represent the concrete (right axis) and the continuous trend lines represent the mortar disks (left axis). The amount of chlorides in the mortar disks is given on the left vertical axis and in concrete on the right vertical axis. In figure 5.20b linear trend lines have been added.



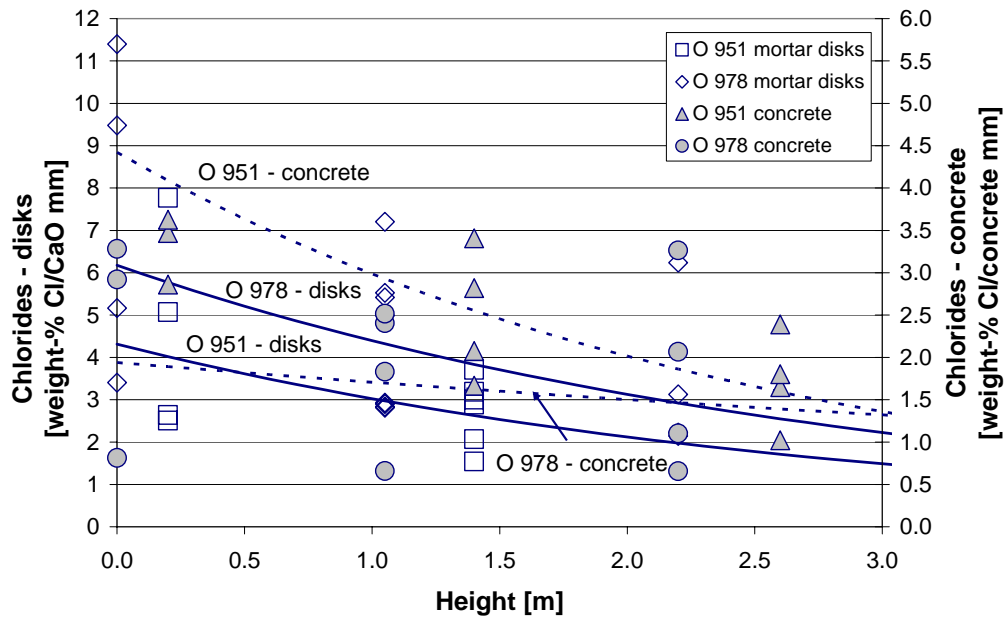


Figure 5.20a: Comparison between the amount of chlorides that have penetrated into the concrete and the mortar disks on bridges O 951 and O 978.

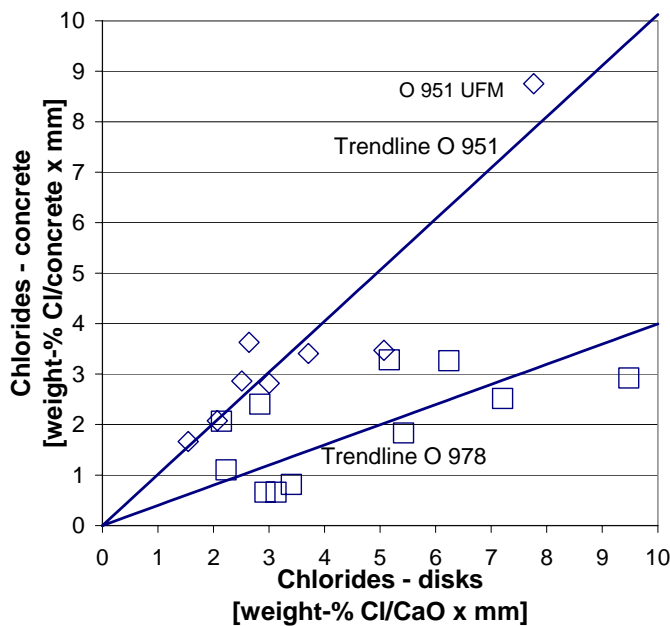


Figure 5.20b: Comparison between the amount of chlorides that have penetrated into the concrete and the mortar disks on bridges O 951 and O 978.

From figure 5.20b it can be seen that the amount of chlorides that have penetrated into the concrete is larger for bridge O 951, while in the mortar disks it is larger for bridge O 978. Since the mortar disks are identical the results from the disks should represent the actual severity of the exposure to chlorides. In Lindvall (2002a), the difference between the amounts of chlorides that have penetrated into concrete and mortar disks is explained by differences in concrete composition and workmanship during construction. The main influencing factor was assumed to be the type of formwork, where bridge O 951 is cast in steel formwork and bridge O 978 in wooden formwork. The type of formwork may influence the surface layer of the concrete, where wooden formwork may give a denser

surface concrete, with low w/b resulting in low chloride diffusivity, since the wood absorbs water from the fresh concrete, and steel formwork may give a less dense surface concrete, resulting in higher chloride diffusivity.

#### 5.4.5 Comparison of chloride ingress into columns and side beams

The differences in chloride ingress into columns and side beams, both on one single bridge and between bridges, have been studied. The exposure to chlorides is different for columns and side beams, where generally columns are exposed to spray and side beams are exposed to splash from passing traffic. Furthermore surfaces in the wet splash zone are directly exposed to rain while they are protected against direct rain in the dry splash zone.

The comparison has been made with chloride ingress data from bridges O 978 (columns) and O 762 (side beam). These two bridges are constructed 2.5 km from each other along the same motorway, which means that they should have comparable exposure conditions. In figure 5.21a chloride ingress profiles from bridges O 762 (filled symbols) and O 978 (unfilled symbols) are shown. The profiles from bridge O 978 come from surfaces facing the traffic towards Göteborg (index FB and MG). The first letter in the index in the profiles from bridge O 978 indicates the level above the road, see figure 5.1.

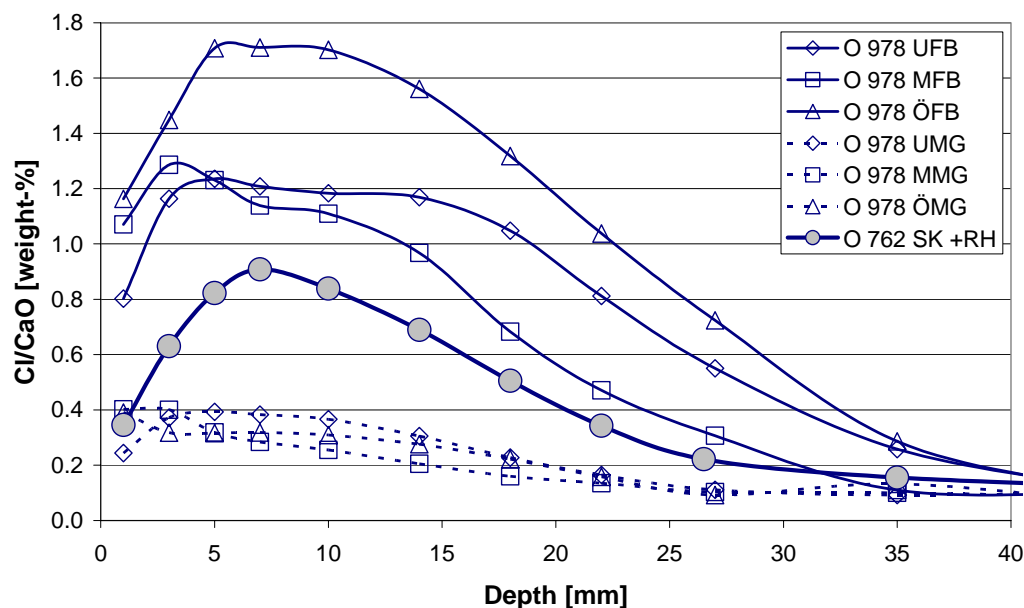


Figure 5.21a: Comparison of the chloride ingress into column (bridge O 978) and side beam (bridge O 762).

From figure 5.21a it can be seen that the chloride ingress into the side beam is somewhere between surfaces facing towards (index FB) and away from (index MG) the traffic.

Additionally the effect of the surface orientation on side beams has been investigated. This has been done with chloride ingress data from side beams on bridges N 434 and O 978. In figure 5.21b chloride ingress profiles from side beams on these bridges are presented. Indexes H and V denote that the profiles come from horizontal and vertical surfaces respectively.

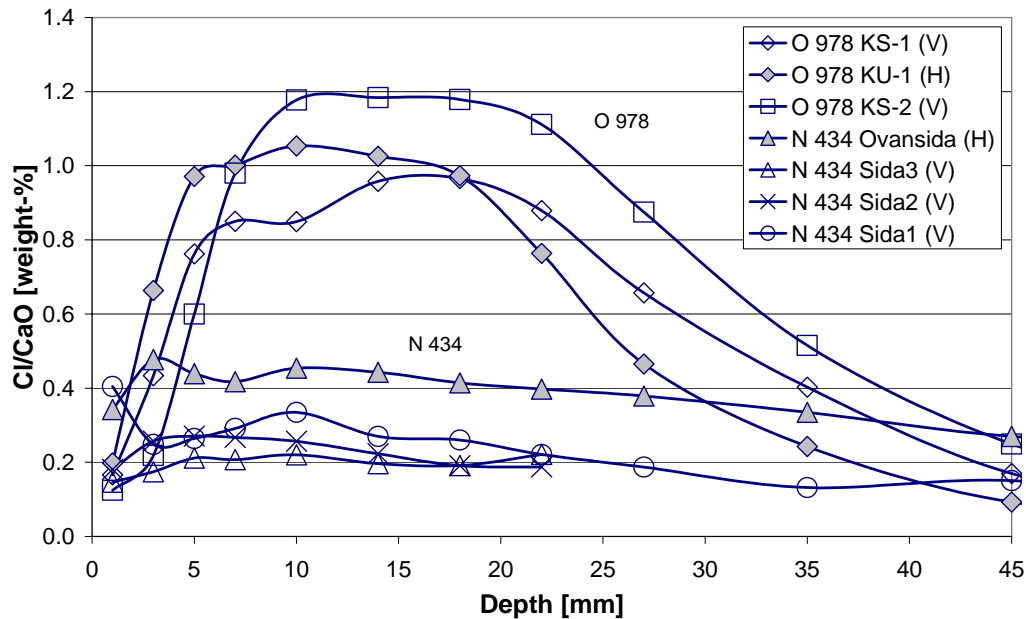


Figure 5.21b: Chloride ingress profiles from side beams on bridges N 434 and O 978.

In figure 5.21 b it can be seen that there is no significant difference in chloride ingress depending on surface orientation. Instead, the difference in chloride ingress between the bridges is considerable, with the chloride ingress in bridge O 978 significantly larger than in bridge N 434. The bridges have approximately the same age and the exposure conditions should be comparable. This indicates that the measured differences in chloride ingress could depend on differences in the concrete properties. Since the bridges have been constructed according to the Swedish building code the concrete compositions should be similar, which means that differences can be related to maintenance, e.g. surface treatments, and repair work. This means that chloride ingress measured into different bridges cannot be directly compared unless the bridges have been constructed and maintained and repaired in similar ways.

The effect of surface orientation has also been investigated on the concrete blocks at the Rv40 field station. In figure 5.22 the amounts of chlorides that have penetrated after 4.5 years of exposure into the concrete in the blocks made from concretes 201 and 236, determined as the areas below chloride ingress profiles (Cl/concrete), are presented. For clarity trend lines have been added to the figure, where the continuous line shows the line of conformity and the dotted line is the trend line for the measured data.

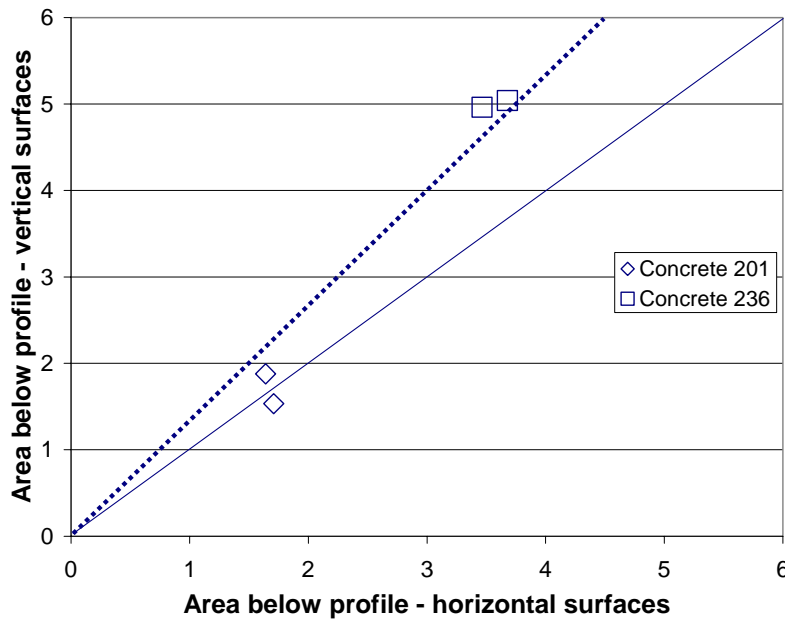


Figure 5.22: The areas below the chloride ingress profiles from concretes 201 and 236 after 4.5 years' exposure.

In figure 5.22 it can be seen that for concrete 201 there are no significant differences in the amounts of penetrated chlorides depending on surface orientation, while for concrete 236 the amounts of penetrated chlorides are somewhat larger for vertical surfaces. Thus the effect of the surface orientation seems to be dependent on the concrete composition. For a concrete with low w/b, the surface orientation does not have any significant effect on the chloride ingress, while for a concrete with high w/b, the chloride ingress is higher into vertical surfaces than into horizontal surfaces. The amount of data, however, is far too small to draw far-reaching conclusions.

## 5.5 Conclusions

Based on the results from the investigations presented in this chapter the following conclusions have been drawn:

- Influence of the exposure conditions.** The presented field studies made in road conditions illustrate how the exposure conditions influence chloride ingress into concrete. The measured chloride ingress and chloride loads show how the exposure conditions vary both between different structures but also within one single structure. Thus, the exposure conditions, and their variations, must be taken into account to model and predict the chloride ingress into concrete exposed along thaw-salted roads.
- Effect of height above the road and orientation towards traffic.** The exposure to chlorides shows a decrease with increasing height above the road. The decrease can be described with a linear function, where the exposure to chlorides at the road surface (height 0.0 m) is equal to 1.0 and at a height of 5.0 m equal to 0.0. The exposure to chlorides is generally highest for surfaces facing towards the traffic, in particular the surfaces facing towards the commuter traffic in the morning hours. However, it should be pointed out that this effect is only significant for roads with commuter traffic in the morning hours, with fairly high speeds. If the speeds of the morning commuter traffic are low other surfaces may also have significant exposure to chlorides.

- **Effect of airstreams around a structure.** Airstreams around a structure, carrying chlorides, have been found to have an influence on the exposure to chlorides. At certain wind directions, the airborne chlorides may be deposited and accumulated on the leeward sides of structures. Usually the leeward sides are only partly exposed to rain, which means that chlorides are not washed away but instead will be accumulated. Furthermore deposition of snow may also have an influence on the exposure to chlorides, where concrete surfaces, on which snow is deposited, are protected from chlorides.
- **Chloride ingress over time in road conditions.** The chloride ingress into concrete structures exposed along thaw salted roads has been found to mainly take place during the first winter season – after the following seasons, the chloride ingress has been found to only increase slowly.

The definition of the exposure time for structures in road conditions is not trivial, since the exposure to chlorides only takes place during approximately 6 months per year (when de-icing salt is spread on the road). The difference in exposure time can be up to half a year, depending on whether the time is defined from the start of exposure or from the start of exposure to chlorides, which makes evaluation of measurements of chloride ingress difficult. Preferably both the total exposure time and the time of exposure to chlorides should be stated to avoid any uncertainties in the definition of the exposure time.

The age of the concrete when it is first exposed to chlorides has been found to have a large effect on the chloride ingress. If the concrete is first exposed to chlorides when it is young and immature, the results will be larger chloride ingress than if the concrete was older and more mature on first exposure. Thus it is important to register when the first exposure to chlorides takes place and the corresponding age of the concrete.

Two consecutive winters have been found to give significantly different chloride ingress into concrete, since the amount of de-icing salt spread on the road depends on the weather conditions and is therefore most likely not similar for two winters. This means that the exposure to chlorides also is different.
- **Chloride ingress into columns and side beams.** The chloride ingress into side beams and columns takes place with different mechanisms. The exposure to chlorides on side beams is mainly due to splash from the traffic and chloride-contaminated snow and slush from the road surface. The exposure to chlorides on columns is mainly due to spray from the traffic. This means that the side beams are exposed to chlorides for a longer period of time than the columns, especially due to remaining chloride-contaminated snow and slush from the road surface. This can be observed in the chloride ingress profiles, where the profiles from side beams have larger convection zones and larger amounts of chlorides that have penetrated into the concrete than the profiles from columns.

Differences in chloride ingress have also been observed on horizontal and vertical surfaces, where the chloride ingress is larger into the vertical surfaces of concrete specimens exposed at the Rv40 field station. However, on chloride ingress data measured in side beams on existing bridges, no effect due to the surface orientation could be observed. Instead, in these data, considerable differences in chloride ingress between different bridges were seen.
- **Each structure should be considered individually.** From the results presented in this chapter it is obvious that it is not possible to directly compare measurements of chloride ingress into concrete from different structures, even if they have been exposed during approximately the same time. The chloride ingress is influenced by many factors, e.g. concrete composition, workmanship during construction, exposure

conditions, age on first exposure to chlorides etc. This means that the most accurate description of the exposure conditions and the resulting chloride ingress will be obtained if each structure is considered individually. Otherwise, if chloride ingress data from different structures are combined, the results may have a large scatter, e.g. shown by Lindvall & Nilsson (2001).

## 6 Models for environmental actions

In this chapter models for environmental actions in marine and road conditions are presented. The models are based on the qualitative models presented in chapter 3 and the quantification is based on the results from the literature study and the field studies in marine and road conditions presented in chapters 3, 4 and 5. The quantified models are later used in chapter 7 for predictions of chloride ingress.

### 6.1 Introduction

The models presented in this chapter describe the environmental actions on surfaces of reinforced concrete structures. The focus has been to describe the environmental actions on reinforced concrete structures subjected to chloride-induced reinforcement corrosion. The models aim to quantify the environmental parameters in the DuraCrete chloride ingress model, since this model has been chosen as an “example model” to exemplify the consequences of variations in the exposure conditions for predictions of chloride ingress into concrete.

The most accurate way to describe the environmental actions on concrete structures is to describe them as surface actions. However, it is not enough to only know the actions outside the concrete, since these actions are influenced by the response of the concrete. Furthermore it is usually difficult to directly measure the environmental actions and therefore the response of the concrete is normally used as a measure of the actions. Additionally many prediction models are derived and quantified from the response of concrete structures, e.g. measured chloride ingress profiles. The response of the concrete is usually measured in terms of moisture and temperature conditions, carbonation and chloride ingress. However, reinforced concrete structures exposed in marine and road conditions, and thus exposed to chlorides, are normally constructed with high-quality concrete (low w/b and high cement content), which means that the carbonation depths are small and therefore not taken into account. Therefore only the chloride, moisture and temperature conditions have been taken into account.

The environmental actions and the response of the concrete, which influence the initiation of reinforcement corrosion, are mainly the exposure to chlorides and the transport properties for chlorides in the concrete. The exposure to chlorides is mainly influenced by the chloride conditions (chloride concentration in the exposure solution at the concrete surface) and to some extent also the temperature and moisture conditions. The chloride transport properties in the concrete are mainly influenced by the moisture and temperature conditions and to some extent the chloride conditions and the degree of carbonation inside the concrete.

The formulation of the models of environmental actions depends on the choice of prediction model, where as mentioned earlier the DuraCrete chloride ingress model has

been chosen as an “example model” in this thesis. The DuraCrete chloride ingress model agrees with models proposed by for example Poulsen, Maage, Helland and Mejlbro, described in e.g. Maage et al (1995 & 1999) Poulsen (1996) and Mejlbro (1996). This means that the models for environmental actions presented in this chapter can be used for these prediction models as well.

In the DuraCrete chloride ingress model the chloride ingress is described with a surface chloride content,  $C_{SN}$ , describing the driving potential of chlorides at the surface of the concrete, and an apparent diffusion coefficient,  $D_a(t)$ , describing the transport properties for chlorides in concrete. These parameters are evaluated by curve fitting of measured chloride ingress profiles to the error function solution of Fick’s 2<sup>nd</sup> law.

The models for environmental actions presented in this chapter have focused on the quantification of the environmental parameters in the DuraCrete chloride ingress model. However, the models can, at least partly, also be used for more general descriptions of the exposure conditions. The chapter has been divided into two parts, where first a general description of the models is given and then more specific models for marine and road conditions are presented.

In this chapter a general description of the parameters in the DuraCrete chloride ingress model is first given. It is also proposed to divide the environmental parameters into a number of uncorrelated “sub-parameters”, to be able to better model the influence of the exposure environment. Then the parameters giving the influence of the concrete properties are described and quantified. After that the parameters giving the influence of the moisture and temperature conditions are described and quantified. Then the parameters giving the variations in chloride ingress over time and chloride threshold level are described and quantified. Finally the specific models for environmental actions in marine and road conditions are described and quantified.



## 6.2 Models for environmental actions – general aspects

### 6.2.1 General

In the original DuraCrete chloride ingress model, the chloride ingress is modelled with two parameters, namely an apparent surface chloride content,  $C_{SN}$ <sup>12</sup>, and an apparent chloride diffusion coefficient,  $D_a(t)$ , see eq. (2.1a).  $D_a(t)$  is expressed as a potential diffusion coefficient,  $D_0$ , measured under standardised conditions, which is transferred with a number of parameters to the actual exposure conditions, cf. eq. (2.1b). In eq. (2.1b) the influence of the exposure conditions is described with parameters affecting  $D_a(t)$ , namely  $k_e$  and  $n$ . Additionally there are also parameters which take into account the influence of the material properties;  $D_0$  (potential chloride diffusion coefficient),  $k_c$  (influence of workmanship),  $n$  (describing the decrease in  $D_a$  with age – combined environmental and material parameter), and test method,  $k_t$ . However, the parameters describing the influence of the material and test method have not been investigated in this study. More information about these parameters and the way they can be quantified is given in for example DuraCrete (2000a) and Gehlen (2000).

As regards the influence of the exposure conditions,  $D_a(t)$  is mainly influenced by the conditions inside the concrete (in terms of temperature and moisture conditions and to some extent the chloride content) while  $C_{SN}$  is mainly influenced by the surface conditions (in terms of equivalent surface chloride concentration). In this study the focus has been to investigate how the chloride and temperature conditions influence the chloride ingress. The moisture conditions have not been specifically investigated, which means that data from other investigations have been used in the modelling.

In the original DuraCrete chloride ingress model, cf. eq. (2.1a) and (2.1b), the influence of the exposure conditions is only described with three parameters, namely  $C_{SN}$ ,  $k_e$  and  $n$ . All effects due to chloride, moisture and temperature conditions are combined in these parameters, which means it is difficult to separate the effects of different influencing factors on a specific parameter. Therefore it is proposed to modify the modelling of  $C_{SN}$  and  $D_a(t)$  from the original DuraCrete model, according to eq. (6.1a) and (6.1b).  $C_{SN}$  is modelled with an equivalent surface chloride content,  $C_{SN,eq}$ , measured in equivalent conditions, which is transferred to the actual exposure conditions with a number of parameters.  $D_a(t)$  is modelled with a potential diffusion coefficient,  $D_0$ , measured in standardised conditions in the laboratory, which is transferred to the actual exposure conditions with a number of parameters. To better model the influence of exposure conditions it is proposed to further subdivide the parameters  $k_{C,e}$  and  $k_{D,e}$  with a number of parameters, according to eq. (6.1a) and (6.1b). All parameters in eq. (6.1a) and (6.1b) are, as a first approach, assumed **uncorrelated**.

$$\begin{cases} C_{SN} = C_{SN,eq} \cdot k_{C,conc} \cdot k_{C,e} \cdot k_{C,test} \\ k_{C,e} = k_{C,Cl} \cdot k_{C,d} \cdot k_{C,h} \cdot k_{C,o} \cdot k_{C,T} \end{cases} \quad (6.1a)$$

where:

- $C_{SN}$ : surface chloride content. [% by weight Cl/binder]
- $C_{SN,eq}$ :  $C_{SN}$  measured in equivalent conditions and concrete quality.  $C_{SN,eq}$  is in marine conditions determined in the submerged zone at 1.0 m depth (chloride

<sup>12</sup>  $C_{SN}$  is similar to  $C_{sa}$  used in chapter 3-5.  $C_{SN}$  is used since this parameter is used in the DuraCrete chloride ingress model.

concentration and temperature of 20g Cl/l and 20°C respectively) and in road conditions at the road surface (vertical surface at 0.0 m distance and height). This parameter is further described and quantified in section 6.2.2. [% by weight Cl/binder]

- $k_{C,conc}$ : parameter that accounts for the influence the concrete composition has on  $C_{SN,eq}$ . This parameter is further described and quantified in section 6.2.2. [-]
- $k_{C,test}$ : parameter that accounts for the influence of the test method. In the study presented in this thesis, this parameter is put to  $k_{C,test}=1.0$ . [-]
- $k_{C,e}$ : parameter that accounts for the influence of the exposure environment. To better model the influence of the exposure environment the parameter  $k_{C,e}$  is subdivided into the following **uncorrelated** parameters,  $k_{C,Cl}$ ,  $k_{C,d}$ ,  $k_{C,h}$ ,  $k_{C,o}$  and  $k_{C,T}$ . [-]
- $k_{C,Cl}$ : parameter that accounts for the influence of chloride concentration in marine submerged conditions on  $C_{SN,eq}$  (if the chloride concentration is other than 20 g/l). This parameter is further described and quantified in section 6.2.3. [-]
- $k_{C,d}$ : parameter that accounts for the horizontal distance to the source of chlorides. This parameter is further described and quantified in section 6.3 and 6.4. [-]
- $k_{C,h}$ : parameter that accounts for the vertical distance to the source of chlorides. This parameter is further described and quantified in section 6.3 and 6.4. [-]
- $k_{C,o}$ : parameter that accounts for the orientation towards the source of chlorides. This parameter is further described and quantified in section 6.3 and 6.4. [-]
- $k_{C,T}$ : parameter that accounts for the influence of temperature on  $C_{SN,eq}$ . This parameter is further described and quantified in section 6.2.3. [-]

The choice to define the equivalent conditions in road conditions as those at the road surface can be questioned since concrete structures are seldom built that close to the road. However, if the conditions at some distance from the road surface are chosen instead, the exposure conditions will also be influenced by effects due to for example distance and orientation to traffic, wind directions etc. This means that the “equivalent exposure conditions” may vary for the same road, depending on where on the road the conditions are defined. Therefore the conditions at the road surface, which in this thesis are assumed to be similar over the whole carriageway, have been chosen as equivalent conditions. Furthermore, with this definition, it will be possible to relate  $C_{SN,eq}$  with the chloride concentration in the solution (brine) on the road surface, if data on this are available, cf. Paulsson & Andersen (1997).

$$\begin{cases} D_a(t) = D_0 \cdot k_{D,c} \cdot k_{D,e} \cdot k_{D,test} \cdot \left( \frac{t_0}{t} \right)^n \\ k_{D,e} = k_{D,RH} \cdot k_{D,T} \end{cases} \quad (6.1b)$$

where

- $D_a(t)$ : apparent diffusion coefficient after a specific exposure time, t. [ $m^2/s$ ]
- $D_0$ : potential diffusion coefficient measured in standardised conditions in the laboratory. This parameter is further described and quantified in section 6.2.2. [ $m^2/s$ ]
- $k_{D,c}$ : parameter that accounts for the curing conditions. This parameter is further described and quantified in section 6.2.2. [-]
- $k_{D,test}$ : parameter that accounts for the influence of test method. This parameter is equal to  $k_t$  in eq. (2.1b) but is for clarity written as  $k_{D,test}$  in eq (6.1b). In the

- study presented in this thesis  $k_{D,test}$  is put to 1.0. Examples of how  $k_{D,test}$  can be quantified are given in DuraCrete (2000a). [-]
- $k_{D,e}$ : parameter that accounts for the environmental conditions. The factor  $k_{D,e}$  is proposed to be subdivided into two **uncorrelated** parameters giving the influence of the RH,  $k_{D,RH}$ , and the temperature,  $k_{D,T}$ , respectively. [-]
- $t_0$ : age at which  $D_0$  is measured (concrete cured in laboratory in standardised conditions). [s]
- $t$ : exposure time. [s]
- $n$ : age factor, giving the decrease in  $D_a$  with time, being partly an environmental parameter. This factor is further described and quantified in section 6.2.4. [-]

## 6.2.2 Influence of concrete properties and chloride conditions

### Introduction

The influence of the concrete properties and chloride conditions is in the modified DuraCrete chloride ingress modelled with the parameters  $C_{SN,eq}$ ,  $k_{C,Cl}$ ,  $D_0$ ,  $k_{C,conc}$  and  $k_{D,c}$ . The equivalent surface chloride content,  $C_{SN,eq}$ , is influenced by a combination of the concrete properties and the exposure conditions (mainly chloride conditions), where  $C_{SN,eq}$  is different for marine and road conditions. However, if the same concrete composition is exposed in both marine and road conditions it is also possible to transfer  $C_{SN,eq}$  from marine to road conditions and vice versa. The potential diffusion coefficient,  $D_0$ , is mainly influenced by the concrete composition. In DuraCrete it is proposed to measure  $D_0$  with NT Build 492 (1999). The parameters  $k_{C,conc}$  and  $k_{D,c}$  are influenced by the concrete composition and curing conditions respectively.

All these parameters are described and quantified in the following sections.

### Equivalent surface chloride content – $C_{SN,eq}$ and the parameter $k_{C,Cl}$

The equivalent surface chloride content,  $C_{SN,eq}$ , is evaluated from chloride ingress profiles measured in concrete exposed in equivalent exposure conditions. In marine exposure conditions the equivalent conditions are at 1.0 m depth in the submerged zone (with a chloride concentration of 20 g/l and a temperature of +20°C), since this zone provides a well defined exposure. In road conditions the equivalent conditions are at 0.0 m distance from and height above the carriageway and facing towards the traffic. Examples of  $C_{SN,eq}$  in marine and road conditions are given in figures 6.1a and 6.1b respectively.

In figure 6.1a (marine conditions) data on  $C_{SN}$  analysed from chloride ingress data from the marine exposure programme are presented. In marine conditions  $C_{SN,eq}$  has been set to  $C_{SN}$  evaluated from concrete exposed at a water temperature of +20°C.  $C_{SN}$  analysed at other temperatures can be recalculated to +20°C by multiplying by the factor  $k_{C,T}$ . Furthermore  $C_{SN,eq}$  depends on the chloride concentration of the seawater, where an increase in the chloride concentration results in an increase in  $C_{SN,eq}$  and vice versa. In figure 6.1a it is exemplified how  $C_{SN,eq}$  and  $k_{C,Cl}$  can be determined for different chloride concentrations in the seawater.

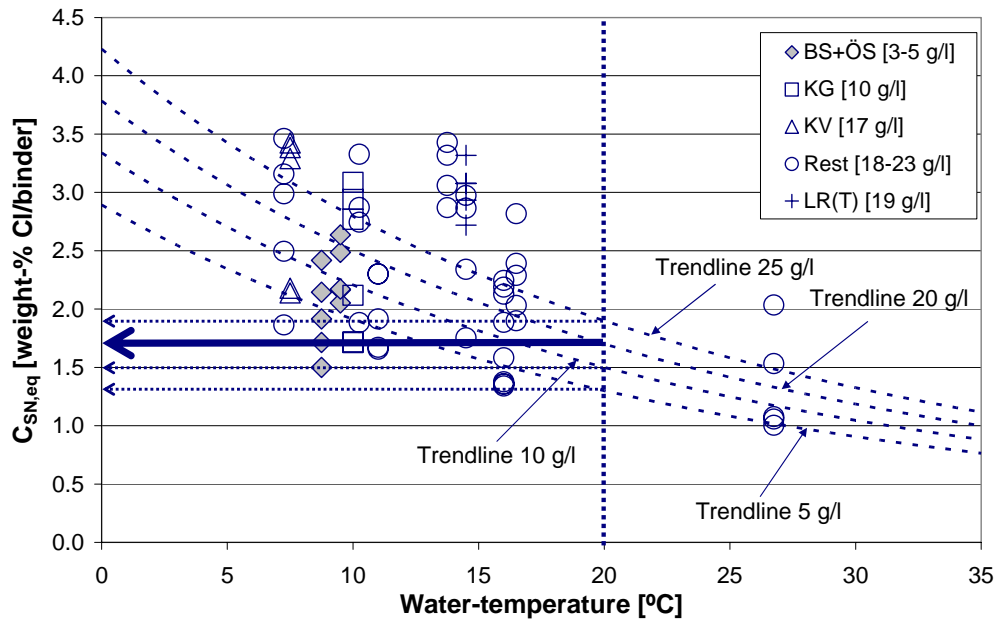


Figure 6.1a:  $C_{SN,eq}$  and  $k_{C,Cl}$  evaluated from measured chloride ingress profiles from the marine exposure programme.

From figure 6.1a it can be seen that  $C_{SN,eq}$  is equal to 1.7 [% by wt Cl/binder] (20 g/l chloride concentration). Additionally the parameter  $k_{C,Cl}$  can be quantified from the data presented in figure 6.1a, by dividing  $C_{SN}$  by  $C_{SN,eq}$  at a water temperature of 20°C. With this procedure the parameter  $k_{C,Cl}$  has been quantified to the following values: 0.76 (5 g/l chloride concentration), 0.88 (10 g/l chloride concentration) and 1.12 (25 g/l chloride concentration).

In figure 6.1b (road conditions) data on  $C_{SN}$  analysed from chloride ingress data from bridges N 434, O 951 and O 978 (25-27 years exposure) are presented together with data from concrete 201 exposed at the Rv40 field station (5 years exposure)<sup>13</sup>. In road conditions  $C_{SN,eq}$  has been set to  $C_{SN}$  evaluated from concrete exposed at the carriageway (0.0 m distance and height) facing towards the traffic.  $C_{SN}$  analysed for other distances and heights above the carriageway and orientations towards the traffic  $C_{SN}$  can be recalculated to  $C_{SN,eq}$  by multiplying by the parameters  $k_{C,d}$ ,  $k_{C,h}$  and  $k_{C,o}$ .  $C_{SN,eq}$  is not temperature dependent since there are no data available in the literature to show this, i.e.  $k_{C,T}=1.0$ . Trend lines have been added in figure 6.1b to show the height-dependence of  $C_{SN}$  for surfaces facing away from and towards the traffic. It should also be noticed that the chloride ingress data in figure 6.1b are measured approximately 3 m from the road surface. The amounts of de-icing salt spread on the roads are approximately the same on the investigated roads, cf. tables 5.1 and 5.4, which means it should be possible to combine the chloride ingress data.

<sup>13</sup> Bridge N 434, O 951 and O 978 are probably constructed with a concrete with  $w/b=0.45-0.50$ , cf. Lindvall (2001), and concrete 201 has  $w/b=0.40$ , cf. Lindvall (2002b).

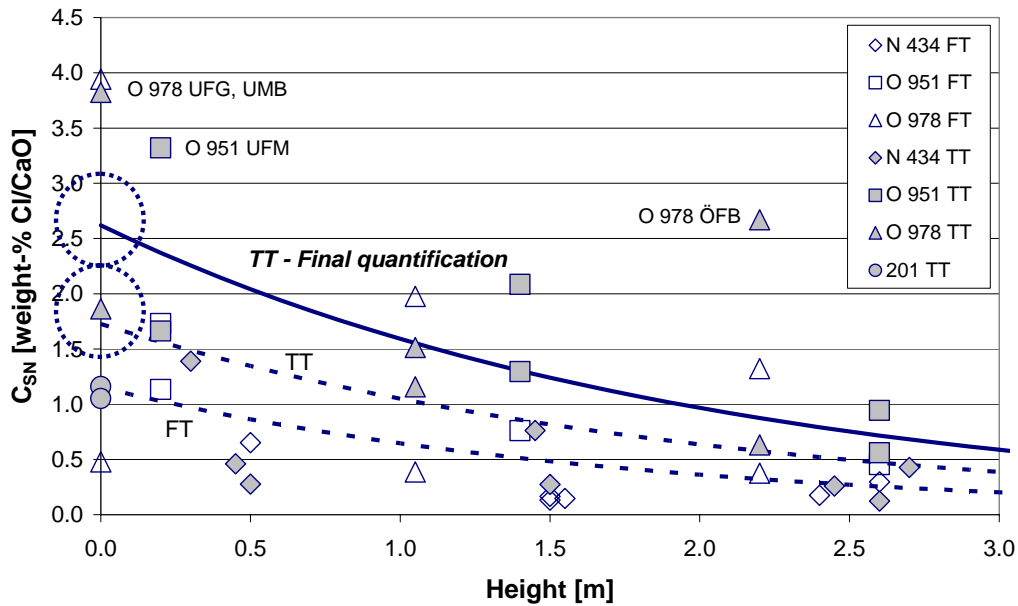


Figure 6.1b:  $C_{SN}$  evaluated from measured chloride ingress profiles from bridges N 434, O 951 and O 978 together with 5 years data from concrete 201 exposed at Rv40 field station.

From figure 6.1b it can be seen the  $C_{SN}$  for surfaces at 0.0 m over the carriageway and facing towards the traffic (index TT) is approximately 1.7 [% by wt Cl/CaO]. However, since the chloride ingress data are measured approximately 3 m from the road surface,  $C_{SN}$  has been multiplied by a factor 1.3 (corresponding to  $k_{C,d} \approx 0.8$  according to figure 6.10a). This means that  $C_{SN,eq}$  should be equal to approximately 2.2 [% by wt Cl/CaO] for this specific concrete exposed in these specific road conditions.

However, as seen in figure 6.1b, the originally quantified  $C_{SN,eq}$  is fairly low (compared with the maximum values of  $C_{SN}$ ) and therefore it has been decided to use a higher value of  $C_{SN,eq}$ , namely  $C_{SN,eq} = 3.4$  [% by wt Cl/CaO]. This value corresponds to  $C_{SN} = 2.6$  [% by wt Cl/CaO] in figure 6.1b. A trend line showing the height dependence of this  $C_{SN,eq}$  has also been added to the figure (denoted **TT - Final quantification**). Assuming that the cement used in the concrete contains 64.9 % by weight CaO<sup>14</sup> the chloride content in the concrete can instead be referred to the cement weight, i.e.  $C_{SN,eq} = 2.2$  [% by wt Cl/binder]. The level of  $C_{SN,eq}$  in road conditions is further discussed in section 7.4.2.

The decisive parameter for the level of  $C_{SN,eq}$  should be, as in marine conditions, the chloride concentration on the road surface. The amount of chlorides available on a road surface follows from the amount of de-icing salt spread on the road, which depends on several factors, e.g. the weather conditions, type of road, equipment used for spreading, type of de-icing salt etc. Furthermore the type of de-icing salt that is spread has also changed over time, since new spreading methods have been developed etc, which means that the amount of chlorides available on the road surface has also changed over time. Consequently the amount of chlorides on a specific road may vary significantly over time, both during one year, but especially between different years, which makes it difficult to exactly define the exposure conditions even for one specific road. However, since no data

<sup>14</sup> This CaO-content is valid for Swedish SRPC *Degerhamn Anläggningscement* (CEM I 42.5 BV/SR/LA).

are available on the correlation between the yearly amount of de-icing salt spread on the road and the chloride concentration in the solution on the road surface, a first rough assumption is that this relationship is linear. This means that if the amount of de-icing salt spread on the road is doubled  $C_{SN,eq}$  is also doubled and so on. However, this relationship is still very uncertain and more research is needed to better quantify it.

Thus  $C_{SN,eq}$  quantified above is only valid for concrete structures exposed along roads where approximately the same yearly amount of de-icing salt is spread, as on the roads along which the investigated structures are located. For other roads, on which other amounts of de-icing salt are spread,  $C_{SN,eq}$  has to be recalculated, with the assumption that  $C_{SN,eq}$  is linearly correlated with the yearly amount of de-icing salt spread on the road. For other types of concretes  $C_{SN,eq}$  has also to be recalculated.

It is also possible to establish a relation between  $C_{SN,eq}$  for marine and road conditions, if similar concrete compositions have been exposed in both marine and road conditions. This is usually not the case, but in two Nordic and Swedish research projects (BMB – Durability of Marine Concrete Structures and BTB – Durability of Road Concrete Structures) some concrete compositions have been exposed in both marine and road conditions, cf. Lindvall & Nilsson (2001b). This means it is possible to compare  $C_{SN,eq}$  for marine and road conditions. In figure 6.2 measured chloride ingress profiles from marine and road conditions for two different concrete compositions<sup>15</sup> are compared. Concretes 202 and 207 have been exposed in road conditions and concretes 1-50 and 3-50 in marine conditions. The indexes “A” and “S” denote exposure in the marine atmospheric and submerged zones respectively.

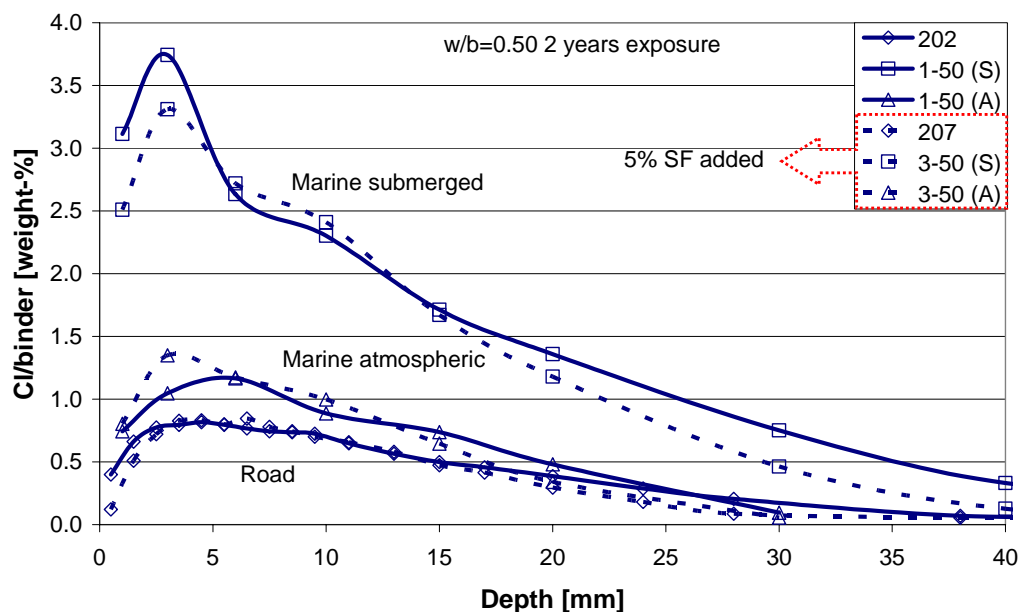


Figure 6.2: Comparison of measured chloride ingress profiles in marine and road conditions. Based on data from Nilsson et al (2000) and Tang (2003).

From figure 6.2 it can be seen that the chloride ingress in road conditions is fairly similar to the chloride ingress in marine atmospheric conditions. The chloride ingress in marine

<sup>15</sup> Concrete **202** and **1-50**: 100% Swedish SRPC (CEM I 42.5 BV/SR/LA) w/c=0.50. Concrete **207** and **3-50**: 95% Swedish SRPC (CEM I 42.5 BV/SR/LA) and 5% SF (Silica Fume) w/b=0.50.

submerged conditions is significantly larger compared with the chloride ingress in the other exposure conditions. The corresponding  $C_{SN}$ , for **concrete 202/1-50**, are 1.11, 3.73 and 1.63 [% by wt Cl/binder] and, for **concrete 207/3-50**, 1.01, 3.78 and 1.56 [% by wt Cl/binder] for road, marine submerged and atmospheric conditions respectively. Thus  $C_{SN,eq}$  in marine conditions is more than 3 times as high as in road conditions for similar concrete compositions.

### Potential diffusion coefficient – $D_0$

As mentioned earlier in DuraCrete it is proposed to determine the potential diffusion coefficient with NT Build 492 (1999). With this method the chloride diffusivity,  $D_{CTH}$  corresponding to  $D_0$ , can be determined on cores, diameter 100 mm, by applying a current over the core forcing chloride ions from a solution of sodium chloride to penetrate into the concrete. After exposure the chloride penetration depth is determined and  $D_{CTH}$  can be evaluated. The method is further described in Tang (1996) and NT Build 492 (1999).

Examples of chloride diffusivities for different concrete compositions and manufacturing conditions measured with NT Build 492 are given in Tang (1996), Tang (1997), DuraCrete (2000a) and Gehlen (2000).

### Parameters $k_{C,conc}$ and $k_{D,c}$

The parameters  $k_{C,conc}$  and  $k_{D,c}$  account for the influence of the concrete properties (differences in  $w/b$ ) on  $C_{SN,eq}$  and of the curing conditions (curing time in moist curing) on  $D_a(t)$  respectively. In figure 6.3a the parameter  $k_{C,conc}$  is expressed as a function of  $w/b$ , where  $k_{C,conc}=1.0$  when  $w/b=0.40$ . In figure 6.3b  $k_{D,c}=1.0$  when the curing time is seven days. The results presented in both figures are based on  $C_{SN,eq}$  determined for OPC concrete with  $w/b=0.40$  and moist-cured for seven days.

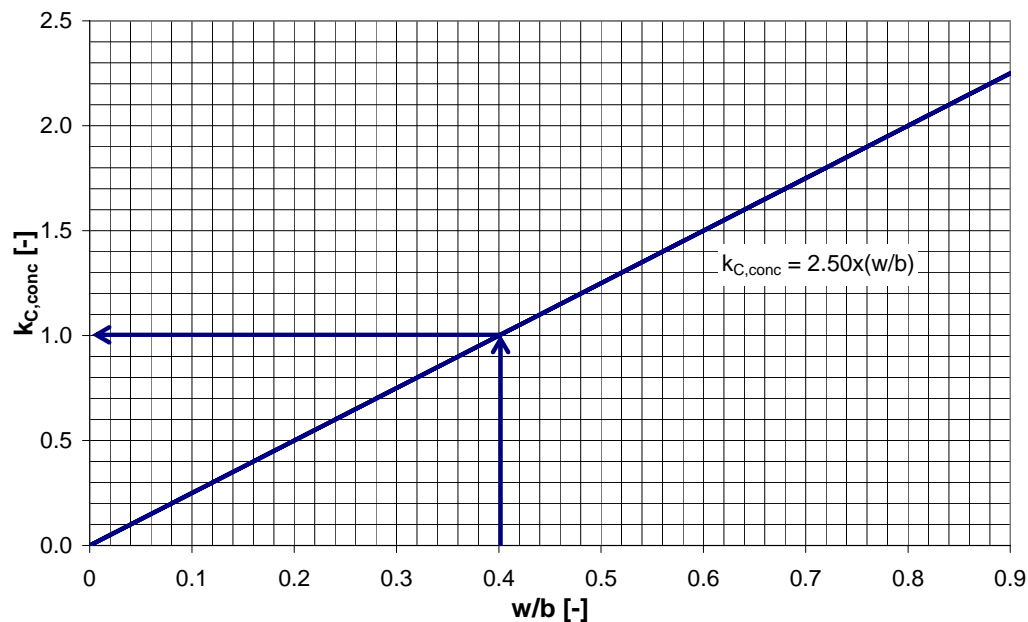


Figure 6.3a: Quantification of the parameter  $k_{C,conc}$ , which gives the influence of concrete composition on  $C_{SN}$  (in terms of  $w/b$ ). Based on data from DuraCrete (2000a).

In figure 6.3a it can be seen that the parameter  $k_{C,conc}$  is greatly influenced by  $w/b$ .

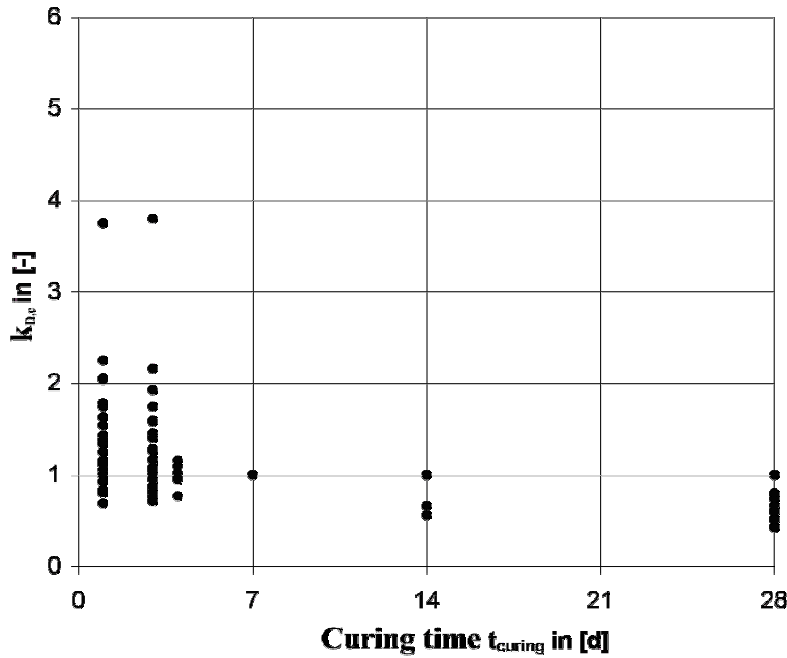


Figure 6.3b: Quantification of the parameter  $k_{D,c}$ , which gives the influence of curing time (moist curing) on  $D_a(t)$ . DuraCrete (2000a).

In figure 6.3b it can be seen that the parameter  $k_{D,c}$  is significantly influenced by the curing time, with  $k_{D,c}$  decreasing with increasing curing time. This means that  $D_a(t)$  decreases with increasing curing time, indicating that the concrete gets more dense.

However, there are more factors influencing both  $k_{C,conc}$  and  $k_{D,c}$ , e.g. type of binder and other types of curing than moist curing, but these factors are not described here. Further information about how the type of binder influences  $k_{C,conc}$  can be found in Nilsson et al (1996), DuraCrete (2000a), and information about how the type of curing influences  $k_{D,c}$  can be found in for example Tang (1997).

### 6.2.3 Influence of moisture and temperature conditions

The moisture conditions in concrete have an influence on the chloride ingress, where the chloride ingress rate, described by  $D_a(t)$ , is significantly influenced by the moisture conditions in the concrete. This influence is described in the modified DuraCrete chloride ingress model with the parameter  $k_{D,RH}$ , cf. eq. (6.1b).

The influence of the moisture conditions on  $D_a(t)$ , in terms of RH, has been studied by several authors, e.g. Saetta et al (1993), Nilsson et al (1997), Climent et al (2000) and Nielsen and Geiker (2003). Models which describe the influence of RH in the concrete on  $D_a(t)$  are given in eq. (6.2a), Saetta et al (1993), and (6.2b), Nilsson et al (1997). In the models, the relationship between  $D_a$  at any RH, and  $D_a(100\% \text{ RH})$  at 100% RH (reference), is given in eq. (6.1b), described by the parameter  $k_{D,RH}$ .

$$k_{D,RH} = \frac{D_a(T, RH)}{D_a(T, 100\%RH)} = \left( 1 + \frac{(1 - RH)^4}{(1 - RH_c)^4} \right)^{-1} \quad (6.2a)$$



where:

$RH_c$ : RH at which  $D(RH_c)=1/2D(100\%RH)$ . Here  $RH_c=83\% RH$ .

$$k_{D,RH} = \frac{D_a(T, RH)}{D_a(T, 100\%RH)} = \begin{cases} 0 & RH < 75\% \\ \frac{0.6}{10} \cdot (RH - 75\%) & 75\% < RH < 85\% \\ 0.6 + \frac{0.4}{15} \cdot (RH - 85\%) & RH > 85\% \end{cases} \quad (6.2b)$$

The parameter  $k_{D,RH}$  is illustrated in figure 6.4a, where eq. (6.2a) and (6.2b) are plotted together with data from Climent et al (2000) and Nielsen and Geiker (2003).

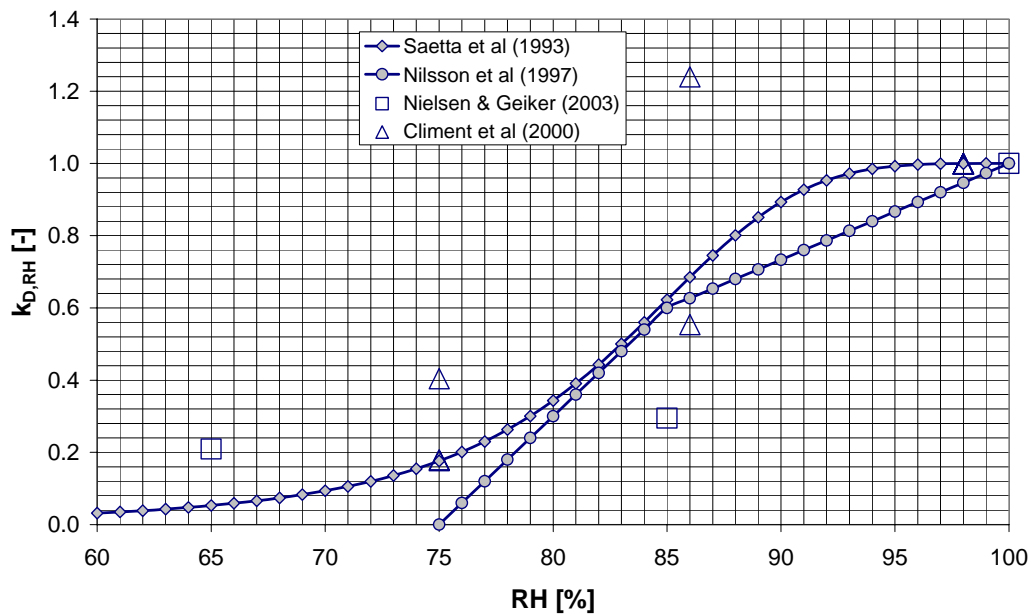


Figure 6.4a: Quantification of the parameter  $k_{D,RH}$ , which gives the influence of RH in the concrete on  $D_a(t)$ . Based on data from Saetta et al (1993), Nilsson et al (1997), Climent et al (2000) and Nielsen and Geiker (2003).

Measurements of moisture conditions in marine conditions are presented in figure 3.13a where it can be seen that RH in marine conditions follows from the exposure zone. RH varies between above 80% RH (submerged zone) and 65-75% RH (atmospheric zone). RH in marine tidal and splash zones is in between the submerged and atmospheric zones. In road conditions RH is almost similar in both dry and wet road environments, cf. figure 3.24a, where RH is 70-85% RH except in the surface near region (0-40 mm), which means that  $k_{D,RH}$  varies with height above the surface. On the basis of the result from figures 3.13a and 3.24a, together with figure 6.4a,  $k_{D,RH}$  has been quantified as follows :

- **Marine submerged conditions.**  $k_{D,RH}=0.40-1.00$
- **Marine tidal and splash conditions.**  $k_{D,RH}=0.05-1.00$
- **Marine atmospheric conditions.**  $k_{D,RH}=0.05-0.20$
- **Road conditions.**  $k_{D,RH}=0.10-0.60$

Obviously the parameter  $k_{D,RH}$  varies significantly and sometimes the levels of  $k_{D,RH}$  can be questioned, e.g. in the marine atmospheric zone where  $k_{D,RH}$  seems too low and gives unrealistically low chloride ingress. Parts of the variations can be explained by the exposure to seawater, the degree of exposure and shelter from rain and solar radiation, but they are also influenced by the degree of self-desiccation in the concrete etc. Due to the large variations in  $k_{D,RH}$  it has been decided to use the following values of  $k_{D,RH}$  in the predictions of chloride ingress made in chapter 7:

- **Marine submerged zone.**  $k_{D,RH}=1.0$
- **Marine tidal and splash zone.**  $k_{D,RH}=0.9$  (tidal zone), 0.4 (splash).
- **Marine atmospheric zone.**  $k_{D,RH}=0.4$  (since the earlier quantified  $k_{D,RH}$  seems too low).
- **Road conditions.**  $k_{D,RH}=0.4$  (dry road environment), 0.6 (wet road environment).

As presented in chapter 4 the temperature conditions in the concrete influence  $C_{SN}$  and  $D_a(t)$ , cf. eq. (4.3a) and (4.4). In eq (6.1a) the temperature-dependence of  $C_{SN}$  is modelled with the parameter  $k_{C,T}$ . In eq (6.1b) the temperature-dependence of  $D_a(t)$  is modelled with the parameter  $k_{D,T}$ . The parameters  $k_{C,T}$  and  $k_{D,T}$  are quantified in eq. (6.3) and illustrated in figure 6.4b.

$$\begin{cases} k_{D,T} = \frac{D_a(T, RH)}{D_a(+20^\circ\text{C}, RH)} = e^{\left[3700\left(\frac{1}{293} - \frac{1}{273+T}\right)\right]} \\ k_{C,T} = \frac{C_{SN}(T, Cl_f)}{C_{SN,eq}(+20^\circ\text{C}, Cl_f)} = e^{\left[3700\left(\frac{1}{273+T} - \frac{1}{293}\right)\right]} \end{cases} \quad [-] \quad (6.3)$$

where:

- $D_a(T, RH)$ :  $D_a(t)$  evaluated from chloride ingress profiles measured in concrete with a temperature  $T$  and a certain  $RH$ .
- $D_a(+20^\circ\text{C}, RH)$ :  $D_a(t)$  evaluated from chloride ingress profiles measured in concrete with a temperature of  $+20^\circ\text{C}$  and a certain  $RH$  (similar to  $RH$  above).
- $C_{SN}(T, Cl_f)$ :  $C_{SN}$  evaluated from chloride ingress profiles measured in concrete exposed in a solution with a temperature  $T$  and a certain chloride concentration in the exposure solution,  $Cl_f$ .
- $C_{SN}(+20^\circ\text{C}, Cl_f)$ :  $C_{SN}$  evaluated from chloride ingress profiles measured in concrete exposed in a solution with a temperature of  $+20^\circ\text{C}$  and a certain chloride concentration,  $Cl_f$  (similar to  $Cl_f$  above).
- $T$ : temperature of the concrete. [ $^\circ\text{C}$ ]

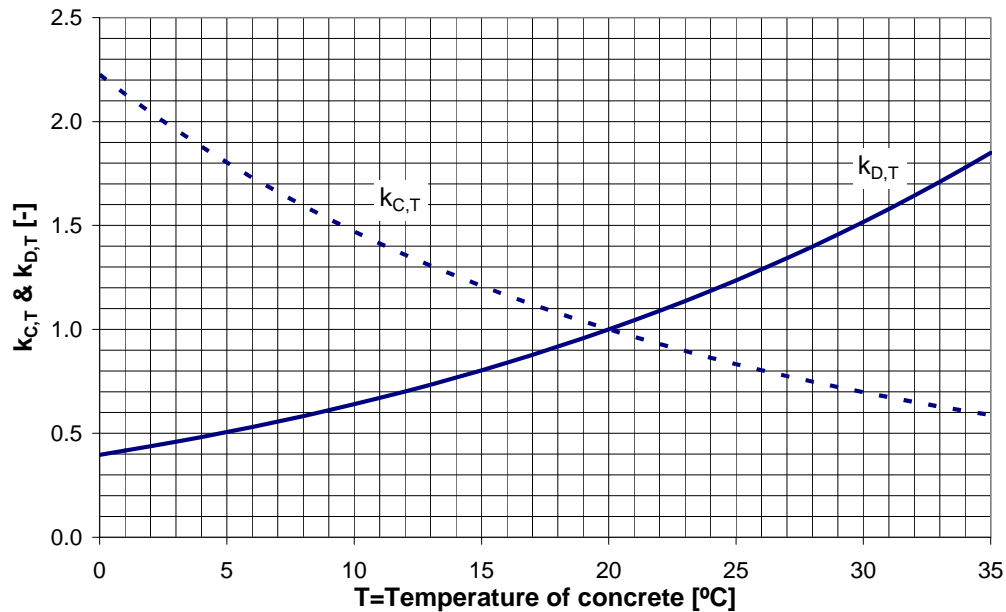


Figure 6.4b: Illustration of the parameters  $k_{C,T}$  and  $k_{D,T}$ .

If no data are available on the moisture and temperature conditions in the concrete, the combined effect of these factors on  $k_{D,e}$  can be evaluated from figure 6.6.

## 6.2.4 Chloride ingress over time

### Age factor – n

In the DuraCrete chloride ingress model, the chloride ingress over time has been modelled with the age factor  $n$ , which describes the decrease in  $D_a(t)$  with increasing exposure time. In figure 6.5 an example is presented of how the age factor,  $n$ , can be quantified. The evaluated  $D_a$ , after different exposure times, are plotted as a function of the exposure time in a log-log scale and the age factor is evaluated as the slope of a linear trend line for the data.  $D_a$  has been evaluated from chloride ingress data measured from concrete 1-40<sup>16</sup> and 1-50<sup>17</sup> exposed in the submerged zone at the Träslövsläge field exposure station. The diamonds and squares denote data from concrete 1-40 and 1-50 and the filled and unfilled symbols exposure in submerged and atmospheric conditions respectively.

<sup>16</sup> Concrete 1-40. SRPC-concrete (Degerhamn Anläggningscement CEM I 42.5 BV/SR/LA). w/c=0.40.

<sup>17</sup> Concrete 1-50. SRPC-concrete (Degerhamn Anläggningscement CEM I 42.5 BV/SR/LA). w/c=0.50.

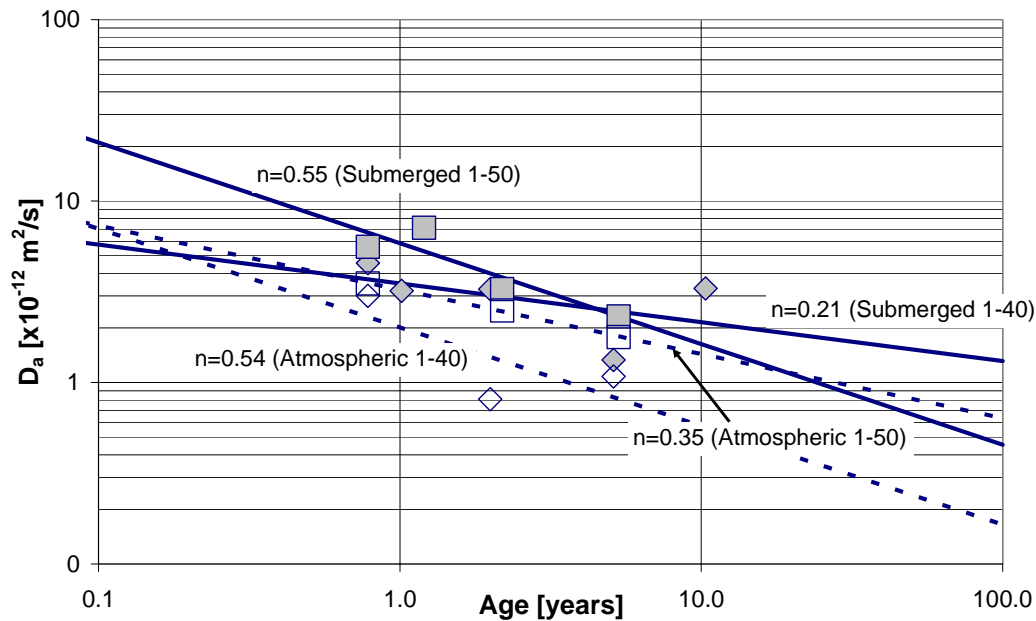


Figure 6.5: Example of quantification of the age-factor,  $n$ . Based on data from Tang (2003).

From figure 6.5 it can be seen that the evaluated age factors (in submerged and atmospheric exposure respectively) are equal to 0.21 and 0.54 (concrete 1-40) and 0.55 and 0.35 (concrete 1-50). The results show that the age factor is higher for concrete 1-40 and lower for concrete 1-50 when chloride ingress data from exposure in submerged and atmospheric conditions are compared. However, the age factors evaluated from figure 6.5 have large uncertainties since they are quantified from data measured on three to five different occasions up to approximately 10 years exposure (for concrete 1-40 in submerged conditions). This means that each data point has a large influence on the quantified age factor, e.g. if the data point after 10 years exposure for concrete 1-40 were unknown the quantified age factor would be significantly different ( $n=0.59$  instead of  $n=0.21$ ). Obviously more data are needed to be able to quantify age factors with less uncertainty. Furthermore from the results in figure 6.5 it is obvious that the age factor is influenced not only by the exposure conditions but also by the concrete composition. In the predictions of chloride ingress in chapter 7 data on the age factor have been taken from DuraCrete (2000a).

The age factor can be quantified by plotting  $D_a$  evaluated from chloride ingress profiles measured after different exposure times, preferably measured on the same concrete to exclude any possible effects due to concrete properties. However, chloride ingress data measured at different exposure times for the same concrete are scarce and therefore chloride ingress data from different concrete compositions and exposure times are usually combined when the age factor is quantified. The result of the quantification may be a large scatter as a result of differences in concrete compositions, analysis methods etc, cf. Lindvall & Nilsson (2001a).

### Definition of exposure time

A factor that influences the results of the quantification of the age factor is the definition of the exposure time. This is a relevant question, since it is possible to define the exposure time either as the total time of exposure or the time of exposure to chlorides. Furthermore the chloride ingress in at least marine atmospheric and road conditions has been found to

almost stop after a certain exposure time, cf. de Rooij & Polder (2002) and Lindvall (2002b).

The definition of exposure time is only clear in marine submerged conditions, where the exposure time to chlorides is similar to the total time of exposure. However, for surfaces above the water surface that are only periodically exposed to chlorides, the time of exposure to chlorides and the total time of exposure are not the same. This difference becomes more significant the longer from the source of chlorides the exposed surface is located. As an example the time of exposure to chlorides, for surfaces high above the water surface in the marine atmospheric zone, can be only a few weeks during the year.

In road conditions the exposure to chlorides only takes place when de-icing salt is spread, i.e. approximately half the year, which means that the time of exposure to chlorides is approximately only half of the total exposure time. The exposure to chlorides may be even shorter at locations where de-icing salt is rarely spread. Thus, depending on when during the year the exposure in road conditions is started, the difference between the total time of exposure and exposure to chlorides can be up to half a year. Additionally, the maturity of the concrete on first exposure to chlorides has been found to have a significant influence on the chloride ingress – this is further discussed below.

### **Effect of maturity on first exposure to chlorides**

The maturity of the concrete on first exposure to chlorides has been found to have a significant influence on the chloride ingress, cf. Lindvall (2002b). It has been found that if the concrete has low maturity on first exposure to chlorides, the chloride ingress is larger compared with chloride ingress into concrete that is more mature. This effect is especially clear in environments with periodic exposure to chlorides, i.e. in marine tidal, splash and atmospheric zones and road conditions. In these environments the main part of the chloride ingress takes place during the first year of exposure to chlorides, which means that the maturity on first exposure to chlorides has a significant influence. Examples of this are given in Lindvall (2002b), where a difference in curing time of only a few weeks, on first exposure to chlorides, has been found to significantly affect the chloride ingress in road conditions.

The effect of maturity can be used to explain the observation that the chloride ingress seems to almost stop in some exposure conditions after a certain exposure time. The increasing maturity of the concrete over time, which gives a more dense concrete, together with pore-blocking effects, will result in a significant decrease in the chloride ingress rate. The result may therefore be, together with effects due to washout of chlorides by rain during summer and autumn, that the chloride content in the concrete is more or less unchanged.

The effect of the maturity of the concrete on first exposure to chlorides is even more pronounced for concrete with binders that have a slower reaction rate than Portland cement, e.g. silica fume. For these concretes it may take up to ten times longer to reach the final degree of reaction, compared with pure Portland cement concrete, Helsing-Atlassi & Kjellsen (2000). The degree of reaction can be related to the density of the concrete and thus the resistance against chloride penetration. This means that if a concrete with secondary binders is exposed to chlorides at early age the chloride ingress may be larger than in a pure Portland cement concrete, due to the comparatively lower degree of reaction.

As discussed earlier the time of exposure to chlorides and the total exposure time are not similar for surfaces above the water surface. If this effect is combined with the effect due to the maturity of the concrete there may be a significant effect on the chloride ingress. This is especially clear in road conditions, where there may be a difference of half a year in the time of exposure to chlorides and the total exposure time. A concrete cast in the late spring will have significantly higher maturity than a concrete that is cast in the late autumn or winter, when first exposed to chlorides, i.e. when de-icing salt is spread on the road. Due to the above effect of the maturity of the concrete, the chloride ingress will be largest in concrete cast in the late autumn or winter.

### **Summary**

Thus, the definition of the exposure time, together with the maturity of the concrete on first exposure to chlorides, is obviously important and should therefore be paid extra attention when measured chloride ingress data are compared. In this thesis the exposure time has been defined as the total time of exposure, since no detailed data are available about the time of exposure to chlorides. The effect of the maturity of the concrete on first exposure to chlorides is also not included, since there are no data regarding this effect. Obviously more research is needed about how the maturity on first exposure to chlorides and the definition of exposure time influence the chloride ingress and the evaluation of measured chloride ingress profiles. Additionally the differences between pure Portland cement concrete and concrete with secondary binders need also to be further investigated.

### 6.3 Models for environmental actions – Marine conditions

In the following section the effects of distance, height and orientation to the source of chlorides, mainly seawater, in marine conditions are described and quantified. These effects are described with the **uncorrelated** parameters  $k_{C,d}$ ,  $k_{C,h}$  and  $k_{C,o}$ . Additionally the combined effects of the moisture and temperature conditions on  $D_a(t)$  at different positions relative to the water surface are exemplified.

#### 6.3.1 General

The exposure to chlorides in marine conditions is mainly influenced by the exposure to seawater, either submerged or from tidal actions, and spray and splash from waves. The main influencing factors are the position relative to the water surface together with the extent of tidal and wave actions. Not only structures in the sea are exposed to marine chlorides, but also structures inland (up to several kilometres from the coastline), since chloride-contaminated spray from breaking waves may be transported with winds inland, cf. Takewaka & Mastumoto (1988), Fitzpatrick (1996), Gustafsson & Franzén (2000) and McGee (2000).

#### 6.3.2 Chloride transport in vertical direction – $k_{C,h}$

Several investigations have shown that there is a decrease in the severity of exposure to chlorides with increasing height above the water level, cf. Fluge (1997), Tang (1997), Wood & Crerar (1997) etc. Furthermore the results from the marine field study presented in this thesis indicate that there is an increase in the severity of the exposure to chlorides with increasing depth. These effects are in eq. (6.1a) modelled with the parameter  $k_{C,h}$ . The quantification of  $k_{C,h}$  requires data on the exposure to chlorides both from the submerged zone (equivalent conditions, where  $C_{SN,eq}$  is defined) and above the water surface. These kinds of data are scarce in the literature – usually the chloride ingress is either measured above or below the water surface. However, in for example Tang (1997) and Wood & Crerar (1997) these kinds of data are available.

In figure 6.6  $k_{C,h}$  is quantified with data from Tang (1997) and Wood & Crerar (1997) together with data from the marine field study presented in this thesis. Included in the figures are also data on variations in  $D_a$  with the position relative to the water surface, where the quotient between  $D_a$  and  $D_a(-1.0\text{ m})$ , at 1.0 m depth, are plotted against position relative to the water surface. This quotient describes how the combined influence of variations in moisture and temperature conditions on  $D_a$  varies with the position relative to the water surface (assuming that the concrete properties are constant over the structure). The data describing  $k_{C,h}$  and the quotient between  $D_a$  and  $D_a(-1.0\text{ m})$  are denoted with **diamonds** and **squares** respectively. The filled and unfilled symbols are based on data from Wood & Crerar (1997) and Tang (1997) respectively, except the data at 0.0 m in the marine tidal zone, which come from the marine exposure programme presented in this thesis (exposure at La Rochelle).

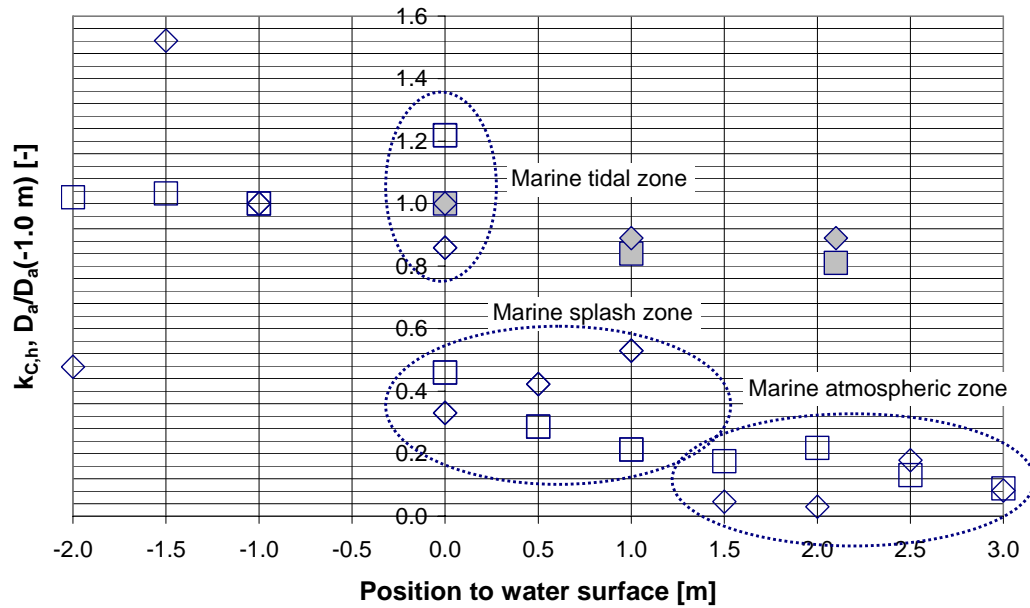


Figure 6.6: Examples of quantification of the parameter  $k_{C,h}$  (diamonds), which gives the effect of vertical distance to the water surface on  $C_{SN}$ . The quotient between  $D_a$  and  $D_a(-1.0 \text{ m})$  (squares) is also added to the figure. Based on data from Tang (1997) and Wood & Crerar (1997).

In figure 6.6 it can be observed that, with the data from Tang (1997),  $k_{C,h}$  decreases significantly with increasing height above the mean water level while it is fairly stable with the data from Wood & Crerar (1997). Similar observations can be made if the quotient between  $D_a$  and  $D_a(-1.0 \text{ m})$  is studied, where the data from Tang (1997) decrease while the data from Wood & Crerar (1997) are fairly stable with increasing height above the water surface.

An explanation for the observed differences between the data from Tang (1997) and Wood & Crerar (1997) can be found if the locations of the structures, where the chloride ingress has been measured, are compared. The data from Tang (1997) come from a structure in the Baltic Sea on the Swedish east coast, while the data from Wood & Crerar (1997) come from a bridge in the North Sea on the Scottish east coast. The wave heights and wind speeds are probably higher on the Scottish east coast than at the Swedish east coast and consequently the exposure to chlorides and moisture (due to driving rain etc) should be more severe for the structure investigated by Wood & Crerar (1997).

It should be noticed that data in figure 6.6 are valid for those specific structures. Data from other structures may be significantly different due to other wave heights, wind directions and speeds etc. Therefore it has been decided to use the following values of the parameter  $k_{C,h}$  in the predictions of chloride ingress in chapter 7, to get a more general description:

- **Marine submerged zone.**  $k_{C,h}=1.00$  [-]. (Equivalent conditions)
- **Marine tidal zone.**  $k_{C,h}=1.00$  [-].
- **Marine splash zone.**  $k_{C,h}=0.80$  [-].
- **Marine (distant) atmospheric zone.**  $k_{C,h}=0.70$  (0.25) [-].



### 6.3.3 Chloride transport in horizontal direction – $k_{C,d}$

There are some investigations on how the exposure to chlorides decreases with increasing distance to the coastline, cf. Takewaka & Mastumoto (1988), Fitzpatrick (1996) and McGee (2000). This effect is in eq (6.1a) modelled with the parameter  $k_{C,d}$ . The quantification of  $k_{C,d}$  requires data on the exposure to chlorides both from or outside the coastline and with increasing distance from the coastline. These kinds of data are available for example in Takewaka & Mastumoto (1988) and McGee (2000). In figure 6.7  $k_{C,d}$  is quantified with data from Takewaka & Mastumoto (1988) and McGee (2000).

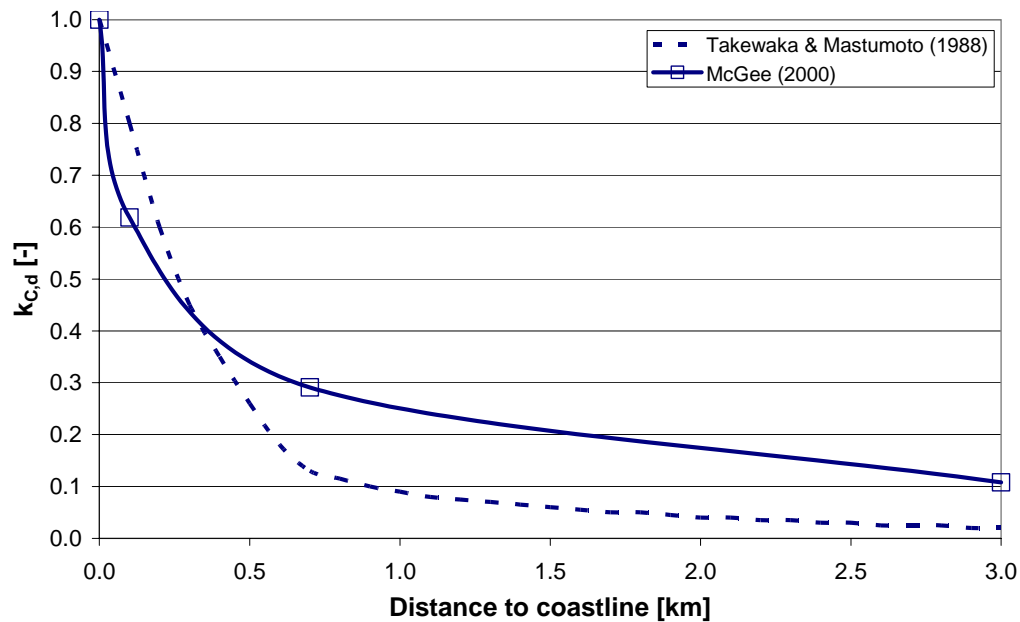


Figure 6.7: Examples of quantification of the parameter  $k_{C,d}$ , which gives the effect of horizontal distance to the coastline on  $C_{SN}$ . Based on data from Takewake & Mastumoto (1988) and McGee (2000).

From figure 6.7 it can be seen that  $k_{C,d}$  decreases rapidly with increasing distance from the coastline, where for example at 1.0 km distance from the coastline  $k_{C,d}$  is between 0.10 and 0.25. However, in the literature there are some data indicating that the marine chlorides may be spread at much longer distances from the coastline than presented in figure 6.7, cf. Gustafsson & Franzén (2000). It has also been shown that transport of marine chlorides inland from the coastline is significantly influenced by the wind direction, cf. Morcillo et al (2000), where it was found that at certain wind directions, defined as “saline winds”, the transport of marine aerosols over land was significantly increased, even at low wind speeds. Therefore the quantified  $k_{C,d}$  in figure 6.7 should be treated more as an indication than an exact measure of the decrease in the exposure to chlorides with increasing distance to the coastline. To get a more specific quantification of  $k_{C,d}$  valid for a certain structure, each structure should be treated separately.

### 6.3.4 Influence of surface orientation – $k_{C,o}$

The surface orientation and shape, together with exposure and shelter from rain, have been found to significantly influence the severity of exposure to chlorides for surfaces exposed above the water surface, cf. Andersen (1996) and Fluge (1997) and others. The effect of surface orientation is in eq. (6.1a) modelled with the parameter  $k_{C,o}$ . In figure 6.8 some examples of how the surface orientation influences the exposure to chlorides, on parts of the Gimsøystraumen bridge, are shown, data from Fluge (1997). The variations in

exposure to chlorides on a column are shown to the left (height above the mean water level is 11.6 m) and on the box girder to the right (bridge deck has a height above the mean water level of 11.6 m) The exposure to chlorides has been measured as the chloride content in the outer 10 mm (box girder) and 15 mm (column) of the concrete. The dominating direction for combined wind and rain is from the south west. Unfortunately no data are available to quantify  $C_{SN,eq}$  (concrete composition, chloride concentration and temperature of seawater etc).

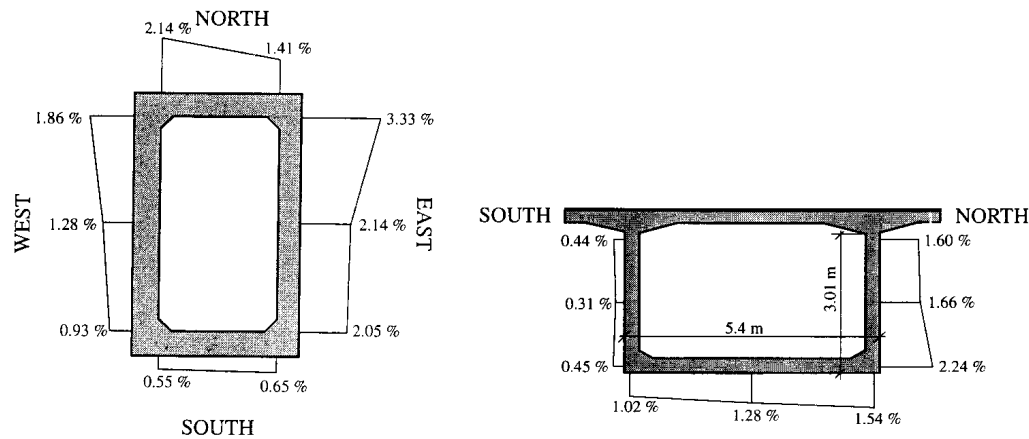


Figure 6.8: Examples of how the surface orientation influences the exposure to chlorides in the marine atmospheric zone. [% by weight Cl/binder]. Fluge (1997).

In figure 6.8 it can be seen that there is a clear effect due to the surface orientation, together with shelter from direct rain, on the severity of exposure to chlorides. In Fluge these variations are explained as effects mainly due to the direction of wind combined with rain, which is from south west. This means that chlorides, deposited on surfaces facing towards south or west, are more probable to be washed away than chlorides deposited on surfaces facing towards east or north. The chloride content in the concrete on these surfaces will instead increase over time.

However, although there are data showing how the surface orientation influences the exposure to chlorides, there are still large uncertainties regarding the significance of influencing factors. Furthermore the effects of surface orientation on the exposure to chlorides are unique for each structure, e.g. due to characteristics of the surrounding terrain etc, which means that each structure should be treated separately, and thus it is not possible to make any general quantification of  $k_{C,o}$ . Therefore the effects of surface orientation on the exposure to chlorides have not been included in the study presented in this thesis, which means that  $k_{C,o}=1.0$ . More research is needed to further clarify the effects of surface orientation and shape together with exposure and shelter from rain.

## 6.4 Models for environmental actions – Road conditions

In the following section the effects on road conditions due to distance, height and orientation to the source of chlorides, mainly de-icing salt spread on roads to prevent slippery road conditions, are described and quantified. These effects are described with the **uncorrelated** parameters  $k_{C,d}$ ,  $k_{C,h}$  and  $k_{C,o}$ .

### 6.4.1 General

Concrete structures in road conditions are, like most outdoor structures, subjected to rapid changes in temperature and moisture conditions and exposure to carbon dioxide. What is special for road structures is that they are exposed to chlorides if de-icing salt is spread on the road. There is also a transport of chlorides to the surroundings of the road, due to drainage, snow ploughing, splash and spray, which means that the road conditions extend over a certain distance from the road itself. Since de-icing salt is only spread during the cold part of the year (the exact period during which de-icing salt is spread varies between different years and locations, even along the same road), concrete structures in road conditions are only exposed to chlorides during parts of the year.

As described in chapters 3 and 5 there are several factors that influence the exposure to chlorides in road conditions, e.g. spread of de-icing salt (type of salt, equipment used for spreading etc), characteristics of traffic (intensities, speeds etc), characteristics of the structure (shape, surface orientations and properties etc) and climate data for the location of the structure (wind speeds and directions, amount of rain etc). However, there are very few data available in the literature on the correlation between these factors and the chloride ingress into concrete exposed along roads where de-icing salt is spread. This is why, in the quantification of the parameters  $k_{C,d}$ ,  $k_{C,h}$  and  $k_{C,o}$ , only effects due to the characteristics of traffic and the structure (mainly surface orientation) have been included.

### 6.4.2 Chloride transport in vertical direction – $k_{C,h}$

There are some investigations on how the exposure to chlorides decreases with increasing height above the road, cf. Fagerlund & Svärd (2001), Lindvall (2002a) and others. This effect is in eq. (6.1a) modelled with the parameter  $k_{C,h}$ . The quantification of  $k_{C,h}$  requires data on the exposure to chlorides at the level of the carriageway and at different heights above this. These kinds of data are available in Fagerlund & Svärd (2001), Lindvall (2002a).

The parameter  $k_{C,h}$  has been modelled with a linear function, see eq (6.4), which describes how  $k_{C,h}$  decreases with increasing height above the road.

$$k_{C,h} = 1 - 0.2 \cdot h \quad [-] \quad (6.4)$$

where:

$h$ : height above the road. [m]

The model, based on data from Fagerlund & Svärd (2001) and Lindvall (2002a), is presented in figure 6.9. The data from Fagerlund & Svärd (2001) and Lindvall (2002a) are denoted by diamonds and squares respectively. The filled and unfilled symbols denote data from surfaces facing towards and away from the traffic respectively.

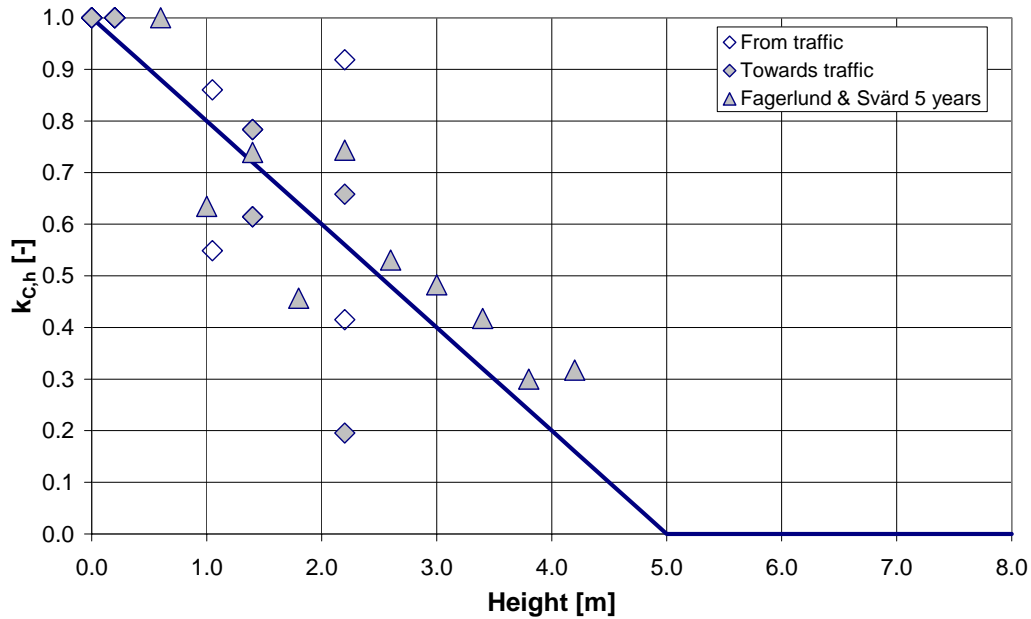


Figure 6.9: Quantification of the parameter  $k_{C,h}$ , which gives the influence of height above the road on  $C_{SN}$ . Based on data from Fagerlund & Svärd (2001) and Lindvall (2002a).

In figure 6.9 it can be observed that there seems not be any significant difference in  $k_{C,h}$  for surfaces facing from and towards the traffic. Thus the model for  $k_{C,h}$  seems not to be dependent on the surface orientation.

#### 6.4.3 Chloride transport in horizontal direction – $k_{C,d}$

Several investigations have shown that there is transport of chlorides from roads, where de-icing salt is spread, in a horizontal direction from the road, cf. McBean & Al-Nassri, Eliasson (1996), Blomqvist & Johansson (1999) etc. The spread of chlorides around a road is mainly affected by the characteristics of the road and the traffic, but also by e.g. the wind conditions around the road. However, in this study only the effects of traffic intensity and speed are included. This is in eq. (6.1a) modelled with the parameter  $k_{C,d}$ . The quantification of this parameter requires data on the exposure to chlorides at different distances from the roads, with different traffic intensities and speeds.

The parameter  $k_{C,d}$  has been modelled with an exponential function, see eq (6.5), which describes how  $k_{C,d}$  decreases with increasing distance to the road. However,  $k_{C,d}$  is dependent not only on the distance to the road but also on the traffic intensity and speed, which is described by the parameter  $d_0$ . This latter parameter gives the distance from the road at which  $k_{C,d}=1.0$ .

$$\begin{cases} k_{C,d} = 1 & d \leq d_0 \\ k_{C,d} = e^{-0.24 \cdot (d - d_0)} & d_0 \leq d \leq d(k_{C,d} = 0.1) \end{cases} \quad [-] \quad (6.5)$$

where

$d$ : distance from the road surface in horizontal direction. [m]

$d_0$ : distance up to which  $k_{C,d}=1.0$ . [m]

The model, together with data from McBean & Al-Nassri (1987) and Blomqvist & Johansson (1999), is presented in figure 6.10a. The quantification of the parameter  $k_{C,d}$  in figure 6.10a is valid for a road with speed limit 50 km/h and low traffic intensity ( $d_0 \approx 1.0$  m, according to figure 6.10b).

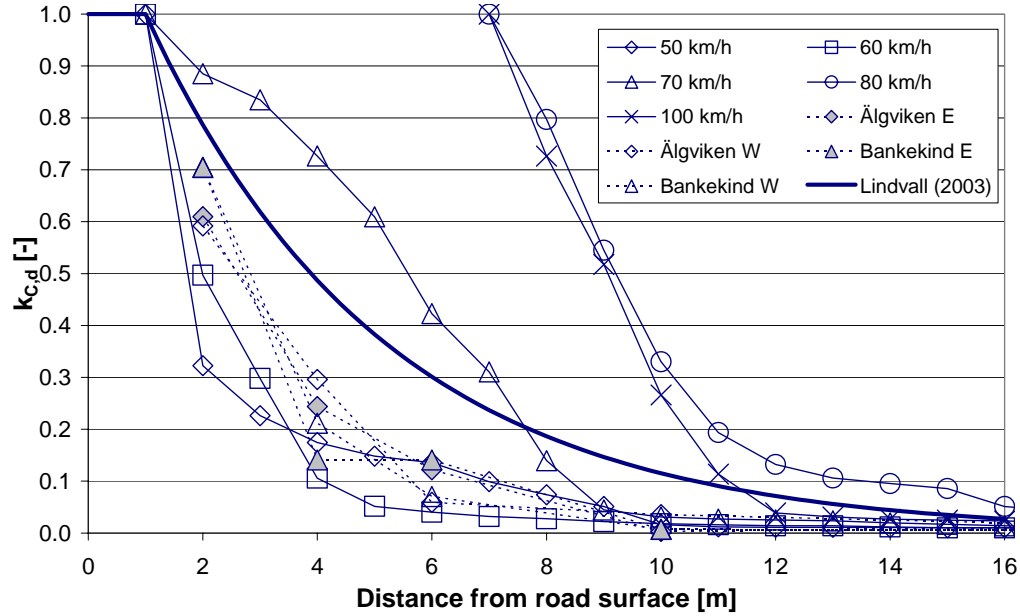


Figure 6.10a: Quantification of the parameter  $k_{C,d}$ , which gives the influence of the distance to the road on  $C_{SN}$ .  $k_{C,d}$  is valid for speeds of 50 km/h. Data from McBean & Al-Nassri (1987) and Blomqvist & Johansson (1999).

The distance up to which  $k_{C,d}=1.0$ , is in eq. (6.5) given by  $d_0$ . The parameter  $d_0$  can be expressed as a function of the speed and traffic intensity according to figure 6.10b.

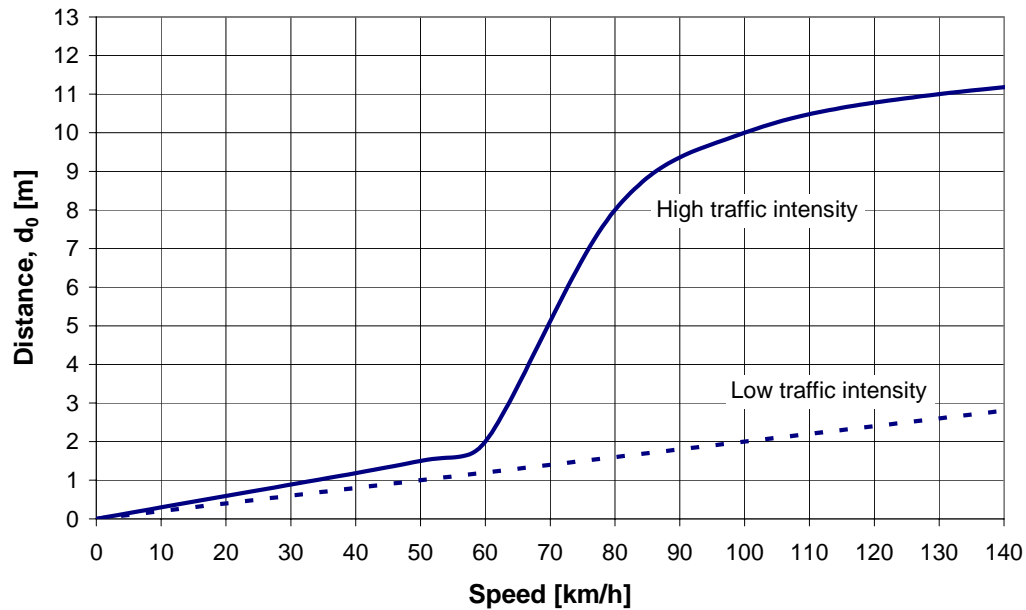


Figure 6.10b: Quantification of the parameter  $d_0$ , which gives the influence of traffic intensity and speed on  $k_{C,d}$ . Based on data from Burton (1992) & Pedersen & Fostad (1996).

The data in figure 6.10b are based on only two reference sources, and may therefore have large uncertainties, but still they give a picture of how the chloride load is a function of the traffic intensity.

The transport of chloride in a vertical direction is also influenced by the wind conditions around the road, especially for structures close to the sea. However, since data on the influence of wind are lacking, this effect has not been included in the model.

#### 6.4.4 Influence of surface orientation – $k_{C,o}$

The results from the investigations in road conditions, presented in this thesis, indicate that there is a difference in the exposure to chlorides depending on the surface orientation. This effect is in eq (6.1a) modelled with the parameter  $k_{C,o}$ , defined in eq (6.6), where surfaces facing towards the traffic are used as reference, cf. figure 6.1b.

$$k_{C,o} = \frac{\text{Exposure to chlorides}}{\text{Exposure to chlorides (TT)}} \quad [-] \quad (6.6)$$

In figure 6.11 the parameter,  $k_{C,o}$ , is quantified with data from Lindvall (2002a). In the figure the relation between the severity in exposure to chlorides for surfaces facing towards and away from the traffic, on bridges O 951 (diamonds) and O 978 (squares), is presented. The severity in exposure to chlorides has been determined as the area below the measured chloride ingress profiles in the mortar disks, cf. figures 5.12a and 5.12b. The determined areas have been combined in pairs along the same road, e.g. surfaces facing towards the traffic from Göteborg and away from the traffic towards Malmö on bridge O 951. In figure 6.11 three linear trend lines have been added: the line of conformity, the trend line for the data and a line describing the result of the quantification of  $k_{C,o}$ .

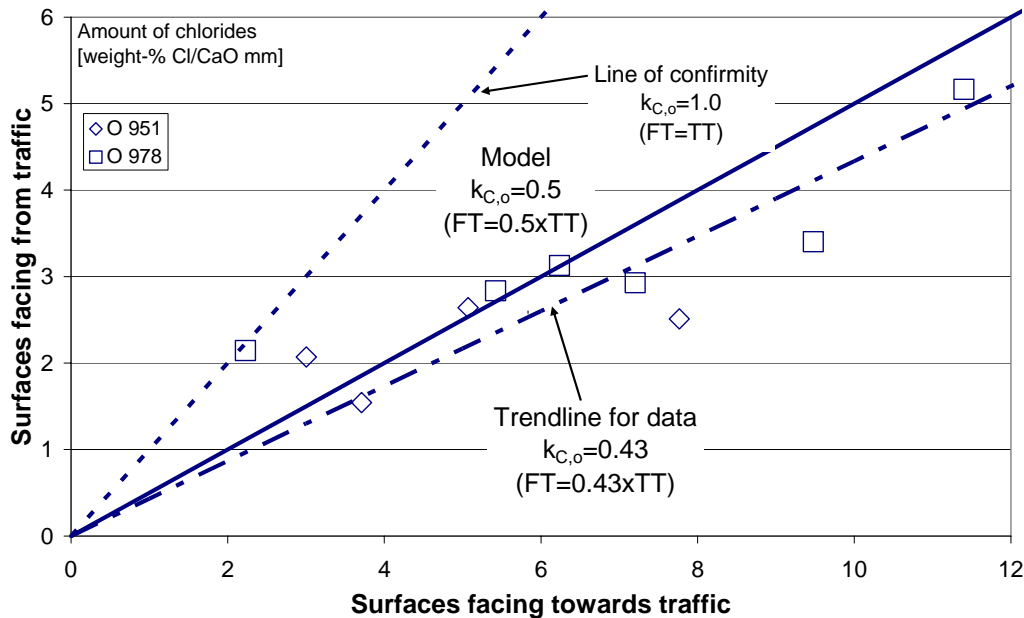


Figure 6.11: Quantification of the parameter  $k_{C,o}$  which gives the influence of surface orientation on  $C_{SN}$ . Data from Lindvall (2002a).

In figure 6.11 it is clear that the surface orientation has a significant effect on the exposure to chlorides. However, as discussed in chapter 5, the variations in exposure to chlorides are unique for each structure – this is certainly the case with the effect of the surface orientation. This means that the data from bridges O 951 and O 978 are only representative for these bridges, where probably the exposure to chlorides for surfaces facing towards the traffic is somewhat high (giving  $k_{C,o}=0.43$  for surface facing away from the traffic). Therefore, to get a more general description of the effect of the surface orientation, the parameter  $k_{C,o}$  has been quantified to 0.5 for surfaces facing away from the traffic. This means that  $C_{SN}$  is twice as high for surfaces facing towards the traffic as for surfaces facing away from the traffic. For surfaces parallel or perpendicular to the traffic  $k_{C,o}=0.5-1.0$  (depending on the local exposure conditions).





## 7 Environmental actions in models of service life

In this chapter, the effects which environmental actions have on predictions of service life with the DuraCrete chloride ingress model, are discussed and analysed. The environmental actions are described with the models presented in chapter 6. In the predictions only the initiation of chloride induced reinforcement corrosion is considered, i.e. the service life is defined as at an end when corrosion is initiated.

### 7.1 Introduction

The influence of the environmental actions on predictions of service life has been demonstrated with the DuraCrete chloride ingress model, described in eq. (2.1a). However, the DuraCrete chloride ingress model predicts the total chloride content in the concrete, which means that the driving potential for chlorides, the surface chloride content  $C_{SN}$ , and the chloride threshold level,  $C_{crit}$ , is described as the **total chloride content** in the concrete.

The predictions have been made mainly with deterministic methods but also with probabilistic methods, where the effects of uncertainties in the parameters in the model are included. In the deterministic predictions the parameters in the model have been described with mean values. The probabilistic predictions have been made with parameters described with means values, standard deviations (SD) and statistical distribution functions. Predictions of chloride ingress have been made both for marine and road conditions, with the emphasis on marine submerged and road conditions. Only **sound concrete**, i.e. without any defects like cracks etc, has been considered.

The results of the predictions of chloride ingress, made both with deterministic and probabilistic methods, have been used for service life predictions, where the concrete covers required to achieve a certain service life have been determined and vice versa. Only the initiation period for chloride induced reinforcement corrosion has been considered in the service life predictions, cf. the service life model presented in figure 2.1. Additionally predictions made with deterministic and probabilistic methods have been compared to demonstrate the effects of uncertainties in the parameters in the model. The effect which reductions of the uncertainties have on the predictions of chloride ingress and service life predictions is also shown.

In this chapter, the input data used in the predictions of chloride ingress are presented first, with the data giving the influence of concrete composition and exposure conditions presented separately. Then the model and the quantified parameters are calibrated against measured chloride ingress data. After that some general deterministic predictions of chloride ingress are made to demonstrate the effects of surface chloride and temperature conditions. Deterministic predictions of chloride ingress in field conditions are then made and the results are discussed and analysed. After that probabilistic predictions of chloride

ingress are made and discussed, to demonstrate the effects of uncertainties in the parameters in the model. Finally conclusions are drawn based on the results and analyses.

## 7.2 Input data – Concrete compositions

### 7.2.1 General

Two different concrete compositions have been chosen to illustrate the effects of the exposure conditions on the chloride ingress:

- I. Swedish SRPC-concrete (CEM I 42.5 BV/SR/LA), w/b=0.40.
- I. Swedish SRPC-concrete (CEM I 42.5 BV/SR/LA), w/b=0.50.

In marine submerged conditions chloride ingress into **both concrete I and II** has been predicted. In the other environments predictions have only been made for **concrete I**.

### 7.2.2 Potential diffusion coefficient ( $D_0$ ) and curing parameter ( $k_c$ )

Data on the parameters which give the influence of concrete composition and workmanship during construction are presented in tables 7.1a ( $D_0$ ) and 7.1b ( $k_c$ ). The data in table 7.1b are based on the data presented in figure 6.3b. Each parameter is described with a mean value,  $\mu$ , a standard deviation, SD, and the type of statistical distribution. For  $D_0$  the reference time,  $t_0$ , i.e. the time after casting at which  $D_0$  is measured, is also specified. Data on the age factor,  $n$ , are given in the section where the influence of the exposure conditions is presented.

Table 7.1a: Data on  $D_0$ . Based on data from Tang (1997).

Concrete	$\mu - D_0$ [ $\times 10^{-12} \text{ m}^2/\text{s}$ ]	SD - $D_0$ [ $\times 10^{-13} \text{ m}^2/\text{s}$ ]	$t_0$ [days]	Statistical distribution
I. (CEM I 42.5 BV/SR/LA)	12.2	12.2 <sup>+</sup>	180	ND (12.2, 1.22)
II. (CEM I 42.5 BV/SR/LA)	19.9	19.9 <sup>+</sup>	180	ND (19.9, 1.99)

ND : Normal distribution.

+ : Coefficient of variation assumed to be 10%, according to Gehlen (2000).

Table 7.1b: Data on  $k_c$ . Based on data from DuraCrete (2000a).

Curing time [days]	$\mu - k_c$ [-]	SD - $k_c$ [-]	Statistical distribution
1	2.400	0.700	Beta (1.667, 1.905, 1.00, 4.00) $1.00 \leq k_c \leq 4.00$
3	1.500	0.300	Beta (2.148, 10.741, 1.00, 4.00) $1.00 \leq k_c \leq 4.00$
7	1	-	Det. (1)
28	0.793	0.102	Beta (4.445, 2.333, 0.40, 1.00) $0.40 \leq k_c \leq 1.00$

Beta : Beta distribution.

In the predictions it is assumed that the concrete has been cured for 7 days, i.e.  $k_c=1$ .

### 7.2.3 Chloride threshold level ( $C_{crit}$ )

The chloride threshold level,  $C_{crit}$ , i.e. the chloride content at the reinforcement at which reinforcement corrosion is initiated, is a decisive parameter for the service life of reinforced concrete structures. Normally reinforcement in concrete is in a passive state, due to the high alkalinity and lack of chlorides and other aggressive ions in the pore

solution of the concrete. The passive state is maintained until the pH in the concrete at the reinforcement is lowered, e.g. due to carbonation or leaching, or a sufficiently high concentration of water-soluble aggressive ions, e.g. chlorides, has reached the reinforcement, and corrosion is initiated. This sufficiently high concentration of aggressive ions is defined as the “threshold level”.

In concrete  $C_{crit}$  is not a single value, but varies greatly depending on the concrete and steel properties and exposure conditions. There are two general definitions of  $C_{crit}$ , Nilsson et al (1996): (i) The minimum chloride content at the reinforcement, which results in pitting corrosion of the reinforcement, and (ii) The chloride threshold level at the reinforcement at a specific time, when damage to the concrete starts. The first definition corresponds to the boundary between initiation and propagation in figure 2.1, while the second definition corresponds to a less well-defined point in the propagation period in figure 2.1. In this thesis the first definition of  $C_{crit}$  has been used.

In the literature  $C_{crit}$  has been found to vary between 0.097-3.04 [% by weight Cl/binder], according to a survey presented in Alonso et al (2000). There are many factors that influence  $C_{crit}$ , e.g. concrete properties, carbonation, moisture and temperature conditions in the concrete, cracks, cast in chlorides, cover thickness, exposure time etc. However, the effects of these parameters on  $C_{crit}$  have not been studied in this thesis. Instead data on  $C_{crit}$  has been taken from Nilsson et al (1997), DuraCrete (2000a) and Gehlen (2000). Based on these references the following levels of  $C_{crit}$  have been chosen for use in the service life predictions (the standard deviation, SD, is also stated):

- **Marine submerged zone.**  $C_{crit}=2.00$  [% by weight Cl<sup>18</sup>/binder] (SD=0.15).
- **Marine tidal, splash and atmospheric zones.**  $C_{crit}=0.60$  [% by weight Cl/binder] (SD=0.15).
- **Road conditions.**  $C_{crit}=0.60$  [% by weight Cl/binder] (SD=0.15).

## 7.3 Input data – Exposure conditions

### 7.3.1 General

In the following section the results of the quantification of the environmental parameters in the DuraCrete chloride ingress model are presented. However, some assumptions have been made to facilitate the description of the exposure conditions. For surfaces below the water level the concrete is assumed saturated (RH=100%) and the temperature is assumed equal to the temperature of the seawater. For surfaces above the water surface the moisture and temperature conditions have been expressed as equivalent surface humidity and temperature conditions and TOW<sup>19</sup>. The equivalent surface temperature has been determined with eq. (3.1) and the equivalent surface humidity has been determined with eq. (3.3). Since heat transport is rapid in concrete, the calculated equivalent surface temperatures have been assumed equal to the temperature in the concrete. The equivalent surface temperature and humidity have been determined for four different intensities of solar radiation,  $I_{solar}$ : 50 W/m<sup>2</sup>, 100 W/m<sup>2</sup>, 200 W/m<sup>2</sup> and 300 W/m<sup>2</sup>, and three different equivalent sky temperatures,  $T_{sky}$ : -5.0°C, -10.0°C and -15.0°C, have been studied. The intensity of solar radiation and sky temperature mainly reflect the degree of cloudiness but also the effects of for example surface orientation and shielding by obstacles. The

<sup>18</sup> Expressed as the total chloride content in the concrete.

<sup>19</sup> TOW – Time Of Wetness, i.e. the time during which a surface is wet, e.g. due to rain, surface condensation etc.

solar radiation intensity decreases and the sky temperature increases with increasing degree of cloudiness. Calculated equivalent surface humidity and temperature conditions are presented in the appendix.

The quantifications of the environmental parameters have been made according to the procedure described in chapter 6.

### 7.3.2 General (marine conditions)

Nine different locations have been chosen to illustrate how different marine exposure conditions influence the chloride ingress into concrete. The following locations have been chosen (the following is stated for each location: sea, the meteorological station where data have been taken and country):

1. The Mediterranean. Meteorological data from Marseille (France).
2. The Baltic Sea. Meteorological data from Kalmar (Sweden).
3. Öresund. Meteorological data from Copenhagen (Denmark).
4. Kattegat. Meteorological data from Göteborg (Sweden).
5. North Sea. Meteorological data from Den Helder (Netherlands).
6. Norwegian Fjord. Meteorological data from Narvik (Norway).
7. Atlantic Ocean around Iceland. Meteorological data from Reykjavik (Iceland).
8. Atlantic Ocean outside Iberian Peninsula. Meteorological data from Lisbon (Portugal).
9. Persian Gulf. Meteorological data from Bandas Abbas (Iran).

Service life predictions have been made in the marine submerged, tidal, splash, atmospheric and distant atmospheric conditions. The chloride ingress has been predicted for **all locations** in the submerged zone. However, in the tidal, splash and atmospheric zones, the chloride ingress has only been predicted for **locations 1 and 4**. The following exposure conditions have been treated in the predictions:

- **Submerged zone (MSZ)**. Exposed to seawater 100% of the total exposure time.
- **Tidal zone (MTZ)**, at the mean water level, i.e. the surface is exposed to seawater approximately 12 hours per day.
- **Splash zone (MSZ)**. Exposed to splash from waves. The extent of splash from breaking waves is 1.0 m above the highest tide level.
- **Atmospheric zone (MAZ)**. 1.0 m above the highest level of the splash zone. The atmospheric zone is above the highest level for the splash zone.
- **Distant atmospheric zone (MDAZ)**. 500 m from the shoreline.

The exposure conditions for these nine locations, in terms of monthly mean temperature and RH in the air, precipitation (amount and days of precipitation) and chloride content and temperature of seawater, are presented in table 7.2. The yearly variations in the exposure conditions are presented in the appendix.

Table 7.2: Exposure conditions in terms of yearly mean temperature and RH in the air (determined from monthly mean values), precipitation (yearly amount and days of precipitation) and chloride concentration and temperature of seawater. Based on data from DMI (1994) and the Levitus seasonal database.

Location	$T_{\text{air}}$	$RH_{\text{air}}$	Precipitation		Seawater		
	[°C]	[%]	Amount [mm]	Days	Temp. [°C]	Cl-conc. [g/l]	Tide [m]
1.	14.3	71.0	546	80	16.0	22.0	0.0
2.	7.3	77.8	471	140	8.8	3.6	0.0
3.	8.6	79.0	600	171	9.5	4.8	0.0
4.	7.8	77.4	670	163	10.0	10.1	0.0
5.	9.7	77.3	706	207	11.0	18.3	±2.5
6.	3.8	76.3	852	197	7.5	17.2	±2.0
7.	5.0	81.8	779	213	7.3	19.5	±2.0
8.	16.6	70.0	708	113	16.5	21.0	±0.5
9.	26.9	62.6	118	7	26.8	23.0	±1.0

### 7.3.3 Quantification of parameters in the DuraCrete-model (marine conditions)

#### General

Data on the parameters which give the influence of the exposure conditions are presented separately for each exposure zone, except for the age factor. In table 7.3 data on the age factor,  $n$ , are presented for concrete exposed in different marine exposure conditions.

Table 7.3: Data on  $n$  for different marine exposure conditions. Based on data from DuraCrete (2000a) and Gehlen (2000).

Binder	Exp. cond.	$\mu - n$ [-]	SD - $n$ [-]	Statistical distribution
Cem I	MSZ	0.30	0.12	Beta (4.075, 9.508, 0, 1)
Cem I	MTZ + MSZ	0.37	0.12	Beta (5.619, 9.568, 0, 1)
Cem I	MAZ + MDAZ	0.65	0.12	Beta (9.619, 9.568, 0, 1)

In the following sections the results of the quantifications of  $C_{\text{SN}}$ , (described by  $C_{\text{SN,eq}}$ , and the parameters  $k_{\text{C,d}}$ ,  $k_{\text{C,h}}$  and  $k_{\text{C,o}}$ ) and  $k_e$  (described by the parameters  $k_{\text{D,RH}}$  and  $k_{\text{D,T}}$ ) are presented. The quantifications have been made according to the procedures described in chapter 6. Examples of the moisture conditions in the concrete are given in figures 3.13a (RH) and 3.13b ( $S_{\text{cap}}$ ).

#### Marine submerged zone

The results of the quantification of  $C_{\text{SN}}$  and  $k_{\text{D,e}}$  in marine submerged conditions are presented in table 7.4. The surface chloride and temperature conditions have been assumed equal to the conditions in the seawater (yearly mean values). The data in table 7.4 are valid for both concretes I ( $w/b=0.40$ ) and II ( $w/b=0.50$ ).

Table 7.4: Results of quantification of  $C_{SN}$  and  $k_{D,e}$  for exposure in marine submerged conditions. Valid for concrete I and II.

Location	$k_{D,RH}$ [-]	$k_{D,T}$ [-]	$k_{D,e}$ [-]	$C_{SN}$ (concrete composition) [% by wt Cl/binder]	
				w/b=0.40 (concrete I)	w/b=0.50 (concrete II)
1.	1.00	0.84	0.84	1.98	2.47
2.	1.00	0.61	0.61	2.01	2.51
3.	1.00	0.63	0.63	1.95	2.44
4.	1.00	0.64	0.64	2.21	2.76
5.	1.00	0.67	0.67	2.40	3.00
6.	1.00	0.57	0.57	2.77	3.46
7.	1.00	0.56	0.56	2.79	3.49
8.	1.00	0.86	0.86	1.94	2.42
9.	1.00	1.33	1.33	1.33	1.66

#### Marine tidal, splash and atmospheric zones

The results of the quantifications of  $C_{SN}$  and  $k_{D,e}$  (for four different equivalent surface humidities and temperatures) in the marine tidal splash, atmospheric and distant atmospheric conditions are presented in tables 7.5a and 7.5b. The data in tables 7.5a and 7.5b are valid for concrete I (w/b=0.40).

The temperature in the concrete has been assumed equal to the surface temperature conditions. The equivalent surface temperature conditions have been determined for the following solar radiations and sky temperatures:  $T_{air}$  (case I),  $T_{sea}$  (case II),  $I_{solar}=50 \text{ W/m}^2$   $T_{sky}=-15.0^\circ\text{C}$  (case III) and  $I_{solar}=300 \text{ W/m}^2$   $T_{sky}=-5.0^\circ\text{C}$  (case IV). Calculated equivalent surface temperatures and humidities are presented in the appendix. The results of the quantification of the environmental parameters for more equivalent surface temperatures are also presented in the appendix.

$C_{SN}$  has been quantified according to eq. (6.1a), where  $C_{SN,eq}$  has been determined from the results presented in figure 6.1a and the parameters  $k_{C,conc}$  and  $k_{C,test}$  have been put equal to 1.0. The parameter  $k_{C,e}$  has been determined according to eq. (6.1b), where the parameters  $k_{C,d}$ ,  $k_{C,h}$  and  $k_{C,o}$  have been determined according to the procedure described in section 6.3.

Table 7.5a: Results of quantification of  $C_{SN}$  for exposure in tidal, splash and atmospheric conditions. Valid for concrete I. [% by weight Cl/binder]

Loc	T	Sp	A	DA
1.	1.98 (1.00)	1.58 (0.80)	1.38 (0.70)	0.48 (0.25)
4.	2.21 (1.00)	1.77 (0.80)	1.55 (0.70)	0.55 (0.25)

The values within brackets in table 7.5a are the products of the parameter  $k_{C,h}$  and the parameter  $k_{C,d}$ . The parameter  $k_{C,d}$  is equal to 1.0 for all exposure zones except for the distant atmospheric zone where  $k_{C,d}$  is equal to 0.35, according to figure 6.7.

The parameter  $k_{D,e}$  has been determined according to eq. (6.1b), where the parameter  $k_{D,T}$  has been quantified from the equivalent surface temperature, according to eq. (6.3).

However, since the moisture conditions above the water surface are uncertain it has been decided, based on the data presented in figures 3.13a and 6.6, to use the following values of  $k_{D,RH}$ : **0.90** in the **tidal (T)** and **0.40** in the **splash (Sp)**, **atmospheric (A)** and **distant atmospheric (DA)** zones.

Table 7.5b: Results of quantification of  $k_{D,e}$  for exposure in tidal, splash and atmospheric zones. [-]

Case	Location		1.		4.	
	$I_{solar}$	$T_{sky}$	T	Sp + A + DA	T	Sp + A + DA
I		$T_{air}$	0.70	0.31	0.52	0.23
II		$T_{sea}$	0.76	0.34	0.58	0.26
III	50 W/m <sup>2</sup>	-15.0°C	0.59	0.26	0.46	0.21
IV	300 W/m <sup>2</sup>	-5.0°C	0.88	0.39	0.70	0.31

In table 7.5b the parameter  $k_{D,e}$  has been determined as the product of the parameters  $k_{D,RH}$  and  $k_{D,T}$ , cf. eq. (6.1b). The parameter  $k_{D,T}$  gives the influence of the temperature of the concrete, which has been assumed equal to the (equivalent) surface temperature (for all surfaces). This means that for example for case III at location 1 the equivalent surface temperature is equal to 10.4, which gives  $k_{D,T}=0.65$ . Since  $k_{D,RH}$  is equal to 0.90 (T) and 0.40 (Sp+A+DA) this means that  $k_{D,e}$  is equal to 0.59 (T) and 0.26 (Sp+A+DA).

### 7.3.4 General (road conditions)

Two different locations have been chosen to illustrate how different road exposure conditions influence the chloride ingress into concrete. For each of these locations the exposure conditions are described in terms of temperature and RH in the air, precipitation (amounts and days of precipitation) and amount of de-icing salt spread on roads, see table 7.6. The yearly variations in the exposure conditions are presented in the appendix.

Table 7.6: Exposure conditions in terms of yearly mean temperature and RH in the air (determined from monthly mean values), precipitation (yearly amount and days of precipitation) and amount of de-icing salt spread on the road. Based on data from DMI (1994), Nilsson (2000) and Golwer (1991).

Location	$T_{air}$	$RH_{air}$	Precipitation		De-icing salt		
	[°C]	[%]	Amount [mm]	Days	Occasions #	Spread [g/m <sup>2</sup> ]	Total [kg/m <sup>2</sup> ]
1. Göteborg	7.8	77.4	670	163	200*	10*	2.0
2. Munich	8.3	78.6	951	180	380*	10*	3.8

♣ : Based on data from section 3.5.

\* : Assumed amount of de-icing salt spread on each spreading occasion.

The severity of exposure to chlorides is dependent on the distance to and height above the road. Three different distances from the road have been considered, viz. **3.0 m** (dry and wet splash zones), **7.0 m** and **12.0 m** (distant road atmosphere), and two speed limits, viz. **50 km/h** and **100 km/h**. Furthermore two different heights above the road have been considered, viz. **0.0 m** and **2.0 m**. A difference is also made between roads depending on the **traffic intensity (high and low)**.

### 7.3.5 Quantification of parameters in DuraCrete-model (road conditions)

#### General

Data on the parameters which give the influence of the exposure conditions are presented separately for each exposure environment, except for the age factor. In table 7.7 data on the age factor,  $n$ , in different marine exposure conditions are presented.

Table 7.7: Data on  $n$  for exposure in road conditions. Based on data from DuraCrete (2000a) and Gehlen (2000)

Binder	Exp. cond.	$\mu - n$ [-]	SD - $n$ [-]	Statistical distribution
Cem I	Road	0.30	0.12	Beta (4.075, 9.508, 0, 1)

The results of the quantifications of  $C_{SN}$  and  $k_{D,e}$  (for four different equivalent surface humidities and temperatures) are presented in tables 7.8a and 7.8b. The temperature in the concrete has been assumed equal to the surface temperatures and examples of the moisture conditions in the concrete are shown in figures 3.24a (RH) and 3.24b ( $S_{cap}$ ). The equivalent surface temperature conditions have been determined for the following solar radiations and sky temperatures:  $T_{air}$  (**case I**),  $I_{solar}=50 \text{ W/m}^2$   $T_{sky}=-15.0^\circ\text{C}$  (**case II**),  $I_{solar}=200 \text{ W/m}^2$   $T_{sky}=-10.0^\circ\text{C}$  (**case III**) and  $I_{solar}=300 \text{ W/m}^2$   $T_{sky}=-5.0^\circ\text{C}$  (**case IV**). The results of the quantification of  $k_{D,e}$  for more equivalent surface temperatures are presented in the appendix.

$C_{SN}$  has been quantified according to eq. (6.1a), where  $C_{SN,eq}$  has been determined from the results presented in figure 6.1b and the parameters  $k_{C,conc}$  and  $k_{C,test}$  are equal to 1.0. The parameter  $k_{D,e}$  has been determined according to eq. (6.1b), where the parameters  $k_{C,d}$ ,  $k_{C,h}$  and  $k_{C,o}$  have been determined according to the procedure described in section 6.4. The data on  $C_{SN}$  presented in table 7.8a are valid for **vertical** surfaces facing **towards** the traffic, i.e.  $k_{C,o}=1.0$ . For vertical surfaces facing away from or parallel to the traffic  $k_{C,o}=0.5-1.0$ , according to what has been described in section 6.4.4, and for horizontal surfaces  $k_{C,o}=0.7$ , as discussed in section 7.4.2. Furthermore  $C_{SN,eq}$  has, as discussed in section 6.2.2, been linearly correlated to the amount of de-icing salt spread on the roads. Since the amount of de-icing salt spread in Munich is 1.9 times as large as in Göteborg, cf. table 7.6,  $C_{SN,eq}$  in Munich should also be 1.9 times as large as in Göteborg. It should be noticed that some of the quantified  $C_{SN,eq}$  are so low that no risk of reinforcement corrosion exists – these values are marked in *italics*. No predictions of the chloride ingress have been made for these cases. The values of  $C_{SN,eq}$  are valid for concrete I (CEM I 42.5 BV/SR/LA w/b=0.40).



Table 7.8a: Results of quantification of  $C_{SN}$  for exposure in road conditions in Göteborg (surfaces facing towards the traffic). [% by weight Cl/binder]

Loc.	$C_{SN,eq}$	Height=0.0 m			Height=2.0 m		
(Dist.) [m]		50 km/h	100 km/h traffic intensity		50 km/h	100 km/h traffic intensity	
			Low	High		Low	High
1. (3.0)	2.20	1.36	1.74	2.20	0.82	1.04	1.32
1. (7.0)	2.20	0.53	0.66	2.20	0.32	0.40	1.32
1. (12.0)	2.20	0.22	0.22	1.43	0.13	0.13	0.86

The values within brackets in table 7.8a denote the horizontal distance to the road.

The parameter  $k_{D,e}$  has been determined from  $k_{D,RH}$  and  $k_{D,T}$ , according to eq. (6.1b), and the parameter  $k_{D,T}$  has been quantified from the equivalent surface temperature, according to eq. (6.3). From the results presented in figure 3.24a, the parameter  $k_{D,RH}$  has been estimated to **0.4** in the **dry splash zone (DSZ)** and **0.6** in the **wet splash zone (WSZ)** and **distant road atmosphere (DRA)**.

Table 7.8b: Results of quantification of  $k_{D,e}$  for exposure in road conditions. [-].

Case	Location:		1		2	
	$I_{solar}$	$T_{sky}$	DSZ	WSZ + DRA	DSZ	WSZ + DRA
I		$T_{air}$	0.23	0.34	0.24	0.36
II	50 W/m <sup>2</sup>	-15.0°C	0.21	0.31	0.21	0.31
III	200 W/m <sup>2</sup>	-10.0°C	0.26	0.39	0.27	0.40
IV	300 W/m <sup>2</sup>	-5.0°C	0.31	0.47	0.32	0.47

## 7.4 Predictions of chloride ingress – general

In this section predictions of chloride ingress are presented. The profiles have been predicted with the modified DuraCrete chloride ingress model, cf. eq. (2.1a) and (2.1b), and the data presented in sections 7.2 and 7.3. First the model with the quantified parameters is calibrated with measured chloride ingress data. Then the effects which the chloride concentration and the temperature of the exposure solution have on the chloride ingress are demonstrated and discussed. Furthermore the level of the chloride threshold level,  $C_{crit}$ , and its influencing factors are discussed.

### 7.4.1 Calibration of the model (marine conditions)

The model and the quantified parameters have been verified by comparing predicted chloride ingress profiles for marine submerged conditions with measured profiles presented by Tang (2003). The profiles presented by Tang (2003) have been measured in concrete slabs with a thickness of 100 mm after 10.3 years of exposure in Träslövsläge (location 4). In figure 7.1 the predicted profiles (unfilled symbols), with an exposure time of 10.3 years, are presented together with the measured profiles (filled symbols). The profiles with index 1-402, with  $w/b=0.40$ , have been exposed in marine submerged conditions. The profiles with index 1-402 Su and 1-402 Su(B) have been measured in the same slab but from different sides.

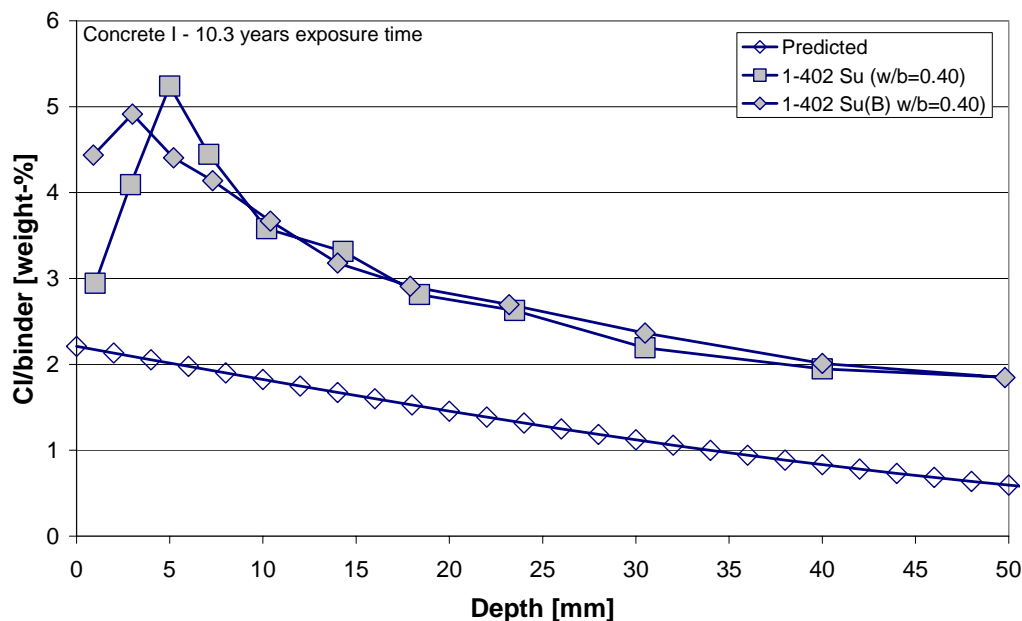


Figure 7.1a: Comparison of predicted and measured chloride ingress profiles after 10.3 years of exposure in Träslövsläge. Measured profiles based on data from Tang (2003).

As seen in figure 7.1a the predicted and measured chloride ingress profiles do not agree at all, the predicted profile is far below the measured profiles. However, the chloride ingress has been measured in slabs that are 100 mm thick and in which chlorides penetrating from both sides have met in the middle of the slab. This can be observed in the measured profiles as a flat plateau in the middle of each profile and therefore the inner part of the profiles cannot be considered representative. Furthermore this means that the DuraCrete model cannot be used to predict the chloride ingress, since this model is derived for diffusion in a semi-infinite medium, i.e. the chloride content is equal to 0.0 at large

depths. Instead it is proposed to use a model that describes diffusion in a finite medium, described by Crank (1975), cf. eq. (7.1).

$$U(x/L, F_0) = \frac{C(x, F_0) - C_0}{C_1 - C_0} = 1 - \frac{4}{\pi} \sum_{n=0}^{\infty} \frac{-1^n}{2n+1} \cdot \exp\left(- (2n+1)^2 \cdot \frac{\pi^2 \cdot F_0}{4}\right) \cdot \cos\left(\frac{(2n+1)\pi}{2} \cdot \frac{x}{L}\right) \quad [-] \quad (7.1)$$

where:

x: depth. [m]

L: half the thickness of the medium. [m]

$F_0$ :  $F_0 = \frac{D_a \cdot t}{L^2} \cdot [-]$

$C_0$ : initial chloride content in concrete. [% by wt Cl/binder]

$C_1$ : surface chloride content. [% by wt Cl/binder]

t: exposure time. [s]

The large difference between the predicted and measured profiles is the level of the chloride content, mainly close to the surface, while the shapes of the profiles are fairly similar. This indicates that the surface chloride content,  $C_{SN}=2.21$  [% by weight Cl/binder] used in the predictions, is too low. Therefore chloride ingress profiles have also been predicted for higher values of  $C_{SN}$ . The predictions have been made with eq (7.1), where  $L=0.05$  [m],  $C_0=0.0$  [% by wt Cl/binder] and  $t=10.3$  [years]. Since the model proposed in eq. (7.1) does not consider the time – dependence in  $D_a$  a constant value of  $D_a=3.10 \cdot 10^{-12}$  [m<sup>2</sup>/s] has been used in the predictions. The predicted profiles are plotted in figure 7.1b, together with the measured profiles presented by Tang (2003).

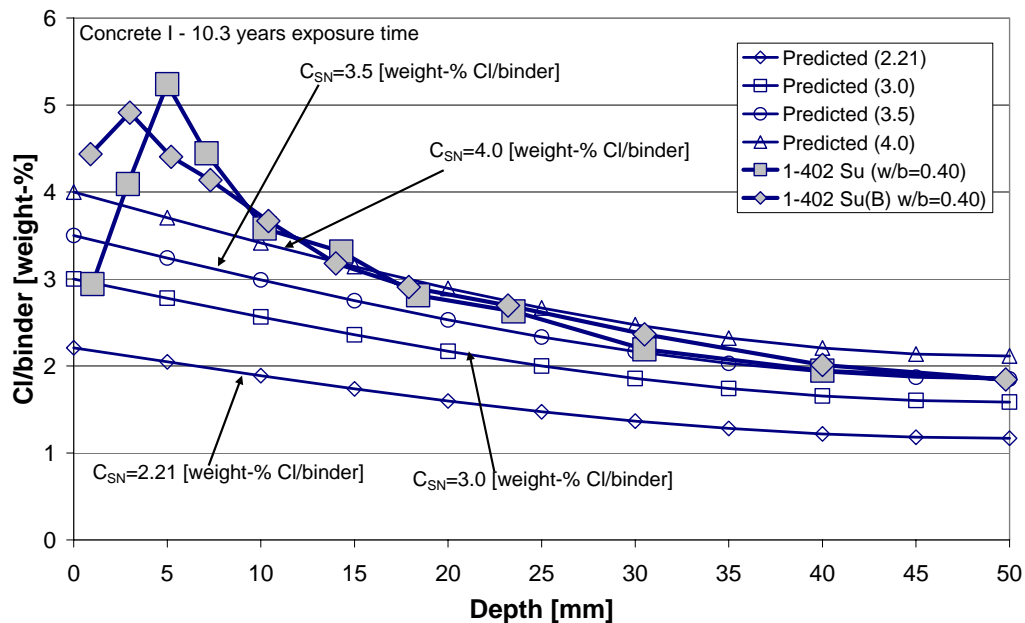


Figure 7.1b: Comparison between predicted and measured chloride ingress profiles after 10.3 years of exposure in Träslövsläge. Measured profiles based on data from Tang (2003).

From figure 7.1b it can be observed that the profiles predicted with higher values of  $C_{SN}$  better agree with the measured profiles, where a more realistic  $C_{SN}$  seems to be approximately 3.5 [% by wt Cl/binder]. It is also more realistic to use the model in eq. (7.1), at least for larger depths, since this model better describes the overlapping of chloride ingress from two sides of the slab. However,  $C_{sa}$  used in the model seems to be too low, alternatively the value of  $D_a$  used is too high (together with the fact that the time dependence of  $D_a$  is not considered), which has the result that the predicted surface chloride contents are significantly lower than the measured chloride contents at the surface.

Since  $C_{SN}$  have been quantified to 2.21 [% by wt Cl/binder] after 1 year of exposure this indicates that  $C_{SN}$  increases with increasing exposure time. Therefore it should be more realistic to model  $C_{SN}$  as a parameter that increases with increasing exposure time. However, in the DuraCrete chloride ingress model  $C_{SN}$  is modelled as a constant over time and therefore it has been decided to use the originally quantified  $C_{SN}$ , according to table 7.4, in the following predictions of chloride ingress.

The predictions made in the marine tidal, splash, distant atmospheric conditions have not been verified. There are some data available from the marine atmospheric zone, presented by Tang (2003), that could be used for verification of the model. However, these data come from a very limited atmospheric zone, with an extension of only some 20 cm, which cannot be considered representative of marine atmospheric conditions. Therefore the model has not been verified in marine atmospheric conditions.

#### 7.4.2 Calibration of model (road conditions)

The model and the quantified parameters have been verified by comparing predicted chloride ingress profiles with measured profiles from the field study of seven bridges around Göteborg. However, it is difficult to directly compare measured and predicted profiles, since the exposure conditions are unique for each bridge, which means that the general definition of the road conditions should therefore represent a worst case valid for several bridges. Consequently the measured profiles in most cases should be lower than the predicted profiles.

Chloride ingress profiles for columns (dry splash zone – DSZ) have been compared with profiles measured in columns on bridge O 951, which was 27 years old at the time of inspection. Chloride ingress profiles have been predicted for surfaces at 3.0 m distance from the traffic, at 0.0 m and 2.0 m height and facing towards the traffic (high traffic intensity and speed=100 km/h). In figure 7.2a predicted (filled symbols) and measured (unfilled symbols) profiles are presented. The profiles with index TT and FT are predicted for surfaces facing towards and away from the traffic respectively. Furthermore the profiles with index UFM/ÖFM and UMG/ÖMG have been measured in surfaces facing towards and away from the traffic respectively. The heights above the road are given within brackets.

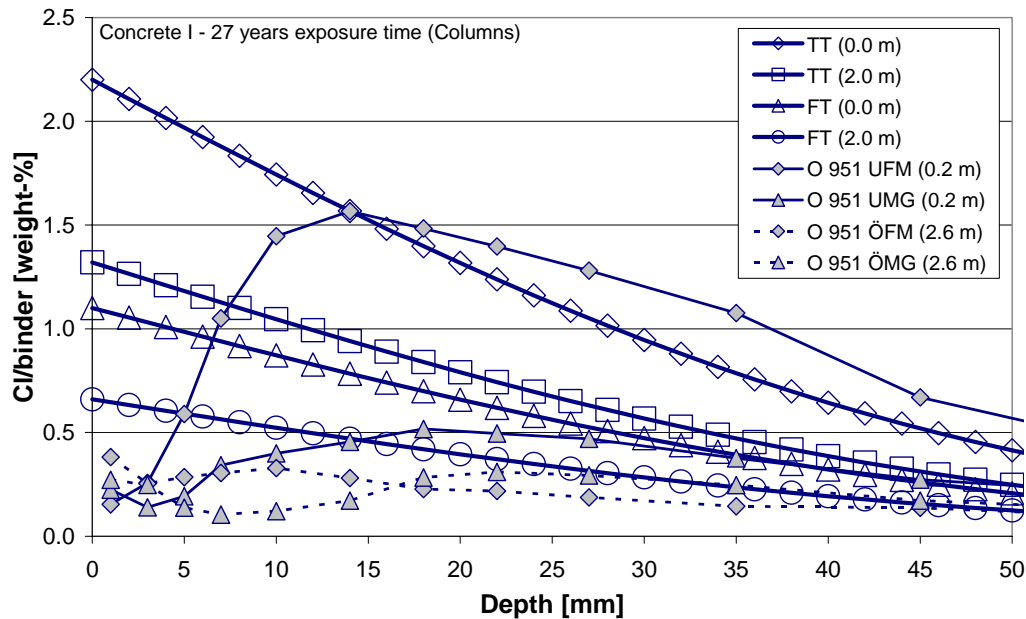


Figure 7.2a: Comparison of predicted and measured chloride ingress profiles in columns after 27 years of exposure on bridge O 951

From figure 7.2a it can be seen that the predicted and measured profiles correlate fairly well. All measured profiles are below the predicted profiles, except the measured profile with index O 951 UFM. However, the difference between this profile and the predicted profile with index TT (0.0 m) is within the observed uncertainty for measured profiles (COV=10-40%). This means that the model and the quantified parameters predict realistic chloride ingress profiles for columns. Therefore it has been decided to use the originally quantified parameters, according to tables 7.7, 7.8a and 7.8b, in the following predictions of chloride ingress in the dry splash zone.

Predicted chloride ingress profiles for side beams (wet splash zone – WSZ) have been compared with profiles measured in columns on bridge O 670 and O 762, which were 30 and 24 years old respectively at the time of inspection. The exposure time in the predictions has been set to 30 years. The predicted profile has been predicted for surfaces at 3.0 m distance from the traffic with high traffic intensity and speed=100 km/h.

In figure 7.2b predicted (filled symbols) and measured (unfilled symbols) profiles are presented. Information about the distance to the traffic is given with brackets in the index for each profile together with information about the exposure time. The numbers 0.7 and 1.0 in the index denote the value of the parameter  $k_{C,o}$ , which is further discussed later. The originally predicted profile is the profile with index **TT (3.0 m) 30y - 1.0**.

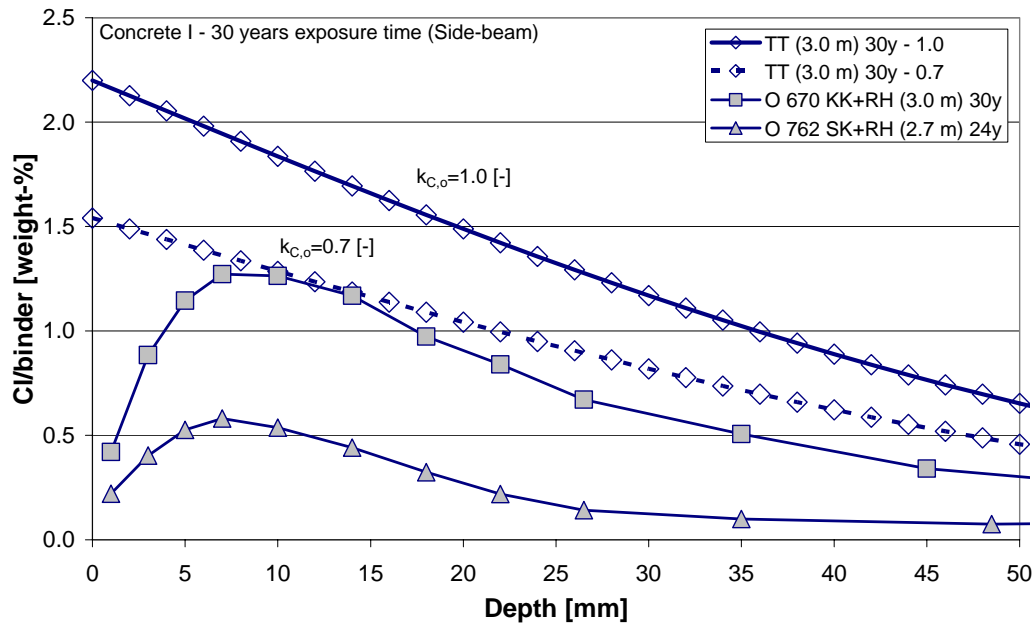


Figure 7.2b: Comparison of predicted (30 years' exposure time) and measured chloride ingress profiles in side beams on bridges O 670 (30 years' exposure time) and O 762 (24 years' exposure time).

In figure 7.2b it can be observed that the measured chloride ingress profiles from side beams on bridges O 670 and O 762 are below the originally predicted chloride ingress profile ( $k_{C,o}=1.0$ ). However, the shape of the measured and predicted profiles is fairly similar. Additionally the predicted chloride penetration depth seems too high. Therefore a reasonable explanation for the difference between the measured and predicted profiles would seem to be that the originally quantified  $C_{SN}$  used in the predictions has been too high.

An evaluation of the measured profiles with the error function solution to Fick's second law has resulted in  $C_{SN}=1.53$  and  $0.70$  [% by weight Cl/binder] for profiles O 670 KK+RH and O 762 SK+RH respectively. The quotients between  $C_{SN}$  for the measured and predicted profiles are thus: **0.70** (O 670 KK+RH) and **0.32** (O 762 SK+RH). Based on this it has been decided to reduce  $C_{SN}$  in predictions by putting the orientation parameter equal to 0.7, i.e.  **$k_{C,o}=0.7$** . To illustrate the effect of  $k_{C,o}=0.7$  a profile predicted with this  $k_{C,o}$  has been added to figure 7.2b. As seen in figure 7.2b this predicted profile corresponds better with the measured profiles from side beams and therefore it has been decided to use  $k_{C,o}=0.7$ , together with the data in tables 7.7, 7.8a and 7.8b, in the predictions of chloride ingress in the wet splash zone and distant road atmosphere.

## 7.5 Predictions of chloride ingress – field conditions

In this section predictions of chloride ingress in field conditions are presented. The service life is defined as at an end when reinforcement corrosion has been initiated, i.e. when the chloride content at the reinforcement is equal to or has exceeded the chloride threshold level,  $C_{crit}$ . Trend lines showing the chloride threshold level have been added to the figures showing the predicted chloride ingress profiles.

In this section only the results of the predictions are presented. The discussions and analyses of the results are made in section 7.6.

### 7.5.1 Marine submerged zone (MSZ)

Predictions of chloride ingress into concrete exposed in the marine submerged zone have been made for both **concretes I and II** (CEM I 42.5 BV/SR/LA w/b=0.40 and 0.50) and for **all exposure locations**. Chloride ingress profiles have been predicted for an exposure time of 100 years. In figures 7.3 and 7.4 the predicted chloride ingress profiles are presented. The chloride threshold level,  $C_{crit}=2.00$  [% by weight Cl/binder], has also been added to the figures.

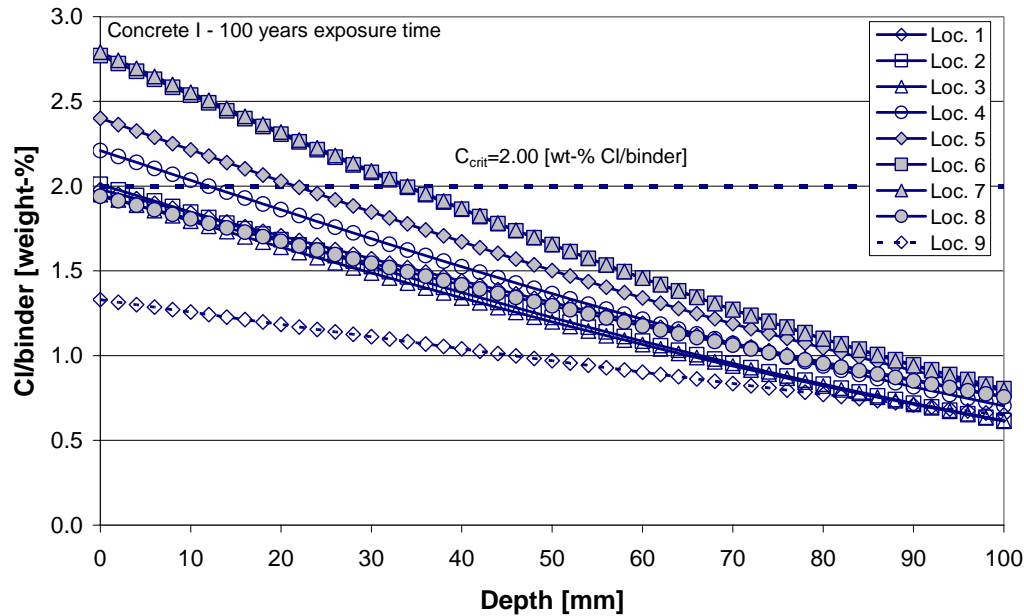


Figure 7.3: Predicted chloride ingress profiles for concrete I for all locations. 100 years' exposure time in submerged conditions.

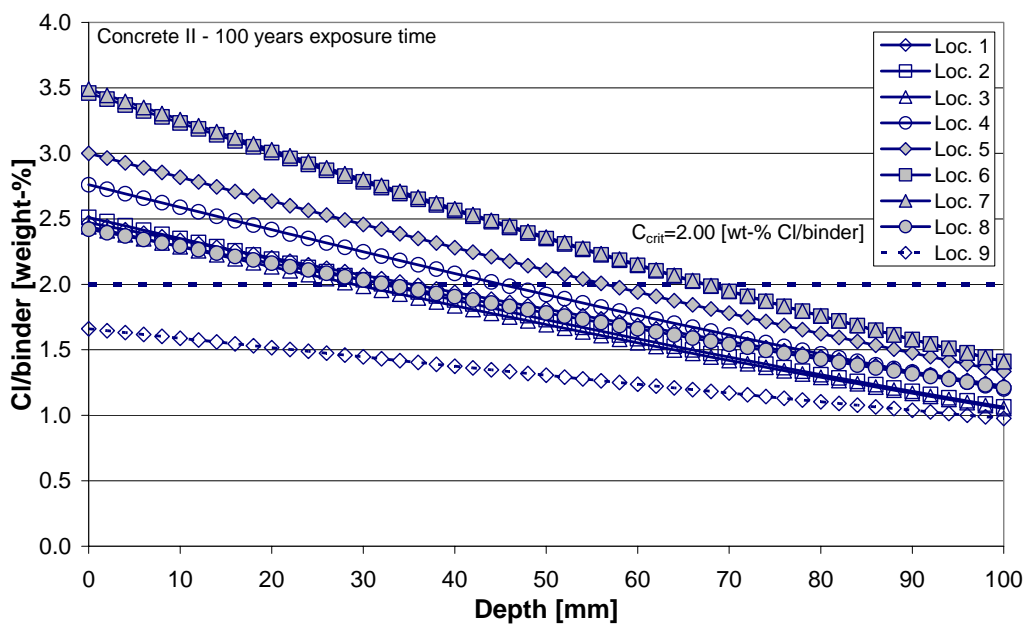


Figure 7.4: Predicted chloride ingress profiles for concrete II for all locations. 100 years' exposure time in submerged conditions.

### 7.5.2 Marine tidal, splash and atmospheric zones

Predictions of chloride ingress into concrete exposed in marine tidal, splash and atmospheric zones have only been made for **concrete I** and for **location 4 (Kattegat)**. Chloride ingress profiles have been predicted for an exposure time of 100 years and for four different surface temperature conditions, cf. table 7.5b. The different cases are indexed with roman numbers in the figures showing the predicted chloride ingress profiles. The profiles are shown in figure 7.5 for **cases III** and **IV** for exposure in splash (Sp), atmospheric (A) and distant atmospheric (DA – 500 m from coastline) conditions. The reason that only these cases are shown is that they represent the minimum and maximum chloride ingress respectively in each exposure zone. However, for tidal conditions (T) profiles for all cases are shown.

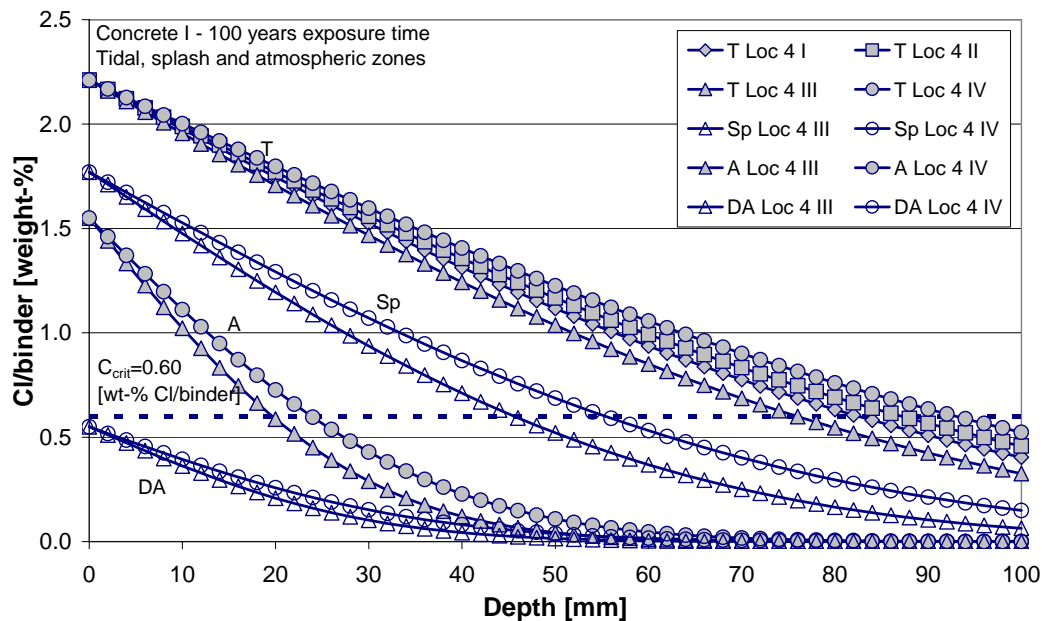


Figure 7.5: Predicted chloride ingress profiles for location 4 (Kattegat). 100 years' exposure time in tidal, splash, atmospheric and distant atmospheric conditions.

### 7.5.3 Road conditions – general

Predictions of chloride ingress into concrete exposed in road conditions have only been made for **concrete I**, for two heights above the road, viz. 0.0 m and 2.0 m and at three different distances from the road, viz. **3.0 m (DSZ and WSZ)**, **7.0 m** and **12.0 m (DRA)**. All profiles have been predicted for an exposure time of 50 years. The profiles from Göteborg and Munich are denoted “Loc 1” and “Loc 2” respectively.

The predictions in the **dry splash zone (DSZ)** have been made for surfaces facing **towards the traffic** for heights of 0.0 m and 2.0 m and also for surfaces facing away **from the traffic** for a height of 0.0 m. In the **wet splash zone (WSZ)** and the **distant road atmosphere (DRA)** all surfaces are treated as if they are facing **towards the traffic**. Furthermore **two speed limits, 50 km/h and 100 km/h** and **two traffic intensities (high and low)** have been considered. Generally the predictions have been made for 100 km/h and high traffic intensity, except for 0.0 m above the road in the dry splash zone (DSZ), where the effects of speed limits and traffic intensities have also been taken into account. Four different surface temperature conditions have been considered, cf. table 7.8b. The



different cases are indexed with roman numbers in the figures showing the predicted chloride ingress profiles.

#### 7.5.4 Dry splash zone (DSZ)

##### Height 0.0 m – distance 3.0 m

Predicted chloride ingress profiles in the dry splash zone, on roads with high traffic intensity and speed of 100 km/h in Göteborg, are shown in figure 7.6a. The chloride ingress has been predicted for surfaces at a height of 0.0 m and a distance of 3.0 m from the road surface, facing towards (TT) and away from (FT) the traffic.

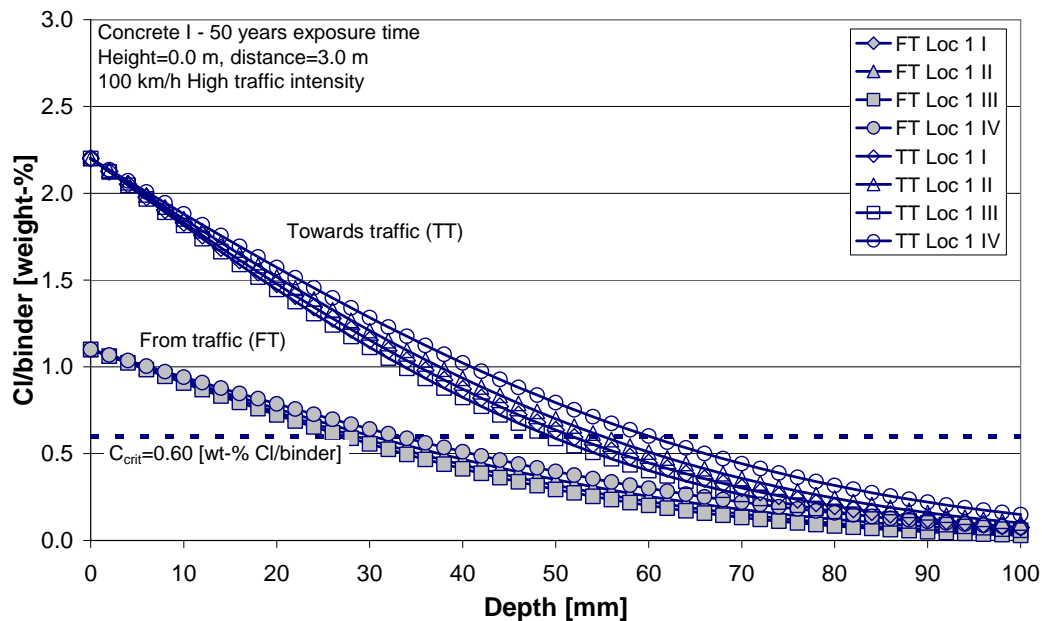


Figure 7.6a: Predicted chloride ingress profiles for Göteborg. 50 years' exposure time in the dry splash zone (height=0.0 m, distance=3.0 m, 100 km/h and high traffic intensity).

Predicted chloride ingress profiles in the dry splash zone, on roads with low traffic intensity and speeds of 50 km/h and 100 km/h in Göteborg, are shown in figure 7.6b. The chloride ingress has been predicted for surfaces at a height of 0.0 m and a distance of 3.0 m from the road surface, facing towards the traffic. It should be noticed that the severity of exposure to chlorides along roads with 50 km/h speed of traffic is approximately similar for low and high traffic intensity, cf. figure 6.10b.

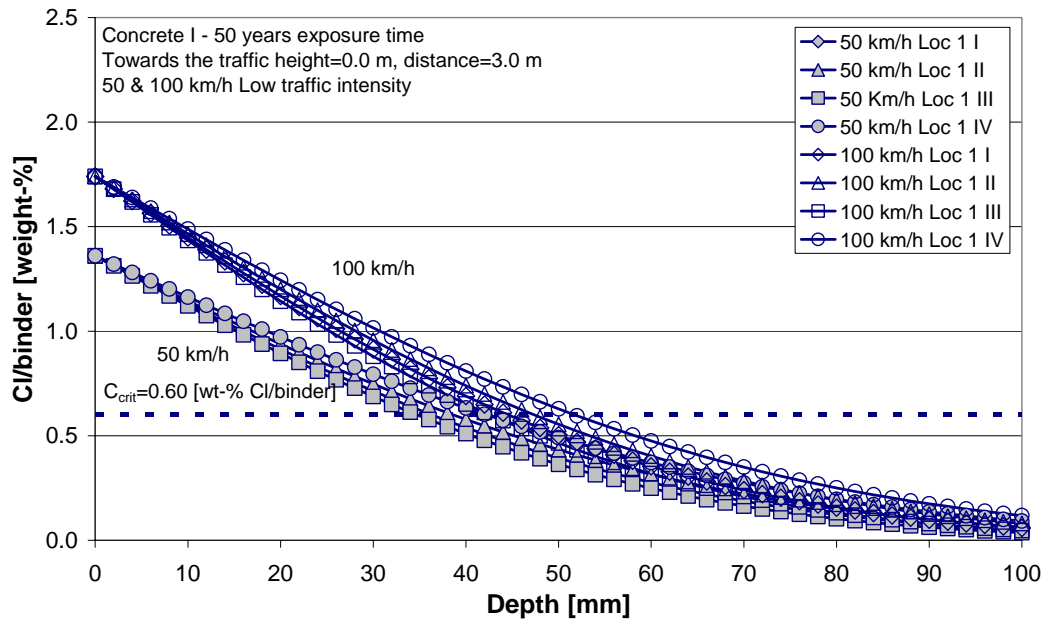


Figure 7.6b: Predicted chloride ingress profiles for Göteborg. 50 years' exposure time in the dry splash zone (height=0.0 m, distance=3.0 m, speeds of 50 & 100 km/h, surfaces facing towards the traffic and low traffic intensity).

Predicted chloride ingress profiles in the dry splash zone, on roads with high traffic intensity and speeds of 50 km/h and 100 km/h in Munich, are shown in figure 7.6c. The chloride ingress has been predicted for surfaces at a height of 0.0 m and a distance of 3.0 m from the road surface, facing towards the traffic.

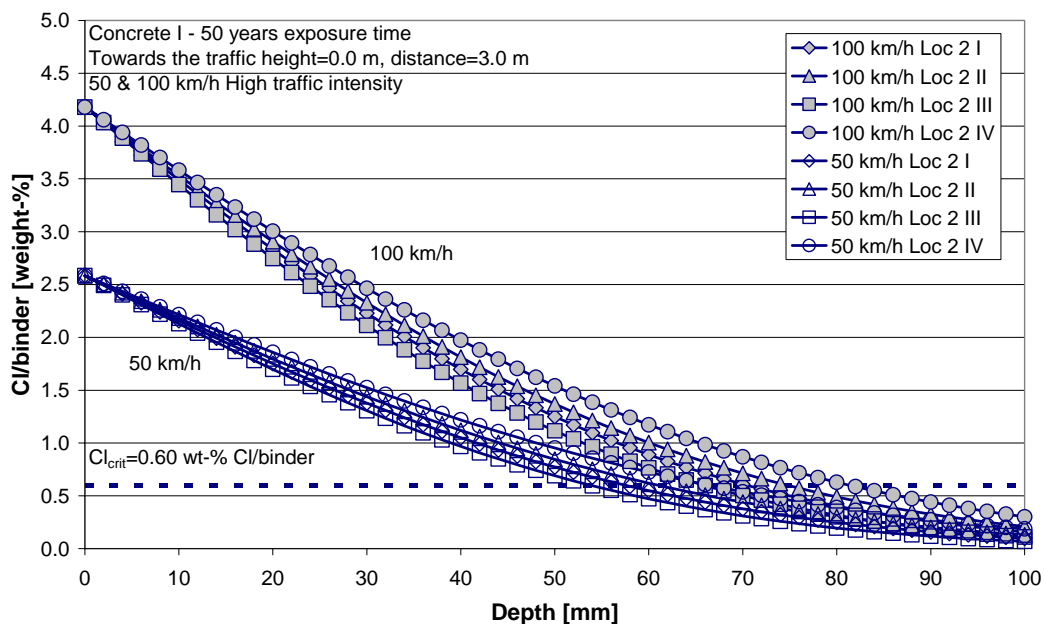


Figure 7.6c: Predicted chloride ingress profiles for Munich. 50 years' exposure time in the dry splash zone (height=0.0 m, distance=3.0 m, speeds of 50 & 100 km/h, surfaces facing towards the traffic and high traffic intensity).

### Height 2.0 m – distance 3.0 m

Predicted chloride ingress profiles in the dry splash zone, on roads with high traffic intensity and speeds of 50 km/h and 100 km/h in Göteborg and Munich, are shown in figures 7.7a and 7.b respectively. The chloride ingress has been determined for surfaces at a height of 2.0 m and a distance of 3.0 m from the road surface, facing towards the traffic.

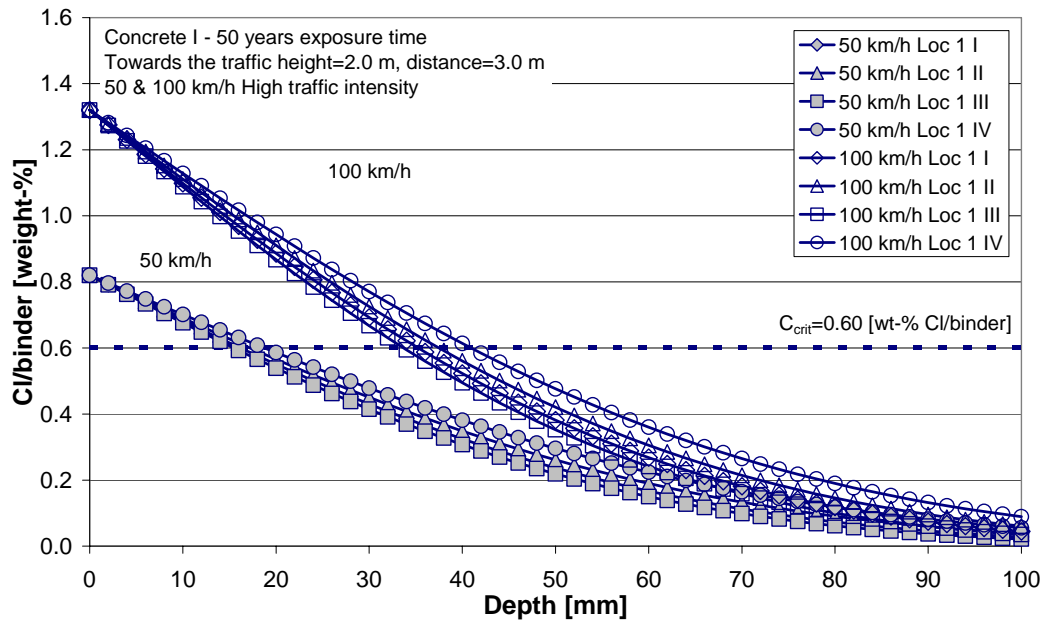


Figure 7.7a: Predicted chloride ingress profiles for Göteborg. 50 years' exposure time in the dry splash zone (height=2.0 m, distance=3.0 m, speeds of 50 & 100 km/h, surfaces facing towards the traffic and high traffic intensity).

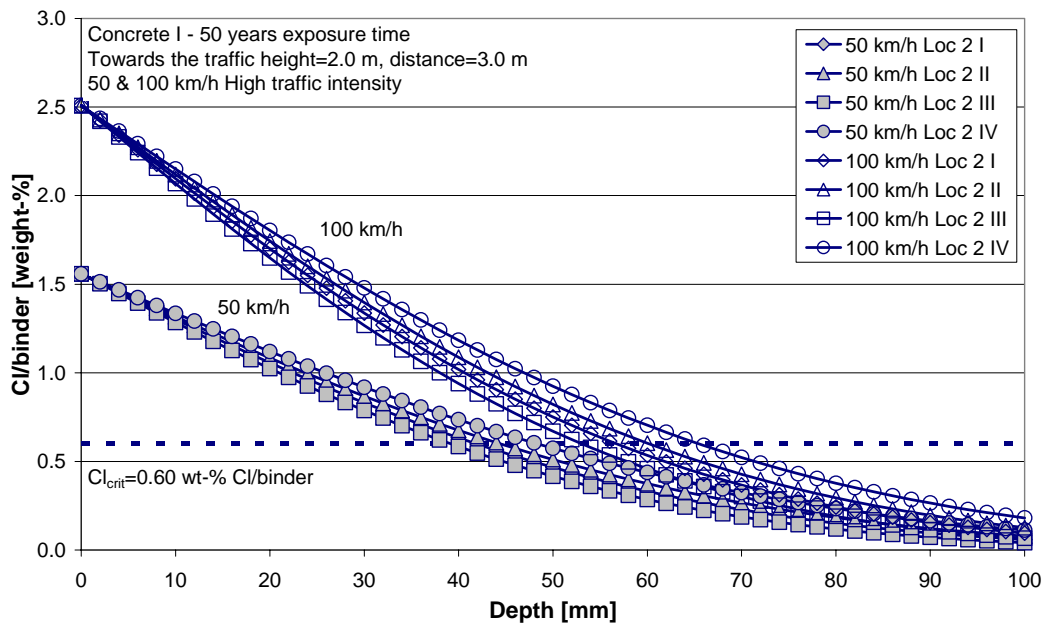


Figure 7.7b: Predicted chloride ingress profiles for Munich. 50 years' exposure time in the dry splash zone (height=2.0 m, distance=3.0 m, speeds of 50 & 100 km/h, surfaces facing towards the traffic and high traffic intensity).

### 7.5.5 Wet splash zone (WSZ)

Predicted chloride ingress profiles in the wet splash zone, on roads with high traffic intensity and speed of 100 km/h in Göteborg and Munich, are shown in figures 7.8a and 7.8b respectively. The profiles have been predicted for heights of 0.0 m and 2.0 m and a distance of 3.0 m from the road surface, for surfaces facing towards the traffic. It should be noticed that  $k_{C,o}=0.7$  has been used in the predictions, as discussed in section 7.4.2.

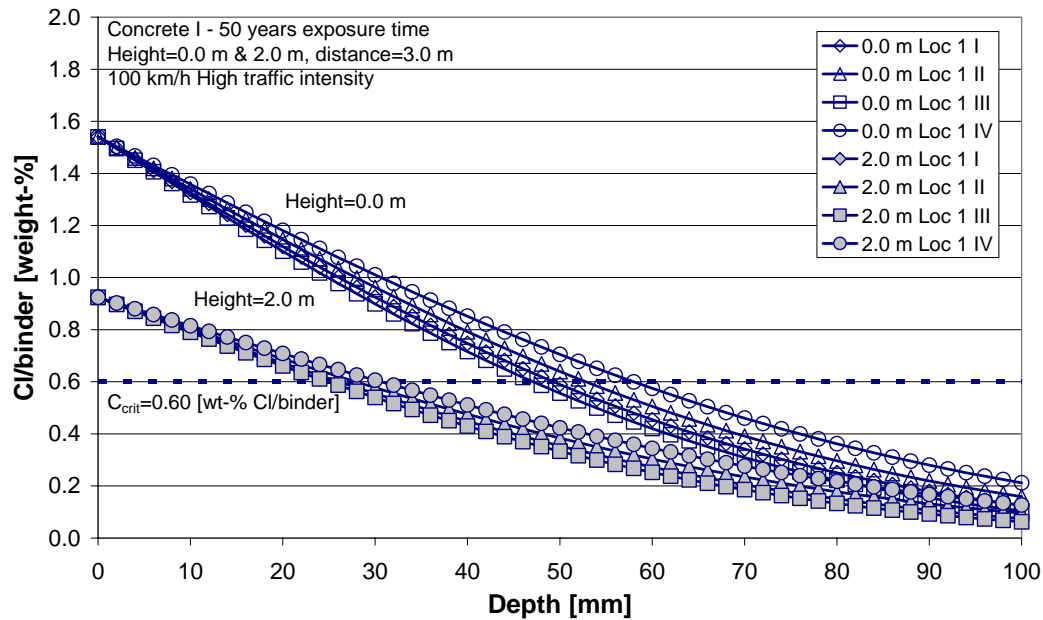


Figure 7.8a: Predicted chloride ingress profiles for Göteborg. 50 years' exposure time in the wet splash zone (heights=0.0 & 2.0 m, distance=3.0 m, speeds of 100 km/h, surface facing towards the traffic and high traffic intensity).

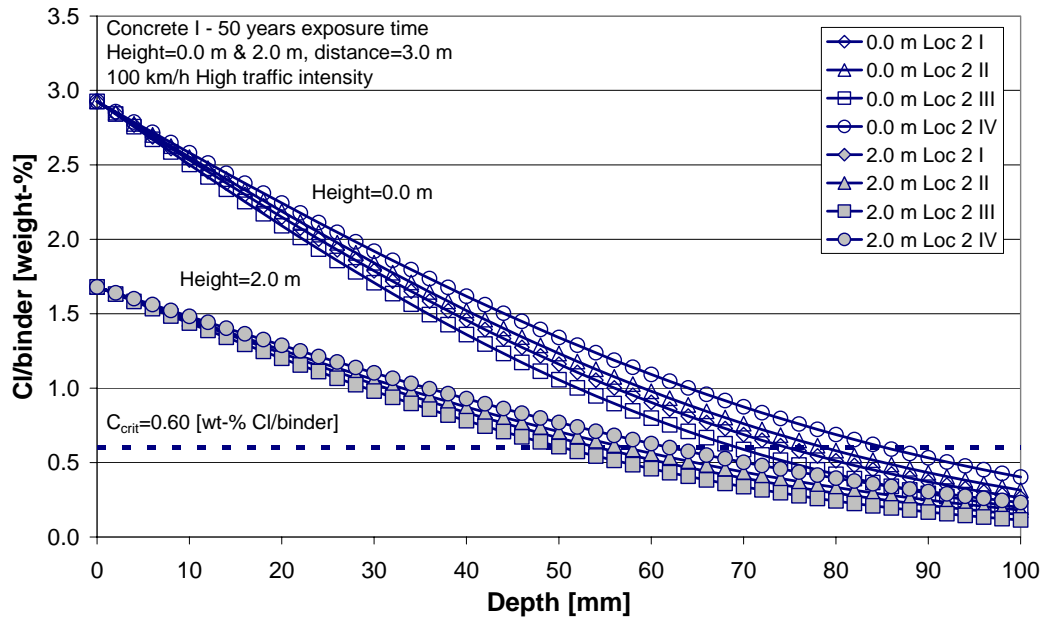


Figure 7.8b: Predicted chloride ingress profiles for Munich. 50 years' exposure time in the wet splash zone (heights=0.0 & 2.0 m, distance=3.0 m, speeds of 100 km/h, surface facing towards the traffic and high traffic intensity).

### 7.5.6 Distant road atmosphere (DRA)

The predicted chloride ingress profiles in the distant road atmosphere, on roads with high traffic intensity and speeds of 50 and 100 km/h in Göteborg and Munich, are shown in figures 7.9a and 7.9b respectively. The profiles have been predicted for heights of 0.0 m and distances of 7.0 and 12.0 m from the road surface, for surfaces facing towards the traffic.

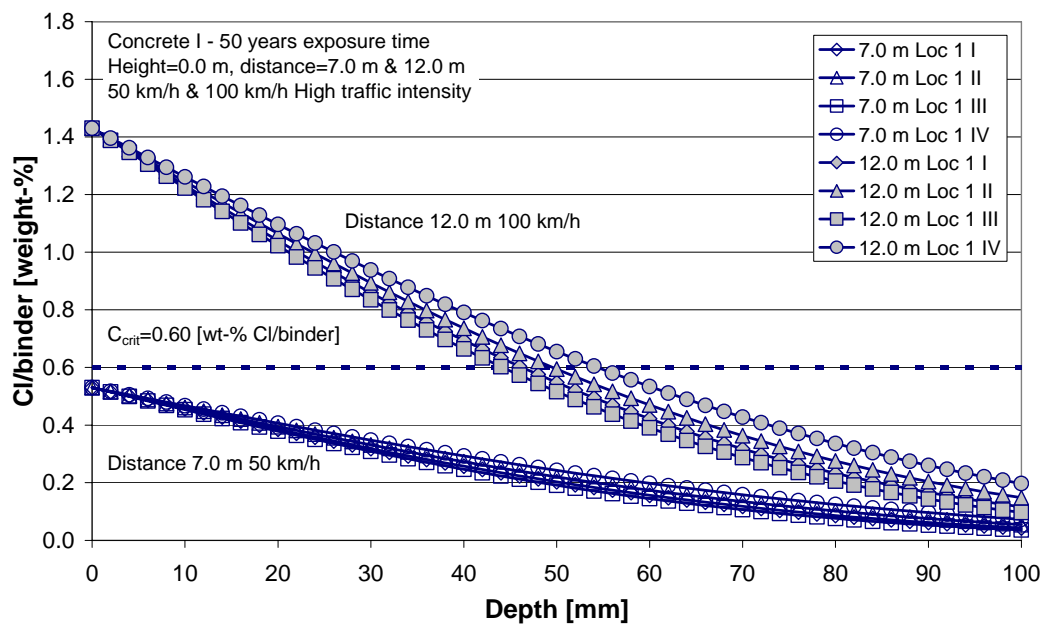


Figure 7.9a: Predicted chloride ingress profiles for the distant road atmosphere in Göteborg. 50 years' exposure time for surfaces 7.0 m (50 km/h) and 12.0 m (100 km/h – high traffic intensity) from the road surface.

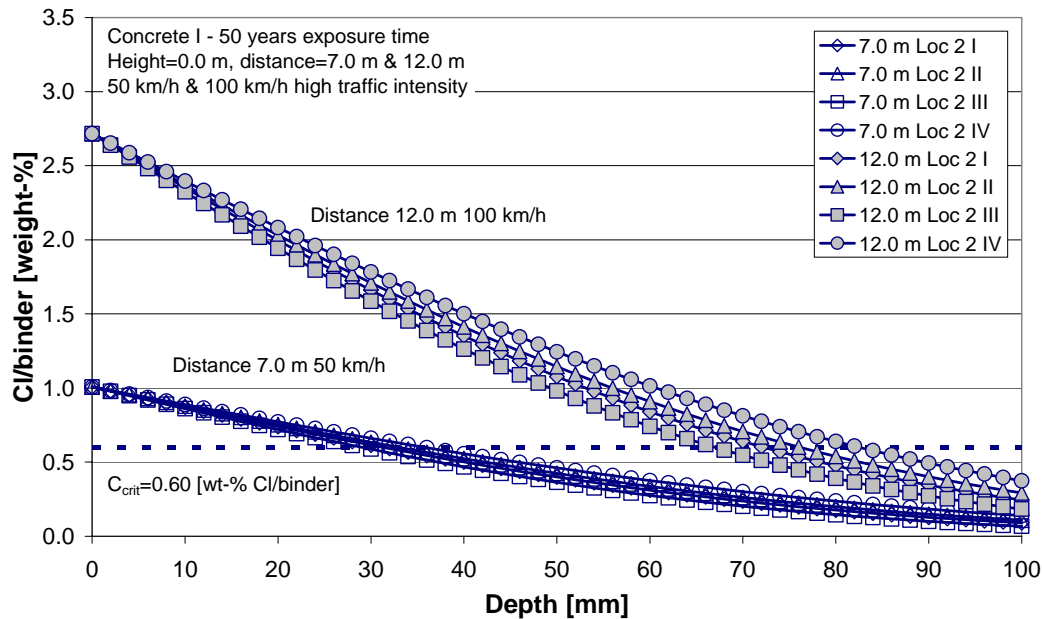


Figure 7.9b: Predicted chloride ingress profiles for the distant road atmosphere in Munich. 50 years' exposure time for surfaces 7.0 m (50 km/h) and 12.0 m (100 km/h – high traffic intensity) from the road surface.

## 7.6 Discussion and analysis – marine and road conditions

In this section the results of the predictions of chloride ingress and service life presented in section 7.5 are examined. The following will be analysed and discussed:

- Effect of chloride and temperature conditions in marine and road conditions.
- Effect of position relative to mean water level and distance to coastline in marine conditions.
- Effect of height above road and orientation towards traffic in road conditions.
- Effect of distance to road and traffic intensity and speed in road conditions.
- Effect of age factor in road conditions.

### 7.6.1 Effect of chloride and temperature conditions

#### Marine submerged conditions

The effects of the chloride concentration and temperature of the seawater at the different locations chosen to illustrate chloride ingress in marine conditions have been investigated. This has been done with the predicted chloride ingress profiles, presented in figures 7.3-7.5.

The effect of the temperature of the seawater can be investigated if the predictions of chloride ingress made at locations<sup>20</sup> 1, 5, 6, 7 and 8 are compared. At these locations the chloride concentration in the seawater is fairly similar, while the yearly mean temperature of the seawater varies, cf. table 7.2. From figures 7.3 and 7.4 it can be observed that the temperature of the seawater significantly influences both the shape and level of the predicted chloride ingress profiles. The profiles get flatter, due to higher  $D_a(t)$ , and the level of the profiles gets lower, due to lower  $C_{SN}$ , with increasing temperature.

<sup>20</sup> Yearly mean temperature of seawater at the chosen locations (shown within brackets): 1 (16.0°C), 5 (11.0°C), 6 (7.5°C), 7 (7.3°C) and 8 (16.5°C).

The predicted concrete covers required to achieve 100 years' service life vary between 0 mm (location 1 and 8) and 34 mm (location 7). The concrete covers of 0.0 mm for location 1 (The Mediterranean) and 8 (Atlantic Ocean outside Iberian Peninsula) are caused by the fact that  $C_{SN} < C_{crit}$ , i.e. there will never be any initiation of reinforcement corrosion. This effect can mainly be attributed to the fact that  $C_{SN}$  decreases, while  $C_{crit}$  is constant, with increasing temperature of the seawater.

The temperature effect on  $C_{SN}$ , if  $C_{SN}$  is defined as the total chloride content, can be explained by a temperature effect on the chloride binding, e.g. as described by Larsen (1998). Since  $C_{crit}$  and  $C_{SN}$  are defined as the chloride content in the concrete, it seems reasonable that there is a temperature effect on  $C_{crit}$  as well. However, depending on how  $C_{SN}$  and  $C_{crit}$  are defined (as free or total chloride content in the concrete) the temperature effect looks different. If  $C_{SN}$  is expressed as the total chloride content in the concrete it should decrease with increasing temperature, assuming that the free chloride content is constant.  $C_{crit}$  (expressed as total chloride content in the concrete) should have a similar temperature dependence as  $C_{SN}$ , i.e.  $C_{crit}$  decreases with increasing temperature and vice versa. This means that the required concrete covers would increase with increasing temperature, which also seems more realistic. However, in the literature data on the influence of temperature on  $C_{crit}$  are scarce and therefore more research is needed to further clarify this important influencing factor.

The effect of the chloride concentration of the seawater can be investigated if the predictions of chloride ingress made at locations<sup>21</sup> 2, 3, 4, 5, 8 and 9 are compared. At these locations the temperature of the seawater is fairly similar (locations 2, 4 and 5 + locations 8 and 9), while the chloride concentration in the seawater varies, cf. table 7.2. From figures 7.3 and 7.4 it can be observed that the chloride concentration of the seawater has only a limited effect on the shape and level of the predicted chloride ingress profiles. Instead the difference between the profiles can be related to different temperatures of the seawater.

The predicted required concrete covers to achieve 100 years' service life vary between 0 mm (locations 3, 8 and 9) and 22 mm (location 5). The low concrete covers at locations 2, 8 and 9 can be explained by the fact that  $C_{SN} \leq C_{crit}$ , where the low  $C_{SN}$  is caused either by low chloride concentration (locations 2 and 3) or high temperature of the seawater (locations 8 and 9).

The effect of exposure in a fjord can be studied if the predictions of chloride ingress made at locations<sup>22</sup> 6 and 7 are compared. The concrete covers required to achieve 100 years' service life for locations 6 and 7 are approximately 34 mm. Thus the effect of exposure in a fjord environment seems to be insignificant.

If the predicted chloride ingress profiles in figures 7.3 and 7.4 are compared the effect of concrete composition can be studied. Obviously the chloride ingress into concrete II is larger ( $w/b=0.50$ ) than into concrete I ( $w/b=0.40$ ), since the former has a less dense pore structure due to a higher  $w/b$ . Furthermore the concrete composition affects both the shape of the profiles and the required concrete covers. As an example the concrete cover,

<sup>21</sup> Mean chloride concentration in the seawater at the chosen locations (shown within brackets): 2 (3.6 g Cl/l), 3 (4.8 g Cl/l), 4 (10.1 g Cl/l), 5 (18.3 g Cl/l), 8 (21.0 g Cl/l) and 9 (23.0 g Cl/l)

<sup>22</sup> Mean chloride concentration in the seawater at the chosen locations (shown within brackets): 6 (17.2 g Cl/l) and 7 (19.5 g Cl/l).

required to achieve 100 years' service life for exposure of concretes I and II at location 4 (Kattegat), is 12 mm and 45 mm respectively.

Some of the required concrete covers predicted from the results presented in figures 7.3 and 7.4 are unrealistically low (locations 1, 2, 3, 8 and 9). As discussed earlier these low concrete covers are a result of the fact that  $C_{SN} \leq C_{crit}$ . In the predictions  $C_{SN}$  depends mainly on the temperature in the concrete, with  $C_{SN}$  increasing with decreasing temperature, cf. table 7.4, and to some extent on the chloride concentration in the seawater, while  $C_{crit}$  is constant. At locations 2 (The Baltic Sea) and 3 (Öresund)  $C_{SN}$  is low since the chloride concentration is low in the seawater, while at locations 1, 8 and 9 (Persian Gulf)  $C_{SN}$  is low because of a high temperature in the seawater. The predicted required concrete covers would probably be more realistic if  $C_{crit}$  was also dependent on the temperature of the seawater, as earlier discussed.

### Marine tidal, splash, atmospheric and distant atmospheric conditions

The combined effects of chloride, moisture and temperature conditions in the concrete on the required concrete covers have been studied by comparing the predicted required concrete covers in the marine tidal, splash and atmospheric zones in Träslövsläge, see figure 7.5. The predictions have been made for the different temperature conditions: (i) **case I** – air temperature, (ii) **case II** – temperature of seawater, (iii) **case III** – equivalent surface temperature with  $I_{solar}=50 \text{ W/m}^2$  and  $T_{sky}=-15.0^\circ\text{C}$  and (iv) **case IV** – equivalent surface temperature with  $I_{solar}=300 \text{ W/m}^2$  and  $T_{sky}=-5.0^\circ\text{C}$ .

In figure 7.5 a clear effect of the temperature conditions can be observed, if the predicted chloride ingress profiles, in each of the marine exposure zones (except the submerged zone), are compared. The required concrete covers increase with increasing temperature and this is especially significant in the marine tidal and splash zones. However, as discussed earlier it is probably not realistic to model  $C_{crit}$  as constant, and it is instead modelled as dependent on the temperature.

The combined effects of chloride and moisture conditions can be evaluated if the predicted concrete covers in the different exposure zones are compared. According to figure 7.5 the covers required to achieve 100 years' service life vary, depending on the temperature conditions in the concrete, between 76-93 mm (MTZ), 46-55 mm (MSZ), 20-24 mm (MAZ) and approximately 0 mm (MDAZ). The largest predicted required concrete covers are, as expected, found in MTZ, with the highest  $C_{SN}$  and  $k_{D,e}$ , and the lowest covers are found in MDAZ, with the lowest  $C_{SN}$  and  $k_{D,e}$ . However, the predicted covers in the atmospheric and distant atmospheric zones are probably too low due to the fact that  $C_{SN}$  used in the predictions has been too low. This is further discussed in section 7.6.2.

### Road conditions

The effect of moisture and temperature conditions on the required concrete covers in the road environment has been studied. In figures 7.6a-7.6c, 7.7a-7.7b, 7.8a-7.8b and 7.9a-7.9b examples of chloride ingress profiles in different road exposure zones and temperature conditions are presented. A selection of these profiles is presented in figure 7.10, where profiles from the dry splash zone (DRZ – 0.0 m height and 3.0 m from the road), the wet splash zone (WSZ – 0.0 m height and 3.0 m from the road) and the distant road atmosphere (0.0 m height and 12.0 m from the road surface) are plotted. All predictions are made for a road with 100 km/h speed and high traffic intensity. The predictions have been made for surfaces at the level of the road and for four different



surface temperature conditions: (i) **case I** – air temperature, (ii) **case II** – equivalent surface temperature with  $I_{\text{solar}}=50 \text{ W/m}^2$   $T_{\text{sky}}=-15.0^\circ\text{C}$ , (ii) **case III** – equivalent surface temperature with  $I_{\text{solar}}=200 \text{ W/m}^2$   $T_{\text{sky}}=-10.0^\circ\text{C}$  and **case IV** – equivalent surface temperature with  $I_{\text{solar}}=300 \text{ W/m}^2$   $T_{\text{sky}}=-5.0^\circ\text{C}$ .

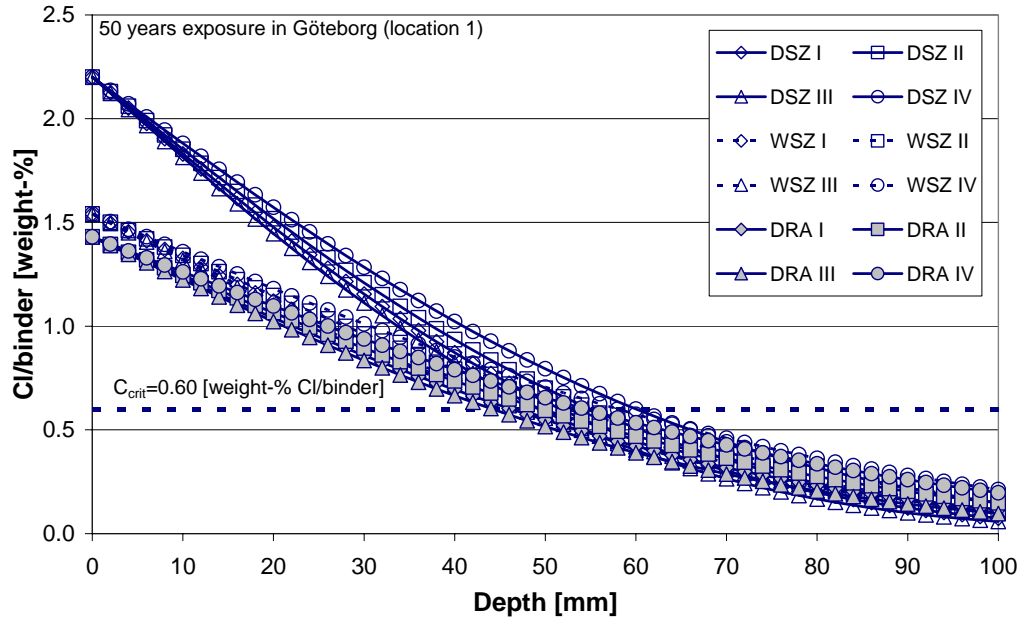


Figure 7.10: Predicted chloride ingress profiles for different road exposure conditions.

In figure 7.10 it can be seen that both the moisture and temperature conditions have a clear influence on the predicted required concrete covers. The influence of the moisture conditions in the concrete can be evaluated if the required concrete covers in the dry and wet splash zones are compared. The predicted required concrete covers are fairly similar in the dry and wet splash zones, despite the lower  $C_{\text{SN}}$  in the wet splash zone<sup>23</sup>, since the concrete also is more moist, resulting in larger  $k_{\text{D,RH}}$  and  $k_{\text{D,e}}$ . The temperature conditions in the concrete can be evaluated if the required concrete covers in each of the exposure zones are compared. The required concrete covers increase with increasing temperature. This can partly be explained by the fact the only  $D_{\text{a}}(t)$  is influenced by the temperature conditions in the concrete, which means that the chloride ingress increases with increasing temperature. However, no measured data are available in the literature to confirm these findings.

### Summary

In marine conditions the predicted chloride ingress profiles and the required concrete covers have been found to be mainly influenced by the temperature and only to some extent by the chloride concentration of the solution at the surface of the concrete. This can mainly be explained by the large temperature dependence of  $C_{\text{SN}}$ , with  $C_{\text{SN}}$  decreasing significantly with increasing temperature.

In road conditions the predicted chloride ingress profiles and the required concrete covers have been found to be influenced by a combination of the chloride, moisture and temperature conditions. The level and shape of the profiles vary depending on the

<sup>23</sup> The chloride ingress has been predicted for a horizontal surface in the wet splash zone, i.e.  $k_{\text{C},0}=0.7$ .

exposure to chlorides, rain and solar radiation. In the dry splash zone the profiles are fairly high and steep due to severe exposure to chlorides but shelter from both rain and solar radiation. In the wet splash zone and distant road atmosphere the profiles are lower and flatter due to less severe exposure to chlorides but exposure to rain and solar radiation.

### 7.6.2 Effect of position relative to mean water level and distance to coastline

The effects of position relative to mean water level and distance to the coastline in marine conditions have been investigated. This has been done with the results presented in figures 7.3 and 7.5, where predicted chloride ingress profiles for exposure in different marine exposure zones in Kattégat (location 4) are presented. The predictions have been made for the different temperature conditions: (i) **case I** – air temperature, (ii) **case II** – temperature of seawater, (iii) **case III** – equivalent surface temperature with  $I_{\text{solar}}=50 \text{ W/m}^2$  and  $T_{\text{sky}}=-15.0^\circ\text{C}$  and (iv) **case IV** – equivalent surface temperature with  $I_{\text{solar}}=300 \text{ W/m}^2$  and  $T_{\text{sky}}=-5.0^\circ\text{C}$ .

The effect of position relative to the mean water level is obvious if the predicted required concrete covers in the different exposure zones are compared, where the largest concrete covers are required in the submerged zone and the smallest concrete covers are required in the distant atmospheric zone. The effect of the distance to the coastline can be studied if the required concrete covers from the atmospheric and distant atmospheric zones are compared. The required concrete covers in the distant atmospheric zone, 500 m from the coastline, are only approximately 1 mm, while in the atmospheric zone the required covers are 20-24 mm.

The predicted concrete covers in the atmospheric and distant atmospheric zones are probably too low, since  $C_{\text{SN}}$  used in the predictions is low, cf. table 7.5a. In investigations made on existing concrete structures, large variations in the exposure to chlorides above the water surface have been observed, cf. Sørensen & Maahn (1982), Fluge (1997) and Andersen (1996). The exposure to chlorides above the water surface was found to largely depend on the characteristics of the structure and surface in question, e.g. height above water surface, surface orientation, airstreams around the structure etc. Thus the modelling of the exposure to chlorides and its variations in these exposure zones is not trivial. Thus there is a need to further investigate the exposure to chlorides, and its variations, especially above the water surface, so that  $C_{\text{SN}}$  may be modelled more realistically.

### 7.6.3 Effect of height above road and orientation towards traffic

The effects of height above the road and orientation towards the traffic in the road environment have been investigated. This has been done with the predicted chloride ingress profiles presented in figures 7.6a, 7.7a and 7.8a-7.8b, where profiles for different surface orientations and heights above the road y are presented.

The effect of the orientation towards the traffic and height above the road is obvious, with the largest concrete covers required for surfaces facing towards the traffic at the level of the road (0.0 m), where also the exposure to chlorides is most severe. The effect of the height above the road can be observed in the predicted required concrete covers. The covers required to achieve 50 years' service life for surfaces facing towards the traffic with speeds of 100 km/h are 49-60 mm (0.0 m height) and 38-41 mm (2.0 m height). The covers required to achieve 50 years' service life for surfaces facing away from the traffic at 0.0 m height above the road are 27-33 mm.

There is also an effect due to the temperature conditions, with the required concrete covers increasing with increasing temperature (cases II and IV), due to an increase in  $D_a(t)$ , which results in larger chloride transport rate. This can be seen if the required concrete covers are studied. The concrete covers to achieve 50 years' service life for a surface at 0.0 m height above the road facing towards the traffic with speeds of 100 km/h are 52 mm (case I), 55 mm (case II), 49 (case III) and 60 mm (case IV). Additionally in figures 7.7a-7.7b the difference in predicted chloride ingress between Göteborg and Munich can be studied. If surfaces along a road with a speed limit of 100 km/h are studied the predicted required concrete covers to achieve 50 years' service life are 34-41 mm in Göteborg and 53-65 mm in Munich. Thus the required concrete covers are approximately 60% larger in Munich than in Göteborg, due to a larger  $C_{SN}$ .

The results in figures 7.6a and 7.7a-7.7b have been compared with measurements of chloride ingress on two of the concrete bridges, bridges O 951 and O 978, investigated by Lindvall & Andersen (2000). These bridges are constructed with concrete compositions similar to concrete I. Measured chloride ingress profiles from the bridges, after 27 and 25 years of exposure respectively, are presented in figure 7.11. The continuous lines denote profiles from bridge O 951 and the dotted lines profiles from bridge O 978. The profiles with index "U" and "Ö" come from approximately 0 m (unfilled symbols) and 2 m (filled symbols) above the road respectively. The distance to the road is 3 m, the traffic intensity is high and the speeds are over 100 km/h.

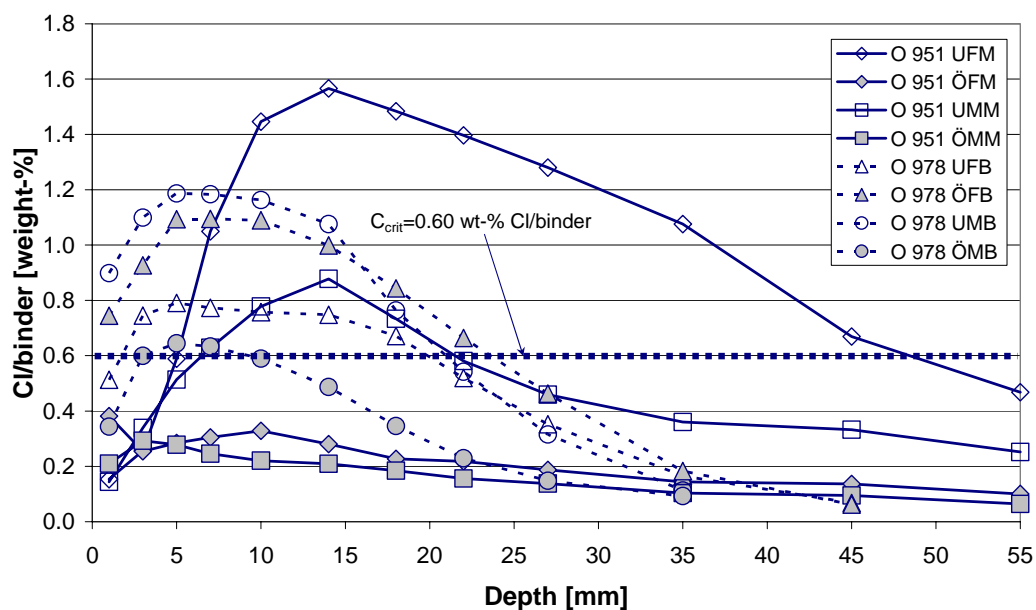


Figure 7.11: Measured chloride ingress profiles from columns on bridges O 951 and O 978. The exposure times have been 27 and 25 years respectively. Data from Lindvall & Andersen (2000).

According to figures 7.6a and 7.7a the concrete covers required to achieve 25 years' service life are 39-47 mm for surfaces 0.0 m above the road and 26-32 mm for surfaces 2.0 m above the road. Compared with the concrete covers evaluated from the measured profiles in figure 7.11 the predicted covers correspond well with the measured chloride ingress (O 951 UFM). However, for the other measured profiles the model overestimates the chloride ingress. There are many possible reasons for this, e.g. the severity of the exposure to chlorides or the potential chloride diffusivity is overestimated in the model.

Furthermore the decrease in chloride diffusivity with time may be underestimated in the model – it has been shown that chloride ingress in concrete exposed in road conditions almost stops after a certain exposure time, cf. Andersen (1997) and Lindvall (2000b).

However, as shown by Lindvall & Andersen (2000) and Lindvall (2002a), the severity of the exposure to chlorides may vary significantly both between different structures but also within one single structure. This means it is not easy to generalize the description of the road environment and to find the most severely exposed spots on a bridge. The exposure to chlorides in road conditions is also influenced by several factors, e.g. the characteristics of the road, traffic and spread of de-icing salt, where the latter two may vary significantly between different years, cf. section 3.5. Consequently the results presented in figures 7.6a and 7.7a should be treated with some caution. Obviously the effects on the severity of exposure to chlorides due to orientation towards traffic and height above the road, distance to the road, traffic speeds and intensity, spread of de-icing salt (type of salt, spreading method) etc, need to be further investigated.

#### 7.6.4 Effect of distance to road and traffic intensity and speed

The effects of distance to the road and traffic intensity and speed have been investigated. This can be done with the predicted chloride ingress profiles presented in figures 7.6a-7.6c, 7.7a-7.7b and 7.9a-7.9b, profiles from structures exposed along roads with different traffic intensities and speed limits, and at different distances from the road. Only surfaces facing towards the traffic are considered since these surfaces have the most severe exposure to chlorides, as discussed earlier.

The most severe exposure to chlorides is found for surfaces exposed along a road with 100 km/h speed and high traffic intensity at 3 m and 7 m from the road surface. The severity of the exposure to chlorides decreases with increasing distance to the road surface, traffic intensity and speed. Thus the least severe exposure to chlorides is therefore found for surfaces exposed in the distant road atmosphere (7 m and 12 m from the road) along roads with 100 km/h speed (low traffic intensity) or 50 km/h speed. These results are in agreement with what has been found by McBean & Al-Nassri (1987) and Blomqvist & Johansson (1999), cf. figure 3.17.

Consequently the largest concrete covers are required for surfaces exposed along a road with 100 km/h speed and high traffic intensity at 3 m and 7 m from the road surface and the smallest concrete cover is required for surfaces exposed along roads with 50 km/h speed of traffic. Predicted required concrete covers to achieve 50 years' service life in Göteborg and Munich respectively are 49.4-60.0 mm and 65.9-81.3 mm for exposure at 3.0 m distance from the road with 100 km/h speed and high traffic intensity. For exposure at 3.0 m distance from roads with 50 km/h speed of traffic the corresponding required concrete covers to achieve 50 years service life are 35-42 mm and 54-66 mm in Göteborg and Munich respectively. Furthermore it should be noticed in figure 7.9a that there is no risk of reinforcement corrosion for surfaces in the distant road atmosphere (7 m and 12 m from the road) along roads with 100 km/h speed of traffic (low traffic intensity) or 50 km/h speed in Göteborg, since  $C_{SN} < C_{crit}$ . However, in Munich, where more de-icing salt is spread resulting in more severe exposure to chlorides, surfaces in the distant road atmosphere, 7 m from roads with 50 km/h or 100 km/h (low traffic intensity), are also subjected to risk of reinforcement corrosion.

### 7.6.5 Effect of age factor in road conditions

The influence of the age factor on the predicted chloride ingress has been investigated, which is illustrated in figure 7.12, where predicted chloride ingress profiles, with different age factors, are presented. The predictions have been made for structures exposed along roads with high traffic intensity and 100 km/h speed at 0.0 m height and 3.0 m distance from the road in Göteborg and Munich. The age factors,  $n$ , used in the predictions have been set to 0.0, 0.19, 0.30 and 0.40 (stated in the figure).

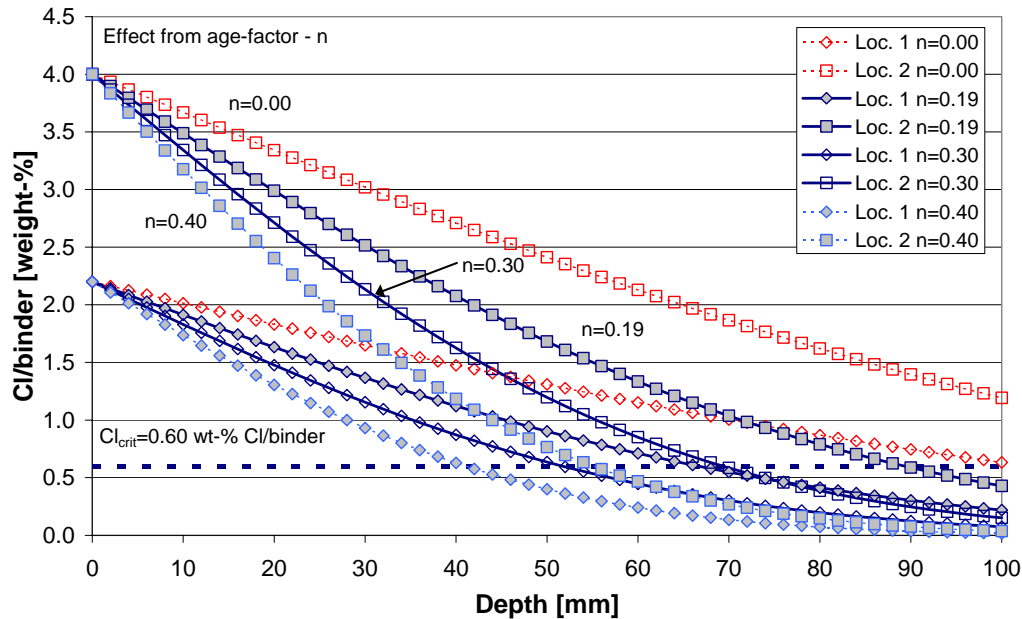


Figure 7.12: Predicted chloride ingress profiles for different values of  $n$ . Exposure both in Göteborg and Munich.

From figure 7.12 it is obvious that the age factor,  $n$ , has a significant influence on the predicted chloride ingress and the corresponding required concrete covers. Low values of  $n$ , i.e.  $D_{\text{eff}}$  decreases little with time, result in large predicted chloride penetration depths, while large values of  $n$  result in small predicted chloride penetration depths. With a service life of 50 years the predicted required concrete covers for location 1 vary between 41 mm ( $n=0.40$ ) and 103 mm ( $n=0.00$ ). Thus the age factor has a large influence on the predicted service life and needs therefore special attention when it is quantified.

### 7.6.6 Effect of chloride threshold level, $C_{\text{crit}}$

As discussed earlier the chosen levels of the chloride threshold level,  $C_{\text{crit}}$ , can be questioned, since  $C_{\text{crit}}$  is influenced by a combination of the chloride, moisture and temperature conditions. The results of predictions should probably be more realistic if  $C_{\text{crit}}$  was expressed as a temperature-dependent parameter. If  $C_{\text{crit}}$  is expressed as the total chloride content in the concrete,  $C_{\text{crit}}$  should consequently decrease with increasing temperature, due to a reduced chloride binding in the concrete.

As a consequence of the temperature effect on  $C_{\text{crit}}$ , the required concrete covers would also increase with increasing temperature, even if the chloride content at the reinforcement remained constant. This means that the required concrete covers should be larger when the temperature in the concrete is high (cases II and IV) and smaller when it is low (cases I and III). Furthermore the extent of reinforcement corrosion is dependent

not only on the chloride content at the reinforcement, but also on the temperature conditions, with the corrosion more severe at higher temperatures.

## 7.7 Probabilistic predictions

### 7.7.1 General

The DuraCrete chloride ingress model was originally developed for probabilistic calculations, where each parameter in the model is described in terms of mean values, standard deviations (indicating the statistical uncertainties) and statistical distribution functions. With probabilistic calculations, the reliability of a structure can be assessed, with the uncertainties of the parameters in the model taken into account. The calculations are based on the performance of the structure, defined by limit states which define the boundaries between desired and undesired or adverse states. In modern building codes two types of limit states are used, viz. ultimate limit states (**ULS**), which refer to the structural safety of structures, and serviceability limit states (**SLS**), which refer to the comfort and functionality of structures. In this study a serviceability limit state has been used, where the risk of initiation of reinforcement corrosion is predicted.

In eq. (7.2a-7.2b) the probabilistic calculations have been made with the following limit state function, where the risk of initiation of reinforcement corrosion, as a function of for example the exposure time, concrete properties or concrete cover, is determined. The risk is expressed as a probability that the limit state is exceeded, a failure probability  $p_f$ , and the service life is defined as at an end when a specific target probability,  $p_{\text{target}}$ , is exceeded.

$$p_f = p \left\{ C_{\text{crit}} - C_{\text{SN}} \cdot \left[ \operatorname{erfc} \frac{d_c / 1000}{2 \cdot \sqrt{D_a(t) \cdot t}} \right] < 0 \right\} < p_{\text{target}} \quad [-] \quad (7.2a)$$

where:

- $p_f$ : failure probability. [-]
- $p$ : probability that a certain event occurs. [-]
- $p_{\text{target}}$ : target probability. [-]
- $d_c$ : concrete cover. [mm]
- $D_a(t)$ : apparent diffusion coefficient determined from eq. (7.2b). [ $\text{m}^2/\text{s}$ ]

$$D_a(t) = D_a(t_0) \cdot \left( \frac{t_0}{t} \right)^n = k_c \cdot k_e \cdot k_t \cdot D_0 \cdot \left( \frac{t_0}{t} \right)^n \quad [\text{m}^2/\text{s}] \quad (7.2b)$$

In the probabilistic calculations the failure probability, for certain concrete covers and concrete properties, has been determined as a function of the exposure time. For the sake of clarity, the failure probability has, in the results of the calculations, been expressed as a reliability index,  $\beta$ , see eq. (7.3).

$$p_f = \Phi(-\beta) \quad [-] \quad (7.3)$$

where:

$\Phi$  standard normal distribution, with  $\mu=0$  and  $SD=1$ . Values of  $\Phi(-\beta)$  can be found in handbooks of statistics, e.g. Box et al (1978).

The following has been investigated in the probabilistic calculations:

- The effect of chloride concentration and temperature of seawater on the reliability of structures exposed in submerged conditions. For this purpose probabilistic service life predictions have been made for concrete structures exposed in the Baltic Sea (location 2), Kattegat (location 4), the North Sea (location 5), Atlantic Ocean around Iceland (location 7), Atlantic Ocean outside Iberian Peninsula (location 8) and Persian Gulf (location 9).
- The effect of the level of  $C_{crit}$  on the reliability of structures exposed in submerged conditions in Kattegat (location 4).
- The effect of thickness and uncertainty of the concrete cover on the reliability of structures exposed in submerged conditions in Kattegat (location 4).
- The effect of orientation towards traffic and height above the road on the reliability of structures exposed in road conditions in Göteborg.

The calculations have been made with the computer program COMREL<sup>24</sup>. All calculations have been made according to FORM (First Order Reliability Methods). The data, and especially their uncertainties, that are used in the predictions are still uncertain, which means that the results of the probabilistic calculations also are uncertain and therefore should be treated with some caution. However, it is possible to update the data with measurements made on structures and thus reduce the uncertainties in the results of the probabilistic calculations.

The results of the probabilistic calculations have also been compared with the results of the deterministic predictions, to demonstrate the effects of uncertainties on the service life predictions.

### 7.7.2 Input data for the probabilistic calculations

Input data used in the probabilistic calculations are given in tables 7.1a-7.1b, 7.3-7.5b and 7.7-7.8b. Data which express the influence of concrete composition (affecting  $D_0$  and  $k_c$ ) and increasing exposure time (affecting  $n$ ) are presented in tables 7.1a-7.1b and 7.3 (marine conditions) and 7.7 (road conditions). Furthermore data which express the influence of the exposure conditions (affecting  $C_{SN}$  and  $k_e$ ) are given in tables 7.4 and 7.5a-7.5b (marine conditions) and 7.8a-7.8b (road conditions).

The statistical uncertainties in  $C_{SN}$  and  $k_e$  are considered in the following way:  $C_{SN}$  has been modelled **normally distributed** with  $COV^{25}$  of 30% and  $k_e$  has also been modelled **normally distributed** with  $COV$  of 20%. The input data on  $C_{crit}$  used to investigate the influence of the level of  $C_{crit}$  is given in table 7.9.

<sup>24</sup> Computer program for probabilistic calculations, programmed by STRUREL. More information about COMREL is available at the website of STRUREL: <http://www.struruel.de>

<sup>25</sup>  $COV$  – Coefficient of variation, cf. eq. (4.1).

Table 7.9: Input data on  $C_{crit}$  used in the probabilistic calculations.

$C_{crit}$	$\mu$	SD	Statistical distribution
0.60	0.60	0.15	Normal (0.60, 0.15)*
0.75	0.75	0.15	Normal (0.75, 0.15)
1.25	1.25	0.15	Normal (1.25, 0.15)
1.50	1.50	0.15	Normal (1.50, 0.15)
2.00	2.00	0.15	Normal (2.00, 0.15) <sup>♠</sup>
2.50	2.50	0.15	Normal (2.50, 0.15)
3.00	3.00	0.15	Normal (3.00, 0.15)

\* : Used for all calculations, except for probabilistic calculations in marine submerged conditions presented in figure 7.13b.

♠ : Used for probabilistic calculations in marine submerged conditions.

The concrete cover,  $d_c$ , has been set equal to **50 mm** with SD=5 mm, modelled with a Beta-distribution – Beta (50, 5, 0, 250)<sup>26</sup>, in all calculations except the ones presented in figures 7.13c and 7.13d. In these figures the effects of variations and uncertainties in the concrete covers have been studied.

### 7.7.3 Results and discussion of probabilistic calculations

In the probabilistic calculations the service life is defined as at an end when the acceptable minimum reliability, i.e. the target reliability, is exceeded. The acceptable minimum reliability depends on the cost of minimising the probability that the limit state is exceeded, in this study the risk of initiation of reinforcement corrosion, in relation to the cost of repairing the structure. Depending on the relation between these costs, the reliability index,  $\beta$ , in a serviceability limit state may vary between 1.0 and 2.0, which corresponds to failure probabilities of 15.866% and 2.275% respectively, Rackwitz (1999). Normally a reliability index of 2.0 is used to define the end of the service life for a serviceability limit state. This corresponds to a case where the cost of minimising the risk that the limit state is exceeded is low and the cost of repairing the structure is high. Trend lines showing  $\beta=1.0$  and 2.0 are included in the figures, where the results of the probabilistic calculations are presented.

The results of the probabilistic calculations are presented in figures 7.13a-7.13d (marine conditions) and 7.14 (road conditions), where the reliability, in terms of the reliability index  $\beta$ , is expressed as a function of the exposure time. In figure 7.13a the effects on the reliability of structures exposed in different marine conditions are illustrated. The calculations have been made with  $C_{crit}=2.00$  [% by wt Cl/binder]. To illustrate the effect of  $C_{crit}=0.60$ , a calculation has also been made with this  $C_{crit}$  for location 4.

<sup>26</sup> Mean concrete cover=50 mm, standard deviation in concrete cover=5 mm, minimum concrete cover=0 mm and maximum concrete cover=250 mm



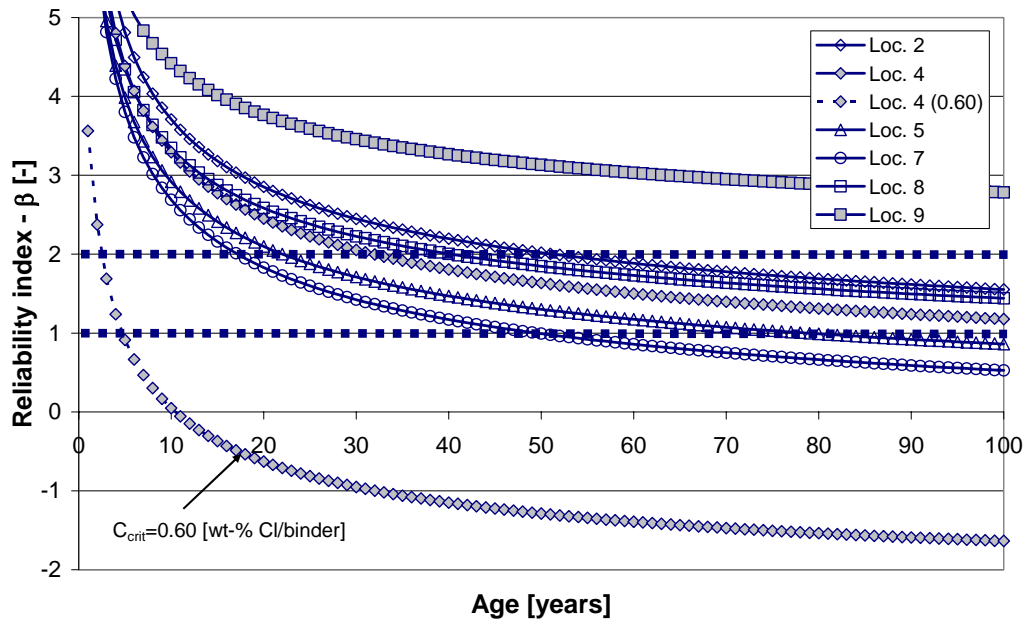


Figure 7.13a: Reliability as a function of the exposure time (marine conditions). Effect of chloride concentration and temperature of seawater.

In figure 7.13a the predictions of service life, with  $\beta=2.0$  ( $C_{crit}=2.00$  [% by wt Cl/binder] and  $d_c=50$  [mm]) are between 18 years (location 7) and >100 years (location 9). With  $\beta=1.0$ , the predicted service life will be considerably longer, e.g. 50 years for location 7. The large variations in calculated reliability indexes presented in figure 7.13a can mainly be attributed to large variations in  $C_{SN}$  between the different locations, cf. table 7.4, while  $C_{crit}$  is constant. This can for example explain that the predicted service life for exposure in the Persian Gulf (location 9) is extremely high (1817 years with  $\beta=2.0$ ). As discussed in section 7.4.3 it would therefore be more realistic to model  $C_{crit}$  as temperature-dependent. Furthermore compared with the service life predicted with deterministic calculations, where the parameters are described with mean values, the probabilistic calculations predict considerably shorter service lives, cf. figure 7.3.

The required concrete covers predicted with probabilistic methods, presented in figure 7.13a, have been compared with the covers predicted with deterministic methods, presented in figure 7.3. The predicted service life ( $d_c=50$  mm) is 32 and 18 years with probabilistic methods ( $\beta=2.0$ ) and 5900 and 300 years for exposure in Kattegat (location 4) and in the Atlantic Ocean around Iceland (location 7) respectively. The reason for the extremely long service lives predicted with deterministic methods is that  $C_{SN}$  is just slightly larger than  $C_{crit}$ . Obviously there is a large difference between the service lives predicted with probabilistic and deterministic methods. This indicates that the uncertainties of the parameters in the model have a large influence on the service life predictions and consequently if the uncertainties can be reduced the service life will be prolonged. There are several ways to reduce the uncertainties, e.g. by controlling the concrete composition, compaction of concrete and/or placement of the reinforcement etc. An illustration of the effects of the uncertainties in the placement of reinforcement are shown in figure 7.13d.

The effect of  $C_{crit}$  can be studied if the calculated reliabilities for location 4 ( $C_{crit}=0.60$  and  $2.00$  [% by wt Cl/binder]) are compared. With  $\beta=2.0$  ( $d_c=50$  mm) the predicted service life varies between 32 and 3 years, with  $C_{crit}=0.60$  and  $2.00$  [% by wt Cl/binder]

respectively. Obviously  $C_{crit}$ , together with its scatter, has great influence on the predictions of service life. The effect of the level of  $C_{crit}$  (for exposure in Träslövsläge) is illustrated in figure 7.13b. The following levels of  $C_{crit}$  have been studied: 0.60, 0.75, 1.25, 1.50, 2.00, 2.50 and 3.00 [% by weight Cl/binder].

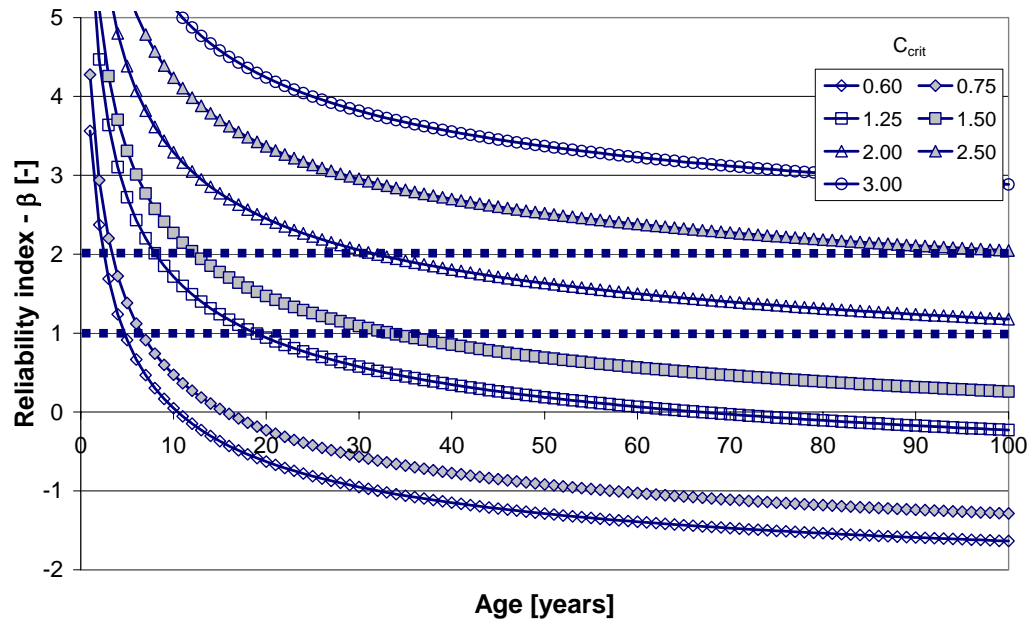


Figure 7.13b: Reliability as a function of the exposure time (marine conditions - Kattegat). Effect of level of  $C_{crit}$ .

From figure 7.13b the effect of the level of  $C_{crit}$  on the predicted service life is obvious. Depending on the chosen level of  $C_{crit}$  the predicted service life ( $\beta=2.0$ ) varies between 3 years ( $C_{crit}=0.60$  [% by wt Cl/binder]) and >100 years ( $C_{crit}>2.50$  [% by wt Cl/binder]).

The effect of the thickness of the concrete cover,  $d_c$ , is illustrated in figure 7.13c. The following concrete covers have been studied in the calculations: 30, 40, 50, 50, 70, 80, 90 and 100 mm. The standard deviation, SD, has been equal to 5 mm in all calculations.

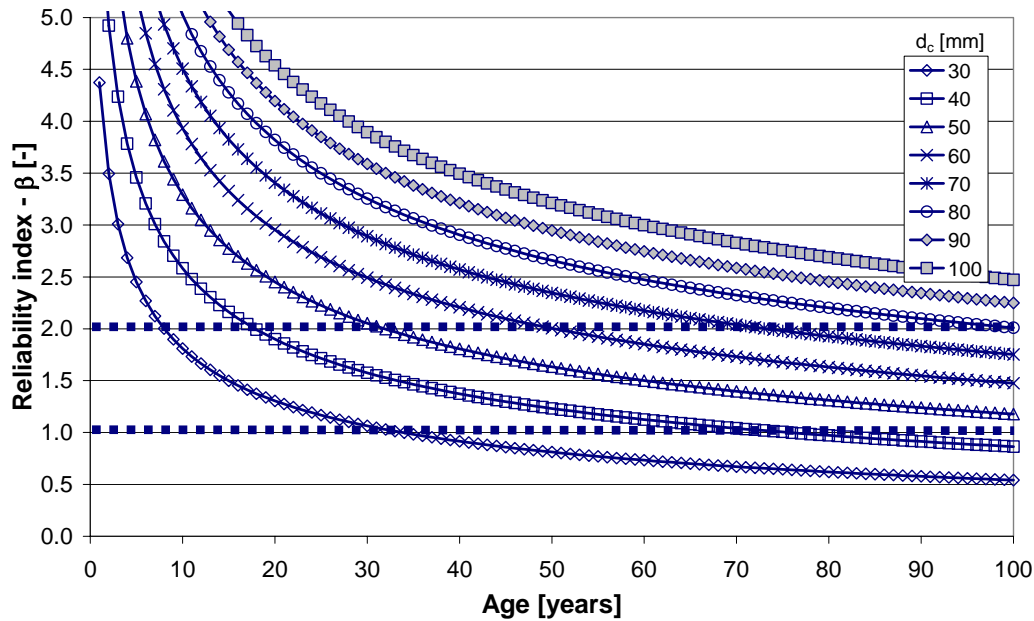


Figure 7.13c: Reliability as a function of the exposure time (marine conditions - Kattgat). Effect of thickness of concrete cover.

From figure 7.13c the effect of  $d_c$  on the predicted service life is obvious, with the predicted service life ( $\beta=2.0$ ) varying between 9 years and >100 years. As expected the predicted service life increases with increasing thickness of the concrete covers,  $d_c$ , with the longest service life achieved for  $d_c=100$  mm.

The effect of uncertainties of the concrete cover,  $d_c$ , is illustrated in figure 7.13d. The uncertainty has been expressed as standard deviations, SD, of the concrete covers, with the following SD included in the calculations: 3, 10, 15, 20, 25 and 30 mm. Calculations have been made for concrete covers of both 50 mm and 60 mm. The indexes denote the mean concrete cover and the standard deviation, where for example 50/10 denotes 50 mm mean concrete cover and 10 mm standard deviation.

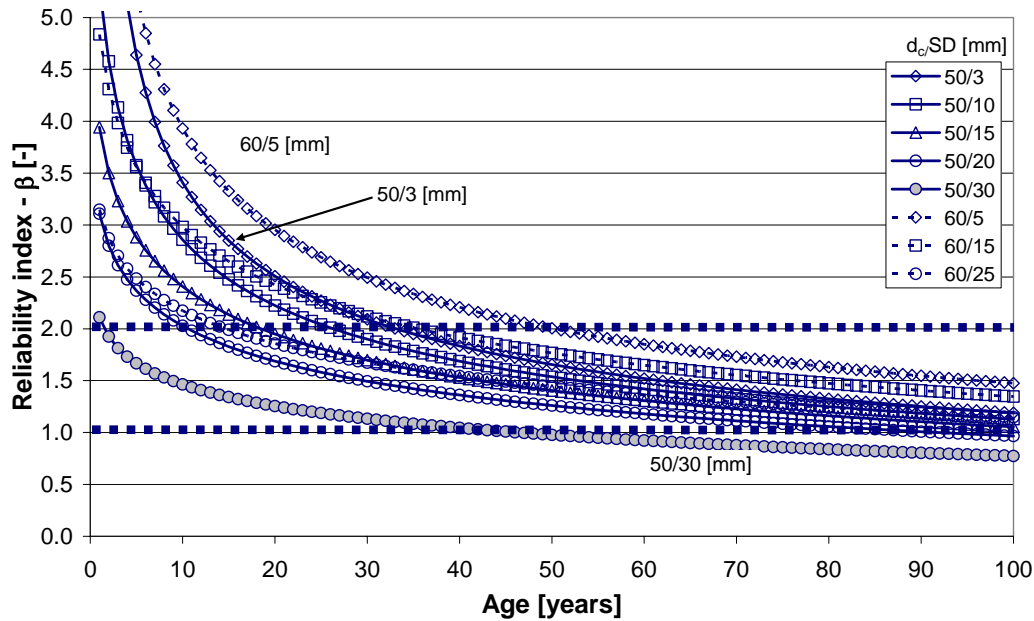


Figure 7.13d: Reliability as a function of the exposure time (marine conditions). Limit state defined as initiation of reinforcement corrosion. Effect of uncertainties in concrete cover.

From the results presented in figure 7.13d it can be concluded that the uncertainty of the concrete cover has a large influence on the predicted service life. The shortest and longest service life is predicted for the concrete cover with the largest and smallest standard deviations respectively (50/30 [mm] and 50/3 [mm]). Furthermore if the mean concrete cover is increased to 60 mm the predicted service life will also increase even if the standard deviation is fairly large – the predicted service lives for 50/3 and 60/16 are similar (34 years with  $\beta=2.0$ ). Consequently if the thickness of  $d_c$  is uncertain the mean concrete cover has to be increased significantly to achieve longer service life.

In figure 7.14 the effects of orientation towards traffic and height above the road are illustrated (exposure in Göteborg). The predictions have been made for a road with 100 km/h speed limit and high traffic intensity. The temperature conditions have been equal to the air temperature. The indexes FT and TT denote surfaces facing away from and towards the traffic respectively and only vertical surfaces have been considered. The distances to and heights above the road are indicated in the figure.

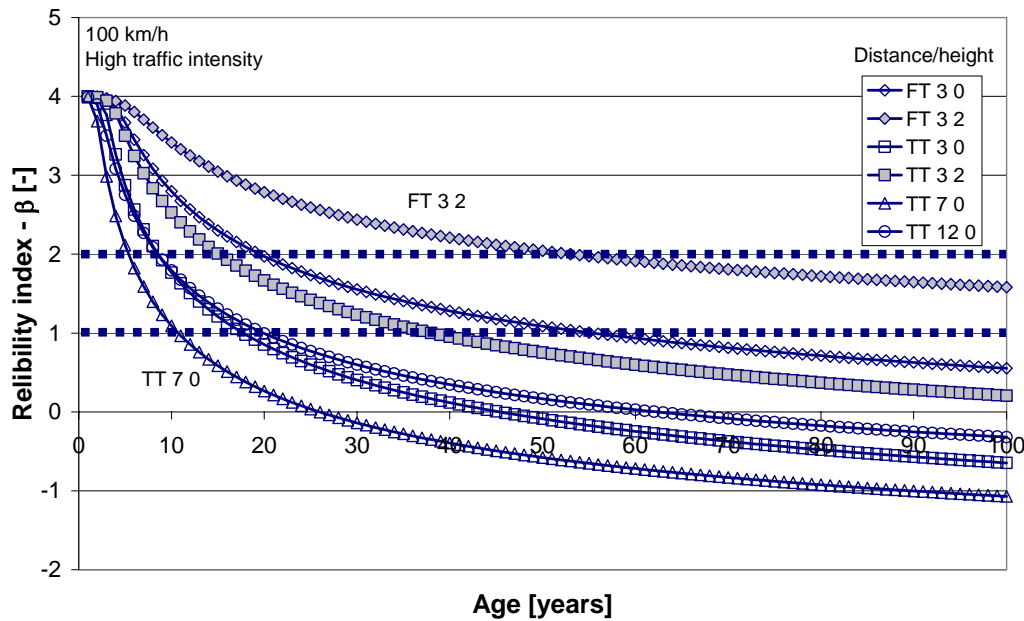


Figure 7.14: Reliability as a function of the exposure time (road conditions – Göteborg). Effect of orientation towards traffic and distance to and height above the road.

As seen in figure 7.14 the orientation, distance and height above the road have a large influence on the reliability of the structures and thus the predicted service life, where they vary between 6 years and 54 years ( $\beta=2.0$ ). The shortest service life is predicted for surfaces facing towards the traffic at 7.0 m from the road and at height 0.0 m (TT 7 0) and the longest service life is predicted for surfaces facing away from the traffic at 3.0 m from the road and at 2.0 m height (FT 3 2). The reason that the service life is shorter for the surface (TT 7 0) than for (TT 3 0 facing towards the traffic at 3.0 m from the road and at height 0.0 m) is the higher value of  $k_{D,e}$ , for (TT 7 0), due to a higher moisture content in the concrete in the wet splash zone than in the dry splash zone.

The service lives predicted with probabilistic methods, presented in figure 7.14, have been compared with predictions made with deterministic methods, presented in figures 7.6a and 7.9a. The service lives predicted with probabilistic methods ( $\beta=2.0$  and  $d_c=50$  mm) are 6 years and 16 years for surfaces facing towards the traffic at 7.0 m distance/0.0 m height and 3.0 m distance/2.0 m height respectively. The service lives predicted with deterministic methods for the same surfaces are 26 and 136 years respectively. As discussed earlier, the uncertainties of the parameters in the prediction model have a large influence on the service life predictions and consequently if the uncertainties can be reduced the service life will be prolonged.

The results presented in figure 7.14 indicate that reinforcement corrosion should be initiated after only 6 years' exposure (surfaces with index TT 7 0). However, the measurements of chloride ingress made in concrete road bridges after 24-30 years exposure indicate that reinforcement corrosion has not been initiated (at least there are no visible signs of reinforcement corrosion at the surface of the concrete), cf. Lindvall & Andersen (2000). Either the model with the quantified parameters is too pessimistic, or the reinforcement is corroding but it has not been observed, since there are no visible signs of corrosion at the surface of the concrete. There are several explanations for the fact that the model and the quantified parameters predict too short service lives, e.g. some

of the quantified parameters have values that are not representative or the standard deviation are too large (representing a pessimistic approach to the uncertainties). An example of a parameter that may have a non-representative value is  $C_{crit}$  – where a constant  $C_{crit}$  has been used in all predictions (independent of temperature etc). As discussed the level of  $C_{crit}$  is of great importance for the predictions of service life.

From the results of the probabilistic calculations presented in figures 7.13a-7.13d and 7.14 it is obvious that the uncertainties and variations in the parameters in the DuraCrete chloride ingress model have a large influence on the predicted service life. The results of the field studies, presented in chapters 4 and 5, show that there are large variations in for example severity in exposure to chlorides, even on one single structure, which shows the significance of considering uncertainties and variations in the boundary conditions in the service life predictions. Therefore, the most accurate service life predictions are probably made with probabilistic methods. With probabilistic methods it is also possible to clarify how the uncertainties in the parameters in the model influence the service life predictions and what consequences reductions of the uncertainties will have. However, probabilistic methods also require that the parameters in the prediction model are statistically quantified, which may require fairly large amounts of data. If low quality data are used for the statistical quantification, the results of the probabilistic calculations may have large uncertainties, cf. Lindvall & Nilsson (2001). Therefore it is important to use data of (fairly) high quality for the statistical quantifications.

## 7.8 Conclusions

In the following sections, conclusions based on the results of the predictions of chloride ingress and service life presented in this chapter are set out. More general conclusions drawn from the work presented in this thesis are presented in chapter 8 “Final discussion and conclusions”.

### 7.8.1 General

The following general conclusions have been drawn from the predictions of chloride ingress and service life:

- Calibration of model.** In marine submerged conditions the model underestimated the chloride contents. In road conditions the model made realistic predictions of chloride ingress in the dry splash zone (vertical surfaces) and overestimated the chloride ingress in the wet splash zone (horizontal surfaces).  
 The underestimation of the chloride ingress in marine submerged conditions was explained by a too low  $C_{SN}$  in the predictions. It was suggested to model  $C_{SN}$  as time-dependent, where  $C_{SN}$  should increase with increasing exposure time. However, since  $C_{SN}$  in the DuraCrete chloride ingress model is constant with time, it was decided to use the originally quantified parameters in the predictions of chloride ingress in marine conditions.  
 The overestimation of the chloride ingress in the wet splash zone was explained by too high  $C_{SN}$  in the predictions. It was therefore suggested to decrease the originally quantified  $C_{SN}$  by a factor 0.7.
- Significance of exposure conditions.** The results of the predictions of chloride ingress and service life demonstrate the significance of the exposure conditions. The exposure conditions directly influence both  $C_{SN}$ , i.e. the driving potential for chlorides, and  $D_a(t)$ , i.e. the transport properties for chlorides in concrete. Furthermore the exposure conditions influence the chloride binding in concrete, which influences the level of both  $C_{SN}$  and the chloride threshold level,  $C_{crit}$ , if these

are defined as total chloride content in the concrete. Since the chloride binding decreases with increasing temperature, both  $C_{SN}$  and  $C_{crit}$  should therefore decrease with increasing temperature. Additionally  $D_a(t)$  is also influenced by the temperature conditions, with  $D_a(t)$  increasing with increasing temperature. However, the increase in  $D_a(t)$  can also be explained by the temperature effect on the chloride binding. The main influencing factors seem to be the temperature conditions and the severity of the exposure to chlorides. In marine submerged conditions the effect of the temperature conditions, while in the other exposure conditions the severity of the exposure to chlorides, were the most significant. The temperature conditions influence the level of both  $C_{SN}$ ,  $C_{crit}$ , and  $D_a(t)$ , while the severity of exposure to chlorides mainly influences  $C_{SN}$ .

- **Comparison of results from deterministic and probabilistic predictions.** The comparison of the results of predictions made with deterministic and probabilistic methods indicate that the uncertainties of the parameters in the prediction model have a large influence on the service life predictions. The results of field studies also show that there are large variations in for example severity in exposure to chlorides, even on one single structure, which shows the significance of considering uncertainties and variations in the boundary conditions in the service life predictions. Therefore, the most accurate service life predictions are probably made with probabilistic methods. However, the parameters in probabilistic models need to be statistically quantified, which requires fairly large amounts of high quality data. If low quality data are used for the quantification the results of the predictions may have large uncertainties.
- **Drawbacks of model.** The DuraCrete chloride ingress model, chosen as an example model, has some drawbacks, due to simplifications. As an example the model assumes that the conditions at the surface and inside the concrete, e.g. moisture and temperature conditions, are constant over time and also over depth. This means that any effects due to variations in equivalent surface conditions over the structure can only be taken into account in a simplified way.

Another example is the surface chloride content,  $C_{SN}$ , which does not change over time. Instead it would be more realistic to model  $C_{SN}$  as increasing with increasing exposure time, at least in marine submerged conditions.

Additionally the chloride ingress is only considered in one dimension, which means that chloride ingress close to sharp corners, where the transport of chlorides takes place in two or three dimensions, will be underestimated. Physical prediction models, which predict chloride ingress in more than one dimension, should be used instead. Furthermore these models consider variations in moisture and temperature conditions and the way they influence the chloride ingress. However, these models need extensive quantification and validation, which means that for the moment they cannot be used in practice, except in special cases, e.g. in submerged conditions with moisture saturated concrete etc.

### 7.8.2 Marine conditions

The following conclusions have been drawn from the predictions of chloride ingress and service life made in marine conditions:

- **Significance of chloride, moisture and temperature conditions.** The chloride and temperature conditions have been found to be factors that mainly influence the chloride ingress into concrete (for a particular concrete). The moisture conditions were not found to significantly influence the chloride, mainly due to the fact that the moisture content in the concrete is fairly high and thus it has no influence on the

transport of chlorides. However, with a lower moisture content in the concrete the transport of chlorides may completely stop.

In submerged conditions the temperature conditions were found to have the most significant effect, while in the other marine exposure conditions the chloride conditions had the most significant effect on the chloride ingress. The chloride conditions follow from the severity of exposure to chlorides and are mainly a function of the distance to the source of chloride, i.e. position to the water surface. The most severe exposure to chlorides takes place in submerged conditions and the severity decreases with increasing distance above the water surface.

- **Position relative to mean water level and extensions of tidal actions and wave heights.** These factors mainly influence the exposure time to seawater, which affects both the severity of exposure to chlorides and the chloride transport properties in concrete. Obviously there is a large difference in the exposure time to seawater depending on whether the exposure takes place above or below the mean water level in the tidal zone. The exposure time to seawater depends also on the wave heights; a structure is exposed to seawater higher up with high waves than with low waves. Consequently, in the tidal and splash zones, it is important to specify where, in relation to the mean water level the exposed surface is situated.
- **Height above the water surface and distance to coastline** (atmospheric zone). This factor mainly influences the severity of exposure to chlorides in the atmospheric zone, with the exposure less severe with increasing height. This means it is important to specify the height above the water surface and the distance to the coastline of the location of the exposed surface.
- **Movement of airstreams around structures and exposure to/shielding from precipitation.** These factors influence both the severity of exposure to chlorides and the chloride transport properties in concrete. Large differences in the severity of exposure to chlorides have also been observed on existing structures. Examples of variations are airborne chlorides which follow airstreams around concrete structures and which may be deposited on the leeward sides of the structures. Depending on the exposure and shelter from direct precipitation surface-near chlorides in the concrete may either be washed away or deposited.

### 7.8.3 Road conditions

The following conclusions have been drawn from the predictions of chloride ingress and service life made in road conditions:

- **Significance of chloride, moisture and temperature conditions.** The chloride and temperature conditions have been found to be factors that mainly influence the chloride ingress into concrete, with the chloride conditions found to have the most significant effect. In the same way as in marine conditions the moisture conditions were not found to significantly influence the chloride ingress, mainly due to the fact that the moisture content in the concrete is fairly high and thus has no influence on the transport of chlorides.  
The chloride conditions follow from the severity of exposure to chlorides, which can be expressed as a function of the amount of de-icing salt spread on the road and the transport to and exposure on the structure. The most severe exposure to chlorides takes place at the road and the severity decreases with increasing distance to the road. However, since there are many factors that influence the exposure conditions, they may also vary significantly between different structures.
- **Characteristics of traffic, e.g. amount of traffic, type and distribution of vehicles, speeds etc.** These factors mainly influence the severity of exposure to



chlorides, with the severity generally increasing with increasing traffic intensity and speeds. However, if the traffic intensity is too high the speeds are reduced and the exposure to chlorides also gets less severe. The type and distribution of vehicles also influence the exposure to chlorides, with the exposure more severe with increasing numbers of heavy vehicles on the road etc.

- **Orientation towards traffic.** This factor mainly influences the severity of exposure to chlorides, with surfaces facing towards the traffic found to be more severely exposed to chlorides than surfaces facing away from the traffic. Furthermore there is an additional orientation effect for structures along roads with commuter traffic; surfaces facing towards the lanes with (moving) commuter traffic in the morning have more severe exposure to chlorides than other surfaces on the structures. This effect is explained by the fact that de-icing salt is normally spread during the night or early morning and thus structures along the lanes with heaviest (moving) traffic also will have the most exposure to chlorides.
- **Height above and distance to road.** These factors mainly influence the severity of exposure to chlorides, with the severity generally decreasing with increasing height above and distance to the road.
- **Characteristics of road and structure, e.g. surroundings of road, shape of structure etc.** These factors mainly influence the severity of exposure to chlorides; the severity may vary significantly due to sheltering effects, airstreams around structures etc. As an example, airborne chlorides that follow airstreams around concrete structures may be deposited on the leeward sides of the structures. Depending on the exposure and shelter from direct precipitation, surface-near chlorides in the concrete may either be washed away or deposited.



## 8 Final discussion and conclusions

### 8.1 General

The overall conclusions that can be drawn from the material presented in this thesis is that the boundary conditions for chloride ingress, following from the exposure conditions, have, as expected, a decisive influence on the service life. The chloride ingress into concrete has been found to be influenced by a combination of the chloride, moisture and temperature conditions, both at the surface and inside the concrete. Since the chloride, moisture and temperature conditions are different in different exposure environments, the chloride ingress is also different in these environments. Large variations in the exposure conditions have been observed, both between different structures but also within one single structure and even one structural part.

The material presented in this thesis also shows that it is not enough to describe the exposure conditions for a concrete structure exposed in marine or road conditions with rough divisions into exposure zones, without any consideration of the true environmental actions and their variations over the structure. The chloride, moisture and temperature conditions, at the surface and inside the concrete, may vary significantly both between different structures, but also within one single structure. The conditions inside the concrete follow from a combination of the surface conditions and the concrete properties. The variations in surface conditions can be related to variations in the exposure to for example rain and solar radiation, due to sheltering effects etc. To include these effects the surface conditions should be expressed as equivalent surface conditions. Therefore each structure should be treated separately, at least for surfaces above the water level, when the exposure conditions are assessed. However, for economic and practical reasons this is usually not possible, and instead the methodology proposed in this thesis can be used, where the exposure to chlorides is measured in one exposure zone, used as a reference, and transferred to the other zones. For this purpose, models have been developed that describe the exposure conditions in marine and road conditions with the focus on chloride ingress.

However, the traditionally used prediction models, which are based on observations from real structures, so-called empirical models, do not fully consider the effect of equivalent surface conditions and their variations. Sophisticated mathematical prediction models, which are based on theories on how transport and binding of different substances take place in materials, so-called scientific models, should be used instead. These models predict the combined chloride and moisture transport and the influence of temperature conditions. However, the models usually also need extensive quantification of input data and verification, especially in unsaturated concrete but also in saturated concrete, which makes it difficult to make reliable predictions in reality with scientific models, except in some special cases, e.g. water-saturated concrete etc. Therefore, in this thesis, it was

decided to use an empirical model for the calculations of chloride ingress, namely the DuraCrete chloride ingress model.

The definition of the exposure time for concrete structures exposed to chlorides is not trivial. A relevant question is whether the exposure time should be defined as the total time of exposure or the time of exposure to chlorides. It is only in marine submerged conditions, where the total time of exposure is equal to the time of exposure to chlorides, that the definition of the exposure time is not open to question. For surfaces above the level of seawater, which are only periodically exposed to seawater, however, the total time of exposure and the time of exposure to chlorides are not similar. This difference becomes even more significant the longer from the source of chlorides the surface is located. In road conditions the exposure to chlorides only takes place when de-icing salt is spread on the road, which means that the time of exposure to chlorides is approximately only half of the year. The time of exposure to chlorides may be even shorter at locations where de-icing salt is rarely spread. Thus, depending on when during the year the exposure in road conditions is started, the difference between the total time of exposure and exposure to chlorides, during the first year of exposure, can be up to half a year. Penetration of chloride further into the concrete, however, will proceed even after the exposure to chlorides at the surface has ceased. The driving potential for this penetration is the chloride content accumulated in the concrete at a certain depth, originating from earlier exposure to chlorides.

The maturity of the concrete on first exposure to chlorides has been found to have a significant effect on chloride ingress. A difference of only a few weeks' curing time (curing in similar conditions) when the concrete is first exposed to chlorides has been indicated to have a significant effect, with the chloride ingress significantly larger into concrete of low maturity. This effect is even more pronounced for concrete with secondary binders like silica fume, due to the slower reaction rate in these concretes. The effect of maturity is especially significant in environments with periodic exposure to chlorides, i.e. in marine atmospheric and road conditions. In these environments the main part of the chloride ingress has been found to take place during the first season/year of exposure to chlorides, which means that the maturity of the concrete on first exposure to chlorides has a significant influence on the chloride ingress. The development of maturity, together with pore blocking effects, can also be used to explain the observation that the chloride ingress almost stops after the first year of exposure, at least in marine atmospheric and road conditions.

It seems reasonable to model chloride ingress in marine and road conditions with the methodology presented in this thesis. The general idea of the methodology is that the chloride ingress is measured in reference conditions and transferred to different exposure conditions, where effects of height, distance and orientation in relation to the reference conditions are taken into account. With this procedure the overall variations in exposure to chlorides on any structure can be assessed if the exposure to chlorides in the reference conditions is known. In marine conditions the submerged zone (1.0 m depth) and in road conditions the conditions at the road surface (0.0 m distance and height) can be used as reference conditions. The choice of reference conditions in road conditions can be questioned since concrete structures are seldom built just at the road. However, if any other distance or height is chosen, the "reference conditions" will be influenced by distance and orientation to traffic, wind directions etc, which means that they may even vary along the same road. Therefore the conditions at the road surface, which are assumed to be similar over the whole road, have been chosen as equivalent conditions.

The predictions of chloride ingress, made with the chosen model and parameters quantified according to the methodology proposed in this thesis, have been calibrated against measured chloride ingress profiles from concrete structures exposed in marine and road conditions. In marine conditions the predictions underestimate chloride ingress, mainly due to a too low surface chloride content used in the predictions. However, it was decided to use the originally quantified surface chloride content, since the chosen prediction model does not include effects due to time dependent surface chloride contents. In road conditions the predictions correlate fairly well with measured chloride ingress profiles in the dry road environment (vertical surfaces), while in the wet road environment (horizontal surfaces) the predictions overestimate the chloride ingress. The surface chloride content used in the predictions was therefore reduced in the wet road environment, to make the predictions better fit the measurements of chloride ingress. Additionally the model used for the predictions does not consider variations in the chloride transport properties of the cover concrete. Thus many of the influencing factors need further investigations to be better explained and to achieve less uncertainty in the quantification of the parameters in the prediction models.

Obviously, the environmental actions may vary significantly over a structure, with severe exposure at unexpected locations due for example to airstreams and water running through joints etc, and normally the positions with the most severe actions are therefore hard to identify easily. Since these positions are of interest when the condition of the structure is assessed, this means that it is difficult to find sampling points that are representative of the structure. However, one way to identify the most severely exposed positions on a structure is to visually observe the environmental actions on the structure in question during days with severe weather, e.g. windy days with rain. Furthermore structures in road conditions should preferably be visually inspected during snowy days, since for example snow may be deposited on the leeward sides of the structure and shield the concrete from exposure to chlorides. Preferably the visual inspections should be made over a certain period, to facilitate a reliable identification of the environmental actions and their variations over the structure.

One parameter that has been found to have a significant effect on the service life predictions for concretes in different exposure conditions is the effect of the temperature in the concrete on the chloride threshold level,  $C_{crit}$ . The temperature effect should be different depending on whether the chloride content is defined as the total or free chloride content in the concrete. Since both  $C_{crit}$  and the surface chloride content,  $C_{sa}$ , are defined as the chloride content in the concrete the temperature should affect both these parameters. Generally it is believed that the amount of bound chlorides decreases with increasing temperature, which means that the total chloride content would also decrease (if the free chloride content is unchanged). However, data that report any temperature effect on  $C_{crit}$  have not been found in the literature. In this thesis only the temperature effect on  $C_{sa}$  has been considered, which means that, since the total chloride content in the concrete is used in the predictions,  $C_{sa}$  decreases with increasing temperature, while  $C_{crit}$  is constant. The consequence of this is that the required concrete cover also decreases with increasing temperature, which is not realistic. Instead the required concrete cover should increase with increasing temperature, which would be the case if the temperature affected  $C_{crit}$  as well (where  $C_{crit}$  would decrease with increasing temperature).

## 8.2 Marine conditions

The exposure conditions in marine conditions have been found to vary significantly, at least for surfaces above the level of seawater. This means that it is not trivial to describe

and model the exposure conditions for surfaces exposed in marine tidal, splash and atmospheric conditions. The position relative to the seawater level has a significant effect on the severity of exposure to chlorides. Additionally there is also a transport of chlorides over land, which means that not only structures in the sea, but also inland from the coastline, are exposed in marine conditions. However, in this thesis the emphasis has been put on investigating, describing and modelling the severity of exposure to chlorides in different marine submerged conditions and only to some extent for surfaces above the level of seawater.

In submerged conditions the severity of exposure to chlorides, indicated by measurements of chloride ingress into concrete, has been found to be influenced by the temperature and chemical composition of the seawater. The main influencing factor has been found to be the temperature of the seawater, with the total chloride content in the concrete higher at low temperatures, while the chloride transport rate is higher at high temperatures. This can be partly explained by an increasing chloride binding with decreasing temperatures and an increasing chloride transport rate with increasing temperatures.

In the other marine exposure conditions the position relative to the water surface has a significant influence on the severity of exposure to chlorides. Above the seawater level the exposure to chlorides takes place with either splash or spray from breaking waves. The extent and severity of the exposure to chlorides is not completely clarified; for example the exposure conditions in the lower and higher parts of the tidal or splash zones are certainly different. Furthermore airborne chlorides, following spray from breaking waves, may be caught by wind and transported long distances, also inland from the coastline, which means that structures not directly in the sea may also be exposed to marine chlorides. Airborne chlorides may also be deposited on the leeward sides of structures, which means that surfaces facing directly towards the sea may not necessarily have the most severe exposure to chlorides. Furthermore the exposure to and shelter from direct rain have a significant influence on the exposure to chlorides, since chlorides that are deposited on surfaces sheltered from direct rain will not be washed away.

Obviously it is not enough to describe the exposure conditions in marine conditions with rough divisions into exposure zones without any consideration of the true environmental actions and their variations over the structure. The most accurate description of the exposure conditions will be obtained only if each structure is considered separately. However, for economic and practical reasons, this is usually not possible, e.g. when new structures are to be designed and built, and instead it is proposed that the methodology described in this thesis should be used, according to which the exposure to chlorides is measured, or determined from environmental data, in one exposure zone (equivalent conditions) and transferred to the other zones.

### **8.3 Road conditions**

The exposure conditions in road conditions have been found to vary significantly both between different structures but also within one single structural part, e.g. columns. Consequently the exposure conditions in road conditions are not trivial to model, especially the exposure to chlorides, which depends on a combination of the amount of chlorides on the road surface and the transport to the surface of the structure. Furthermore the moisture and temperature conditions, at the surface and inside the concrete, also vary, depending on the exposure to and shelter from direct rain and solar radiation. However, in this thesis the emphasis has been put on investigating, describing and modelling the

severity of exposure to chlorides, and for concrete structures exposed along different roads on which de-icing salt is spread.

The severity of the exposure to chlorides along a road depends on the amount of chlorides available on the road surface. The amount of chlorides on the road surface follows from the amount of de-icing salt spread on the road, which depends on several factors, e.g. the weather conditions, type of road, equipment used for spreading, type of de-icing salt etc. Furthermore the types and amounts of de-icing salt which is spread on roads have changed over time, due to environmental considerations and the development of new spreading methods etc, which means that the amount of chlorides available on the road surface has changed over time. Consequently the available amount of chlorides on a specific road may vary significantly over time, both during one specific year, but especially between different years, which makes it difficult to exactly define the exposure conditions even for one specific road.

The exposure to chlorides also takes place up to a certain distance from and height above the road, since there is a transport of chlorides from the road surface, as splash and spray in both the horizontal and vertical directions, and by drainage. In the horizontal direction the exposure to chlorides is largest at the carriageway and decreases with increasing distance. In the vertical direction the exposure to chlorides has been found to be largest at the level of the carriageway and for surfaces facing towards the traffic. The exposure to chlorides decreases with increasing height above the road. Additionally the transport of chlorides in both the horizontal and vertical directions from the road depends on the characteristics of traffic, e.g. traffic intensity and speeds, types of vehicles etc, and the weather conditions, with the amount of splash and spray larger when the road surface is moist. Since the characteristics of the traffic and the weather conditions are different for different bridges it is hard to generalise the description of the exposure conditions in road conditions.

Obviously, it is not enough to describe the exposure conditions along thaw-salted roads with rough divisions into general exposure zones. The exposure to chlorides is mainly influenced by the amounts of chlorides on the road surfaces and the speed of the traffic. Furthermore, the occasions when de-icing salt is spread on the road affect the amount of chlorides on the road surface. The amounts and occasions of de-icing salt spread depend on several factors, which means that the amount of de-icing salt may vary significantly both between different roads but also along one road. Furthermore the amounts of de-icing salt that are spread have decreased in recent years, due to environmental considerations but also changes in the types of spreading equipment etc. The transport of chlorides from the road surface to the surroundings is also influenced by several factors, with the significance of the factors being more or less unique for each structure. This means it is difficult to directly compare the severity of exposure to chlorides on different structures, even if they are exposed fairly close to each other along the same road. Thus the most accurate description of the exposure conditions will be obtained if each structure is considered separately. However, for economic and practical reasons, this is usually not possible, e.g. if a new structure is to be designed and built, and instead it is proposed that the methodology described in this thesis should be used, where the exposure to chlorides is measured in one exposure zone (equivalent conditions) and transferred to the other zones.





## 9 Future research

Obviously, many of the factors that influence the service life of reinforced concrete structures need to be further investigated. The object of these further investigations is to learn more about the influencing factors and the way they are related to each other, and in this way reduce uncertainties in service life predictions. This means that the service life predictions can be better used to make more optimal designs and also to better plan and optimize for future inspections and maintenance.

In the following sections proposals are given for future research, first from a general point of view and then more specifically for marine and road conditions. Since this thesis has only treated the influence of the exposure conditions on initiation of reinforcement corrosion, only proposals for future research into the influence of the exposure conditions are presented. A division has been made into proposals for future research regarding chloride ingress in general, and more specifically chloride ingress under marine and road conditions.

### 9.1 Chloride ingress – in general

Based on the overall results of the study presented in this thesis the following is proposed for future research, to be further investigated and explained:

- Factors influencing chloride transport properties in concrete and surface chloride conditions.** The results presented in this thesis show that more data are needed on the relation between the driving potential and the transport properties of chlorides, and their variations, for chloride penetration into concrete and influencing factors. Examples of influencing factors are chloride, moisture and temperature conditions in the concrete together with the chloride concentration in the solution at the surface of the concrete.

The significance of these factors can for example be investigated by parallel measurements of chloride, moisture and temperature conditions in concrete exposed in both field and laboratory conditions. The exposure should be made in different chloride and temperature conditions. To avoid any influence due to the concrete properties similar concrete compositions should be used. Furthermore the chloride transport properties over time need to be further investigated and quantified.
- Factors influencing chloride binding and the chloride threshold level,  $C_{crit}$ .** The results presented in this thesis show that the chloride binding has a large effect on chloride penetration into concrete and the chloride threshold level,  $C_{crit}$ . Therefore more data are needed on the significance of the factors that influence the chloride binding, e.g. pH, moisture and temperature conditions in the concrete, chloride content in concrete etc. The results of the service life predictions presented in this thesis show that one factor that has a large effect on  $C_{crit}$  is the temperature of the

concrete. However, no data have been found in the literature regarding this effect and therefore more research is needed.

The significance of the factors influencing chloride binding can for example be investigated by measurements of chloride binding isotherms for concrete exposed in different conditions, e.g. moisture and temperature conditions etc, in both field and laboratory conditions. Parallel with these measurements the chloride threshold level should also be determined. This can be done by determinations of the chloride content at the reinforcement together with investigations of the corrosion activity (either visually or with indicative methods, e.g. potential measurements etc).

- **Significance of the maturity of concrete on first exposure to chlorides.** The maturity of the concrete on first exposure to chlorides has been indicated to have a significant influence on chloride ingress, cf. Lindvall (2002b). Therefore it is proposed to further study the influence of the maturity of concrete on first exposure to chlorides and the corresponding chloride ingress. Additionally the differences between the effect of maturity for pure Portland cement concrete and concrete with secondary binders need also to be further investigated.  
The effect of the maturity of concrete on first exposure to chlorides can for example be investigated by measurements of chloride ingress into concretes of different compositions exposed in similar exposure conditions at different ages.
- **Definition of exposure time.** The definition of the exposure time (total time of exposure or time of exposure to chlorides) and its influence on the evaluation of measured chloride ingress profiles need to be further investigated. Furthermore the observations that the chloride ingress stops after a certain exposure time, cf. de Rooij & Polder (2002) and Lindvall (2002b), needs to be further investigated to arrive at a better explanation. There are some earlier investigations where the effect of differences in total time of exposure and time of exposure to chlorides can be determined, cf. Tang (1997) where concrete specimens have been exposed in artificial tidal conditions in the laboratory. However, data are also needed from concrete exposed in field conditions, in both marine and road conditions.  
The influence of the definition of exposure time can for example be investigated by measurements and analyses of chloride ingress into concrete periodically exposed to chlorides, e.g. in road conditions. Parallel with measurements of chloride ingress, both the total time of exposure and the time of exposure to chlorides are registered. The time of exposure to chlorides can be determined as the time when the concrete is exposed to seawater, in marine tidal and splash conditions, or when chlorides are available on and transported from thaw-salted roads and deposited on concrete. The availability and transport of chlorides from road surfaces depend on several factors, e.g. spread of de-icing salt, moisture conditions on the road surface, wind speeds and directions, characteristics of traffic etc.

## 9.2 Marine conditions

Based on the results of the investigations and predictions of chloride ingress into concrete exposed in marine conditions the following is proposed for future research, to be further investigated and explained:

- **Exposure conditions in marine submerged conditions.** More data are needed on exposure conditions in marine submerged conditions, e.g. the influence of the chemical composition and temperature of seawater and depth. These factors have to some extent been investigated in the study in marine conditions presented in this

thesis, but they need to be further investigated so that they may be more accurately quantified and the uncertainties of the parameters  $C_{SN,eq}$ ,  $k_{C,Cl}$ ,  $k_{C,T}$  and  $k_{D,T}$  in eq. (6.1a) and (6.1b) reduced in this way.

The exposure conditions and their variations in submerged conditions can for example be investigated by making field studies like the one presented in this thesis, both at similar and other exposure locations. The focus of these additional field studies should be to further investigate the influencing factors in marine submerged conditions, and the way they are correlated to each other, to reduce the uncertainties in the parameters used in service life models. Furthermore chloride, moisture and temperature conditions could be studied in concrete exposed at different depths, to further investigate the effect of depth below the water surface.

- **Exposure conditions in marine tidal and splash conditions.** The variations in exposure conditions in the marine tidal and splash zones, e.g. the way the position relative to the mean water level influences the exposure to chlorides and direct rain, need to be further investigated. An example of what should be investigated is how the exposure to chlorides varies between the lower and higher parts of the tidal zone. Other proposals for future research are the way the extent of the splash zone can be expressed as a function of the wave heights, the geometry of the structure and possible shelter from direct rain. Data on the influence of these factors can be used to quantify and reduce the uncertainties of the parameters  $k_{C,d}$ ,  $k_{C,h}$ ,  $k_{C,o}$ ,  $k_{C,T}$ ,  $k_{D,RH}$  and  $k_{D,T}$  in eq. (6.1a) and (6.1b).

The exposure conditions and their variations in tidal, splash and atmospheric conditions can for example be studied by making parallel investigations of the chloride, moisture and temperature conditions in concrete together with measurements of the exposure to chlorides at different positions on one single structure. To exclude any effects due to variations in concrete properties, concrete specimens manufactured under similar conditions should be used for the exposure.

- **Exposure conditions in the marine atmospheric zone.** Additional data are needed on how the exposure conditions in the atmospheric zone vary, e.g. the way the height above the water surface, the geometry of the structure, surface orientation and possible shelter from direct rain influence the exposure to chlorides and direct rain. Other proposals for future research are the way the exposure to chlorides over land varies depending on the distance to the coastline and wind directions and speeds. Data on the influence of these factors can be used to quantify and reduce the uncertainties of the parameters  $k_{C,d}$ ,  $k_{C,h}$ ,  $k_{C,o}$ ,  $k_{C,T}$ ,  $k_{D,RH}$  and  $k_{D,T}$  in eq. (6.1a) and (6.1b).

The exposure conditions and their variations in the marine atmospheric zone can for example be studied by making parallel investigations of the chloride, moisture and temperature conditions in the concrete together with measurements of the exposure to chlorides at different positions on one single structure and/or at different distances from the coastline. To exclude any effects due to variations in concrete properties, concrete specimens manufactured under similar conditions should be used for the exposure.

- **Significance of marine growth.** Data are needed on the way marine growth influences the severity of exposure to chlorides, especially in submerged conditions, but also in other marine exposure conditions. The influence of marine growth can for example be studied by parallel investigations of chloride ingress into surfaces that are cleaned and not cleaned from marine growth

during the exposure. To exclude any effects due to variations in concrete properties, concrete specimens manufactured under similar conditions should be used for the exposure.

### 9.3 Road conditions

Based on the results of the investigations and predictions of chloride ingress into concrete exposed in marine conditions the following is proposed for future research, to be further investigated and explained:

- Significance of spreading of de-icing salt.** The spreading of de-icing salt on roads and the way this influences the exposure conditions need to be further investigated, e.g. how the exposure to chlorides can be correlated with the amount of chlorides that is available on the road surface. The amount of chlorides available on the road surface can be correlated to the amount and type of de-icing salt spread on the road and this correlation needs to be further investigated. The amount of chlorides spread on the road may vary significantly between different structures and over time, due to weather conditions, characteristics of the road and traffic etc. These data can be used to quantify and reduce the uncertainties of the parameters  $C_{SN,eq}$  and  $k_{C,Cl}$  in eq (6.1a). The influence due to spreading of de-icing salt can for example be investigated by making parallel studies of the spread of de-icing salt on a road and the chloride ingress into concrete exposed along the same road. Additionally parallel registrations of the amounts of de-icing salt spread on the road together with measurements of the chloride concentration in the surface water on the road should be made. To exclude any effects due to variations in concrete properties, concrete specimens manufactured under similar conditions should be used for the exposure.
- Significance of characteristics of road and traffic (types of vehicles, speed and intensity).** More data are needed on how the characteristics of the road and traffic influence the exposure conditions. Examples of factors that influence the road characteristics, and need to be further investigated, are the type of road, number of lanes, presence of hard shoulders etc, and traffic. Factors that influence the traffic characteristics and that need to be further investigated are e.g. types of vehicles (amount of heavy traffic), speed and/or traffic intensity etc. The characteristics of road and traffic influence both the amount of de-icing salt spread on the road, since more de-icing salt is spread on main roads than local roads, and the transport of chlorides from the road to the surroundings, with higher speeds giving a larger transport of chlorides etc. Data on the influence of the characteristics of the road and traffic can be used to quantify and reduce the uncertainties of the parameters  $C_{SN,eq}$ ,  $k_{C,Cl}$ ,  $k_{C,d}$ ,  $k_{C,h}$  and  $k_{C,o}$  in eq (6.1a). The effects due to the characteristics of road and traffic on the exposure conditions can be investigated by making parallel investigations of the chloride, moisture and temperature conditions in the concrete together measurements of the exposure to chlorides on concrete exposed along different roads. Preferably the investigations should be made at similar positions relative to the road on all investigated structures, to exclude any effects due to the position relative to the road etc. However, it is difficult to only investigate how just one of the factors which describe the characteristics of the road and the traffic will influence the exposure to chlorides, since usually several factors vary between different roads. To exclude any effects due to variations in concrete properties, concrete specimens manufactured under similar conditions should be used for the exposure.

- **Significance of distance to and height above road.** The influence of the distance to and height above the road on the severity of exposure to chlorides needs to be further investigated. The exposure to chlorides at the road depends principally on the characteristics of the road and the traffic. The exposure of road structures to chlorides, at a certain distance to and height above the road, depends also on their distance to and height above the road, since the severity of the exposure decreases with increasing distance and height. This decrease is also partly influenced by the characteristics of the road and traffic, with the chlorides spread over a longer distance at high speeds and traffic intensities. However, the effects of the distance to and height above the road are not fully known, which means that the shape of the curve describing the decrease in the exposure to chlorides with increasing distance and height has large uncertainties. Data on the influence of the distance to and height above the road can be used to quantify and reduce the uncertainties of the parameters  $k_{C,d}$  and  $k_{C,h}$  in eq. (6.1a).

The effect of the distance to and height above the road can for example be investigated by parallel measurements of the exposure to chlorides at different distances and/or heights above the road on one single structure. If data from different structures are combined, the effects due to the characteristics of the road and traffic will also be included in the comparison. To exclude any effects due to variations in concrete properties, concrete specimens manufactured under similar conditions should be used for the exposure.

- **Significance of orientation towards traffic.** More data are needed on how the orientation towards the traffic influences the severity of the exposure to chlorides. The effect of the orientation towards the traffic is especially significant close to large cities with commuter traffic during the morning and afternoon. However, the significance of the effect of orientation towards the traffic on the severity of exposure to chlorides is still uncertain, since data presented in this thesis come from only two specific bridges. Data on the influence of the orientation towards the traffic can be used to quantify and reduce the uncertainties of the parameter  $k_{C,o}$  in eq (6.1a).

However, this requires data from more structures to get a more general picture of the significance of the surface orientation.

The effect of the orientation towards the traffic can for example be investigated by parallel measurements of the exposure to chlorides around columns, with different orientations towards the traffic, at the same heights above and distances to the road. To exclude any effects due to variations in concrete properties, concrete or mortar specimens manufactured under similar conditions should be used for the exposure.

- **Significance of exposure to and shelter from direct rain.** Additional data are needed on how exposure to and shelter from direct rain influence the exposure to chlorides. Chlorides in the concrete close to the surface of structural elements exposed to direct rain may be washed away, while on structural elements sheltered from direct rain the chlorides may instead be enriched. Furthermore the exposure to direct rain has an influence on the moisture conditions in the concrete and consequently on the transport of chlorides. Data on the influence of the exposure to and shelter from direct rain can be used to quantify and reduce the uncertainties of mainly the parameter  $k_{D,RH}$  in eq. (6.1b).

The effects due to the exposure to and shelter from direct rain can for example be investigated by parallel measurements of the chloride and moisture conditions in concrete on one single structure, exposed to and sheltered from direct rain. To

exclude any effects due to variations in concrete properties, concrete specimens manufactured under similar conditions should be used for the exposure.

## 10 References

AASHTO (1984), Standard Method of Sampling and Testing for Total Chloride Ion in Concrete and Concrete Raw Materials, American Association of State Highway and Transportation Officials, Designation: T 260-84, Washington, 1984.

Alavizadeh-Farhang, A. & Paulsson, J. (1997), Measurements on seasonal and daily temperature distribution across a concrete bridge slab due to change of ambient temperature and solar radiation, in proceedings of *Nordic Mini-seminar of the Nordic Concrete Federation on Moisture Measurements in Concrete Constructions Exposed to Temperature and Moisture Variations*, VTT Symposium No. 174, Espoo, 1997, pp. 20-42.

Alonso, C., Andrade, C., Castellote, M. & Castro, P. (2000), Chloride threshold values to depassivate reinforcing bars embedded in a standardized OPC mortar, *Cement and Concrete Research*, Vol. 30. No. 7, 2000, pp. 1047-1055.

Andersen, A. (1996), Moisture and chloride profiles in a column in the Vejle fjord bridge after 18 years of exposure to marine environment, Publication P-96:7, Department of Building Materials, Chalmers University of Technology, Göteborg, 1996. 12 pp.

Andersen, A. (1997), Investigation of chloride penetration into bridge columns exposed to de-icing salt, HETEK-report No. 82, Danish Road Directorate, Copenhagen, 1997, 37 pp.

Andersen, A., Hjelm, S., Janz, M., Johannesson, B., Pettersson, K., Sandberg, P., Sørensen, H., Tang, L. & Woltze, K. (1998), Total chloride profiles in uncracked concrete exposed at Träslövsläge Marine Field Station, Report TVBM-7126, Division of Building Materials, Lund Institute of Technology, Lund, 1998.

Andersson, L.G. (2001), Personal communication, Department of analytical and marine chemistry, Chalmers University of Technology, Göteborg, 2001.

Åstebøl, S.O., Pedersen, P.A., Røhr, P.K., Fostad, O. & Soldal, O. (1996), Effekter av veisaltning på jord, vann og vegetasjon (The effects from salting of roads on soil, water and vegetation), MITRA No 05/95, Forskningsparken i Ås AS, Oslo, 1996, 63 pp. (in Norwegian).

Bäckman, L. (1980), Vintervägsaltets miljöpåverkan (The environmental impact of de-icing salt), VTI-rapport nr. 197, Swedish National Road and Transport Research Institute, Linköping, 1980, 62 pp. (in Swedish)

Basheer, L., Kropp, J. & Cleland, D.J. (2001), Assessment of the durability of concrete from its permeation properties: a review, *Construction and Building Materials*, No. 15,

pp. 93-103, 2001.

Bentz, D.P. (2000), A Computer Model to Predict the Surface Temperature and Time-of-Wetness of Concrete Pavements and Bridge Decks, NISTIR 6551, Building and Fire Research Laboratory, National Institute of Standards and Technology, Gaithersburg, 2000, 19 pp.

Bentz, E.C. & Thomas, M.D.A (2001), Life-365 Service Life Prediction Model - Computer Program for Predicting the Service Life and Life-Cycle Costs of Reinforced Concrete Exposed to Chlorides, *Manual to Life-365*, W. R. Grace Construction Products, Master Builders, and the Silica Fume Association, 2001, 56 pp.

Blomqvist, G. & Johansson, E.-L. (1999), Airborne spreading and deposition of de-icing salt – a case study, *The Science of the Total Environment*, Vol. 235, 1999, pp. 161-168.

Blomqvist, G. (1998), Impact of De-icing Salt on Roadside Vegetation – A Literature Review, VTI rapport 427A, Swedish National Road and Transport Research Institute, Linköping, 1998, 35 pp.

Boddy, A., Bentz, E., Thomas, M.D.A. & Hooton, R.D. (1999), An overview and sensitivity study of a multimechanistic chloride transport model, *Cement and Concrete Research*, Vol. 29, No. 6, 1999, pp. 827-837.

Borlinger, A. (1996), The Heat Exchange between Building Surfaces and their Environment, in proceedings of the 4<sup>th</sup> *Symposium on Building Physics in the Nordic Countries*, Helsinki, 1996.

Box, G.E.P., Hunter, W.G. & Hunter, J.S. (1978), Statistics for Experimenters, John Wiley & Sons, New York, 1978, 653 pp.

Bradshaw, A., Hung, B. & Walmsley, T. (1995), Trees in the Urban Landscape. Principles of Practice, E. & FN. Spon, London, 1995. 272 pp.

Broomfield, J. P. (1997), Rebar corrosion – What do we know for sure, in proceedings of *International Conference on Repair of Concrete Structures – From Theory to Practice in a Marine Environment* (edited by A. Blankvoll), Svolvær, 1997, pp. 35-47.

Burton, R. (1992), Scourge of the Planes, *The Horticulturist*, No. 3, Vol. 1, 1982, pp 28-30.

CEB (1989), Durable Concrete Structures, Bulletin 183, Comité Euro-International du Béton (CEB), Lausanne, 1989, 120 pp.

CEB (1997), New Approach to Durability Design – An example for carbonation induced corrosion, Bulletin 238, Comité Euro-International du Béton (CEB), Lausanne, 1997, 138 pp.

Climent, M.A., de Vera, G., López, J., García, C. & Andrade, C. (2000), Transport of Chloride through non-saturated concrete after an initial limited chloride supply, in proceedings of the 2<sup>nd</sup> *International RILEM Workshop on Testing and Modelling the Chloride Ingress into Concrete* (edited by C. Andrade & J. Kropp), Paris, September



2000, pp. 173-187.

Concrete in coastal structures (1998), edited by R.T.L. Allen, Thomas Telford, London, 1998, 301 pp.

Crank, J. (1975), The Mathematics of Diffusion, Oxford Science Publications, 2<sup>nd</sup> edition, New York, 1975. 414 pp.

DMI (1994), Jordens klima – Guide til vejr og klima i 156 lande (The climate of the Earth – Guide to weather and climate in 156 countries), edited by Juncher-Jensen, J. & Cappelen, J., Danish Meteorological Institute, Copenhagen, 1994, 259 pp. (in Danish).

Dobson, M.C. (1991), De-icing Salt Damages to Trees and Shrubs, Forestry Commission Bulletin 101, HMSO, London, 1991, 64 pp.

Dragstedt, J. (1980), Vejsalt og vejtræer (De-icing salt and roadside trees), Laboratorierapport 46, Statens Vejlaboratorium, Roskilde, 1980, 77 pp. (in Danish)

DuraCrete (1997), Design Framework, Document BE95-1347/R1, The European Union – Brite EuRam III, Contract BRPR-CT95-0132, Project BE95-1347, CUR, Gouda, 1997, 165 pp.

DuraCrete (1998), Modelling of Degradation, Document BE95-1347/R4-5, The European Union – Brite EuRam III, Contract BRPR-CT95-0132, Project BE95-1347, CUR, Gouda, 1998, 174 pp.

DuraCrete (1999), Models for Environmental Actions on Concrete Structures, Document BE95-1347/R3, The European Union – Brite EuRam III, Contract BRPR-CT95-0132, Project BE95-1347, CUR, Gouda, 1999, 273 pp.

DuraCrete (2000a), Statistical Quantification of the Variable in the Limit State Functions, Document BE95-1347/R9, The European Union – Brite EuRam III, Contract BRPR-CT95-0132, Project BE95-1347, CUR, Gouda, 2000, 130 pp.

DuraCrete (2000b), General Guidelines for Durability Design and Redesign, Document BE95-1347/R15, The European Union – Brite EuRam III, Contract BRPR-CT95-0132, Project BE95-1347, CUR, Gouda, 2000.

Eliasson, Å (1996), Spridning av vägsalt kring vägar (The spread of de-icing salt around roads), Project work 20p, Department of Physical Geography, University of Göteborg, Göteborg. 1996, 34 pp. (in Swedish).

Fagerlund, G. & Svärd, J. (2001), Kartering av kloridbelastning vid Riksväg 40 – Resultat från 5 vintersäsonger (Mapping of the chloride load around a Swedish main road exposed to de-icing salts – Results after 5 winter seasons), Report TVBM-7162, Division of Building Materials, Lund Technical University, Lund, 2001, 12 pp. (in Swedish).

Fitzpatrick, R.A. (1996), Corrosion of concrete structures in coastal areas, *Concrete International*, Vol. 18, No. 7, 1996, pp. 46-47.

Fluge, F. (1997), Environmental loads on coastal bridges, in proceedings of *International*

*Conference on Repair of Concrete Structures – From Theory to Practice in a Marine Environment*, Svolvær, 1997, pp 89-98.

Frederiksen, J.M. (2000), Chloride threshold values for service life design, in proceedings of the 2<sup>nd</sup> *International RILEM Workshop on Testing and Modelling the Chloride Ingress into Concrete* (edited by C. Andrade & J. Kropp), Paris, September 2000, pp. 397-414.

Frederiksen, J.M. (2001), How to apply the HETEK model in the road environment – 1999, in proceedings of Nordic Miniseminar of *Prediction Models for Chloride ingress and corrosion initiation in concrete structures* (edited by L.-O. Nilsson), Publication P-01:6, Department of Building Materials, Chalmers University of Technology, Göteborg, 2001.

Frey, R., Balogh, T. & Balázs, G.L. (1994), Kinetic method to analyse chloride diffusion in various concrete, *Cement and Concrete Research*, Vol. 24, No. 5, 1994, pp. 863-873.

Gaal, G.C.M., van Beek, A., Bakker, J.D. & Walraven, J.C. (2003), Coefficient of diffusion derived from structures exposed to chloride more then 60 years old, in the proceedings of 2<sup>nd</sup> *International RILEM Workshop on Life Prediction and Aging Management of Concrete Structures* (edited by D.J. Naus), Paris, May 2003, pp. 21-29.

Gehlen, C. (2000), Probabilistische Lebensdauerbemessung von Stahlbetonbauwerken – Zuverlässigkeitsbetrachtungen zur wirksamen Vermeidung von Bewehrungskorrosion (Probability-based service life design of reinforced concrete structures – Reliability studies for prevention of reinforcement corrosion), Heft 510, *Deutscher Ausschuss für Stahlbeton*, Berlin, 2000, 106 pp. (in German).

Glass G.K. & Buenfeld, N.R. (1995), Chloride threshold levels for corrosion induced deterioration of steel in concrete, in proceedings of the *International RILEM Workshop on Chloride Penetration into Concrete* (edited by L.O. Nilsson & J.P. Ollivier), St-Rémy-lès-Chevreuse, October 1995, pp. 429-440.

Golwer, A. (1991), Belastung von Böden und Grundwasser durch Verkehrswege (Exposure on soil and ground water from roads), *Forum Städte-Hygiene*, No. 42, pp. 266-275. (in German)

Grefstad, K.A. & Grindland, O. (1997), Corrosion conditions on Gimsøystraumen bridge and other Norwegian coastal bridges, in proceedings of *International Conference on Repair of Concrete Structures – From Theory to Practice in a Marine Environment* (edited by A. Blankvoll), Svolvær, 1997, pp 133-142.

Gustafsson, M. E. R. & Franzén L. G. (2000), Inland transport of marine aerosols in southern Sweden, *Atmospheric Environment*, Vol 34, No. 2, pp. 313-325, 2000.

Hagentoft, C.-E. (2000), Building Physics Fundamentals, Report R-2000:1, Department of Building Physics, Chalmers University of Technology, Göteborg, 2000, 194 pp.

Harderup, E. (1995), Klimatdata för fuktberäkningar – Väderdata från tio meteorologiska mätstationer i Sverige (Climate data for moisture calculations – Weather data from ten meteorological stations in Sweden), Report 3025, Department of Building Technique,

## Chapter 10 References

Lund University, Lund, 1995, 50 pp. (in Swedish)

Hedenblad, G. (1988), Effect of soluble salt on the sorption isotherm, Report TVBM-3035, Division of Building Materials, Lund Institute of Technology, Lund, 1988, 9 pp.

Helsing-Atlassi, E. & Kjellsen K.O. (2000), Hydrationsutveckling och strukturutveckling (Hydration and structural development), chapter 8 in *Betonghandboken Högpresterande betong – Material och utförande* (edited by Christer Ljungkrantz), Svensk Byggtjänst, Stockholm, 2000, pp. 107-139. (in Swedish).

Högberg, A. (1998), Microclimate Description: To Facilitate Estimating Durability and Service Life of Building Components Exposed to Natural Outdoor Climate, Publication P-98:5, Department of Building Physics, Chalmers University of Technology, Göteborg, 1998.

IBP (1995), Weather data file for Holzkirchen 1991, made available by the Institute für Bauphysik, Holzkirchen, 1995.

Izquierdo, D., Andrade, C. & de Rincón, O. (2000), Statistical analysis of the diffusion coefficients measured in the piles of Maracaibo's bridge, in proceedings of the 2<sup>nd</sup> *International RILEM Workshop on Testing and Modelling the Chloride Ingress into Concrete* (edited by C. Andrade & J. Kropp), Paris, September 2000, pp. 135-148.

Jacquet, J., Jeppesen, P.S. & Jacobsen, H.J. (1992), Vintertjeneste for primære veje – stade og udviklingsmuligheder (Winter maintenance for primary roads – state-of-the-art and possibilities for development), Road department, Danish Road Directorate, Copenhagen, 1992, 134 pp. (in Danish)

Kelsey, P.D. & Hootman, R.G. (1992), De-icing salt dispersion and effects on vegetation along highways, case study: de-icing salt deposition on the Morton arboretum, in *Chemical de-icers and the environment* (edited by F.M. D'Itri), Chelsea, Michigan. 1992, pp. 253-281.

Kobysheva, N.V. (1992), Guidance material on the calculation of climatic parameters used for building purposes, WMO – No. 665, World Meteorological Organization, Geneva, 1992, 210 pp.

Kompen, R., Blankvoll, A., Berg, T., Noremark, E., Austnes, P., Grefstad, K., Kristiansen, B., Bonsak, B. & Halden, J. (1997), OFU Gimsøystraumen bru – Sluttrapport: Klimapåkjennning og tilstandsvurdering (OFU Gimsøystraumen bridge – Final report: Environmental loads and condition assessment), Publikasjon no. 85, Norwegian road administration, Oslo, 1997, 229 pp. (in Norwegian).

Langille, A.R. (1976), One season's salt accumulation in soil and trees adjacent to a highway, *Hort Science*, Vol. 11, No. 6, 1976, pp. 575-576.

Larsen, C.K. (1998), Chloride binding in concrete – Effect of surrounding environment and concrete composition, Report 1998:101, Department of structural engineering, Norwegian University of Science and Technology, Trondheim, 1998, 325 pp.

Levitus seasonal database, Data on temperature variations in the seawater at the exposure

locations found at <http://ingrid.ldgo.columbia.edu/SOURCES/.LEVITUS/.SEASONAL> (the Levitus seasonal database).

Lindvall A. & Nilsson L.-O. (2001a), Original quantification of the environmental parameters in the DuraCrete chloride ingress model, in proceedings of *Nordic Miniseminar on Prediction Models for Chloride ingress and corrosion initiation in concrete structures* (edited by L.-O. Nilsson), Publication P-01:6, Department of Building Materials, Chalmers University of Technology, Göteborg, 2001.

Lindvall A. & Nilsson L.-O. (2001b), Studies of the Effect of Secondary Cementitious Materials on Chloride Ingress, in proceedings of *Workshop on Durability of exposed concrete containing secondary cementitious materials* (edited by D. Bager), Nordic Concrete Federation, Hirtshals, November 2001, pp. 159-178.

Lindvall, A. & Andersen, A. (2000), Undersökning av kloridinträngning, armeringskorrosion, frysning och fukttillstånd på sju brokonstruktioner exponerade för tössalter (Investigations of chloride penetration, reinforcement corrosion, freezing and moisture conditions on seven bridge structures exposed to thaw-salts), Publication P-00:8, Department of Building Materials, Chalmers University of Technology, Göteborg, 2000, 130 pp. (in Swedish – also available in English). Can be downloaded from “<http://www.bm.chalmers.se/research/publika/rapporte.htm>”.

Lindvall, A. (2001), Environmental Actions and Response – Reinforced Concrete Structures exposed in Road and Marine Environments, Publication P-01:3, Department of Building Materials, Chalmers University of Technology, Göteborg, 2001, 320 pp. Can be downloaded from “<http://www.bm.chalmers.se/research/publika/rapporte.htm>”.

Lindvall, A. (2002a), Mapping of the chloride load around two Swedish reinforced concrete bridges, Publication P-02:2, Department of Building Materials, Chalmers University of Technology, Göteborg, 2002, 52 pp. Can be downloaded from “<http://www.bm.chalmers.se/research/publika/rapporte.htm>”.

Lindvall, A. (2002b), Chloride ingress in a Swedish road environment – Five years exposure for three concrete compositions, Publication P-02:4, Department of Building Materials, Chalmers University of Technology, Göteborg, 2002, 42 pp. Can be downloaded from “<http://www.bm.chalmers.se/research/publika/rapporte.htm>”.

Lindvall, A. (2003), Chloride ingress data from field exposure, at twelve different marine exposure locations, and laboratory exposure, Publication P-03:1, Department of Building Materials, Chalmers University of Technology, Göteborg, 2003, 53 pp. Can be downloaded from “<http://www.bm.chalmers.se/research/publika/rapporte.htm>”.

Löfgren, S. (2000), Vägsaltets effekter på mark- och vattenkemin i små skogsområden i sydöstra Sverige (The effects from de-icing salt on the chemistry in soil and water in small wooded areas in the southeastern part of Sweden), Vägverket publikation 2000:35, The Swedish National Road Administration (Vägverket), Uppsala, 2000, 44 pp. (in Swedish).

Long, A.E., Henderson, G.D. & Montgomery, F.R. (2001), Why assess the properties of near-surface concrete?, *Construction and Building Materials*, Vol. 15, 2001, pp. 65-79.

Maage, M., Helland, S. & Carlsen, J.E. (1997), Service life prediction of concrete in

- marine environment, in proceedings of *International Conference on Repair of Concrete Structures – From Theory to Practice in a Marine Environment* (edited by A. Blankvoll), Svolvær, 1997, pp 177-187.
- Maage, M., Helland, S. & Carlsen, J.E. (1999), Chloride Penetration into concrete with light weight aggregates, LIGHTCON Report No. 3.6, STF22 A98755, SINTEF, Trondheim, 1999.
- Maage, M., Poulsen, E., Vennesland, Ø. & Carlsen, J.E. (1995), Service life model for concrete structure exposed to marine environment, Initiation period, LIGHTCON Report No. 2.4, STF70 A94082, SINTEF, Trondheim, 1995.
- McBean, E. & Al-Nassri, S. (1987), Migration pattern of de-icing salt from roads, *Journal of Environmental Management*, Vol. 25, 1987, pp.231-238.
- McCormick, M. & Thiruvathukal, J. (1981), Element of Oceanography, Saunders College publishing, Philadelphia, 1981.
- McGee, R. (2000), Modelling of chloride ingress in Tasmanian bridges, in proceedings of the 2<sup>nd</sup> *International RILEM Workshop on Testing and Modelling the Chloride Ingress into Concrete* (edited by C. Andrade & J. Kropp), Paris, September 2000, pp. 149-160.
- Mehta, P.K. (1991), Concrete in the Marine Environment, Elsevier applied science, London, 1991.
- Meijers, S.J.H. (2003), Computational Modelling of Chloride Ingress in Concrete, *Dissertation*, Delft University of Technology, Delft, 2003, 170 pp.
- Mejlbro, L. (1996), The complete solution to Fick's second law of diffusion with time-dependent diffusion coefficient and surface concentration, in *Durability of Concrete in Saline Environment*, (edited by P. Sandberg), Cementa, Danderyd, 1996.
- Mejlhede-Jensen, O. (1998), Chloride ingress in Cement Paste and Mortar measured by Electron Micro Analysis, Technical Report Series R No. 51, Department of Structural Engineering and Materials, Technical University of Denmark, Lyngby, 1998.
- Möller, J. S. (1994), Measurements of carbonation in cement based materials, Publication P-93:11, Departments of Building Materials, Chalmers University of Technology, Göteborg, 1994, 93 pp.
- Morcillo, M., Chico, B., Mariaca, L. & Otero, E. (2000), Salinity in marine atmospheric corrosion: its dependence on the wind regime existing in the site, *Corrosion Science*, Vol. 42, 2000, pp. 91-104.
- Neville, A.M. (1995), Properties of concrete, Longman, London, 1995.
- Nielsen, E.P. & Geiker, M.R. (2003), Chloride diffusion in partially saturated cementitious material, *Cement and Concrete Research*, Vol. 33, No. 1, 2003, pp. 133-138.
- Nilsson, B.-G. (2000), Personal communication, *Vägverket* (The Swedish road

administration), Göteborg.

Nilsson, L.-O. (1980), Hygroscopic moisture in concrete – drying, measurements and related material properties, Report TVBM-1003, Division of Building Materials, Lund Institute of Technology, Lund, 1980, 162 pp.

Nilsson, L.-O. (1996), Interaction between microclimate and concrete – a prerequisite for deterioration, *Construction and Building Materials*, Vol. 10, No. 5, pp. 301-308.

Nilsson, L.-O. (2000), A numerical model for combined diffusion and convection of chloride in non-saturated concrete, in proceedings of the *2<sup>nd</sup> International RILEM Workshop on Testing and Modelling the Chloride Ingress into Concrete* (edited by C. Andrade & J. Kropp), Paris, September 2000, pp. 261-275.

Nilsson, L.-O. (2001), Overview of Prediction models for chloride ingress into concrete structures, in proceedings of *Nordic Miniseminar on Prediction Models for Chloride ingress and corrosion initiation in concrete structures* (edited by L.-O. Nilsson), Publication P-01:6, Department of Building Materials, Chalmers University of Technology, Göteborg, 2001.

Nilsson, L.-O., Andersen, A., Tang, L. & Utgenannt, P. (2000), Chloride ingress data from field exposure in a Swedish road environment, Publication P-00:5, Department of Building Materials, Chalmers University of Technology, Göteborg, 2000, 21 pp. Can be downloaded from “<http://www.bm.chalmers.se/research/publika/rapporte.htm>”.

Nilsson, L.-O., Poulsen, E., Sandberg, P., Sörensen, H.E. & Klinghoffer, O. (1996), Chloride penetration into concrete – State of the Art (Transport processes, corrosion initiation, test methods and predictions models), HETEK-report No. 53, Danish Road Directorate, Copenhagen, 1996. 151 pp.

Nilsson, L.-O., Sandberg, P., Poulsen, E., Tang, L., Andersen, A. & Frederiksen, J.M. (1997), A System for estimation of Chloride ingress into Concrete – Theoretical background, HETEK-report No. 83, Danish Road Directorate, Copenhagen, 1997. 168 pp.

NT Build 492 (1999), Chloride migration coefficient from non-steady state migration experiments, Nordtest method, 1999, 8 pp.

OECD (1989), Curtailing usage of de-icing agents in winter maintenance, Road Transport Research, Organisation for Economic Co-operation and Development (OECD), Paris, 1989, 126 pp.

Oke, T.R. (1987), Boundary Layer Climates, Routledge, Second edition, London, 1987.

Page, C.L., Short, N.R. & El Tarras, A. (1981), Diffusion of chloride ions in hardened cement pastes, *Cement and Concrete Research*, Vol. 11, No. 3, pp. 395-406.

Paulsson, J. & Andersen, A. (1997), Measurements on seasonal and diurnal variations of environmental conditions surrounding a heavily trafficked bridge structure, in proceedings of *International Conference on Repair of Concrete Structures – From Theory to Practice in a Marine Environment* (edited by A. Blankvoll), Svolvær, 1997, pp. 144-152.

## Chapter 10 References

- Paulsson-Tralla, J. (2001), Personal communication, StockholmKonsult (now Carl Bro), Stockholm.
- Pedersen, P.A. & Fostad, O. (1996), Effekter av veisaltning på jord, van og vegetasjon (Effects from spread of de-icing salt on soil, water and vegetation), Hovedrapport del I, Institutt for plantefag, Norges landbrukshøgskole/Forskningsparken i Ås AS. (in Norwegian).
- Polder, R.B. (1996), Durability of new types of concrete for marine environment, CUR-report 96-3, CUR, Gouda.
- Polder, R.B., de Rooij, M.R., de Vries, H. & Gulikers, J. (2003), Observed Penetration in Marine Concrete Structure after 20 years in North Sea Environment, presented at *workshop on Risk based maintenance of Structure*, TU Delft, Delft, January 2003.
- Poulsen, E. (1996), Estimation of Chloride ingress into Concrete and Prediction of Service Lifetime with Reference to Marine RC Structure, in *Durability of Concrete in Saline Environment*, (edited by P. Sandberg), Cementa, Danderyd, 1996.
- Rackwitz, R. (1999), *Zuverlässigkeitsbetrachtungen bei Verlust der Dauerhaftigkeit von Bauteilen und Bauwerken* (Reliability aspects at loss of durability of structural parts and structures), In *Kurzberichte aus der Bauforschung* 40, No. 4, Stuttgart, 1999, pp. 297-301. (in German)
- Randrup, T.B. & Pedersen, L.B. (1996), Vejsalt, træer og buske – En litteraturundersøgelse om NaCl's effekter på vedplanter langs veje (De-icing salt, trees and bushes – A literature study of the effects from NaCl on plants along roads), Report No. 64, Danish Road Directorate, Copenhagen, 1996, 69 pp. (in Danish)
- Rooij de, M.R. & Polder, R. (2002), Unpublished data, TNO (Netherlands Organisation for Applied Scientific Research, Delft, 2002.
- Saetta, A.V., Scotta, R.V. & Vitaliani, R.V. (1993), Analysis of Chloride Diffusion into Partially Saturated Concrete, *ACI Materials Journal*, Vol. 90, No. 5, 1993, pp. 441-451.
- Salt Institute (1995), De-icing Salt And Our Environment, Informational guide for public policy makers, Salt Institute, Alexandria, VA, 1995, 25 pp.
- Salt Institute (1999), The Snowfighter's handbook, Salt Institute, Alexandria, VA, 1999, 22 pp.
- Samson, E. & Marchand, J. (1999a), Numerical Solution of the Extended Nernst-Planck Model, *Journal of Colloid and Interface Science*, Vol. 215, 1999, pp. 1-8.
- Samson, E., Lemaire, G., Marchand, J. & Beaudoin, J.J. (1999b), Modeling chemical activity effects in strong ionic solutions, *Computational Materials Science*, Vol. 15, 1999, pp. 285-294.
- Samson, E., Marchand, J., Robert, J.-L. & Bournazel, J.-P. (1999c), Modelling ion diffusion mechanisms in porous media, *International journal for numerical methods in*

*engineering*, Vol. 46, 1999, pp. 2043-2060.

Sandberg, P. & Larsson, J. (1993), Chloride binding in cement pastes in equilibrium with synthetic pore solution, in proceedings of *Nordic Miniseminar on Chloride penetration into concrete structures* (edited by L.-O. Nilsson), Publication P-93:1, Department of Building Materials, Chalmers University of Technology, Göteborg, 1993.

Sandberg, P. (1995), Critical evaluation of factors affecting chloride initiated reinforcement corrosion in concrete, Report TVBM-3068, Division of Building Materials, Lund Institute of Technology, Lund, 1996, 116 pp.

Sandberg, P. (1998), Chloride initiated reinforcement corrosion in marine concrete, Report TVBM-1015, Division of Building Materials, Lund Institute of Technology, Lund, 1998, 86 pp.

Sandberg, P. (1999), Studies of chloride binding in concrete exposed in a marine environment, *Cement and Concrete Research*, Vol. 29, No. 4, pp. 473-477.

Sandberg, P., Tang, L. & Andersen, A. (1998), Recurrent studies of chloride ingress in uncracked marine concrete at various exposure times and elevations, *Cement and Concrete Research*, Vol. 28, No. 10, 1998, pp. 1489-1503.

Sandberg, U. (1977), Mätning av stänk från fordon på våt vägbana (Measurement of splash and spray generated by vehicles on wet roads), VTI-rapport 124, Swedish National Road and Transport Research Institute, Linköping, 1977, 46 pp. (in Swedish with English abstract)

Sandberg, U. (1980), Efficiency of Spray Protectors – Tests 1979, VTI-rapport 124, Swedish National Road and Transport Research Institute, Linköping, 1980, 82 pp.

Siemes, A. J. M., Vrouwenvelder, A. C. W. M. & van den Beukel, A. (1985), Durability of buildings: a reliability analysis, *HERON*, Vol 30, No. 3, 1985, Delft, pp. 1-48, 1985.

Sørensen, B. & Maahn, E. (1982), Penetration rate of chloride in marine concrete structures, *Nordic Concrete Research*, Publication No. 1, The Nordic Concrete Federation, Stockholm, 1982.

Sørensen, H.E. (1992 & 1993), Test Report. Project Durability of Marine Concrete Structures, Test reports AECprov92-060, -074, -082 & 93-033, AEC, Vedbaek, 1992 & 1993.

Svennerstedt, B. (1989), Ytfukt på fasadmateriel (Surface moisture on facade materials), The National Swedish Institute for Building Research, TN:16, Gävle, 1989, 181 pp. (in Swedish)

Svenska Betongföreningen (2003), Vägledning för val av exponeringsklass enligt SS-EN 206-1 (Guidance for choice of exposure class according to SS-EN 206-1), Betongrapport nr 11, Swedish Concrete Association, Stockholm, 2003, 26 pp. (in Swedish).

Takewake, K. & Mastumoto, S. (1988), Quality and cover thickness of concrete based on the estimation of chloride penetration in marine environments, in the proceedings of 2<sup>nd</sup>



## Chapter 10 References

- international conference on concrete in marine environment*, 21-26 August 1988, ACI, Detroit, 1988, pp 381-400.
- Tang, L. & Andersen, A. (2000), Chloride ingress data from five years field exposure in a Swedish marine environment, in proceedings of the 2<sup>nd</sup> *International RILEM Workshop on Testing and Modelling the Chloride Ingress into Concrete* (edited by C. Andrade & J. Kropp), Paris, September 2000, pp. 105-119.
- Tang, L. & Nilsson, L.-O. (1993), Chloride binding capacity and binding isotherms of OPC pastes and mortars, *Cement and Concrete Research*, Vol. 23. No. 2, 1993, pp. 247-253.
- Tang, L. & Sandberg, P. (1996), Chloride penetration into concrete exposed under different conditions, in proceedings of the 7<sup>th</sup> *International Conference on the Durability of Building Materials and Components* (edited by C. Sjöström), Stockholm, May 1996, pp. 453-461.
- Tang, L. & Utgenannt, P. (1998), Measurements of chloride flow along a highway, Proceedings of the 2<sup>nd</sup> *International Conference on concrete in severe conditions*, Tromsø, 1998.
- Tang, L. (1996), Chloride Transport in Concrete – Measurement and Prediction, Publication P-96:6, Department of Building Materials, Chalmers University of Technology, Göteborg, 1996, 88 pp.
- Tang, L. (1997), Chloride penetration profiles and diffusivity in concrete under different exposure conditions, Report E-97:3, Department of Building Materials, Chalmers University of Technology, Göteborg, 1997, 53 pp.
- Tang, L. (2002), Tang-Nilsson Method for Determination for Chloride Binding Isotherm, Unpublished material, Department of Building Materials, Chalmers University of Technology, Göteborg, 2002.
- Tang, L. (2003), Estimation of cement/binder profile parallel to the determination of chloride profile in concrete – Nordtest project 1581-02, SP Report 2003:7, SP Swedish National Testing and Research Institute, Borås, 2003.
- Texas University (2003), Map showing exposure locations in marine exposure programme downloaded from “<http://www.lib.utexas.edu/maps/>”, General Libraries, The University of Texas, Austin, 2003.
- Truc, O. (2000), Prediction of Chloride Penetration into Saturated Concrete – Multi-Species Approach, Report P-00:4, Department of Building Materials, Chalmers University of Technology, Göteborg, 2000, 179 pp.
- Tuutti, K. (1982), Corrosion of steel in concrete, fo 4.82, CBI (*Swedish Cement and Concrete Research Institute*), Stockholm, 1982.
- Utgenannt, P. & Petersson, P.-E. (2001), Frost Resistance of Concrete Containing Secondary Cementitious Materials – Experience from Three Field Exposure Sites, in proceedings of *Workshop on Durability of exposed concrete containing secondary*

## Chapter 10 References

*cementitious materials* (edited by D. Bager), Nordic Concrete Federation, Hirtshals, November 2001, pp. 97-112.

Utgenannt, P. (2002), Personal communication, SP Swedish National Testing and Research Institute, Borås, 2002.

Volkwein, A., Dorner, H. & Springenschmid, R. (1986), Untersuchungen zur Kloridkorrosion der Bewehrung von Autobahn-Brücken aus Stahl- oder Spannbeton (Investigation of chloride induced reinforcement corrosion in highway bridges made of steel or reinforced concrete), Forschung Strassenbau und Strassenverkehrstechnik, Heft 460, Berlin, 1986. (in German).

Wallbank E.J.H. (1989), The performance of concrete in bridges – A survey of 200 highway bridges, HSMO publication, prepared for the Department of Transport, London, 1989, 96 pp.

Weber, D. (1982), Untersuchung von Umwelteinflüssen auf Ingenieur Bauwerke der Berliner Stadsautobahn (Investigation of the environmental load on structures in the motorways in Berlin), BAM 12, No. 2, Berlin, Germany. 1982. (in German).

Wirje A. & Offrell, P. (1996), Kartering av miljöladd – Kloridpenetration vid Rv40 (Mapping of environmental load – Chloride penetration at Rv40), Report TVBM-7106, Division of Building Materials, Lund Institute of Technology, Lund, 1996. 41 pp. (in Swedish).

Wood, J.G.M. & Crerar, J. (1997), Tay road bridge: Analysis of chloride ingress variability & prediction of long term deterioration, *Construction and Building Materials*, Vol. 11, No. 4, 1997, pp. 249-254.

## Appendix

The following are presented in the appendix:

- **Meteorological data for exposure locations**, presented as monthly mean values of RH and temperature of the air and precipitation. Additionally data on the chloride concentrations in and temperature of seawater at the marine exposure locations are also presented.
- **Calculations of equivalent surface humidity and temperature conditions** for the chosen marine and road locations for some chosen solar radiation intensities,  $I_{\text{solar}}$ , and sky temperatures,  $T_{\text{sky}}$ .
- **Quantifications of the environmental parameter  $k_{\text{D,e}}$**  in marine and road conditions.

### Meteorological data

Nine marine and two road locations have been chosen to illustrate how different exposure conditions influence chloride ingress into concrete. For each location the exposure conditions have been described in terms of the temperature and RH of the air, precipitation (amounts and days of precipitation) and for marine conditions the chloride concentrations and temperature of seawater. The yearly amounts of de-icing salt spread in road conditions are presented in table 7.6. The following marine locations have been chosen (the following is stated for each location: sea, the meteorological station where data have been taken from and country):

1. The Mediterranean. Meteorological data from Marseille (France).
2. The Baltic Sea. Meteorological data from Kalmar (Sweden).
3. Öresund. Meteorological data from Copenhagen (Denmark).
4. Kattegat. Meteorological data from Göteborg (Sweden).
5. North Sea. Meteorological data from Den Helder.
6. Norwegian Fjord. Meteorological data from Narvik (Norway).
7. Atlantic Ocean around Iceland. Meteorological data from Reykjavik.
8. Atlantic Ocean outside Iberian Peninsula. Meteorological data from Lisbon (Portugal).
9. Persian Gulf. Meteorological data from Bandas Abbas (Iran).

The following road locations have been chosen:

1. Göteborg (Sweden). Meteorological data from Göteborg.
2. Munich (Germany). Meteorological data from Munich.

## Appendix

The yearly variations in the monthly mean temperature and RH of the air and the amount of precipitation (melted form) for the chosen marine locations are presented in figures A. 1a-A.1c.

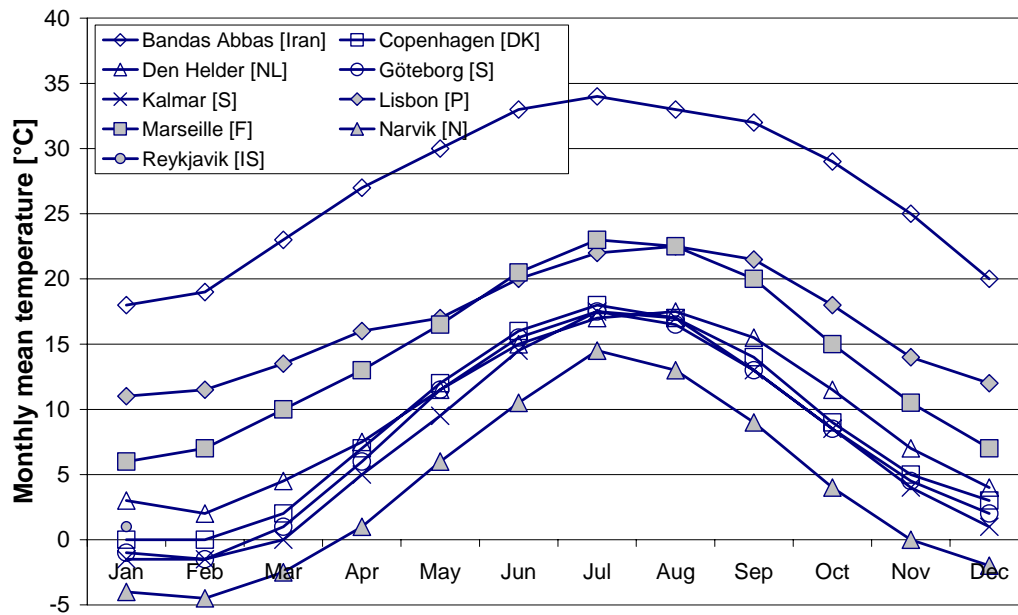


Figure A.1a: Yearly variations in monthly mean temperature of the air at the chosen marine exposure locations. Based on data from DMI (1994).

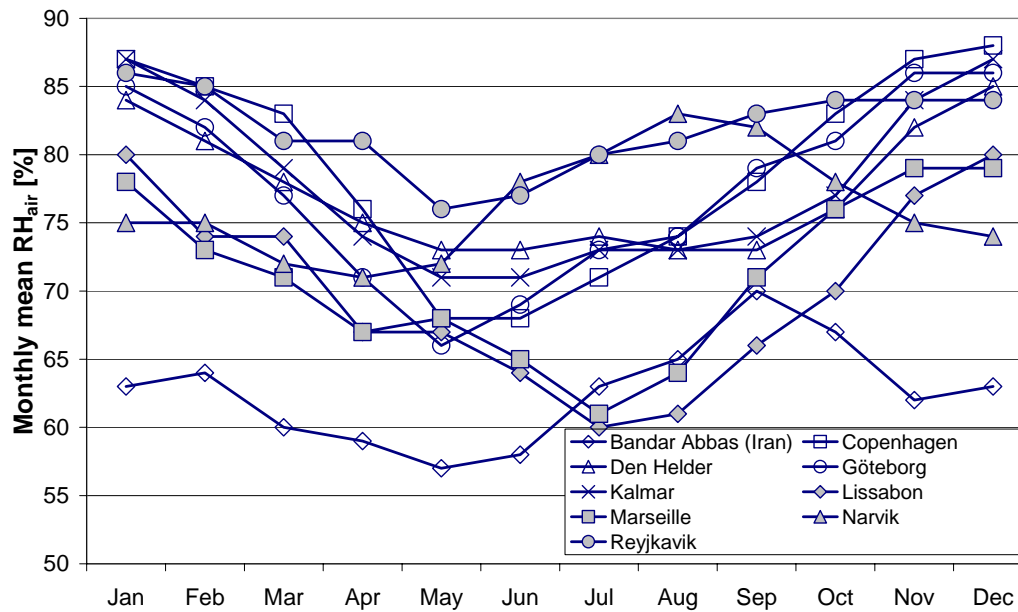


Figure A.1b: Yearly variations in monthly mean RH of the air at the chosen marine exposure locations. Based on data from DMI (1994).

## Appendix

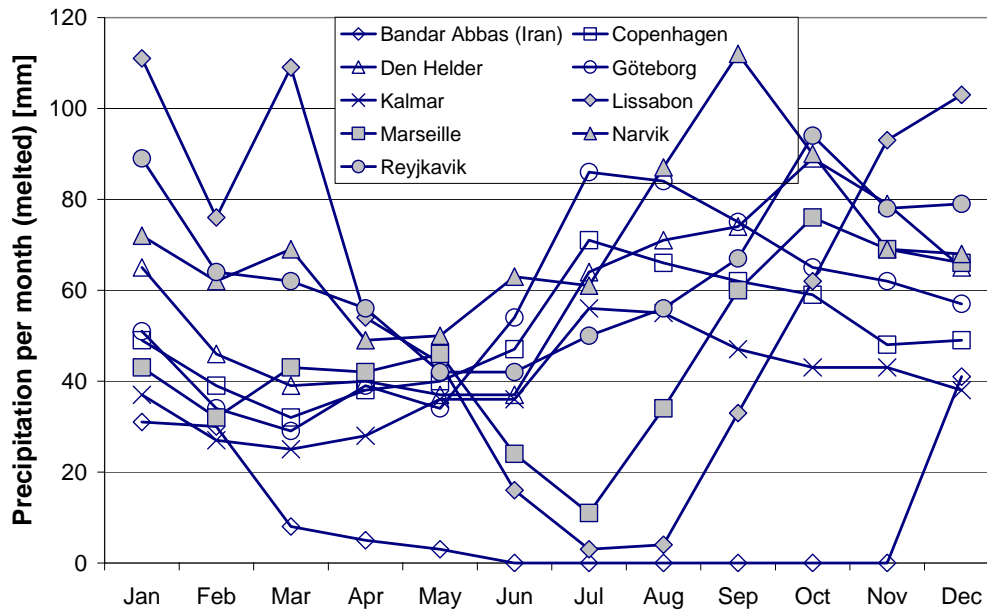


Figure A.1c: Yearly variations in monthly mean amounts of precipitation (melted form) at the chosen marine exposure locations. Based on data from DMI (1994).

The exposure conditions at the chosen marine exposure locations have also been registered as the chloride concentration and temperature of the seawater. Data on the chemical composition and temperature of the seawater at the marine exposure locations are presented in figures 4.3a and 4.3b.

The yearly variations in the monthly mean temperature and RH of the air and precipitation (melted form) for the chosen road locations are presented in figures A.2a-A.2c.

## Appendix

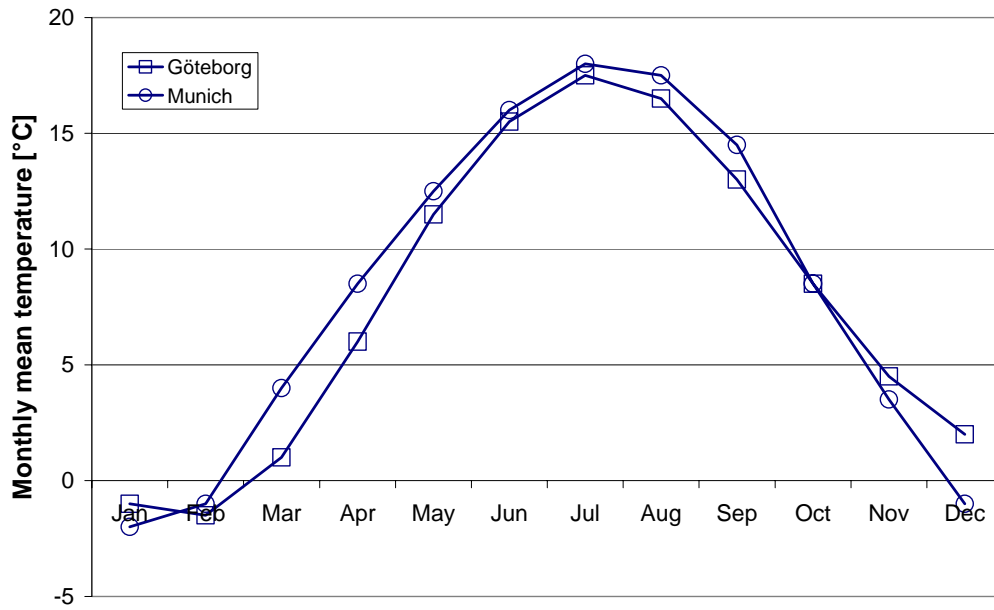


Figure A.2a: Yearly variations in monthly mean temperature of the air for the chosen road locations. Based on data from DMI (1994).

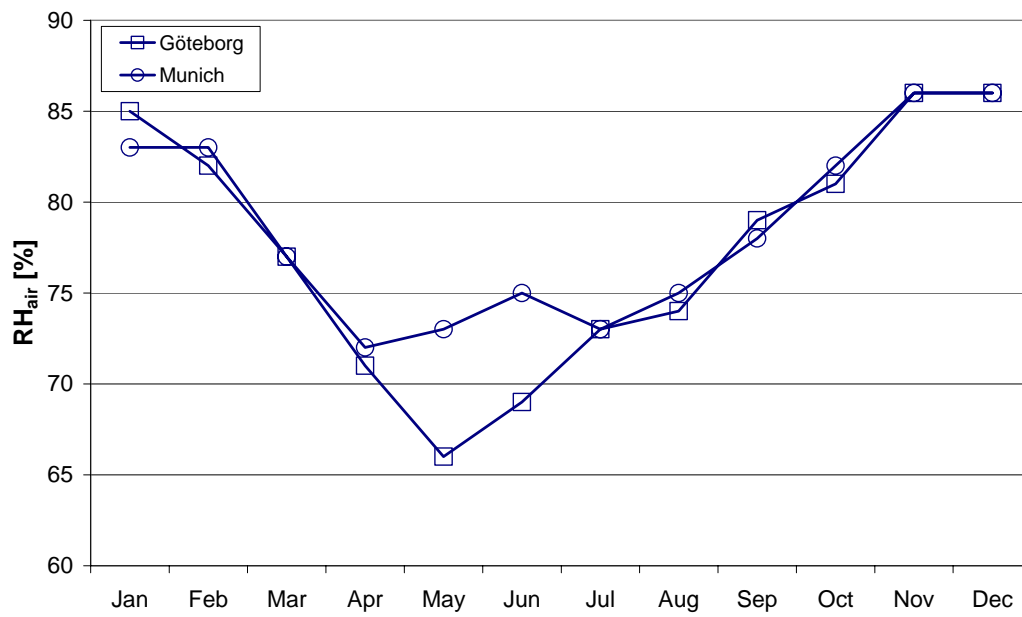
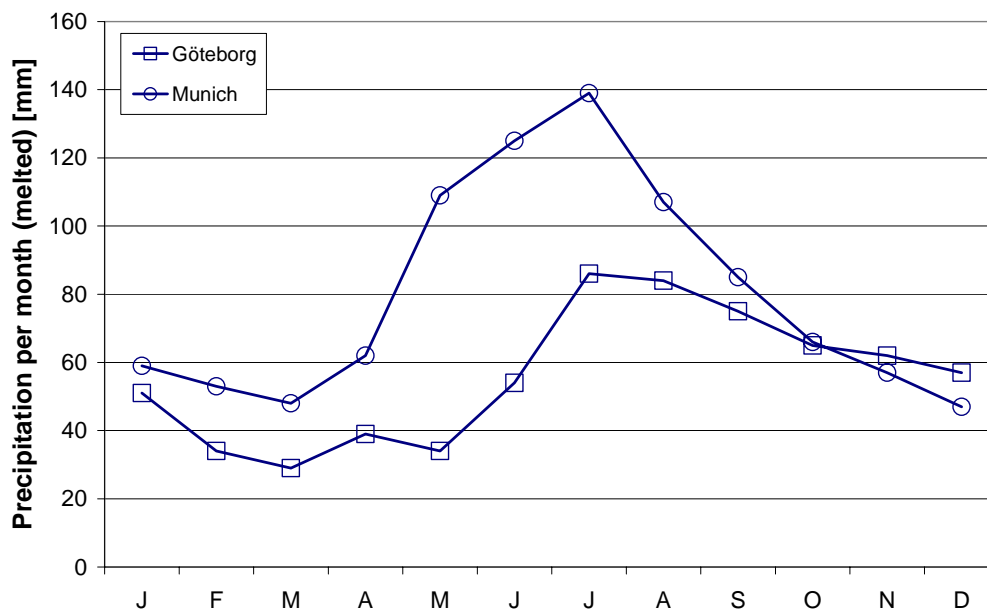


Figure A.2b: Yearly variations in monthly mean RH of the air for the chosen road locations. Based on data from DMI (1994).

## Appendix



*Figure A.2c: Yearly variations in monthly mean amounts of precipitation (melted form) for the chosen road locations. Based on data from DMI (1994)*

The numbers of days with precipitation each month at the chosen exposure locations are shown in table A.1. Each exposure location is denoted by a number, denoting the location, and whether the exposure is marine (M) or road (R), e.g. “1. M” denotes data valid for marine exposure in the Mediterranean.

## Appendix

*Table A.1: Number of days with precipitation each month at the chosen exposure locations. Based on data from DMI (1994).*

Month	1. M	2. M	3. M	4. M	5. M	6. M	7. M	8. M	9. M	1. R	2. R
Jan	8	14	17	15	21	15	20	15	2	15	16
Feb	6	12	13	12	18	14	17	12	2	12	16
March	7	10	12	10	17	16	18	14	1	10	13
April	7	10	13	12	15	15	18	10	0	12	15
May	8	10	11	10	13	16	16	10	0	10	15
June	4	10	13	12	12	17	15	5	0	12	17
July	2	12	14	14	15	15	15	2	0	14	16
Aug	5	12	14	14	15	19	16	2	0	14	16
Sep	6	11	15	16	18	21	19	6	0	16	13
Oct	8	12	16	15	20	20	21	9	0	15	13
Nov	9	13	16	16	21	14	18	13	0	16	15
Dec	10	14	17	17	22	15	20	15	2	17	15
<b>Yearly</b>	<b>80</b>	<b>140</b>	<b>171</b>	<b>163</b>	<b>207</b>	<b>197</b>	<b>213</b>	<b>113</b>	<b>7</b>	<b>163</b>	<b>180</b>

## Equivalent surface humidity and temperature

### General

Equivalent surface humidity and temperature conditions have been calculated for surfaces above the water surface, in marine conditions, and for all surfaces, in road conditions. The equivalent surface conditions have been determined for four different solar radiation intensities,  $I_{\text{solar}}$ : 50 W/m<sup>2</sup>, 100 W/m<sup>2</sup>, 200 W/m<sup>2</sup> and 300 W/m<sup>2</sup>, and three different sky temperatures,  $T_{\text{sky}}$ : -5.0°C, -10.0°C and -15.0°C. The yearly mean air temperature and RH, for each location, have been used as input data in the calculations. The corresponding equivalent surface humidity and temperature conditions have been determined, according to eq. (3.1) and (3.3), with the following input data:

- **a**, The absorption factor for short-wave radiation,  $a=0.7$  [-] (concrete surfaces).
- **$\alpha_{\text{cv}}$** , the convective heat transfer coefficient,  $\alpha_{\text{cv}}=20$  [W/m<sup>2</sup>K] (which corresponds to a wind speed=5 [m/s]).
- **$\alpha_{\text{r}}$** , the radiative heat transfer coefficient, where  $\varepsilon=0.90$  [-]. [W/m<sup>2</sup>K]

### Marine conditions

In tables A.2a-A.2c  $T_{\text{s,eq}}$  and  $\text{RH}_{\text{s,eq}}$  calculated for different sky temperatures and solar radiation intensities, are presented for the chosen marine locations.



## Appendix

*Table A.2a: Calculated  $T_{s,eq}$  and  $RH_{s,eq}$  for the chosen marine locations.  $T_{sky}=-5.0^{\circ}\text{C}$ .*

Loc.	$I_{\text{solar}}=50 \text{ W/m}^2$		$I_{\text{solar}}=100 \text{ W/m}^2$		$I_{\text{solar}}=200 \text{ W/m}^2$		$I_{\text{solar}}=300 \text{ W/m}^2$	
	$T_{s,eq}$	$RH_{s,eq}$	$T_{s,eq}$	$RH_{s,eq}$	$T_{s,eq}$	$RH_{s,eq}$	$T_{s,eq}$	$RH_{s,eq}$
1.	12.2	80.4	13.7	73.6	16.6	61.8	19.4	52.0
2.	6.6	81.3	8.0	74.1	10.9	61.7	13.8	51.6
3.	7.7	83.8	9.1	76.5	12.0	63.8	14.9	53.4
4.	7.0	81.4	8.5	74.2	11.4	61.8	14.2	51.7
5.	8.5	83.0	10.0	75.8	12.9	63.3	15.8	53.0
6.	3.7	76.5	5.2	69.5	8.1	57.6	11.0	48.0
7.	4.7	83.3	6.2	75.8	9.1	62.9	12.0	52.4
8.	14.1	81.4	15.5	74.6	18.4	62.8	21.3	53.0
9.	22.3	81.5	23.7	75.1	26.6	63.9	29.4	54.6

*Table A.2b: Calculated  $T_{s,eq}$  and  $RH_{s,eq}$  for the chosen marine locations.  $T_{sky}=-10.0^{\circ}\text{C}$ .*

Loc.	$I_{\text{solar}}=50 \text{ W/m}^2$		$I_{\text{solar}}=100 \text{ W/m}^2$		$I_{\text{solar}}=200 \text{ W/m}^2$		$I_{\text{solar}}=300 \text{ W/m}^2$	
	$T_{s,eq}$	$RH_{s,eq}$	$T_{s,eq}$	$RH_{s,eq}$	$T_{s,eq}$	$RH_{s,eq}$	$T_{s,eq}$	$RH_{s,eq}$
1.	11.3	85.0	12.8	7.8	15.6	65.2	18.5	54.9
2.	5.7	86.1	7.2	78.4	10.0	65.2	12.9	54.4
3.	6.8	88.7	8.2	80.8	11.1	67.3	14.0	56.3
4.	6.1	56.1	7.6	78.5	10.5	65.3	13.4	54.5
5.	7.7	87.8	9.1	80.1	12.0	66.8	14.9	55.9
6.	2.9	80.9	4.3	73.5	7.2	60.9	10.1	50.6
7.	3.9	88.1	5.3	80.2	8.2	66.5	11.1	55.3
8.	13.2	86.0	14.6	78.8	17.5	66.2	20.4	55.9
9.	21.3	86.1	22.8	79.3	25.6	67.4	28.4	57.5

## Appendix

*Table A.2c: Calculated  $T_{s,eq}$  and  $RH_{s,eq}$  for the chosen marine locations.  $T_{sky}=-15.0^{\circ}\text{C}$ .*

Loc.	$I_{\text{solar}}=50 \text{ W/m}^2$		$I_{\text{solar}}=100 \text{ W/m}^2$		$I_{\text{solar}}=200 \text{ W/m}^2$		$I_{\text{solar}}=300 \text{ W/m}^2$	
	$T_{s,eq}$	$RH_{s,eq}$	$T_{s,eq}$	$RH_{s,eq}$	$T_{s,eq}$	$RH_{s,eq}$	$T_{s,eq}$	$RH_{s,eq}$
1.	10.4	89.9	11.9	82.2	14.8	68.9	17.6	57.9
2.	4.8	91.1	6.3	82.3	9.2	68.9	12.1	57.4
3.	5.9	93.9	7.4	85.5	10.2	71.1	13.1	59.4
4.	5.3	91.2	6.7	83.0	9.6	69.0	12.5	57.6
5.	6.8	92.9	8.2	84.7	11.1	70.6	14.0	59.0
6.	2.0	85.7	3.5	77.8	6.4	64.3	9.3	53.4
7.	3.0	93.3	4.5	84.8	7.4	70.2	10.3	58.4
8.	12.3	91.0	13.7	83.3	16.6	70.0	19.5	59.0
9.	20.4	91.0	21.8	83.8	24.7	71.2	27.5	60.6

### Road conditions

In tables A.3a-A.3c  $T_{s,eq}$  and  $RH_{s,eq}$  calculated for different sky temperatures and solar radiation intensities, are presented for the chosen road locations.

*Table A.3a: Calculated  $T_{s,eq}$  and  $RH_{s,eq}$  for the chosen road locations.  $T_{sky}=-5.0^{\circ}\text{C}$ .*

Loc.	$I_{\text{solar}}=50 \text{ W/m}^2$		$I_{\text{solar}}=100 \text{ W/m}^2$		$I_{\text{solar}}=200 \text{ W/m}^2$		$I_{\text{solar}}=300 \text{ W/m}^2$	
	$T_{s,eq}$	$RH_{s,eq}$	$T_{s,eq}$	$RH_{s,eq}$	$T_{s,eq}$	$RH_{s,eq}$	$T_{s,eq}$	$RH_{s,eq}$
1.	7.0	81.4	8.5	74.2	11.4	61.8	14.2	51.7
2.	7.4	83.1	8.8	75.7	11.7	63.1	14.6	52.8

*Table A.3b: Calculated  $T_{s,eq}$  and  $RH_{s,eq}$  for the chosen road locations.  $T_{sky}=-10.0^{\circ}\text{C}$ .*

Loc.	$I_{\text{solar}}=50 \text{ W/m}^2$		$I_{\text{solar}}=100 \text{ W/m}^2$		$I_{\text{solar}}=200 \text{ W/m}^2$		$I_{\text{solar}}=300 \text{ W/m}^2$	
	$T_{s,eq}$	$RH_{s,eq}$	$T_{s,eq}$	$RH_{s,eq}$	$T_{s,eq}$	$RH_{s,eq}$	$T_{s,eq}$	$RH_{s,eq}$
1.	6.1	86.1	7.6	78.5	10.5	65.3	13.4	24.5
2.	6.5	87.9	8.0	80.1	10.8	66.7	13.7	55.7

*Table A.3c: Calculated  $T_{s,eq}$  and  $RH_{s,eq}$  for the chosen road locations.  $T_{sky}=-15.0^{\circ}\text{C}$ .*

Loc.	$I_{\text{solar}}=50 \text{ W/m}^2$		$I_{\text{solar}}=100 \text{ W/m}^2$		$I_{\text{solar}}=200 \text{ W/m}^2$		$I_{\text{solar}}=300 \text{ W/m}^2$	
	$T_{s,eq}$	$RH_{s,eq}$	$T_{s,eq}$	$RH_{s,eq}$	$T_{s,eq}$	$RH_{s,eq}$	$T_{s,eq}$	$RH_{s,eq}$
1.	5.3	91.2	6.7	83.0	9.6	69.0	12.5	57.6
2.	5.6	93.0	7.1	84.7	10.0	70.4	12.9	58.8

## Input data – Environmental parameters

### General

The DuraCrete model for chloride ingress, cf. eq. (2.1a), has been chosen to demonstrate how the developed models for environmental actions influence service life predictions. In the DuraCrete model the chloride ingress is modelled as a combination of the influence of the concrete composition, the workmanship during construction and the exposure environment. The parameters that describe the influence of the concrete composition and

## Appendix

the workmanship during construction are described and quantified in chapter 7. The influence of the exposure environment is modelled with the following parameters, according to the modification of the DuraCrete chloride ingress model described in eq. (6.1a) and (6.1b):

- $k_{D,e}$ . Constant parameter that accounts for the influence of the exposure environment on  $D_0$ .  $k_{D,e}$  can be divided into the parameters  $k_{D,RH}$ , which accounts for the influence of moisture conditions, in terms of the relative humidity (RH) of the concrete, and  $k_{D,T}$ , which accounts for the influence of temperature conditions in the concrete. [-]
- $C_{SN}$ . Surface chloride content (total chloride content), which describes the driving potential for chloride transport at the surface of the concrete. The results of the quantifications of this parameter are presented in chapter 7. [% by weight Cl/binder].
- $C_{crit}$ . Chloride threshold level (as total chloride content) at the reinforcement when reinforcement corrosion is initiated (threshold concentration). This parameter is further described in chapter 6. [% by weight Cl/binder].
- $n$ . Age factor, which describes the decrease in the chloride diffusion coefficient,  $D_a(t)$ , with increasing exposure age. The results of the quantifications of this parameter are presented in chapter 7. [-].

All these parameters can be modelled as stochastic parameters to include uncertainties related to the concrete composition, workmanship during construction and exposure environment etc.

In the following sections the results of the quantification of the parameter  $k_{D,e}$ , in marine and road conditions, are presented.

### Marine conditions – $k_{D,e}$

In table A4 examples of quantified  $k_{D,e}$  are shown for locations 1 (The Mediterranean) and 4 (Kattegat). The parameter  $k_{D,e}$  has been determined from  $k_{D,RH}$  and  $k_{D,T}$  according to eq. (6.1b) where the parameter  $k_{D,T}$  has been quantified from the equivalent surface temperature, according to eq. (6.3). The parameter  $k_{D,RH}$  can be quantified according to figure 6.3 and with data from figure 3.13a. However, since the moisture conditions above the water surface are uncertain it has been decided to use the following values of  $k_{D,RH}$ : **0.90** in the **tidal (T)** and **0.40** in the **splash (Sp), atmospheric (A) and distant atmospheric (DA) zones**.

## Appendix

*Table A.4a: Quantified  $k_{D,e}$  for exposure in marine tidal, splash and atmospheric conditions. [-]*

Location		1.		4.	
$I_{\text{solar}}$	$T_{\text{sky}}$	$T$	$Sp + A + DA$	$T$	$Sp + A + DA$
	$T_{\text{air}}$	0.70	0.31	0.52	0.23
	$T_{\text{sea}}$	0.76	0.34	0.58	0.26
50 W/m <sup>2</sup>	-5.0°C	0.60	0.28	0.47	0.22
50 W/m <sup>2</sup>	-10.0°C	0.58	0.27	0.45	0.21
50 W/m <sup>2</sup>	-15.0°C	0.56	0.26	0.44	0.21
100 W/m <sup>2</sup>	-5.0°C	0.64	0.30	0.51	0.24
100 W/m <sup>2</sup>	-10.0°C	0.62	0.29	0.49	0.23
100 W/m <sup>2</sup>	-15.0°C	0.59	0.28	0.47	0.22
200 W/m <sup>2</sup>	-5.0°C	0.73	0.34	0.58	0.27
200 W/m <sup>2</sup>	-10.0°C	0.70	0.33	0.56	0.26
200 W/m <sup>2</sup>	-15.0°C	0.68	0.32	0.53	0.25
300 W/m <sup>2</sup>	-5.0°C	0.83	0.39	0.66	0.31
300 W/m <sup>2</sup>	-10.0°C	0.80	0.38	0.63	0.30
300 W/m <sup>2</sup>	-15.0°C	0.77	0.36	0.61	0.29

The parameter  $k_{D,e}$  can be modelled normally distributed with a coefficient of variation of 20%, in accordance with Gehlen (2000).

### Road conditions – $k_{D,e}$

In table A4b examples of quantified  $k_{D,e}$  are shown for the chosen road locations. The parameter  $k_{D,e}$  has been determined from  $k_{D,RH}$  and  $k_{D,T}$  according to eq. (6.1b) and the parameter  $k_{D,T}$  has been quantified from the equivalent surface temperature, according to eq. (6.3). The parameter  $k_{D,RH}$  can be quantified according to figure 6.3 and with data from figure 3.24a. From the results presented in figure 3.24a, the parameter  $k_{D,RH}$  has been estimated to **0.4** in the **dry splash zone (DSZ)** and **0.6** in the **wet splash zone (WSZ)** and **distant road atmosphere (DRA)**.

## Appendix

*Table A.4b: Quantified  $k_{D,e}$  for exposure in road conditions. [-].*

<b>Location:</b>		<b>Göteborg [S]</b>		<b>Munich [D]</b>	
$I_{\text{solar}}$	$T_{\text{sky}}$	DSZ	WSZ + DRA	DSZ	WSZ + DRA
	$T_{\text{air}}$	0.23	0.34	0.24	0.36
50 W/m <sup>2</sup>	-5.0°C	0.22	0.33	0.23	0.64
50 W/m <sup>2</sup>	-10.0°C	0.21	0.32	0.22	0.33
50 W/m <sup>2</sup>	-15.0°C	0.21	0.31	0.21	0.31
100 W/m <sup>2</sup>	-5.0°C	0.24	0.36	0.24	0.36
100 W/m <sup>2</sup>	-10.0°C	0.23	0.34	0.23	0.35
100 W/m <sup>2</sup>	-15.0°C	0.22	0.33	0.22	0.34
200 W/m <sup>2</sup>	-5.0°C	0.27	0.41	0.28	0.42
200 W/m <sup>2</sup>	-10.0°C	0.26	0.39	0.27	0.40
200 W/m <sup>2</sup>	-15.0°C	0.25	0.38	0.26	0.44
300 W/m <sup>2</sup>	-5.0°C	0.31	0.47	0.32	0.47
300 W/m <sup>2</sup>	-10.0°C	0.30	0.45	0.30	0.46
300 W/m <sup>2</sup>	-15.0°C	0.29	0.43	0.29	0.44

The parameter  $k_{D,e}$  can be modelled normally distributed with a coefficient of variation of 20%, in accordance with Gehlen (2000).